

Bringing Glass Giants to life

Fabrication of mass-optimized structural glass components of complex form

Bringing Glass Giants to life

Fabrication of mass-optimized structural glass components of complex form

by

Menandros Ioannidis

5627338

in partial fulfilment of the requirements for the degree of

Master of Science

in

Architecture, Urbanism & Building Science

Track of

Building Technology

Mentors: Dr. Ing. Faidra Oikonomopoulou Chair of Structural Design & Mechanics
Dr. Ing. Marcel Bilow Chair Building Product Innovation

Consultants: Dr. Telesilla Bristogianni
Dr. Charalampos Andriotis
Ir. Anna Maria Koniari

5th July 2023



My biggest gratitude goes to **Onassis foundation** for honouring me with their generous scholarship, which made it possible for me to pursue my studies abroad and realize my full potential. Your contribution was of utmost importance. Thank you!

First and foremost, I would like to express my sincere gratitude to my main mentor Dr. Ing. **Faidra Oikonomopoulou** for her constant support and excitement throughout my thesis. For always being available, supportive, enthusiastic and engaged with the project. Thank you for your guidance and for been a constant source of inspiration.

Secondly, I extend my deepest appreciation to my second mentor Dr. Ing. **Marcel Bilow** for his insightful contribution and consultations. Thank you for always helping me see through a different point of view and encourage me to reach the fullest of my potential. And of course thank you for the really cool lab pictures! They are a great memory from my time here.

To Dr. Ing. **Telesilla Bristogianni** I am thankful for the continuous assistance and input regarding the experiments, lab work, and equipment. Your countless meetings and personal time devoted to helping me were invaluable, and without your support and hands on help, the experimental part of my thesis would not have been possible.

Ing. **Anna Maria Koniari** I am grateful for generously sharing your work and expertise on topology optimization. Thank you for always been available to answer my questions and give advice.

Dr. **Charalampos Andriotis** thank you for the meetings from your personal time and the constructive input on topology optimization and output verification.

Special thanks are due to **ExOne**, especially to **Andreas Muller** and to **Leonhard Stöckle** for providing the 3D printed sand moulds used in the experiments and for their valuable input throughout the thesis.

I would also like to express my appreciation to **HÜTTENES ALBERTUS Chemische Werke GmbH** for sponsoring the coatings necessary for the experiments. I extend my special thanks to **David Hein** for the communication and feedback during the thesis.

I am grateful to TU Darmstad, Prof. **Seel, Matthias Martin** and **Chhadeh, Philipp Amir** for their valuable input on 3D printing of glass.

I would like to thank ir. **Hans Hoogenboom** from VR-lab for offering the computer used for the optimization of the geometry.

A heartfelt thank you to **Paul de Ruiter** thank you very much for allowing me to use the 3D printers, materials and equipment at the LAMA lab for my final prototype.

I would also like to thank **Daniel Frank Massimino** from **Evenline** for providing a sample of 3D printed glass.

Lastly, this thesis marks the end of an intense and transformative two-year period that has forever changed my perception of the boundaries of architecture. I would like to express my gratitude to my friends here and abroad and family for their unwavering support throughout this unique phase of my life. Without your physical and moral support, none of this would have been possible.

Marialena thank you for taking the pictures with the prototype. **Jasmine** and **Adalberto** thank you for the help with 3D printing. **Jullz, Juan, Olga, Pavlos, Charalampos, Jasmine, Daniela, Marialena, Nathaniel, Martijn, Alina** and **Eva** for your advice and feedback on the presentation. **Areti** and **Alexandre** thank you for been supportive and understanding.

Finally, I would like to devote this work in the memory of my beloved **parents**. Although they are no longer alive, their upbringing and love is reflected in this achievement. Hope you are proud.

Current research conducted at TU Delft focused on utilizing structural Topology Optimization (TO) for designing large monolithic cast glass structures with maximum stiffness and minimum mass. These structures demonstrated improved manufacturability in terms of time, energy, and cost efficiency due to their mass efficiency, which results in shorter annealing times. However, the complex geometries and customization of these forms posed challenges in terms of fabrication.

The manufacturability of intricate glass structures is explored by analysing and comparing three possible fabrication methods for three-dimensional glass structures with complex and customized geometries. The methods examined are:

- (i) Kiln casting in disposable moulds,
- (ii) Waterjet cutting and lamination of float glass panes,
- (iii) Additive manufacturing of glass.

The assessment of these methods is based on a set of criteria related to structural performance, visual quality, fabrication limitations, and sustainability. This comparative study act as a guide to the design of a case study and the selection of the preferred fabrication method. An all-glass topologically optimized bridge observatory in Vikos Gorge, Greece, is chosen as the design case. Based on the comparative study and a set of soft criteria, casting in disposable moulds is selected as the preferred fabrication method.

However, glass casting currently faces major drawbacks that restrict its potential. The two main drawbacks that this thesis tries to address are:

Rough and opaque surface quality (main focus): This issue is tackled through **laboratory experimentation** with the aim of achieving good surface quality immediately after demoulding. The experiments involve the use of different types of disposable 3D printed sand moulds (3DPSM) and application of refractory coatings and coating combinations at various maximum firing temperatures.

Lack of redundancy: Redundancy is explored **through research by design** and the implementation of design strategies (segmentation, zoning, fabrication methods combination) to ensure the feasibility of the structure.

The end result of this thesis is a comprehensive study on how an all-glass structure with complex and customized shape can be realized. The experimental part of the research yielded improved results, indicating that the combination of refractory coatings and 3DPSM has the potential to bring such glass components to life, reduce the need for post-processing, and simplify the fabrication process.

Given the limitations of time and knowledge within a master's thesis, further research is suggested to validate and evaluate the results obtained.

Table of Contents

1. RESEARCH FRAMEWORK	11
1.1. Background	12
1.2. Problem statement	14
1.3. Objective	15
1.4. Research question	16
1.5. Methodology	16
1.6. Time planning	17
2. CASE STUDY	21
2.1. Site.....	22
2.2. Design principles	23
2.3. Precedence/ built projects	24
3. GLASS	25
3.1. Introduction.....	26
3.2. Types of glass.....	26
3.3. Brief history of glass fabrication.....	27
3.4. Structural use of glass	27
3.5. Planarity of laminated float glass elements	29
3.6. Exploration of structural glass potential	31
3.7. Challenges	34
3.8. Discussion	38
4. FABRICATION METHODS	39
4.1. Abrasive Waterjet (AWJ) cutting of float glass and lamination.....	40
4.2. Glass casting.....	44
4.3. 3D printing of glass	52
4.4. Fabrication methods comparison/ conclusions.....	57
5. ASSESSMENT CRITERIA	59
5.1. Structural.....	61
5.2. Optical	66
5.3. Sustainability	70
5.4. Fabrication limitations.....	73
5.5. Conclusions	78
6. FABRICATION EXPERIMENTATION	81
6.1. Overview.....	82
6.2. Experiments set up	83
6.3. Annealing schedules	85
6.4. Coatings experiments	88
6.5. Hot pouring	104
6.6. Conclusions	107
6.7. Discussion – Next steps.....	109
7. FINAL DESIGN & REDUNDANCY	113
7.1. Software limitations	114
7.2. Custom algorithm for TO of glass (Koniari, 2022).....	116
7.3. Load cases	116
7.4. Design domain and input data	117
7.5. Geometry optimization	119
7.6. Research through design/ redundancy of bearing structure.....	119
7.7. Research through design/ redundancy of side rails and floor	124
7.8. Detailing	131
7.10. Verification of bearing structure.....	136
7.9. Assembly sequence	136
7.11. Final geometry.....	138
8. PROTOTYPING	147
8.1. Scaling up the coatings results	148
8.2. Prototyping	152
8.3. Fabrication.....	155
8.4. Full size fabrication	167
9. CONCLUSIONS & REFLECTION	171
9.1. Conclusions	172
9.2. Limitations	174
9.3. Discussion	174
9.4. Next steps	177
9.5. Reflection.....	180
10. REFERENCES	183
11. APPENDIX	189

1

RESEARCH FRAMEWORK

Introduction, background information, framework, methodology and research questions.

1.1. Background

Glass is an optically transparent, durable, and infinitely recyclable material (Musgraves et al., 2019) with high compressive strength¹ which makes it ideal for architectural and structural applications in the built environment. Currently only **laminated float glass** is used in structural applications. While these applications are redundant and safe, they are governed by the 2-dimensionality of the flat panes made by the prevailing float glass industry (Le Bourhis, 2014).

Latest developments in fabrication methods of glass, such as **3D printing of glass** (Inamura et al., 2018; Klein, 2015) and **casting** of glass (Bhatia, 2019; Bristogianni, 2022; Damen, 2019; Oikonomopoulou, Bristogianni, Barou, Jacobs, et al., 2018; Oikonomopoulou, 2019) display the attempt to escape from the 2D design space and explore the potential of 3D components for architectural applications.

Literature review show that 3D printing of glass displays great future prospect but is still in an embryotic stage allowing only for relative small-scale objects. Casting of glass shows great potential in large scale 3D structural applications (e.g., Crystal house, Giant Magellan blank, Mirage, Qaammat Pavillion, Optical house) but realised examples of complex shapes and at large scale are limited to telescope blanks (Figure 1).

For the realization of customized and complex 3D structural glass components, design, material and fabrication particularities need to be addressed. Starting with glass peculiarities. Glass requires lengthy annealing process, as displayed in the work of (Klein, 2015; Oikonomopoulou, 2019; Koopman, 2021; Koniari, 2022) regarding cast glass, mass and thickness of the designed object increase the annealing time exponentially; skyrocketing the cost and the feasibility of such voluminous glass components (Figure 1). Though the implementation of mass optimization, specifically utilizing topology optimization², the annealing time can be minimized, leading to a more feasible and cost-efficient production (Damen, 2019; Koniari, 2022).

Glass as a material has significantly different tensile and compressive strength. Existing conventional software (e.g., ANSYS) usually implement von Mises failure criterion which is more suitable for ductile materials that have similar values of tensile and compressive strength values (Bruggi & Duysinx, 2012). Recent development of custom algorithm for topology optimization (TO) of glass as part of the thesis of (Koniari, 2022), is able to account for the brittle nature of the material and significantly different values in the tensile and compressive strength, the annealing time limitation and the need for uniform mass distribution, unique to glass.

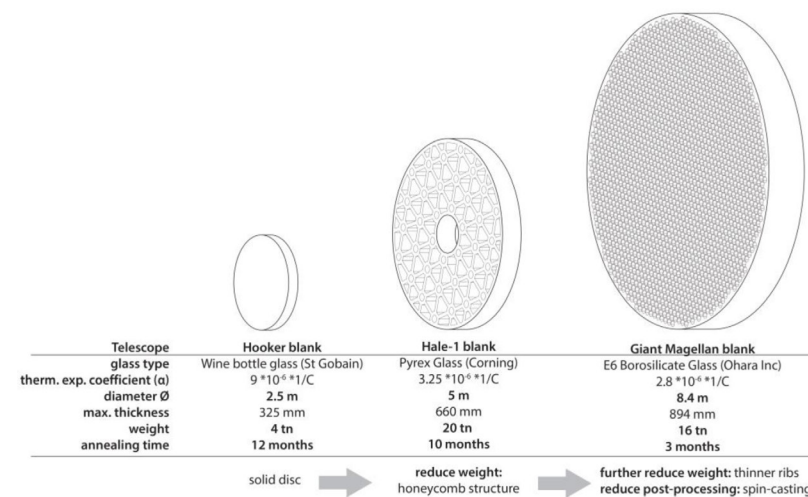


Figure 1 : Reduction of annealing time through the implementation of mass and max. thickness reduction., left solid blank, middle: honeycomb structure, right: denser grid with thinner elements, derived from (Oikonomopoulou, 2019), based on data from (Zirker, 2005)

1. Different values are stated in the bibliography. For float soda-lime glass compressive strength as high as 1000 MPa is reported (Ashby & Jones, 2006; Weller et al., 2008). In Granta EduPack 2021 R2 a compressive strength for soda-lime glass is stated in a range of 300-420 MPa and for borosilicate glass in the range of 260-350 MPa. "In practice strength values between 14-70MPa are reported for common glass products and reach a maximum of 2.1GPa for freshly drawn glass fibers (Varshneya 2013)."(Bristogianni, 2022)

2. "Topology optimization of solid structures involves the determination of features such as the number and location and shape of holes and the connectivity of the domain." (Bendsøe & Sigmund, 2004)



Figure 2 : Bründl Kaprun flagship store sky walk made from laminated float glass (seele, 2021).

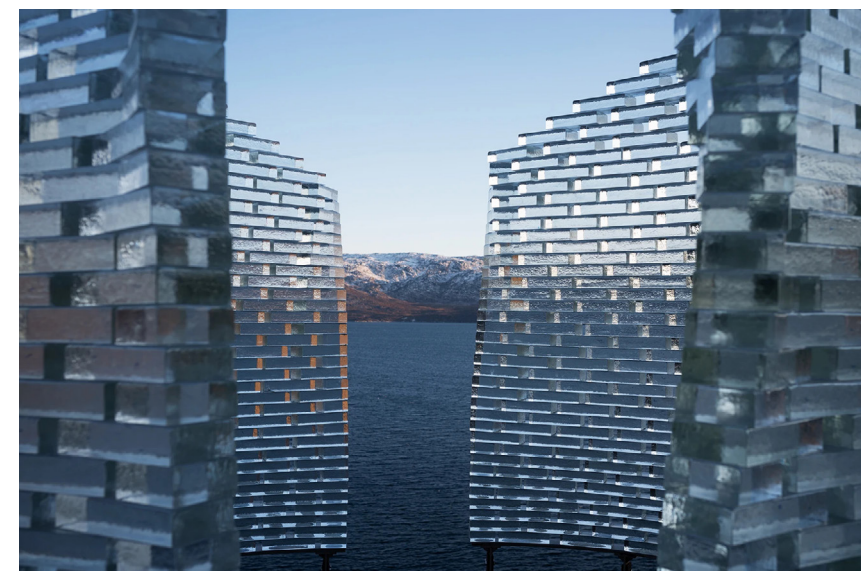


Figure 3 : Qaammat Pavillion, adhesively bonded cast glass structure, photo credits: Julien Lanoo. (2021)



Figure 4 : Optical house, cast glass bricks © Koji Fuji / Nacasa & Partners Inc (2012)

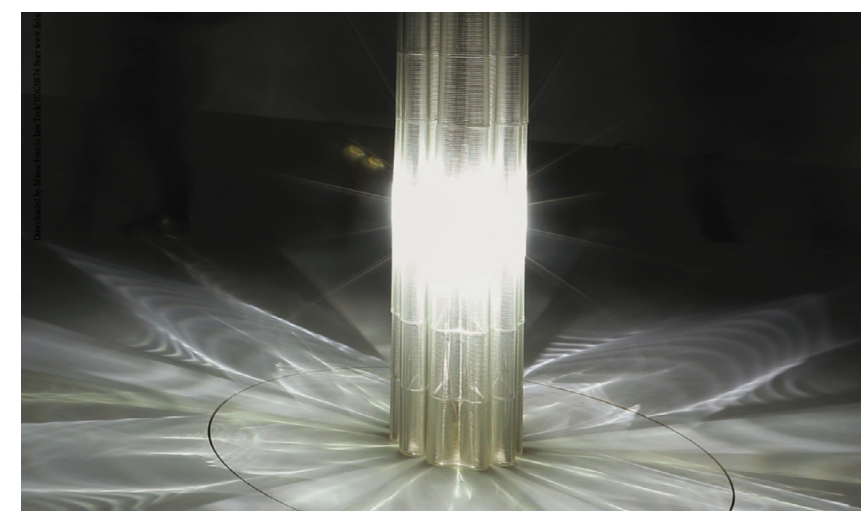


Figure 5 : Glass column fabricated using 3D printing of glass(Inamura et al., 2018)



Figure 6 : Glass I, 3D printing of glass (Image credit: Andy Ryan) (Klein, 2015)

Custom developed tools such the one described above, show great potential towards the more efficient design of mass optimized glass components in the future.

TO designs, even though they contribute greatly to an optimized shape of feasible annealing time, they also result in complex, customized forms that are challenging and cost-ineffective to produce with the currently available fabrication mould methods (e.g., permanent moulds or disposable moulds of low accuracy). Successful implementation of 3d printed sand moulds (3DPSM) for casting a topologically optimized steel node realised by Arup and 3Dealise (Galjaard et al., 2015) underlies the potential of such fabrication method on glass casting. Extensive research in kiln casting using disposable moulds has been conducted at TU Delft by (Bristogianni, 2022; Oikonomopoulou, 2019) and complimented by the master thesis of (Bhatia, 2019; Damen, 2019) that dive into the potential of using 3D printed sand moulds in kiln casting of glass. On the one side mould technology is mature enough allowing for shape and size freedom, high level of accuracy and relative low cost. On the other side rough opaque surface quality, that requires post processing underlines the need for research towards this direction. First experiments done by (Giesecke & Dillenburger, 2022) using different binders and coatings, tested with hot pouring technic, show great promise regarding surface and finishing quality of cast glass elements. Up to today there is no extensive testing of the most promising binders and coatings on kiln casting of glass elements.



Figure 7 : experiments using different coatings, top kiln casting, bottom foundry casting (Giesecke & Dillenburger, 2022)

To sum up, cast glass is constricted by the current means of fabrication but recent developments pave the way for complex shaped structural applications of cast glass. This vision is highlighted in numerous MSc thesis (Bhatia, 2019; Damen, 2019; Koniari, 2022; Koopman, 2021; Naous, 2020; Stefanaki, 2020) within TU Delft that dare to design novel structures of cast glass.

1.2. Problem statement

Main problem

Emerging design tools and fabrication methods show potential towards three-dimensional structural applications of glass. Custom design tools for TO help overcome limitations in the annealing time and material peculiarities unique to glass. While design tools have evolved overcoming the limitations posed by the nature of the material, production methods of the generated complex and customized geometries and recent innovations in fabrication methods are still under-explored.

Currently there is no comparative research/ study between the different fabrication methods for structural 3D glass components.

Sub problems

Structural performance, optical quality, sustainability and feasibility are imperative in glass structures. Findings from the comparative study are used to design and specify an all-glass structural cantilever as a case study:

Structural performance: Cast glass structures display no redundancy and have lower design strength than laminated glass.

Optical quality: So far structural glass components via lamination or 3D printing have compromised transparency displaying directional transparency. Transparency in cast glass shows an opaque rough surface when produced with the current disposable mould methods. Cast glass has the potential to have a smooth and fully transparent surface if produced with a steel mould.

Sustainability: casting shows great recycling potential, reducing the environmental impact when compared to the predominant fabrication method of float glass.

Feasibility: Apart from laminated glass, structural applications using alternative fabrication methods for complex glass elements are under-represented in the built environment.

1.3. Objective

Literature review

The research is based on thorough literature review of state-of-the-art research papers, publications, conference lectures and personal communication with companies (ExOne, Hüttenes Albertus (HA) Chemische Werke GmbH) and institutions (TU Darmstadt, MIT) to familiarize with concepts of glass, fabrication methods (casting in 3D printed sand moulds, 3D printing of glass and lamination of waterjet parts), case studies/ precedence of built and research projects and topology optimization in structures. The main aim of the research is to categorize the different fabrication methods for glass using a set of criteria: structural, optical, sustainability and fabrication limitations/ feasibility. Each criterion is broken down into sub criteria that are analysed per fabrication method. The set of criteria allow for the qualitative comparison of the different fabrication methods and define interrelations/ correlations between the criteria for each of the fabrication methods.

Case study

The comparative study acts as a guide for the design of the case study. The fabrication method for the realization of the case study is chosen based on a set of soft criteria established during the preliminary design phase. An all-glass topologically optimized cantilever observatory is chosen as the design case and kiln casting with disposable moulds is the selected fabrication methods. The existing 2D TO algorithm developed by (Koniari, 2022) and ANSYS workbench commercial software is used for the generation and structural verification of the geometry. Full documentation, detailing, construction sequence, transportation plan is produced during this phase.

Lab experiments

Surface quality and transparency are investigated by a series of experiments conducted on the glass lab of TU Delft. Set of experiments as follows:

1. Testing of annealing schedules and their effect on mould binders (ExOne)
2. Experiments with different coatings on disposable 3D printed sand moulds produced by (ExOne) with the most promising binder. The goal is to investigate if surface quality and transparency can be improved, thus reducing the need for post processing and cost. Small cylindrical shaped specimens, comparative analysis and examination with the microscope are the results of this part (ExOne and HÜTTENES ALBERTUS Chemische Werke GmbH).
3. Prototyping (segment or scaled model) of the case study geometry that also acts as a scaled up verification of the optimal set up derived from the previous.

Finally, redundancy/ safety is explored through research by design during the development of the case study.

1.4. Research question

As stated above there is limited knowledge regarding the fabrication potential of 3D glass components with complex and customized form. This leads to the research question of this thesis which is:

Which **fabrication method** is the most promising for **mass-optimised** and **customized glass** components of complex form?

Comparative study in terms of **optical quality, structural performance, sustainability** and **fabrication limitations/feasibility** for such components, fabricated via 3 different methods:

- **Lamination** of AWJ cut glass parts
- **Kiln casting** with the aid of disposable 3D printed sand moulds
- **3D printing of glass** – literature review only

Sub question

Focusing on kiln-casting using disposable 3D printed sand moulds (3DPSM):

A. How to improve the **surface quality** and **optical quality** of structural glass elements?

- Which is the preferred firing schedule and maximum temperature that glass can be cast on the provided 3DPSM?
- Which is the potential of applying different coatings on 3D printed sand moulds in improving the surface quality and finishing texture of complex-shaped cast glass components?

B. How to improve **redundancy** and **safety** of structural glass elements?

- In which ways can design help improve safety of cast glass structures?

1.5. Methodology

This thesis is split into 4 parts:

- literature review
- case study
- lab experiments
- prototyping

For literature review extensive research on current papers and publications is conducted to familiarize with the concepts of glass, fabrication methods (casting in 3D printed sand moulds, 3D

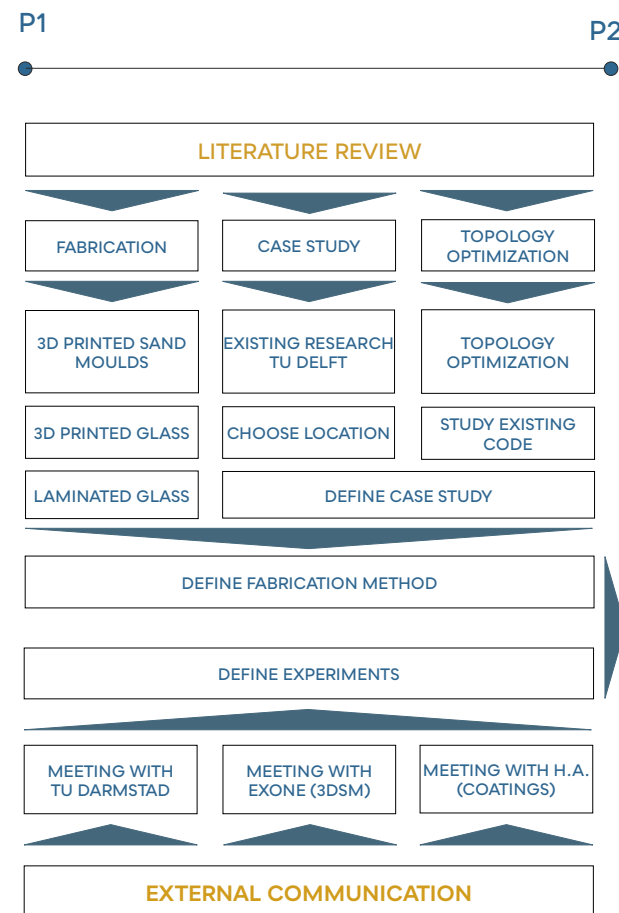
printing of glass and lamination of waterjet parts), case studies/ precedence research of built and research projects and topology optimization in structures. The product from the first phase is an extensive comparative study on complex shaped glass components fabricated with the 3 different manufacturing techniques base on a set of criteria. After P2 research through design (case study) and experimental tasks run in parallel.

Case study

An all-glass topologically optimized cantilever observatory in Vikos gorge in Greece is chosen as the design case and kiln casting with disposable moulds is the selected as the fabrication method for the bearing structure.

Lab experiments

Lab experiments are split in two sets. Material sponsorship has been secured for the series of the experiments, by ExOne company for the 3D printed sand moulds and by HÜTTENES ALBERTUS Chemische Werke GmbH for the coatings.



The first set of experiments deals with the effect of annealing schedule on the carrying capacity of 3D printed sand moulds. Sand mould pieces are placed in the oven following different annealing cycles to determine if and how the prolonged exposure to heat affects the structural integrity of the moulds (results are evaluated qualitative performing scratch and brittleness tests).

The second set of experiments has to do with the application of different coatings and combination of coatings on the 3D printed sand moulds. Surface and optical quality of kiln-cast glass specimens is access and compared with samples produced without coating. Conclusion from the first experiment (if applicable) are used in these experiments.

Prototyping

Prototyping considers the knowledge obtained by research through design and lab experiments. Part of or a scaled model of the designed structure is realised in cast glass as a proof of concept.

1.6. Time planning

Between P1 and P2, literature review, choosing of the case study, location for the case study and company/ institution communication takes place.

After P2 and P3 the feedback from P2 is implemented, literature review continues, research through design begins (case study), first set of experiments takes place, and second set of experiments start.

Between P3 and P4 the design of the case study solidifies, structural verification and detailing of the structure is done. Meanwhile the rest of the experiment sets begin. Tests finish by the end of P4, while first reflections and conclusions are added.

Between P4 and P5 a prototyping of the glass cantilever is fabricated via kiln casting, feedback from P4 is incorporated in the work and final report and presentation is prepared.

See (Figure 9) for the weekly time planning.

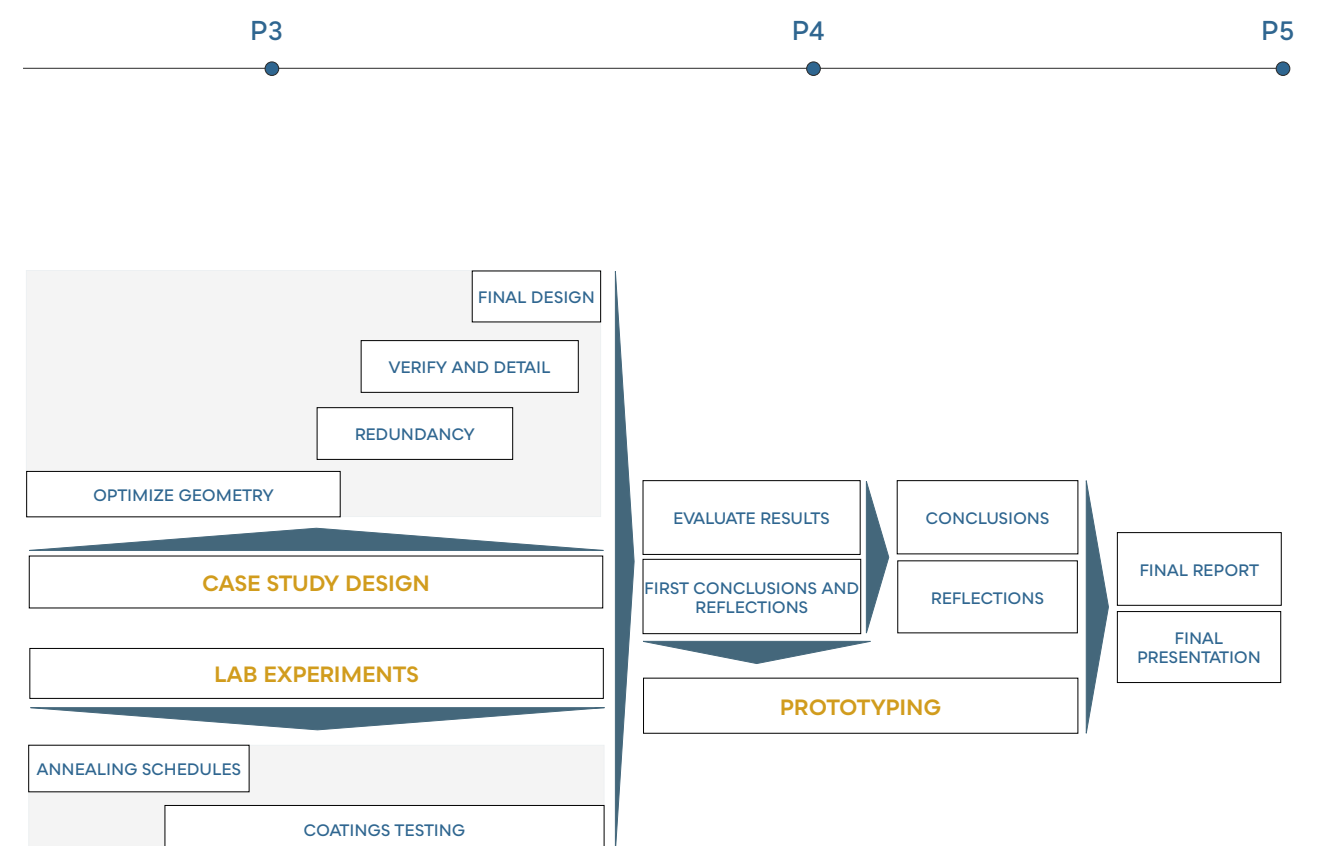
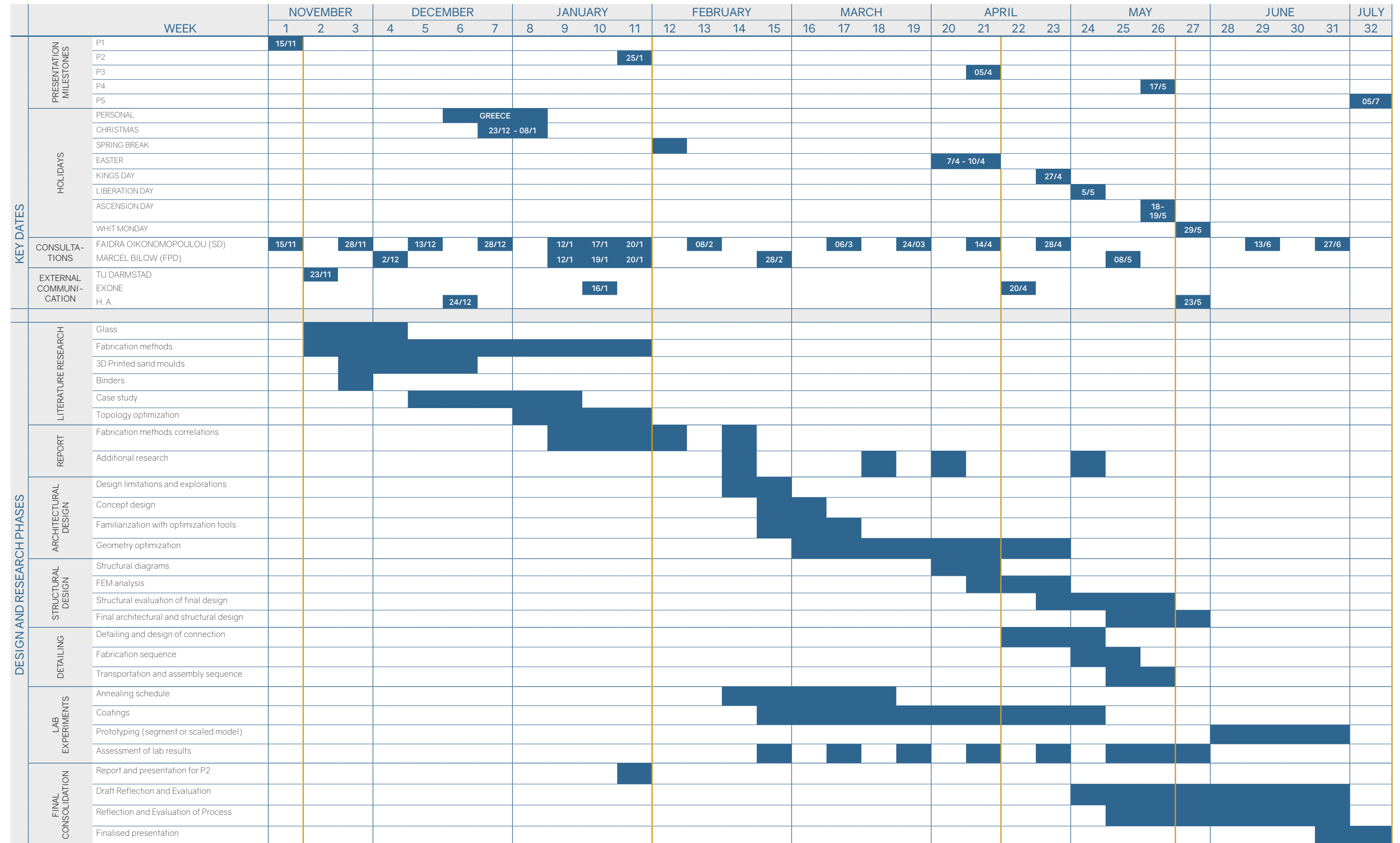


Figure 8 : Timeline outline

Figure 9 : Weekly planing



2

CASE STUDY

This chapter introduces the case study. The aim is to arrive at the design of a cast glass cantilever (bridge) observatory in Oxya viewpoint of Vikos Gorge in Greece. Literature review indicates that topology optimization shapes with intricate design relate to asymmetry in the structure. Cantilevers are supported only on one side and display both tension and compression adding an additional level of complexity and can fully utilize the ability of the custom algorithm developed by (Koniari, 2022) for glass. Precedence research shows examples of all glass cantilevers (made out of laminated glass) of up to 10 m. in length (seele, 2021) which act as reference for the design.

2.1. Site

Vikos Gorge is part of Vikos-Aoos National Park, located in the Northwest Greece. According to (Guinness World Records 2005, 2004) is the “deepest relative to its width” gorge in the world. It has a length of approximately 30 km, depth between 120-1350 m. and width from few meters to 2500 m (Wikipedia, 2022). The gorge is runner by Voidomatis river tributary of Aoos. The landscape is a protected area of unique natural beauty. Oxya viewpoint offers breathtaking views of Voidomatis river and the gorge (Figure 11). The location is easily accessible through an approx. 100 m long well paved and maintained path (Figure 10). The car park is located at the beginning of the path. Access to the viewpoint.

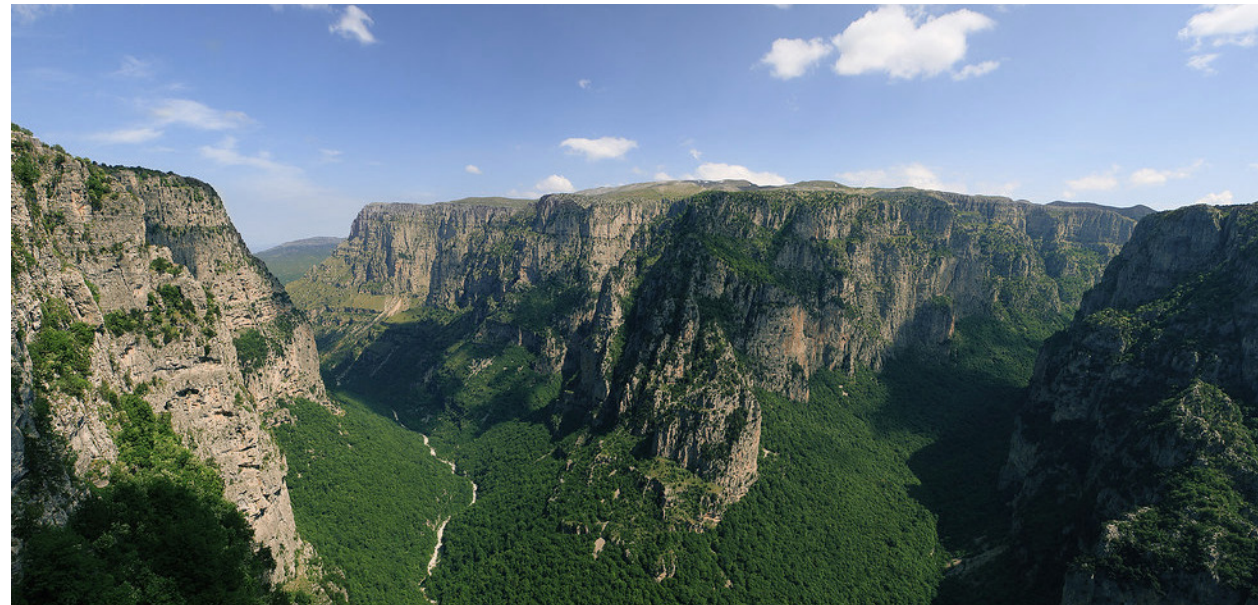
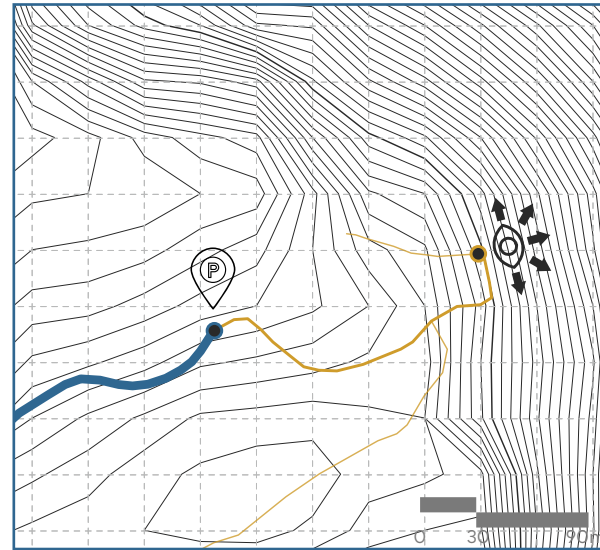


Figure 10 : Topography of location and view from eye level at Oxya viewpoint. Image source: googlemaps.com.

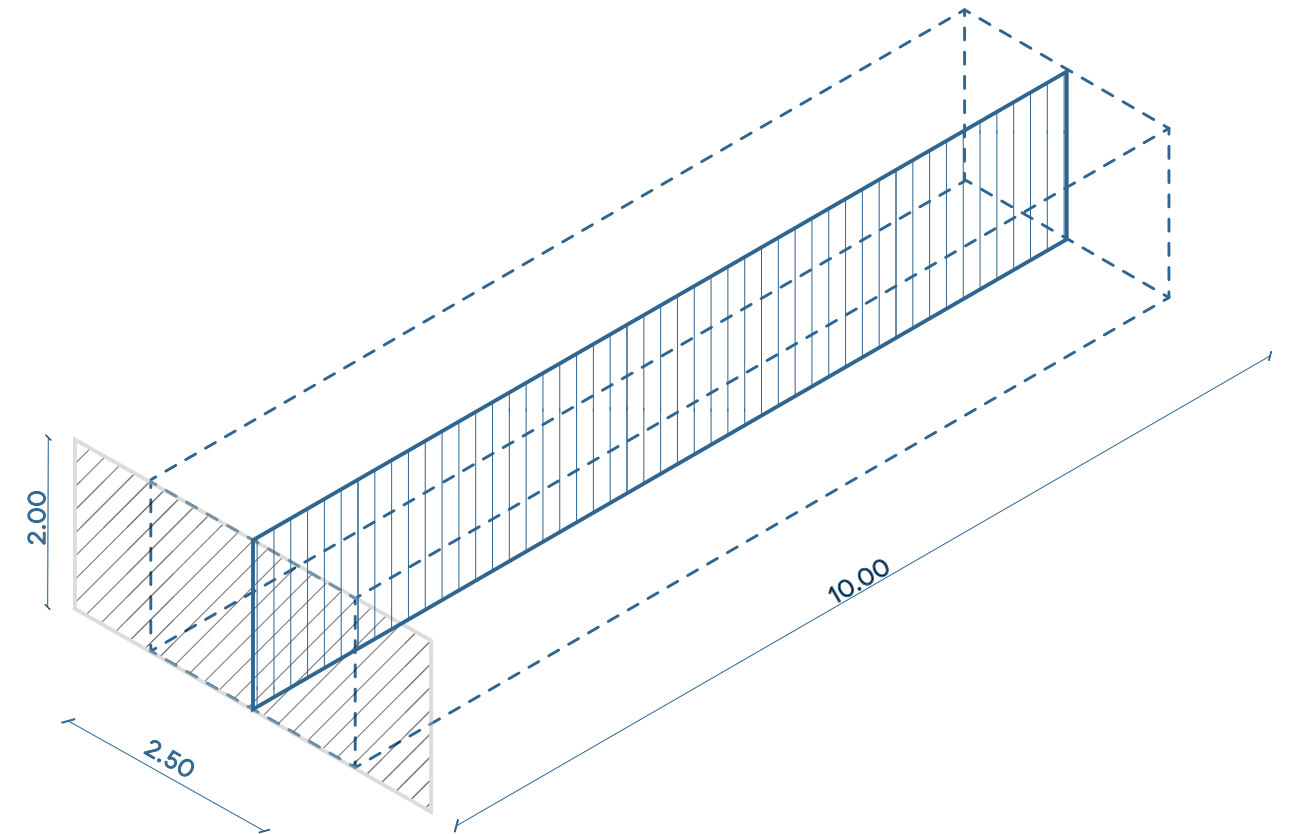


Figure 11 : Design domain for the case study

2.2. Design principles

While the location receives a lot of visitors every day no conscious design has taken place to facilitate this need. The only structure present is the stone wall that protects the visitors from falling over the edge. A location with such a unique natural beauty requires a minimally invasive design with nominal optical footprint that offers an unobstructed view of the surroundings. A topologically optimized structure will add a unique structure/ experience to the location that can acts as a landmark (innovative and daring structure) that boosts local tourism. Finally, the design of the case study should be respectful of the environment produced with the most sustainable fabrication method available for glass (Figure 12).



Figure 12 : design principles/ soft criteria for the design

2.3. Precedence/ built projects

As a starting point for the case study already built project are researched to draw inspiration from. A characteristic example of architectural intervention at a location of unique natural beauty is that of Grand Canyon Skywalk at Eagle point, AR, USA. This project offers an unprecedented view of the Grand Canyon for its visitors. Its glass bridge extends approximately 21 meters over the rim of the canyon offering a clear view of 1200 meters to the Canyon floor below through its glass floor. This structure is robust enough to hold the weight of 70 Boeing 747 fully loaded with passengers. While the structure is robust its trade-off is the high visual impact on the environment due to the use of conventional structural elements made from steel (Figure 13, Figure 14).

A more recently built example of a glass bridge is that of Skywalk for Bründl Sports (2021) (Figure 15). The all-glass cantilever is 10m in length and 2 meters in width and is part of a retail centre in the Austrian Alps. The bearing elements of the structure are made of glass, manufactured through the lamination of float glass panes. Steel is only used for the connection of the elements and for fixing the walkway to the building. This case study showcases the architectural potential of an all-glass structure at a location of unique natural beauty and acts as the main inspiration for the design of this thesis.



Figure 13 : Top view of Grand Canyon Skywalk at Eagle point (Giroux Glass, n.d.)



Figure 14 : Side view of Grand Canyon Skywalk where the conventional steel structure can be seen (Giroux Glass, n.d.)



Figure 15 : Skywalk for Bründl Sports and the Austrian Alps on the background. Glass structure blends with the environment creating minimal visual obstruction and offers a unique architectural experience (Blocher Partners, n.d.)

3

GLASS

Short introduction of glass properties and manufacturing history. Current applications of structural glass and limitations posed by the material's nature and the currently available fabrication methods are presented.

3.1. Introduction

Glass offers a range of exceptional and distinctive characteristics to architects, engineers, artists, and others, making it a highly sought-after material across various industries such as construction, automotive, boating, interior design, optics, glassware, art, tableware, and data cables. Its combination of transparency, strength, recyclability and longevity makes it an ideal choice for various applications. Depending on the composition, glass can appear transparent or translucent, coloured or clear (Bontemps & Cable, 2008; Musgraves et al., 2019).

Glass is a material that is formed by solidifying a liquid and has a consistent composition. Its transparency is the result of the complex and random arrangement of its molecules and the lack of crystal lattice formulation. As glass is a combination of various molecular bonds, it does not have a specific chemical formula. This also means that it does not have a fixed melting point when heated, instead it transitions from a solid to a liquid state gradually. Unlike other crystals, glass has properties that do not vary depending on the direction in which they are measured. Glass is known for its amorphous isotropy, which means that its properties remain the same regardless of the direction of the material (Schittich & Lenzen, 2007).

In general glass is a durable material that is resistant to most acids and alkaline solutions except for hydrofluoric acid. The noncorrosive nature of glass and its chemical inertness makes it ideal for maintenance free structures.

Glass is a recyclable material that can be recycled endlessly without losing its quality (Musgraves et al., 2019; Nijssse, 2003).

Glass has high theoretical compressive strength higher than any other structural material currently used with reports of 1000 MPa (Ashby & Jones, 2006; Weller et al., 2008) (Table 1).

Mechanically, glass can have some elastic deformation, but it doesn't yield plastically. The covalent bonds between atoms cannot repair themselves after being broken (Veer, 2007). Thus, glass is characterised as a brittle material.

3.2. Types of glass

The three main types of glass used are soda-lime-silica glass, borosilicate glass and quartz glass. Soda-lime-silica glass is considered the standard glass, commonly used for façade glazing, bottles, and jars, while borosilicate glass is preferred for applications that require greater temperature resistance due to its lower thermal expansion coefficient compared to soda-lime-silica glass. This type of glass is widely used in cookware, lab equipment, medical devices, lighting, and optics. Other types of glass such as lead glass and aluminosilicate glass (e.g., thin glass) are used for various other applications. The table below gives an overview of the different properties of each of the glass families.

Table 2: Indicative values for most common types of glass (Information retrieved from ANSYS Granta Edu-Pack 2022 R1 software)

Types of glass	Density (kg/m ³)	Young's modulus (GPa)	Price (€/kg)	Expansion coefficient α (10 ⁻⁶ /°C)
Quartz glass	2170-2200	62-74	5.29-8.83	0.48-0.52
Soda lime glass	2440-2520	68-72	1.2-1.41	8.92-9.28
Borosilicate glass	2200-2370	61-64	3.61-6.03	3.5-3.7
Lead glass	3950-3990	53-55	3.54-5.3	8.8-9.2
Aluminosilicate glass	2470-2520	84-88	1.2-1.4	4.5-4.69

3.3. Brief history of glass fabrication

Glass is an ancient material created in the ancient Mesopotamia and Egypt around 4500 years ago (Klein, 2015; Musgraves et al., 2019; Rasmussen, 2012). Over the centuries glass has been manufactured with a plethora of technics and different recipes. Casting of glass is indeed one of the earliest technics dating back to 15th century BC (Trentinella, 2003). Important moments in the manufacturing history of glass are the invention of: the glass blowing at the 1st century BC, the cylinder method around 2nd century BC, the crown or disk method on the 4th century BC, the plate glass casting on the 17th century and the float glass process in the mid-20th century (Musgraves et al., 2019).

The earliest application of glass relates to jewelry and art. During the Roman times glass first appeared as glazing to allow light in the interior of buildings. Until the Middle Ages glass as glazing remained a privilege for the upper classes and church (as stained glass). In the 17th century the use of clear glass is preferred over the use-stained glass affected by the rationalism movement. Later in the mid-19th century, the idea of architectural glass comes to life with the realization of the Crystal palace (1851) designed by Sir Joseph Paxton. Crystal palace changed the production and construction methods through a series of innovations⁴ that introduced. While this is the first application of architectural glass the glass itself is not structural and it is supported by a lightweight cast iron skeleton.

The advent of the float glass manufacturing process by Pilkington in 1959 (Pilkington company, n.d.) less than a century ago allowed the application of glass in all-glass building envelopes and later on as structural glass façades (Cruz, 2013). Over the course of its history glass has transitioned from a fragile and opaque material to a durable, optically transparent, structural material that shows immense potential in architectural and structural applications of the future.

3.4. Structural use of glass

Structural use of glass has only been going on for some decades. Compared to steel or concrete that are used for approx. 200 years and 100 years respectively. Due to its unique and contradictory properties is believed that in the next years will be used more widely as a structural material (Nijssse, 2003). Recently there is an increasing amount of research and projects regarding the structural applications of glass. Glass is preferred over other materials for its transparency, its durability and its good mechanical properties (especially its compressive strength). Float glass pieces are laminated together with a transparent interlayer, forming structural elements. One of the earliest example of structural use of float glass is the Centre Administratif (Figure 17) (Brunet Saunier Architecture, 1995). Laminated float glass sheets form cruciform load-bearing glass columns that are capable of bearing up to 50 tons each (Cruz, 2013).



Figure 16 : Glass properties

Table 1: Theoretical compressive strength of most common structural materials, edited from (Bhatia, 2019)

Material	Compressive strength (MPa)
Aluminium (T6)	469
Structural steel (A36)	400
Concrete	40
Glass	>1000

4. Construction of The Crystal Palace began in 1850, and the building was completed in just five months, largely due to the use of prefabricated materials. Pieces such as standard-sized glass panes, cast iron, and laminated wood, were built in Birmingham, and assembled on-site, enabling the process to be completed much faster than traditional building methods. This innovative approach to construction was a significant factor in the speedy completion of The Crystal Palace (Zoeller & Muscato, n.d.).

Yurakucho canopy at the Yurakucho metro station in Tokyo, Japan (Figure 18) is an all-glass cantilever structure, designed by Rafael Viñoly Architects and engineered by the British company Dewhurst Macfarlane & Partners. The canopy covers an 8m by 4.8 m staircase to the metro station. The total size of the canopy is 10.5 m. by 5 m. The structural concept is based on a series of cantilevered beams that are bolted together effectively transferring the moment and shear loads to a steel torsion support. The arch cantilevered beams are made of laminated glass and acrylic sheets. Each beam is made from four elements that are bolted together at the middle and end of their length. The number of blades is reduced from four to one towards the end of the structure. The arch beams are fixed to the horizontal steel beam by V shaped steel elements (Lusas, n.d.).

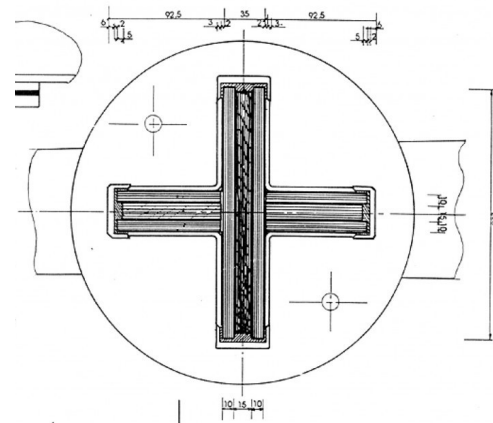


Figure 17 : Top, view of the glass column from the interior of the building, Bottom: glass column detail from Centre Administratif (Brunet Saunier Architecture, 1995)

Processes such as tempering, heat and chemical strengthening have intensified the applications and research of structural elements made from laminated glass. A more recent example is the Apple Store, Fifth Avenue in New York (Figure 19) (Bohlin Cywinski Jackson, 2006). In this example, fins comprised of several layers of float glass are laminated together forming the column and beams of the structure. The structural elements interconnect resulting in a structural-steel free glass cube structure. The design has been revisited in 2011, the number of fins and beams were reduced, further refining the design and the transparency of the structure.



Figure 19 : Apple Store, Fifth Avenue in New York (Bohlin Cywinski Jackson, 2006)

3.5. Planarity of laminated float glass elements

The first projects that utilized glass for structural applications were comprehensive and ahead of their time, pushing the boundaries in design and manufacturing. In the earliest, implementation redundancy was a major concern. According to (Nijse, 2003) in the Centre Administratif project the structure has sufficient redundancy being able to carry the loads of the roof even after the failure of one column element. This is partially due to the

steel elements in the structure (Cruz, 2013).

Apart from redundancy these projects display the limitations imposed by the prevailing presence of float glass industry⁵. All the elements that shape the building components are practically 2D limiting the shape and expression freedom.

It is possible to create pseudo-3D shapes made from multiple sheets of glass often seen in art. The artist Ben Young creates 3D shaped sculptures. Lamination of multiple layers is also possible as seen in the work of Dustin Yellin (Yellin, n.d.) where he creates 3D collages by embedding mixed media into individual laminated glass panes. The result is usually bulk and heavy with the need of a minimum overlap area to allow for adequate surface for lamination. The resolution of the shapes is governed by the thickness of the glass pane. Laminating multiple pieces becomes increasingly difficult (the artist results in the use of glue). Extensive literature research has yielded that Industrially fabricated examples employ no more than 11 layers (Eckersley O'Callaghan, 2018) (usually confined to 5-6 layers) (Li & Ren, 2011). This is due to practical limitations linked to autoclave lamination process (forming of bubbles due to uneven pressure - compromise of optical quality, cost).

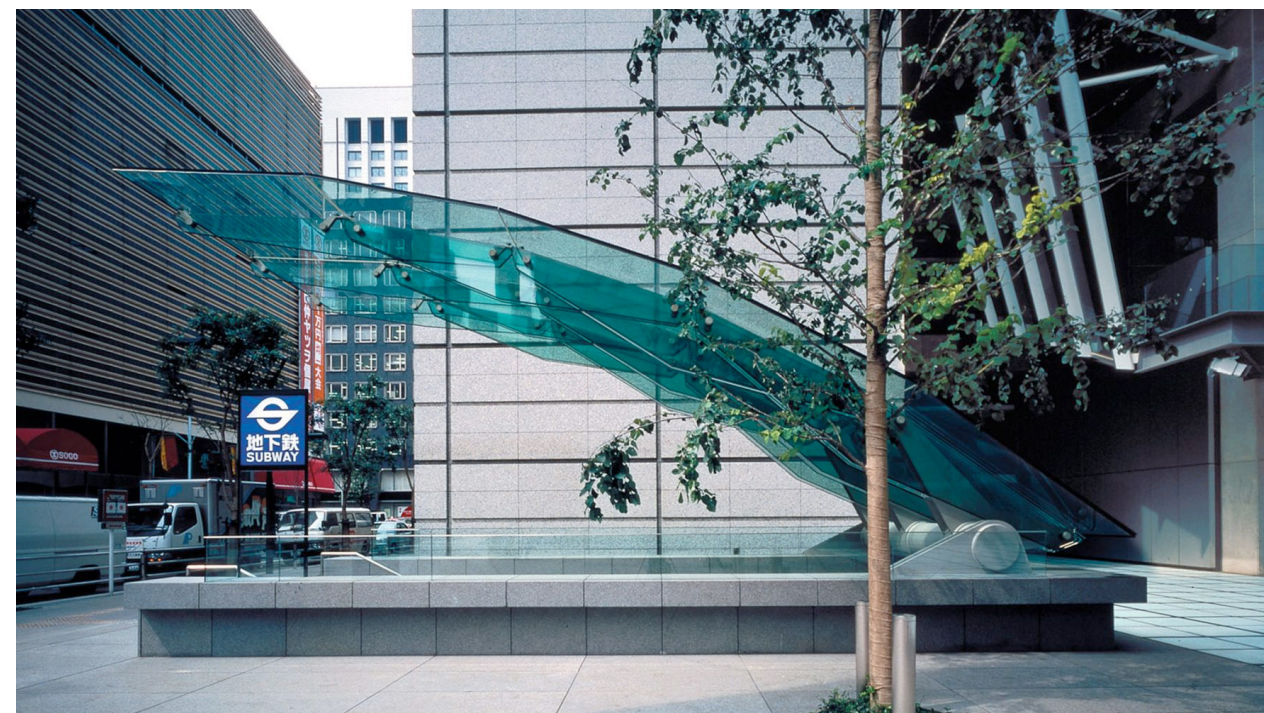


Figure 18 : Yurakucho canopy in Tokyo Japan (Rafael Viñoly Architects, 1997)



Figure 20 : In the project Glass wipe by (Eckersley O'Callaghan, 2018) were up to 11 layers of glass are laminated using SentryGlass interlayer.

5. As stated in the work of (Le Bourhis, 2014) and (Oikonomopoulou, 2019) at present 90% of the flat glass used in the building industry is been produced by the float glass method. Float glass is preferred over other production methods for its superior transparency, its relative low cost, its wide availability and the standardized size of the panels.

The most extreme realized example is that of house Laminata, glass House in Leerdam, Netherlands by KARO (2002) (Figure 24). The house is built by approximately 13000 factory-cut 10mm sheets of float glass (Nolan, 2001), glued on site with a silicon-based sealant. The house took 4-5 years from concept to construction mainly due to the research needed in finding a suitable adhesive (Divisare, n.d.).



Figure 21 : Laminated glass sculpture, source: <https://www.demilked.com/glass-sheets-wave-sculpture-ben-young/>

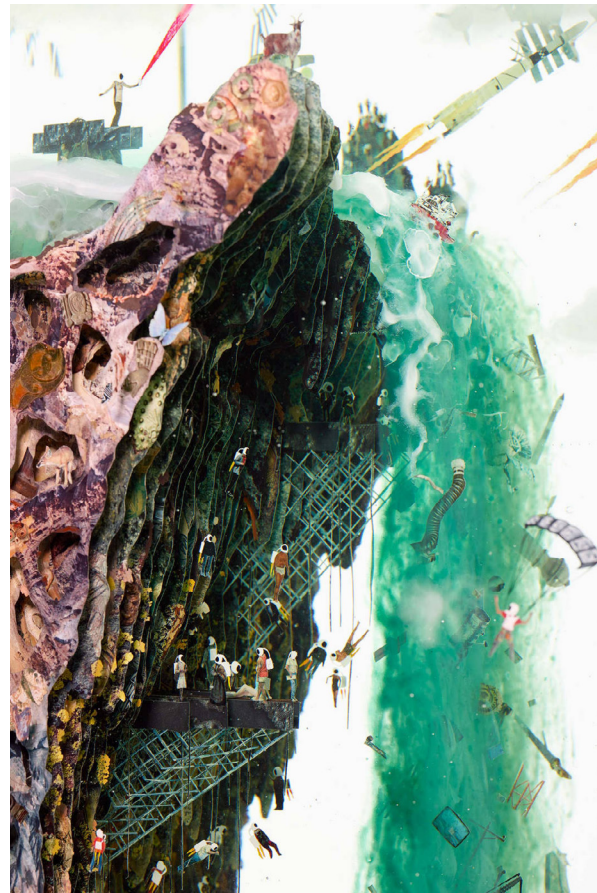


Figure 22 : The Politics of Eternity (detail), 2019, Glass, Collage, Acrylic, Steel, (Yellin, n.d.)

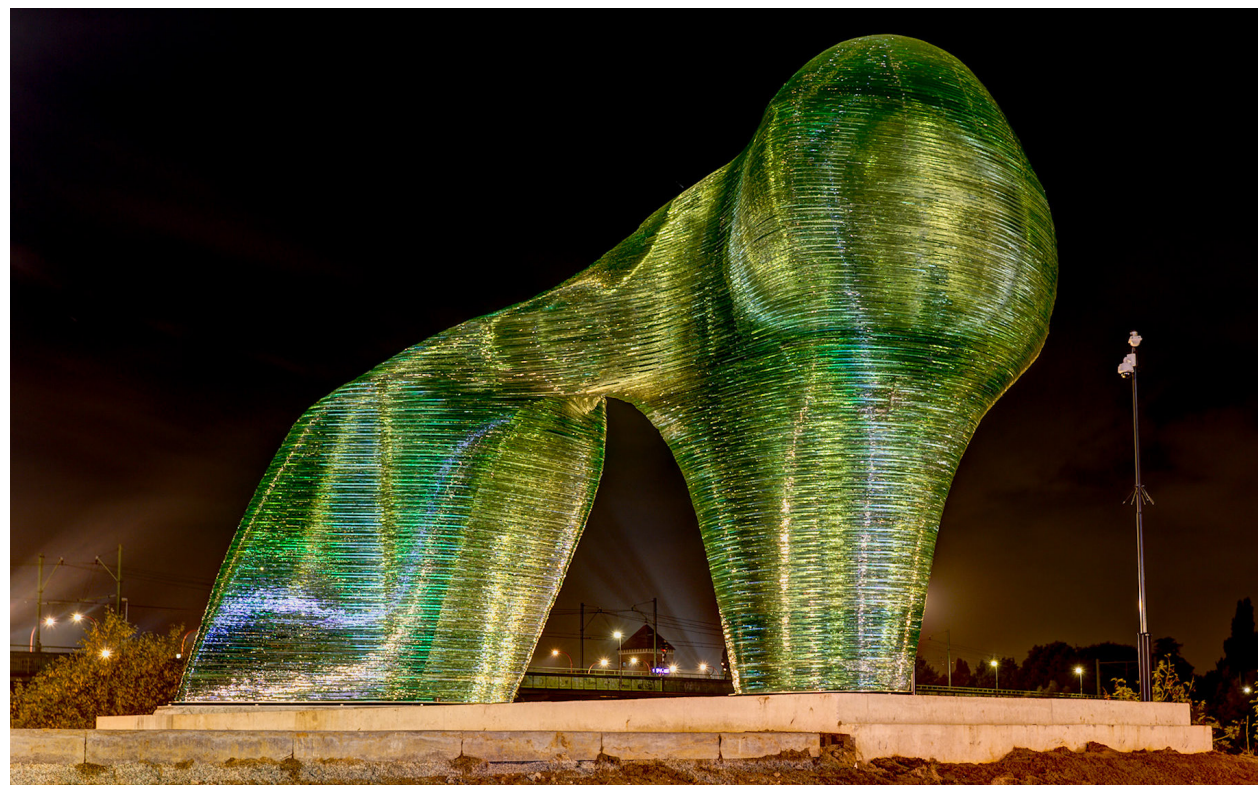


Figure 23 : Glass sphinx sculpture in Venlo, Netherlands, fabricated using float glass. Image credit: Twan van den Hombergh



Figure 24 : House laminata, image credits: Luuk Kramer (Divisare, n.d.)(<https://divisare.com/projects/387294-kruunenberg-architecten-luuk-kramer-laminata-a-house-of-glass>)

3.6. Exploration of structural glass potential

“ GLASS WILL NEVER SEEM THE SAME AGAIN AND MOST PROBABLY WILL NEVER BE USED IN QUITE THE SAME WAY “(Nolan, 2001)

Lately architects and engineers are trying to escape the 2Dimensionality that comes with the lamination of float glass panels by further specifying the material in novel applications, utilizing emerging technologies and fabrication techniques.

Glass casting is promising, allowing the production of 3Dimensional structural building components with greater shape freedom than that of the laminated components. Characteristic examples are the Atocha memorial (Figure 25), the Crown Fountain, the Optical House and the Crys-

tal House (Figure 26)(Oikonomopoulou, Singh Bhatia, et al., 2020). These projects use repetitive cast glass elements of simple shape and up to 10 kg of mass (Oikonomopoulou, Singh Bhatia, et al., 2020). The mass and shape freedom limitations in these projects relate to the lengthy annealing time and the cost of producing high accuracy steel or graphite moulds.

The research potential of structural applications of cast glass is evident in the plethora of master thesis from (Bhatia, 2019; Damen, 2019; Koniari, 2022; Koopman, 2021; Naous, 2020; Stefanaki, 2020) within TU Delft. The above-mentioned theses focus on novel structural cast glass applications for column, connection nodes in grid shell, bridges, dome and slab respectively (Figure 27, Figure 28, Figure 29, Figure 30). Topology optimization to minimize the mass and the annealing time



Figure 25 : Atocha memorial, cast glass bricks, image source: (Tensinet, n.d.)

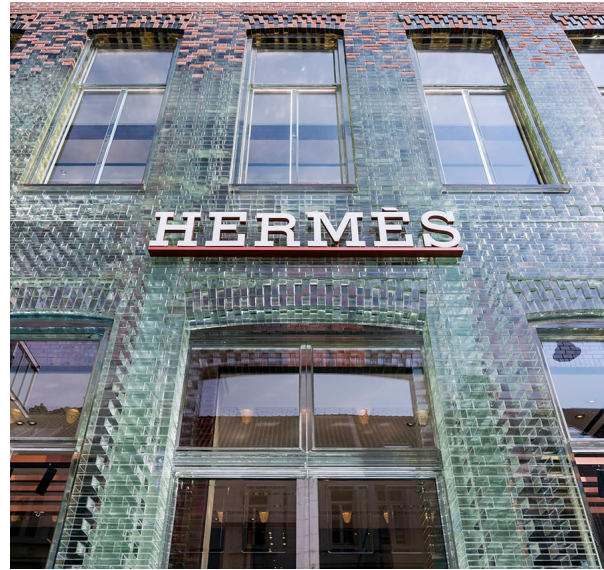


Figure 26 : Crystal house, cast glass, image source: (MVRDV, 2016)

is used in all the examples. The result is a complex and custom shape that escapes the brick-like elements displayed in the previous examples. The shape complexity of the envisioned glass giants requires new and innovative fabrication techniques to be produced in a feasible and efficient way. New fabrication methods for moulds that utilize additive manufacturing and research regarding coatings that are currently used for metal casting display great promise in the production of such components.

Additive manufacturing of glass is new but already displays potential in shape freedom. The structural applications of 3D printed glass elements are limited in scale. The largest scale project is the Glass II (Inamura, 2017a)(Figure 31). This project used 3D printing of glass (FDM method) for the fabrication of several freestanding columns of complex geometry. Due to the size limitations of the fabrication method, the columns are segmented and printed in parts. After the fabrication is complete the parts are assembled and held together with the help of a vertical steel rod running through the column's core (Inamura, 2020). Additive manufacturing of glass with other methods than that of FDM has been explored (Zhang et al., 2021) but so far and to the knowledge of the author FDM displays the greatest potential in structural

application and is the only one with available but limited structural test data (Inamura et al., 2018).

Yet, the lack of established properties and design guidelines, the relative low tensile strength⁶ of glass that is at least an order of magnitude lower than its compressive strength (Oikonomopoulou, 2019) and its brittle nature (that causes spontaneous failure), makes such 3D glass components less favourable for structural applications (Inamura et al., 2018).

6. In Granta EduPack 2021 R2 a tensile strength for soda-lime glass is stated in a range of 30–35 MPa and for borosilicate glass in the range of 22–32 MPa. (O' Regan 2014) reports that the tensile strength of soda-lime glass is 45 MPa.



Figure 27 : Topologically optimized glass column, concept as part of the thesis of (Bhatia, 2019)

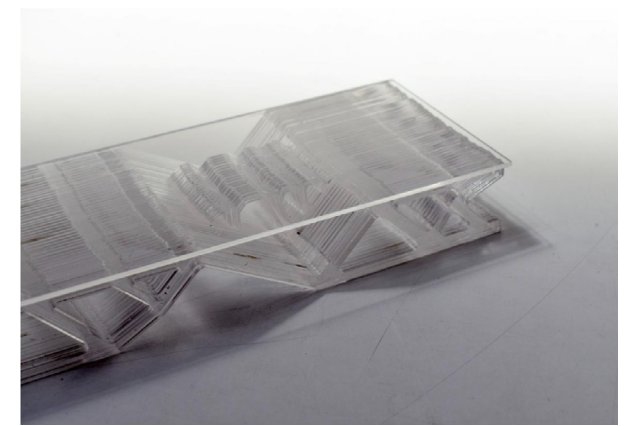


Figure 28 : Topologically optimized glass bridge, concept as part of the thesis of (Koniari, 2022)

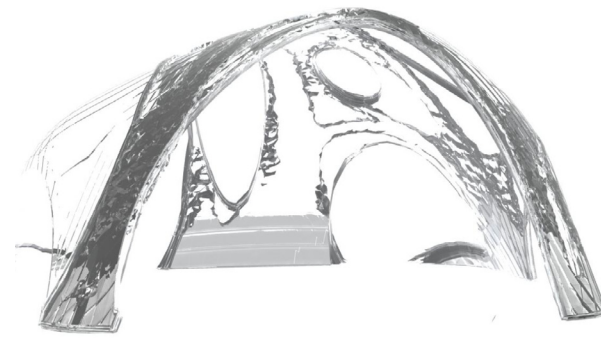


Figure 29 : Topologically optimized glass dome, concept as part of the thesis of (Naous, 2020)

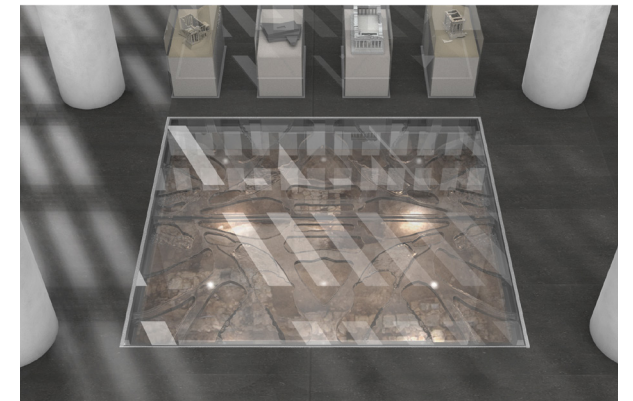


Figure 30 : Topologically optimized glass slab, as part of the thesis of (Stefanaki, 2020)



Figure 31 : Glass II, 3D printed glass column (Inamura, 2017a)

3.7. Challenges

There are two main reasons why we do not see realized examples of glass giants. The first one is linked to the glass peculiarities as a material. The second has to do with fabrication limitations involved in the manufacturing process.

3.7.1. Glass peculiarities

Glass is a brittle material, thus is unable to plastic deformation and failure is sudden, always caused by pick local tensile stresses. Due to its nature, glass requires a lengthy annealing time to properly cool down and avoid any residual stress concentration. The higher the mass or thickness of the cross section of the designed object the exponentially longer the annealing time required. Annealing time increases the cost and energy involved in the process, as the glass objects need to remain at high temperatures and cool down in a controlled manner inside an annealing lehr. To design feasible glass structures the implementation of topology optimization is considered as the most sensible solution.

A set of geometrical limitation imposed by the brittle nature of glass and the annealing time are:

- the homogeneous distribution of mass to allow for even cooling of the object, if parts of the component are considerably thinner can cool down faster shrinking at a different leading to stress concentration and cracking,
- the minimum and maximum cross section to be within a sensible range to allow for annealing on a timely manner and avoid uneven mass distribution,

- sharp corner/ edge should be avoided since they can create pick stresses and cracking of the glass object.

3.7.2. Fabrication limitations

While TO can result in the design of a feasible structures in terms of energy, time and cost, the geometry is highly complex and customized, e.g., TO grid shell node of (Figure 32). Fabricating such shapes introduces a different set of challenges per manufacturing method available for glass. In lamination of waterjet cut float glass would mean lots of waste generation (cut offs) and difficulty in lamination of multiple layers. In casting, the use of a high-precision steel mould would not make sense cost-wise and an existing low-precision disposable mould would imply a lot of post-processing increasing costs, manufacturing time and reducing accuracy. In 3D printed glass size is the main limiting factor.

The advent of additive manufacturing (AM) created new possibilities for more traditional fabrication methods such as casting. A successful example of combined implementation of additive manufacturing (AM) in casting and topology optimization in a structural application is the steel node engineered by Arup. The steel node is part of a tensegrity roof in the Hague designed by ELV Architecten (Galjaard et al., 2015). Most of the nodes in this structure have a different shape and different anchoring points. Production of elements with this degree of complexity using a traditional manufacturing such as welding was considered extremely laborious. That was the driving factor that led to the development of a mass customization process.

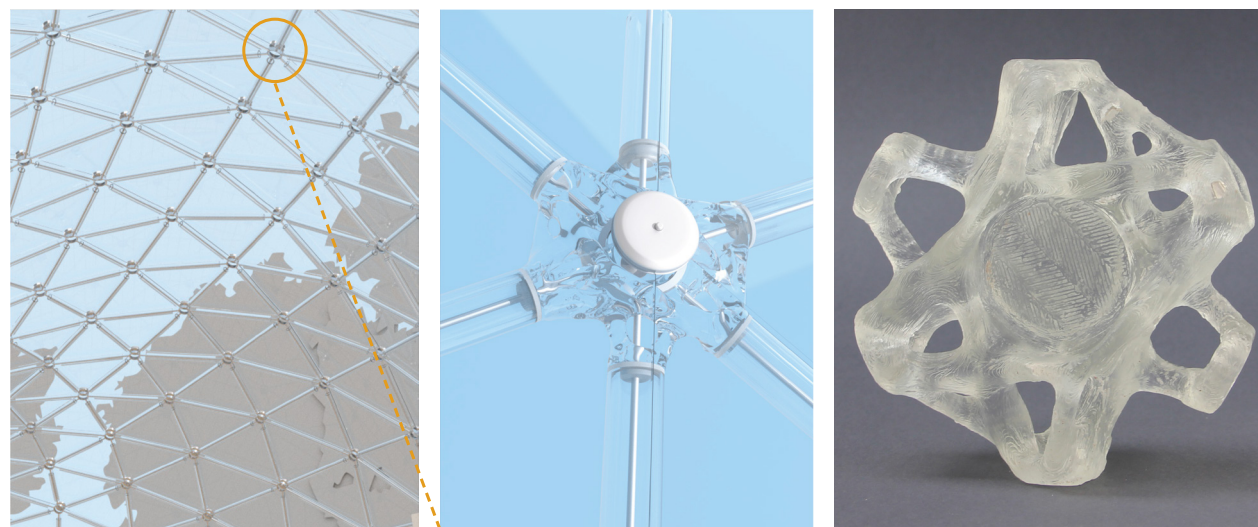


Figure 32 : Intricate shapes generated by TO of glass, grid-shell all glass node (Damen, 2019)

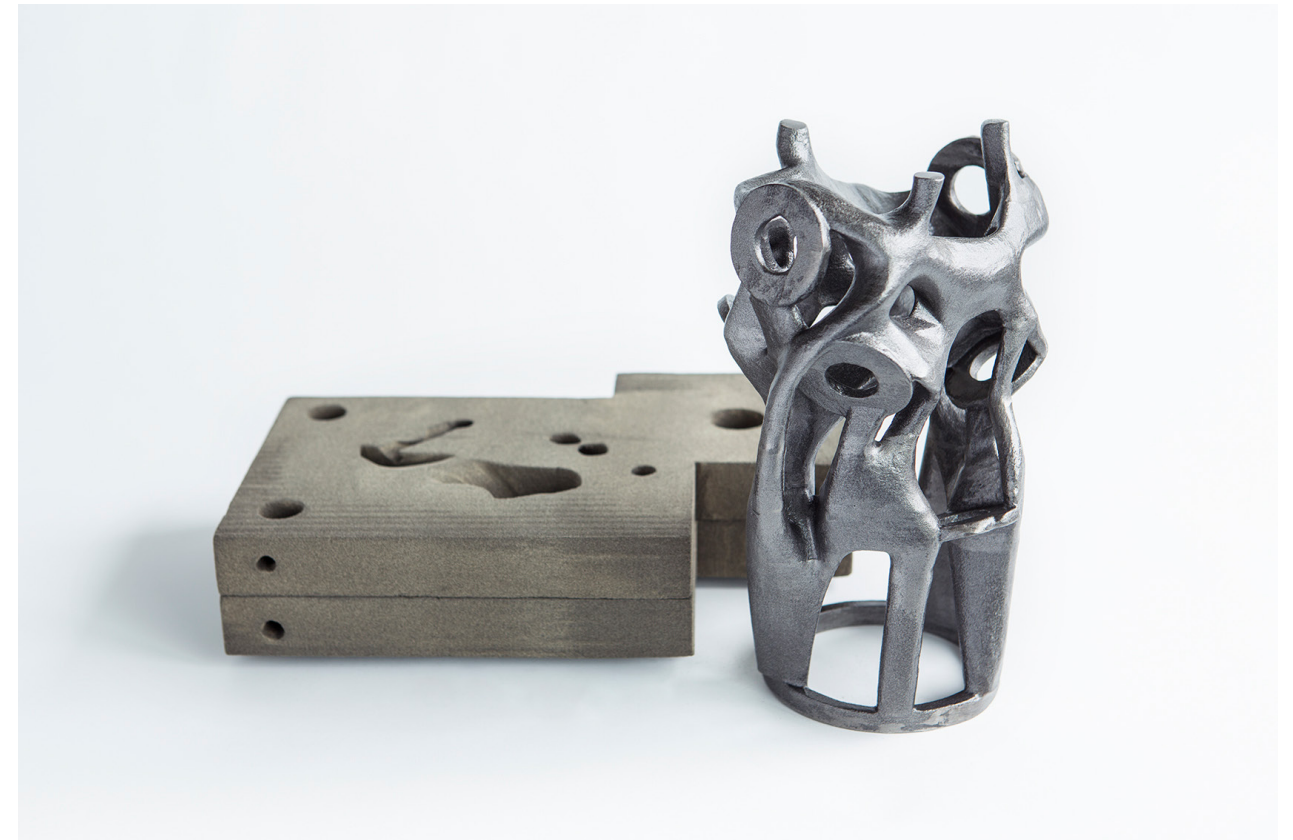


Figure 33 : Topologically optimized steel node cast in 3D printed sand mould (Sand Printing Makes Complex Cast-Structural Parts Affordable - Arup, n.d.) image credits: Davidfotografie

Each of the nodes was topologically optimized resulting in a complex geometry. To produce this geometry Direct Metal Laser Sintering (DMLS) AM (additive manufacturing) method was used. This method at the time was expensive, had no manufacturing standards and no structural data to verify the integrity of the structure. The company came to the realization that a more traditional method was better suited to manufacture such elements.

Casting using 3d printed sand moulds (3DPSCM) combines a standardized fabrication method (casting with sand) with additive manufacturing, allowed the production of the complex shaped nodes in a cost and time efficient way. The standardized production method ensured the structural performance of the elements (Figure 33).

The node example uses metal which is a ductile material that can be optimized using the existing FEM software's. Glass is a brittle material and as mentioned at p.9 requires specialized for mass optimization. Even though the successful implementation of TO and AM paves the way to produce glass with less restrictions and using a more effi-

cient work-flow there are still a lot of challenges. The main challenges are related with the computational skills required, the complexity of the design tools and the time consuming post process of the geometry with the current software available as stated by (Bhatia, 2019; Galjaard et al., 2015).

Dbt group from ETH has implemented 3DPSCM for casting complex and customized shapes in concrete. Prototype A and B are the 2 examples (Figure 36, Figure 39) of topologically optimized slabs casting such moulds (Jipa et al., 2016). Different optimization methods were used in each of the slab.

For prototype A 3 fixed supports are used as boundary conditions. The goal of the optimization was to reduce the material by 80% while minimizing the deformation under uniform surface load. Optimization is done using the free plug-in Millipede for McNeal Rhinoceros⁷. The result for the optimization is a grayscale bitmap which is translated to material distribution. This image is vectorised and extruded arriving at a 3D geometry.

7. Plug-in requires Grasshopper to run. Grasshopper is part of McNeal's Rhinoceros 7 commercial software.



Figure 34 : 3D printed sand mould produces by binder jetting additive manufacturing method, Mould inside sand box, probably after drying.



Figure 35 : Cleaning up the excess sand from the cured 3D printed sand moulds. This mould is used for the fabrication of prototype A.

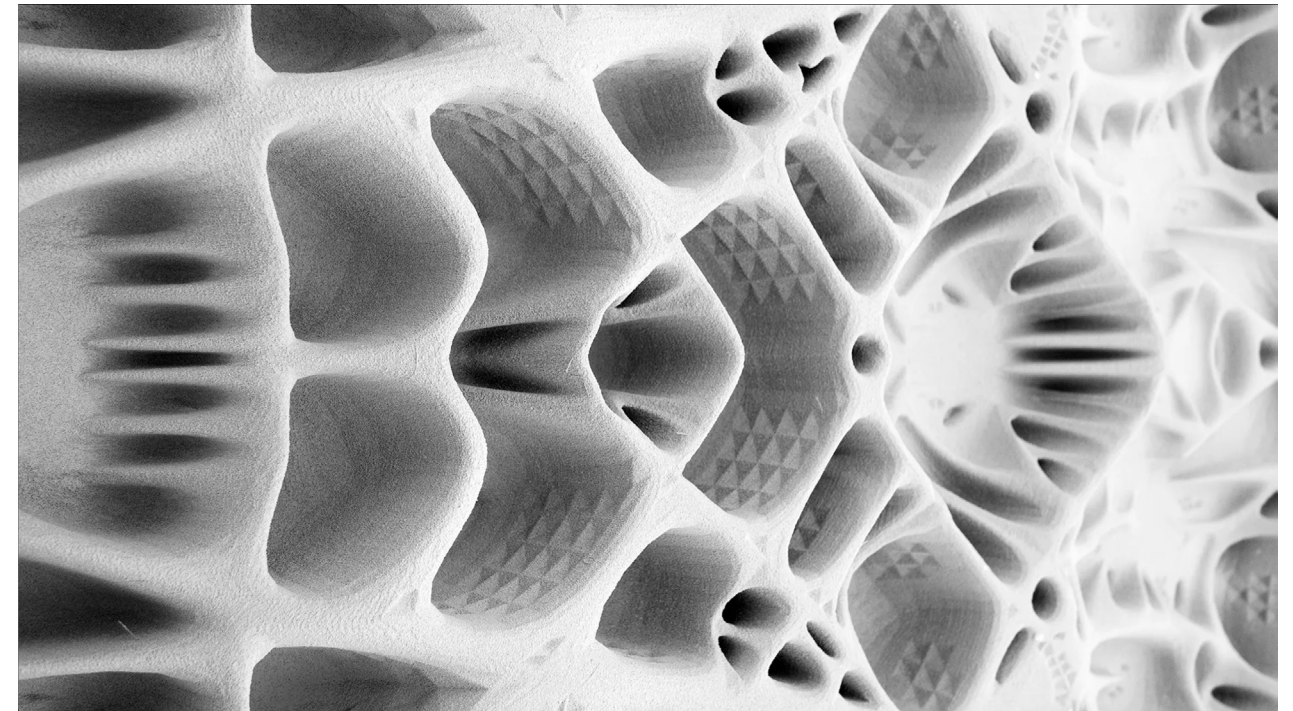


Figure 36 : Final prototype geometry using Ultra-High Performance Fibre Reinforced Concrete (UHPFRC) with steel fibres (Jipa et al., 2016), image source (dbt, 2017).

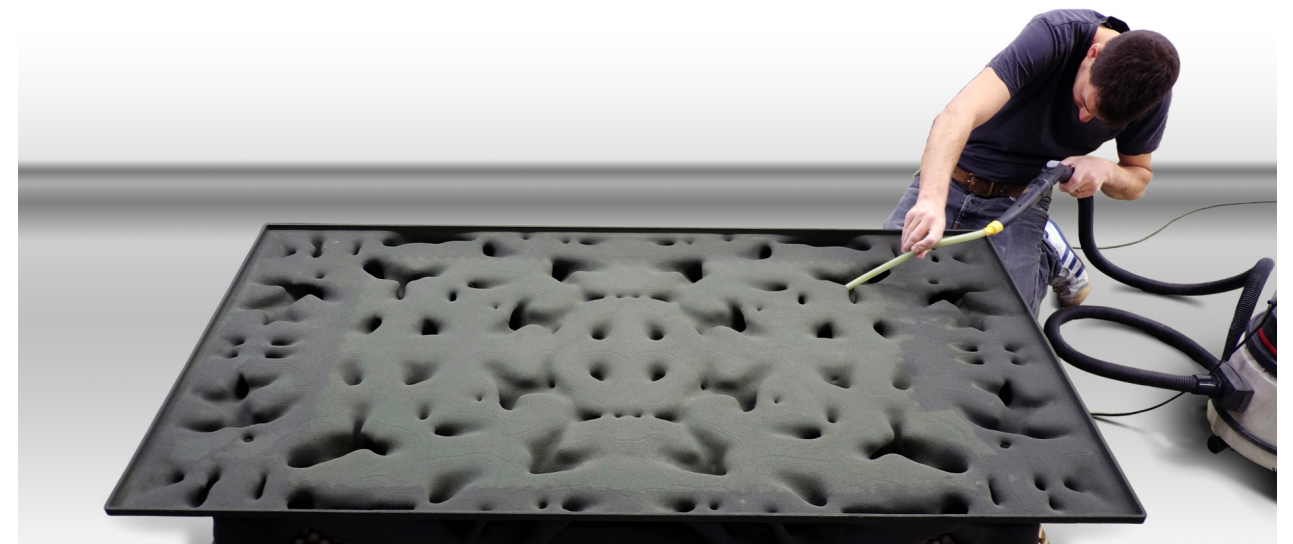


Figure 37 : Removal of unconsolidated sand and infiltration with epoxy resin to increase the strength of the material. Prototype B mould (Jipa et al., 2016)



Figure 38 : Removal of unconsolidated sand and infiltration with epoxy resin to increase the strength of the material. Prototype B mould (Jipa et al., 2016)



Figure 39 : Prototype B as realised (Jipa et al., 2016)

Prototype B has 4 fixed support points. In this case, Simulia ABAQUS⁸ commercial software was used for the topology optimization. The optimization aims at reducing the initial volume by 82% while minimizing the stress in the slab.

In both cases above, the generated geometry is post processed before the moulds are printed. The post processing is based on the fabrication limitations⁹ and to ensure reliable casting¹⁰ (Jipa et al., 2016). This indicates that similar limitations are expected on the fabrication of cast glass elements produced via kiln casting and the use of disposable 3DPS moulds.

3.8. Discussion

This chapter introduced the main challenges involved in the fabrication of “glass giants”. While the material peculiarities can be address somewhat effectively with the current means, fabrication potential remains under-explored. On the following chapters the most prominent fabrication methods are thoroughly analysed based on a set of criteria arriving at a comparative table that highlights the potential and limitations of each fabrication methods for voluminous glass structural components.

The finding will support the choice of fabrication method for the case study and the research on safety leading to the final design.

4

FABRICATION METHODS

This chapter focuses on the different fabrication methods for building components made of glass. There are three fabrication techniques that are within the scope of this thesis: 1) Abrasive waterjet cut and laminated float glass, 2) kiln casting of glass on disposable moulds and 3) 3D printing of glass.

8. Simulia ABAQUS software utilises SIMP(Solid Isotropic Material with Penalization) (see chapter 3.8) algorithm which is considered to be more robust (Damen, 2019; Jipa et al., 2016)

9. Limitations relative to complexity of the geometry such as thin/ fragile elements that can break during casting or narrow segments that will not allow post processing.

10. Radii and cross sections to allow the flow of concrete.

4.1. Abrasive Waterjet (AWJ) cutting of float glass and lamination

Method description

Lamination of AWJ cut elements is a combination of subtractive and additive manufacturing techniques. To produce an AWJ cut laminated float glass structural elements 3 fabrication steps are involved. First the float glass production, then the AWJ cutting of the parts and lastly the lamination.

Starting with the float glass (Figure 41) production starts with the batch. The batch is the glass recipe that most commonly consist of sand, lime, dolomite, soda and sulphate. Glass cullet can be added in the mixture and helps reduce the melting time. Purity of the raw materials and effective mixing are important to ensure homogeneity. The batch is then dropped in the furnace; the furnace contains already melt glass. Flames above the glass surface control the temperature which for this stage is approx. 1550-1600°C. When melting is complete the glass moves at the end of the furnace where its temperature is reduced via a constant flow of cold air from 1400°C to 1100°C. This step prepares the glass for the next step, the float tank. Glass is poured in a molten tin pool. Glass at this point has similar viscosity to honey and spreads evenly, forming a flat sheet of glass. Edge rollers adjust the width of the of the glass sheet. Flow at the entrance of the float tank and the edge rollers on the sides control the thickness of the glass pane. The float glass leaves the float bath at 600°C. At this point it is solid enough and can glide on top of metallic roller. The next step is the Lehr. The Lehr allows for glass to anneal gradually. Lehr is split in 2 parts. The first is the annealing zone where the

permanent stress are fixed (600-480°C). While glass is above the annealing point (approx. 525°C for soda-lime glass (Shelby, 2005)) viscosity allows for molecular rearrangement and release of any internal stress. The second part is the cooling zone. Glass exits this zone at approx. 80-50°C. Finally, glass edges are trimmed, and glass is inspected for any flaws. Flawed parts are aromatically rejected, crushed and used as cullets in the batch. The rest of the glass panes are cut to size and stored. As both surfaces are fire finished, they need no grinding or polishing (Saint-Gobain, n.d.).

Next step is the AWJ cutting of glass. Literature suggests that glass is first cut with the use of AWJ and then laminated. Tempering is performed after cutting as it is not possible to cut heat-strengthened or tempered glass using this method. AWJ cutting of laminated glass is possible but can lead to loss in accuracy and increase in cutting time compromising the cost and the quality of the final product (ShivajiRao & Satyanarayana, 2020). Abrasive waterjet cutting is a subtractive manufacturing technic that uses high pressure water jet combined with abrasive material to cut material in sheets. A computer-controlled head and nozzle with up to 5-axis allow for precise cutting under different and varying angles. AWJ cutting can cut between a broad range of materials from metals to stone and glass. For each material different setting for the pressure, the abrasive size and flow rate are used for optimal cutting and surface quality of the edge (ShivajiRao & Satyanarayana, 2020). AWJ cutting of glass panes can led to rough or non-perpendicular edges (kerf angle) that require post processing to avoid stress concentration and premature failure of glass.

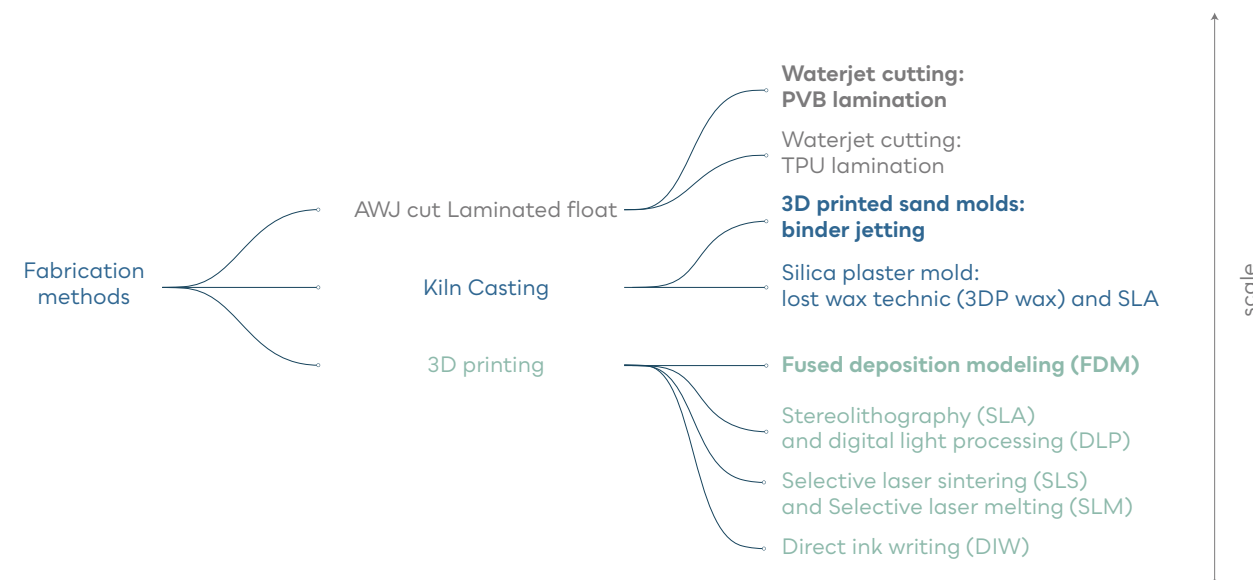


Figure 40 : Fabrication methods for glass within the scope of this thesis.

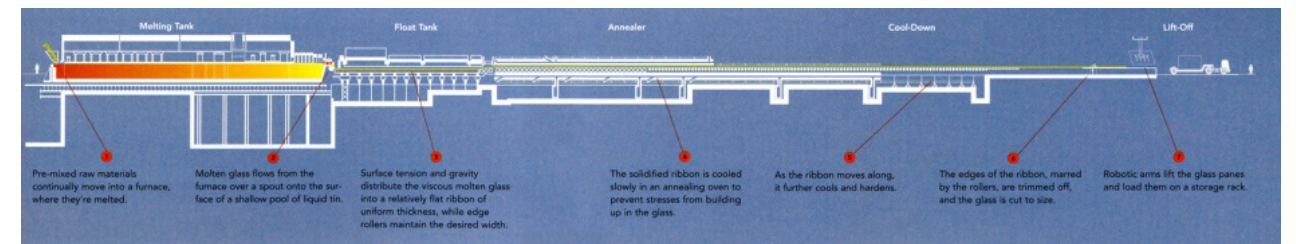


Figure 41 : Float glass production line (Corning museum of glass, 2011)

Common water jet cutters have a 3-axis head that can only move in X,Y and Z axis. The most advanced machines have 5-axis heads (Figure 43). Additional axis are A-axis for perpendicular movement and the C-axis for rotation around the Z-axis (Figure 42). 5-axis machines are more accurate, have improved cutting speed, more versatility in angles and complex geometries and can reduce the kerf angle¹¹ (Jet Edge, n.d.)

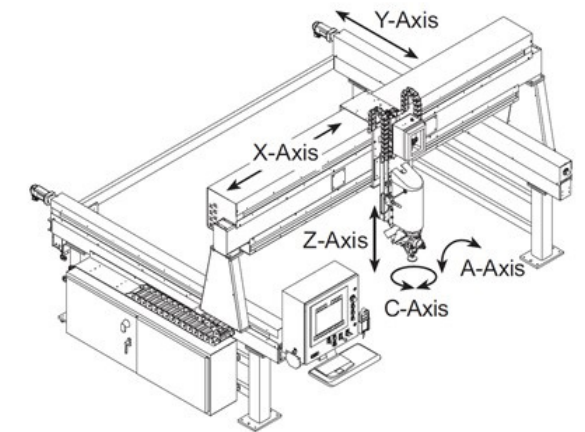


Figure 42 : Axis of waterjet cutter (Jet Edge, n.d.)

Finally, the lamination stage. Before this stage, tempering of the glass can occur if applicable. Sheet lamination is one of the 7 different categories of additive manufacturing according to the (ASTM F42) (American society of testing and materials, n.d.). In lamination polyvinyl butyral (PVB) is most widely used interlayer due to its high light transmittance, mechanical strength, good adhesion to glass and cost (Yang, 2021). Other interlayers such as SentryGlass® and polyurethane (PU)¹² are used depending on the desired design application. Interlayer is in the shape of rolls of 0.38 mm or 0.76 mm, thicker interlayer can be achieved by applying 2 or more layers (Centre for the Protection of National Infrastructure, 2019). Glass plies are washed, centred and stacked (Figure 44,45). During the stacking phase the interlayer is laid between 2 or more lites of glass. The glass is then heated and pressed to remove trapped air and seal the edges for the autoclave. Lastly the piece enters the autoclave where under pressure and heat (up to 12 bars and between 135-145°C for PVB) the lamination is complete (Olabisi & Adewale, 2015).

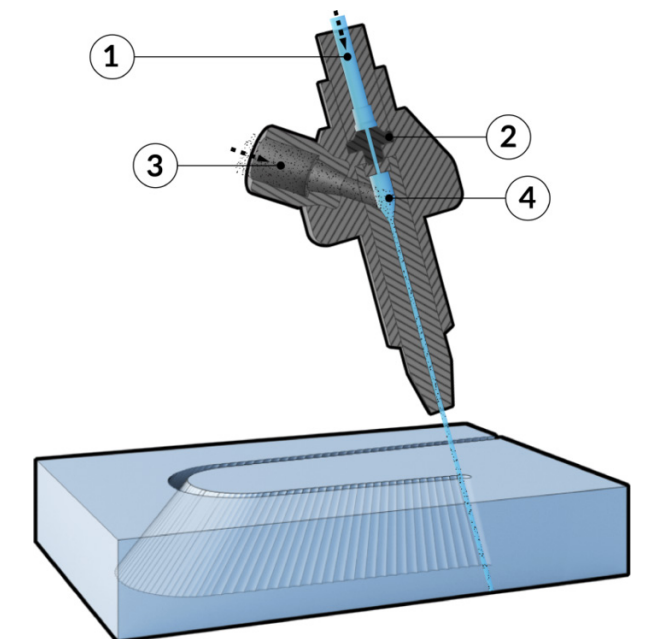


Figure 43 : 5 axis AWJ head, (<https://www.manufacturingguide.com/en>)

11. "Kerf is defined as the difference in the amount of material removed from the top of the specimen to the bottom along the thickness. The angle that defines the kerf width along the thickness is referred to as kerf angle" (ShivajiRao & Satyanarayana, 2020)

12. PU offers high tensile strength, toughness, resistance to UV, abrasion and chemical degradation but comes at a higher price (Martín et al., 2020). It is primarily used for safety and ballistic resistant glass applications.

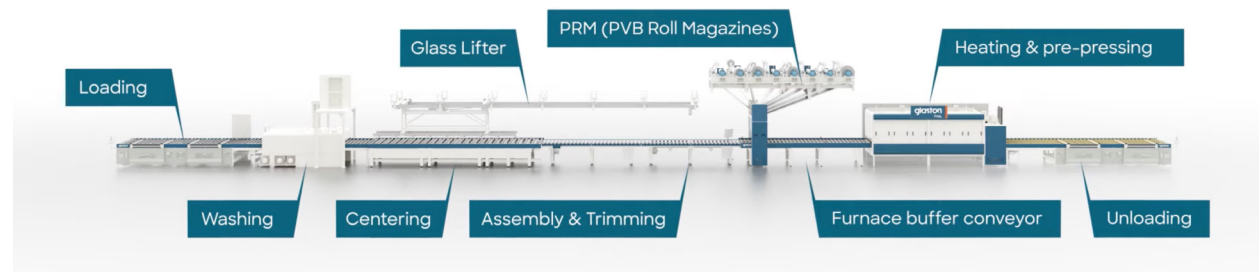


Figure 44 : Lamination process, (glaston, n.d.)



Figure 45 : Lamination of a 20 m.. long piece of float glass, <https://www.sedak.com/en/skills/laminating/>

Potential

The mechanical properties and the failure behaviour of laminated components is well documented and proved in the built environment. Structurally wise glass elements fabricated with this method have increased safety and predictable post failure behaviour due to the number of layers and the adhesive nature of the interlayer. Such structures are serviceable after failure. Optical wise the transparency of the component depends on the orientation of the layers in combination with the viewing angle. The finishing quality of the components is good due to the high standards of the float glass industry. Laminated components can be easily connected with other glass elements of other structural elements by embedding metal plates and/or special connections between the interlayer and require minimal post processing.

Limitations

Sustainability wise laminated building components are hard to recycle due to the interlayers that require additional effort to remove and can lead to contamination of the glass. During the waterjet cutting a lot of glass is discarded in the form of cut-out pieces which makes the method less material efficient. AWJ cutting can introduce edge flaws resulting in need for post processing. There are

also some fabrication limitations connected with the shape freedom and size governed by the glass panels and autoclaves dimensions and the lamination process requirements. For example, there is a practical limit on the number of glass layers that can be laminated together, typically not exceeding 5-7. Finally, the complex fabrication method adds cost to the final product.

Applications (Built examples/ references)

Structural glass building components built with this method have been realized early on. As seen in the previously described example Centre Administratif (1995), Yurakucho canopy (1997), Apple store on the 5th Avenue (2005, 2011) and more recently the all-glass walkway at Bründl Sports Flagship Store (2021).

Bründl Sports Flagship Store (2021) (Figure 46) is a ski rental retail center located close to the Kaprun ski resort in the Austrian Alps. The centre was design by Blocher partners and engineered by Seele. The most prominent feature of the building is the 10 m. long all-glass walkway that allows for the unobstructed view of mountains and river. The main structural elements are made from 6 layers of 12 mm heat strengthened laminated float glass with total dimensions of 11 by 1.8 m.

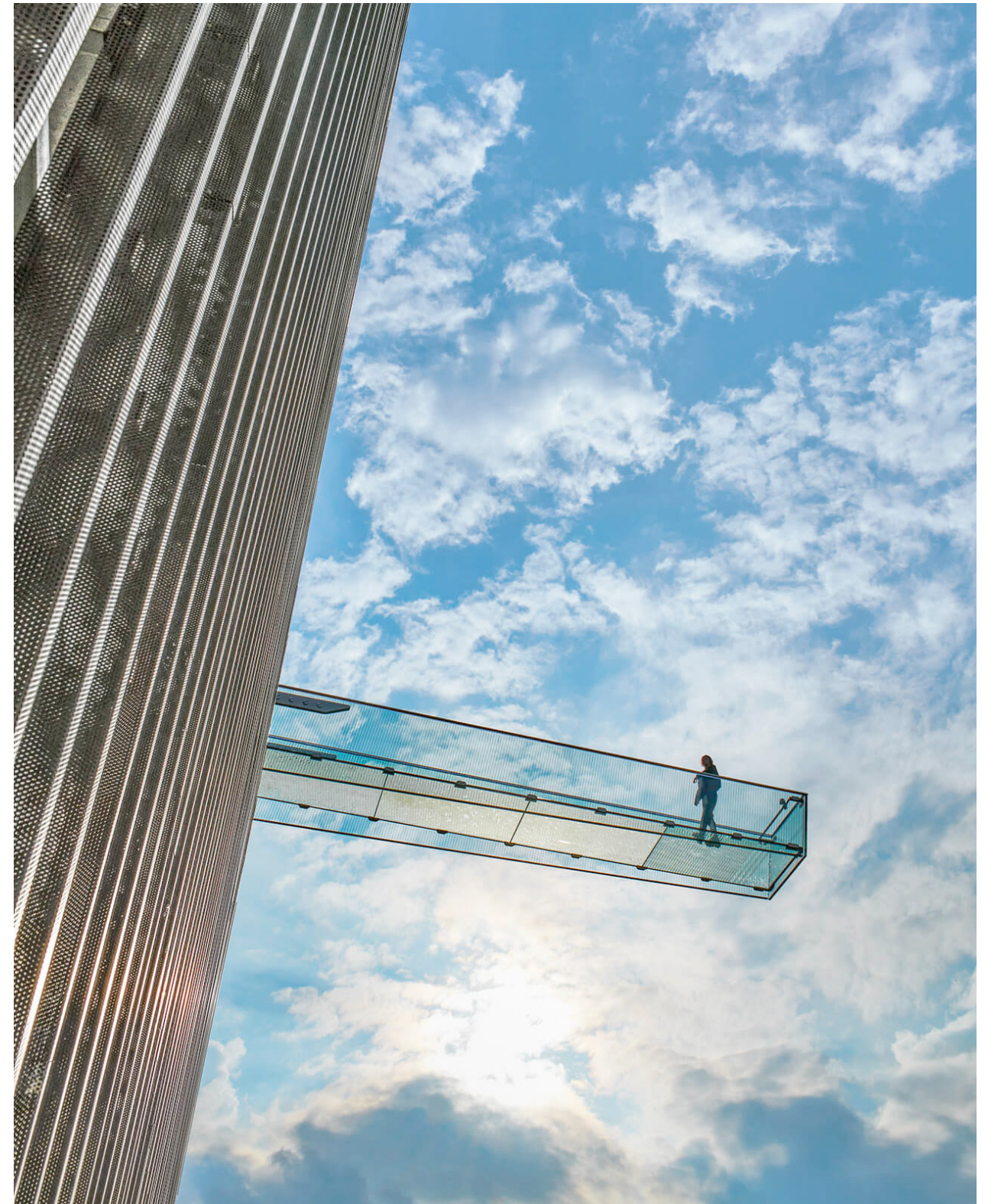


Figure 46 : Skywalk for Bründl Sports, (seele, 2021)

Placed at the sides of the walkways these elements act both as the support for the cantilevering walkway and as fall protection. They are fixed to the building using stainless steel tension fasteners at the upper part and rest against supports on the lower part (seele, 2021).

This example is a great source of inspiration since it highlights the possibilities of all-glass structures. While it lacks the shape complexity seen on the Yurakucho canopy, it validates safety and feasibility for glass, opening possibilities towards topologically optimized cast glass structural components.

4.2. Glass casting

Method description

Casting is one of the oldest glass shaping techniques. Recent developments in fabrication methods allow for a hybrid utilization of the well tested techniques of the past and new means such as additive manufacturing, enhancing the fabrication potential, alleviating previous limitations and restrictions.

Casting can be primary or secondary (Figure 47-48). Primary casting refers to the formation of glass from its raw ingredients (Cummings, 2002). The most common way to work with primary casting of glass is by hot-forming (melt-quenching). In secondary casting solid glass is used in various shapes (i.e., sheets, rods, marbles, grains, powder, cullets). Glass parts are heat up until they melt and flow into the shaped mould (Cummings, 2002). The most common shaping technique for secondary casting is kiln casting. Apart from the initial material difference, primary casting of glass requires two ovens, one for melting and one for annealing of the glass, whilst in secondary casting firing and annealing happen at the same oven.



Figure 47 : Primary casting or hot pouring (top), image credits: Marcel Bilow. Secondary casting or kiln casting (bottom) (Oikonomopoulou, 2019)

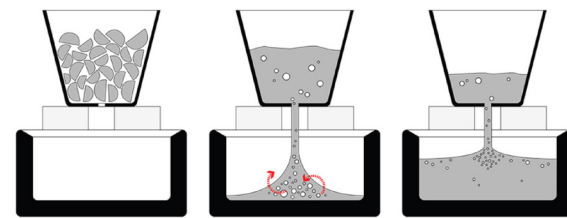


Figure 48 : Kiln casting process using a flowerpot filled with glass pieces that when melt flow through the hole at the bottom filling the mould with glass (Oikonomopoulou, 2019).

Firing temperatures are usually lower for secondary casting since the glass is already formed. Firing allows for melting and homogenization between the glass interfaces of the solid cullets. In secondary casting the solid glass parts are placed on a separate pot on top of the mould that has a hole at the bottom. When temperature is above softening point, glass melts and flows through the hole in the mould. Depending on the desired geometry and if the mould is open on one end (e.g., beam, cube) the mould can be designed with some extra space at the top. The mould is filled in with glass parts and some extra material is placed on top to account for the gaps. In that case the glass melts and from the effect of gravity fills the desired shape without the need of a separate container (pot).

Potential

Among the merits of cast glass are:

- high level of non-directional transparency (Figure 49),
- recyclability,
- zero glass waste,
- homogeneity
- and lower firing temperatures than float glass.

Limitations

On the downside cast glass elements require a lengthy annealing process. Annealing time plays a significant role when casting glass. Glass requires adequate time to allow for proper annealing and release of any residual stresses. Internal stress relief is a function of viscosity. The higher the viscosity the lower the probability for molecular rearrangement that leads to stress release. Strain point is the temperature below which any stress is considered as permanent (Watson, 1999).



Figure 49 : Transparency of cast glass as seen in the facade of Crystal House (MVRDV, 2016)

Based on information provided by the manufacturer (Bulls-eye Glass, n.d.) for thick float glass slabs (Koopman, 2021) in his MSc thesis arrives at Equation 1 for annealing time in cast glass:

Equation 1:

$$T = 0.0156 \cdot t^2 + 0.139 \cdot t + 0.7266, h.$$

T : Time in hours

t : Thickness in mm

In this first approximation is noticeable that the annealing time exponentially increases with the thickness of glass. A typical example in cast glass are the telescope banks (figure 1) which confirm the link between annealing time and mass, max. thickness and mass distribution. (Equation 1) is a good first approximation but is based on data for glass panels that are cooled from top and bottom side at the same time.

More complex shape cast glass elements require a somewhat more elaborate approach on the annealing time calculation. (Koniari, 2022) used a formula defined by (Hubert, 2015) which considers material properties and allowable residual stresses.

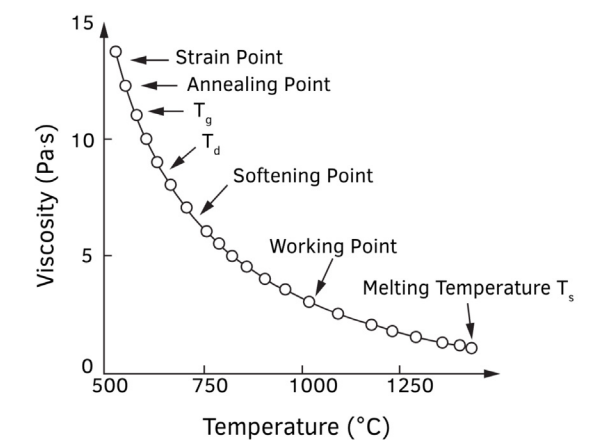


Figure 50 : Typical curve for viscosity as a function of temperature for a soda-lime-silica melt (NIST Standard No. 710). Defined viscosity points are indicated on the figure. Source:(Shelby, 2005).

Equation 2:

$$h = \frac{\sigma}{E\alpha_{ex}\rho c_p d^2 b (1-\mu)\lambda}, \text{K/s}$$

where:

σ : allowable permanent stress

d: characteristic dimension, radius in case of a sphere

b: shape factor

E: Young's modulus of the material (MPa)

α_{ex} : thermal expansion coefficient (K⁻¹)

ρ : density (kg/m³)

c_p: specific heat (J/(kg*K))

μ : Poisson's ratio

λ : thermal conductivity (W/(m*K))

(Equation 2) defines the cooling rate in °K/s and confirms the assumption of (Equation 1) (the bigger the characteristic dimension, thus thickness of glass elements, the cooling rate is exponentially slower). The advantage of this formula is that it can discern between distinct types of glass¹³.

Another limiting factor in kiln cast glass is the mould. The surface of the mould that is in contact with glass can lead to roughness and reduced accuracy. Open and pressed mould (Figure 51) made from steel or graphite can achieve high surface quality and accuracy but are costly and better suited for large production volume with hot pouring method (Bhatia, 2019; Koopman, 2021; Oikonomopoulou, Bhatia, et al., 2020). While the resulting surface quality using the later moulds is superior to the former, high geometrical complexity can also

be a challenge.

Literature study and previous experiments highlight multiple benefits in the use of disposable moulds over permanent, steel moulds, for the fabrication of customized kiln cast glass. Steel or graphite moulds are expensive and require advanced CNC methods for bespoke shapes (Oikonomopoulou, Bhatia, et al., 2020; Oikonomopoulou, Bristogianni, Barou, Veer, et al., 2018). Thus far, disposable moulds (silica plaster though investment casting/lost wax technique and 3d printed sand moulds (3DPSM) fabricated with binder jetting) require post processing to achieve optical transparency and good surface quality (Oikonomopoulou, Bhatia, et al., 2020). Some lesser issues regarding shape limitation relate to the use of disposable moulds.

Applications (Built examples/ references)

Complex shapes of cast glass are often seen in sculptures. Characteristics examples are the airy forms by Karen La Monte (Figure 52). Other examples are the solid glass sculptures from Roni Horn (Figure 53) (e.g., Water Double, v.1 with a height of 132 cm and diameter of 134 – 142 cm (Hauser & Wirth, n.d.).

The largest manufactured monolithic piece of cast glass is the Giant Magellan Telescope with a diameter of 8.4 m and thickness of 894 mm. The telescope blank was cast on a Silica-alumina fibre mould and annealed inside a custom revolvinglehr for 3 months (Oikonomopoulou, 2019; Zirker, 2005).

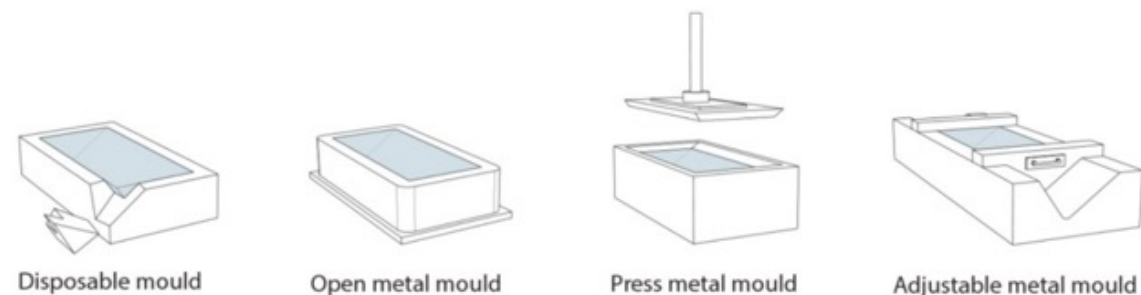


Figure 51 : Different types of moulds as described in the work of (Oikonomopoulou, Bristogianni, Barou, Veer, et al., 2018)

13. e.g., borosilicate glass has lower thermal expansion coefficient (3.1 – 6 * 10⁻⁶ /K) than soda lime (9 * 10⁻⁶ /K) and can be annealed at ~50% of the time needed for soda lime glass (according to EN572-1:2004)



Figure 52 : Reclining Dress Impression with Drapery, 2009, (48.3 x 154.9 x 57.2 cm), Smithsonian American Art Museum, © Karen LaMonte



Figure 53 : Water Double, v.1, © Roni Horn, image credits: © Ron Amstutz

4.2.1. Kiln casting of glass on disposable moulds

3D printed sand moulds: binder jetting

Method description

Traditional sand mould technique requires two positive halves. The positive halves are imprinted on a sand bed producing the two negatives of the object. The two parts are combined with the addition of vents and pouring basin into the final mould.

Binder jetting is one of the seven different categories of additive manufacturing according to the ASTM (American society of testing and materials) (ASTM F42). The 3D model of the object is digitally sliced into layers (1). For each layer, a thin layer of fine sand is applied on the printing table where a liquid binder agent is selectively applied by a computer-controlled head. The process is repeated until the object is complete. By applying binder only on the negative of the object the final mould is produced (2). After this the printing box containing the print and the excess sand is placed in a microwave oven for drying (ExOne, 2021). Microwave drying usually takes 15-45 minutes and it is considered better than a conventional oven as requires less time and allows for more reliable drying from the inside out (3). Excess sand is then removed at first using an automated process (4) and fine de-sanding is performed manually with the use of pressurized air (5). Moulds are then inspected and stored at a dry environment. Excess sand is reused for future moulds.

Potential

The biggest advantage of the 3DPSM is their relative low manufacturing cost, high level of precision and size accuracy¹⁴ and relative low production time¹⁵. In theory the recovered sand from the moulds can be reused or recycled creating a more circular fabrication cycle.



Figure 54 : Production process of 3DPSM according to (ExOne, 2021)

14. +/- 0.1 mm as reported by Arup Amsterdam, subject to the grain size used (Oikonomopoulou, Singh Bhatia, et al., 2020)

15. From a few hours to some days (Oikonomopoulou, Singh Bhatia, et al., 2020)

Limitations

The production of 3DPSM has several limitations. Due to the need for material removal after casting and support of the mould fully closed cavities are not possible. The thickness of the mould walls must be adequate to be able to withstand the hydrostatic pressure build up during casting. Sharp corners must be avoided to ensure that no air bubbles or unfilled volumes are present during casting. The filleting of the radii ensures also that no stress concentration is created on the final component (limitation of the material as well as the fabrication technique).

Even though it is not technically required in terms of fabrication method, splitting the mould in pieces helps with the release of the object after casting and allows for the homogeneous application of surface coatings. Surface coatings are necessary due to the rough surface of the mould and the tendency of sand particle to merge with the glass surface after casting (Bhatia, 2019; Damen, 2019; Giesecke & Dillenburger, 2022; Oikonomopoulou, Singh Bhatia, et al., 2020)

Applications (Built examples/ references)

Companies such as 3Dealize, Concr3de, Voxeljet and ExOne have already utilized the technology in casting metal objects of complex form. As seen in the example of the steel node engineered by Arup.

Glass casting in 3D printed sand moulds has been tested in the MSc thesis of (Bhatia, 2019) and of (Damen, 2019). The former has tested different coatings to improve surface quality. The result while encouraging need a lot of manual post processing (polishing) to account for the surface roughness. Some additional testing with different coating has been done by (Giesecke & Dillenburger, 2022) but the most promising coatings has been tested for foundry casting (hot pouring) and not for kiln casting. Yet, structural performance of the elements produced have not been tested on

Table 3: Comparative table between different binders for 3D printed sand moulds ((ExOne, 2023)

Binder type	FURAN Cold-Hardening Binder System	CHP Cold-Hardening Binder System	HHP Hot-Hardening Binder System	INORGANIC Inorganic Binder System
Hot strength	5-8**	7-10	9-10	3-4
Filigree character	5-6	10	7-8	8-9
Strength	7-8	8-10	9-10	5-6
Environmental impact	3	6	5	10
Finishing	3	10	7-8	9

Characteristics dependent on precise sand and binder combination. Scale is 1-10, with 10 indicating most ideal conditions ** with additive

cast glass produced via this method.

There are different binders used to produce 3d printed sand moulds. According to (ExOne, 2023) the 4 types of binders used in the production of the moulds are:

- Furan,
- CHP,
- HHP and
- Inorganic (referred also as Anorganik (Oikonomopoulou, Bhatia, et al., 2020)

Previous research by (Bhatia, 2019; Giesecke & Dillenburger, 2022; Oikonomopoulou, Singh Bhatia, et al., 2020) shows that CHP and Inorganic binders are better suited for the kiln casting being able to withstand heat up to 900°C for a prolonged period of time without losing their binding capabilities. The use of 3DPSM bound with inorganic binder for hot pouring of up to 1200°C is also confirmed by experiments at ETH.

CHP binder is a phenolic binder. In the research work of (Bhatia, 2019) after firing the colour of the



Figure 55 : Prototype of topologically optimized glass column. The prototype was produced using 3DPSM at the glass lab at TU Delft (Bhatia, 2019)

binder evaporated and the mould could easily be scratch but remained intact. The size of the test sample was small so for casting of bigger items this might be an issue. Inorganic is a water glass binder. This type of binder displays no change after firing and is hard to scratch showing promise for casting of larger components. From Table 3 we can conclude that inorganic is the best binder in terms of environmental impact and finishing quality.

Coatings can be applied to the mould ensuring a better surface quality, higher transparency and reduced roughness. Foundry casting experiments conducted by (Giesecke & Dillenburger, 2022) using 3DPSM fabricated with CHP and Inorganic binders and coated with a combination of Zirko-fluid and graphite-water dispersion yielded promising results. Experiments on kiln casting using same 3DPSM by (Bhatia, 2019; Oikonomopoulou, Bhatia, et al., 2020) at TU Delft indicate that crystal cast has good results. Further experimentation on 3DPSM with the above-described binders and combinations of the most promising coatings is part of this thesis.

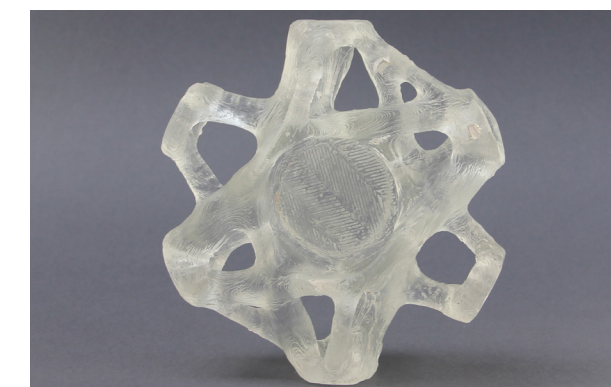


Figure 56 : Prototype of topologically optimized grid shell node fabricated using the lost wax technique (3d printed wax positive and silica plaster negative for glass casting) (Damen, 2019)

KILN CASTING @ 900 °C



FOUNDRY CASTING @ 1200°C



Figure 57 : The use of various coatings for glass casting on 3DPMSM , edited from (Giesecke & Dillenburger, 2022)

Kiln casting: lost wax technique/ 3DP wax based filament and SLA

Method description

Investment casting with the lost wax technique is one of the oldest known metal-forming techniques dating back to the 3rd millennium B.C. A positive wax model of the desired geometry is created. The positive wax model is then dipped or cast around with clay or other material. The object is left to solidify and dry. After drying the mould is placed in the oven and fired burning the wax away, leaving the negative imprint of the shape. The mould is then ready to be cast. After casting the mould is broken to release the cast object. Due to the nature of the mould material the cast element requires post processing and cleaning to improve surface quality.

Potential

Traditionally the positive wax model had to be made manually. Recent research shows the possibility of 3D printing using wax-based filament (Wax Filament, n.d.) with the FDM^m (fused deposition modelling) method. The 3d printing object produced by FDM^m method can have an infill pattern on the inside reducing the material needed (compared to solid wax) as current research by the glass group at TU Delft displays. The bigger advantage of the 3d printed wax technique is the accuracy when compared to traditional lost wax technique or other methods such as the use of foam that can be later removed. Another advantage is the ability to use a computational work-flow that

allows for flexibility and ease in adjustments simplifying the work flow. Using SLA^m (Stereo-lithography Apparatus) method to print the positive of the mould can result in greater accuracy and better surface definition in the final product (Glass group TU Delft). SLA^m uses a vat of liquid photo-polymer resin that is selectively cured under light emitted by a computer-controlled laser system. The parts of the resin exposed to the light polymerize turning into solid parts (American society of testing and materials, n.d.).

Limitations

The most common material for investment casting with the lost wax technique is silica plaster. Silica plaster (Crystalcast) has low manufacturing cost but comes with some major shortcoming as it has low level of precision and low max. firing temperature (around 1000°C)(Oikonomopoulou, Singh Bhatia, et al., 2020). The mould material is brittle; thus, it is recommended only for kiln casting. Other limitations connected with this technique are the edges radii and the need for open cavities to allow for removal of the mould material after casting.

Applications

Application of this method has been tested by the glass lab team at TU Delft. Complex shape, such as the dinosaur in the figures, was tested to understand the difference between printing methods and to study the surface quality effect on the mould.



Figure 58 : Example printed with FDM method and wax-based filament (top). Layering is visible at the mould after the firing of the wax-based filament (bottom). Photo credits: Anna Maria Koriari (2022).

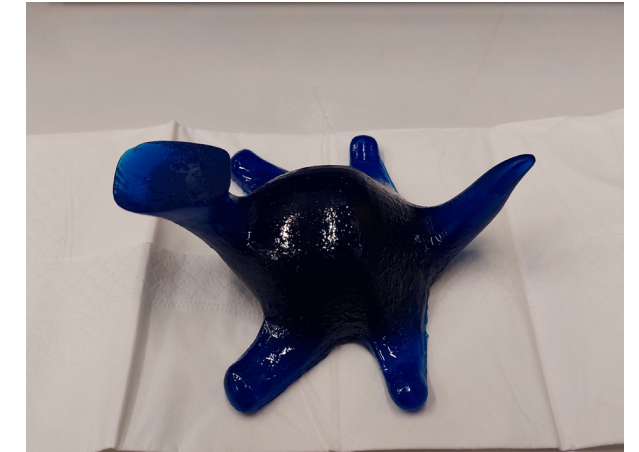


Figure 59 : Example printed with SLA on wax-based photosensitive resin. Smoother surface with no visible layering. Photo credits: Anna Maria Koriari (2022).



Figure 60 : Accuracy of the FDM printer is lower at around 1-2 mm which creates a visible pattern on the mould surface after the wax is burned off.

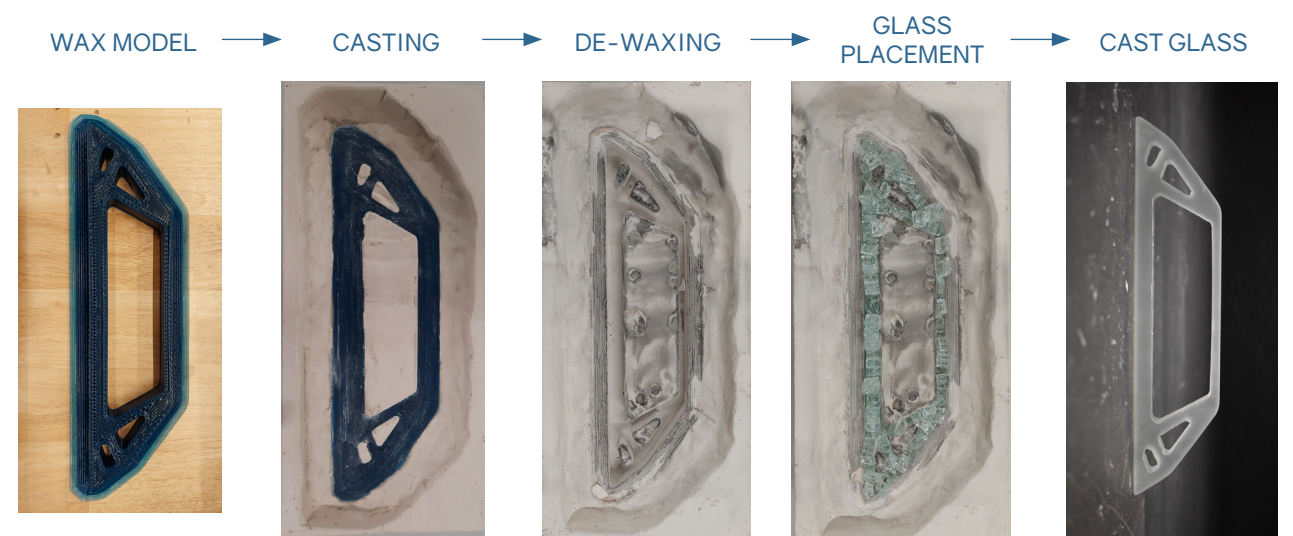


Figure 61 : Accuracy of the FDM printer is lower at around 1-2 mm which creates a visible pattern on the mould surface after the wax is burned off.

While unfortunately the glass dinosaur negative mould was not cast it gave a good insight on how to set up the printer. Printing using wax-based filament is challenging as it requires specific settings (nozzle temperature and speed), bed heating and can sometimes result in warp geometries while printing.

After the above-mentioned tests two sets of topologically optimized beams were printed on wax based filament using FDM 3d printing. The wax printed were then used to make silica plaster moulds implementing the lost wax technique. The process involves printing the wax positive of the mould, casting on Crystalcast, drying, de-waxing by heating in the oven, placing the glass and placing the mould again in the oven for kiln-casting and finally get the end up with the glass piece (Figure 61). This process is more laborious than the use of 3DPSM and involves a lot of steps, the use of an oven two times(once for de-waxing and one for kiln casting) and has high waiting time for printing and drying. The glass components produced via this method required polishing and grinding to achieve a better surface quality.

4.3. 3D printing of glass

(categorized as in (Zhang et al., 2021))

The advent of additive manufacturing in glass allowed for 3D printing of glass components with a variety of ways¹⁶ opening new possibilities for complex shaped glass elements. Each method comes with its own set of advantages/ disadvantages and is suitable for different kind of applications. In this sub chapter these methods are briefly presented to give an idea about the current state of each of the different AM methods of glass.

4.3.1. Fused Deposition modelling (FDM)

Method description

Fused deposition modelling or FDM has been invented and patented by Stratsys company(Zhang et al., 2021). In general, this method is based on continuous filament feeding through a computer-controlled heated nozzle. The head moves within the printable volume, depositing material layer by layer on the printer's bed (Figure 63). The nozzle and or the plate can move around within the printable area.

Micron3DP and MIT (MIT News Office, 2015) developed a system for printing silica glass. The G3DP is the first model developed and is extensively presented in the master's thesis of (Klein, 2015).

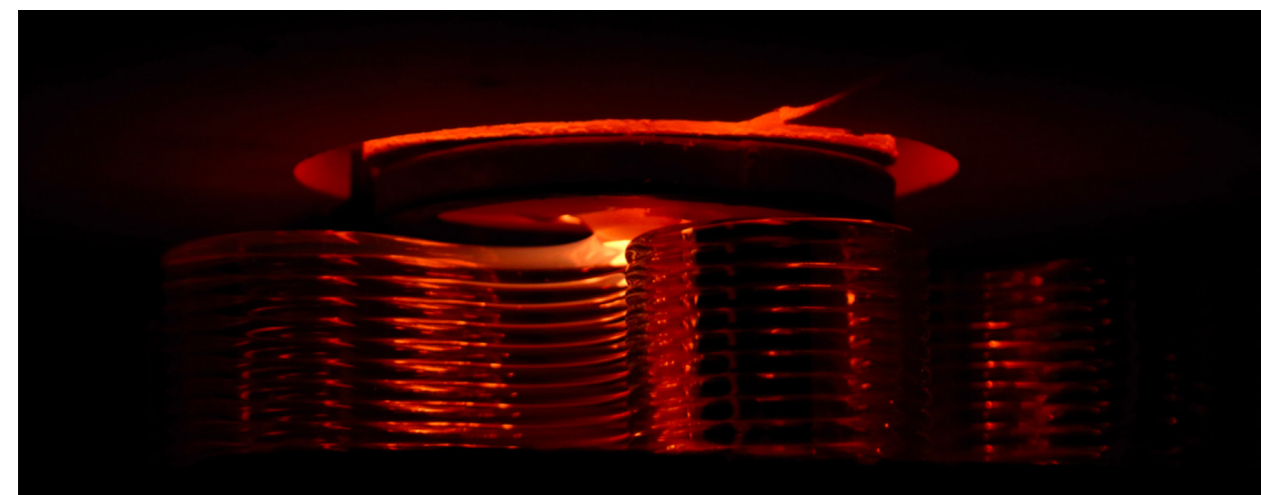


Figure 63 : FMD 3D printing of glass in the making (Inamura, 2017b)

The second iteration, the G3DP2, allowed for more accurate prints and improvements in speed and printable volume. The development of this printer was part of the master's thesis of (Inamura, 2017b).

Since glass requires a controlled annealing process, adjustment to the FDM technology was necessary. The set-up has improved over the years, but the main principal remains the same. There are two main elements in this system. The Kiln cartridge and the print annealer (Figure 64). On the kiln cartridge glass cullets are placed for melting inside a crucible. At the end of the crucible is the nozzle that allows for the flow of the glass. The system is gravity based. Since glass is a viscous fluid even at high temperatures the team had to explore different nozzle sizes both in length and in diameter of the nozzle head to achieve the optimal flow. Another

limitation to that system is the need for frequent refilling since the pressure level affects the flow rate. The nozzle deposit glass layer by layer at a constant rate within the print annealer. The temperature of the printer annealer is controlled to avoid uneven cooling of the printed glass component. Temperature gradient of approximately 350°C between the 5 last printed layers is crucial for the stability and solidification of the structure, higher temperature difference can lead to crack propagation and uneven stress concentration(Klein, 2015). When the print of an element completes the flow of glass from the nozzle stops either by reducing the temperature in the kiln cartridge or by manually cooling down the nozzle head. In the examples of G3DP and G3DP2 the printed objects are moved into a separate annealing chamber.

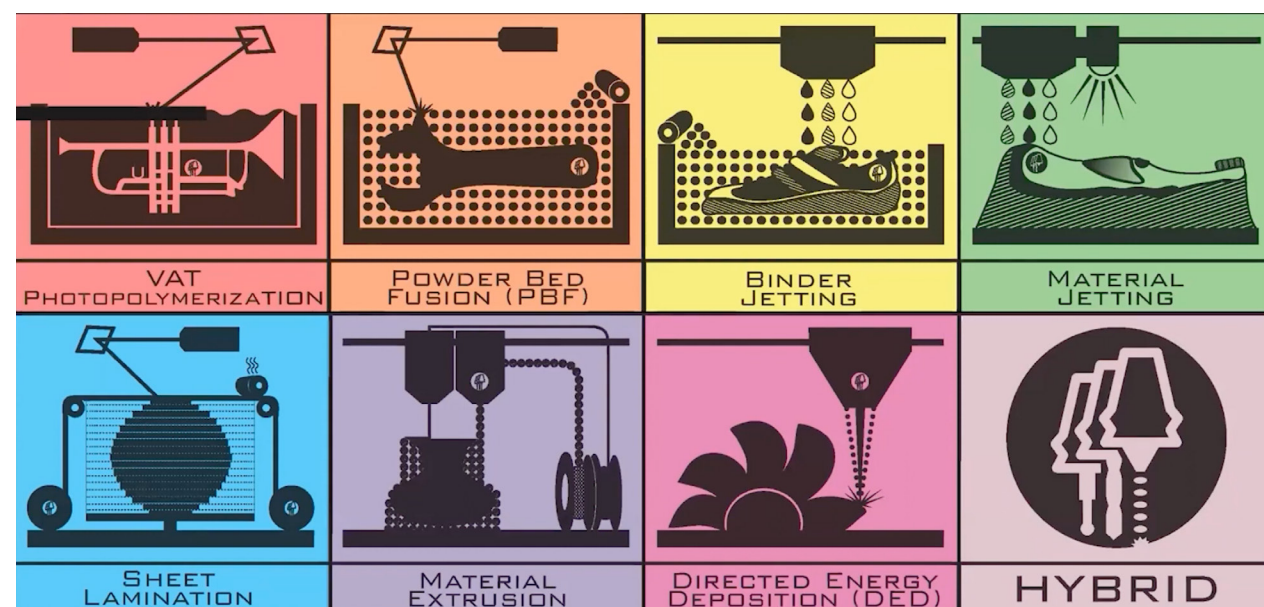


Figure 62 : 7 categories of additive manufacturing as defined by (American society of testing and materials, n.d.).www.hybridmanutech.com

16. Extrusion of glass in the molten state (FDM), direct ink (particle base) writing, laser assisted filament melting and stereolithography patterning of ink at room temperature (SLA) (Moore et al., 2020; Zhang et al., 2021)

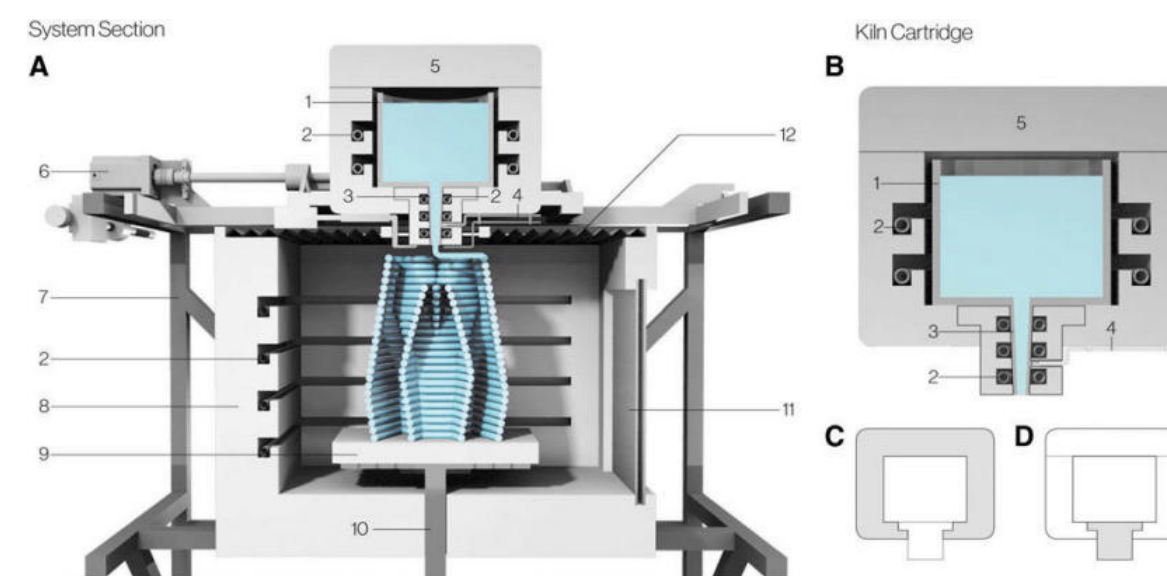


Figure 64 : FA G3DP print annealer. (B) the kiln cartridge, (C) Kiln crucible, and (D) nozzle.: (1) the crucible, (2) heating elements, (3) the nozzle, (4) the thermocouple, (5) removable feed access lid, (6) stepper motors, (7) printer frame, (8) print annealer, (9) ceramic print plate, (10) z-drive train, (11) ceramic viewing window, and (12) insulating skirt.(Klein et al., 2015)

Potential/ Limitations/ Applications

This method shows great potential as it can produce objects of substantial size as seen in the realized glass columns (Figure 65), project Glass II (Inamura, 2017a). The speed and accuracy of printing has been improved over the years. Preliminary structural testing has been performed giving more insight into the structural values, the safety of such glass objects and the surface quality. Shape freedom is high but size is still limited. On the downside the components that are produced

with this method are not optically transparent and present anisotropic behaviour, both affected by the layering. Other limitations relate to time and cost efficiency/ feasibility.

Over additive manufacturing (AM) technologies according to (Choi et al., 2017) have been used to manufacture ceramic parts with complex shapes, and are currently being applied to the casting industry to reduce the inconvenience of mould making. Opening new possibilities for glass manufacturing.

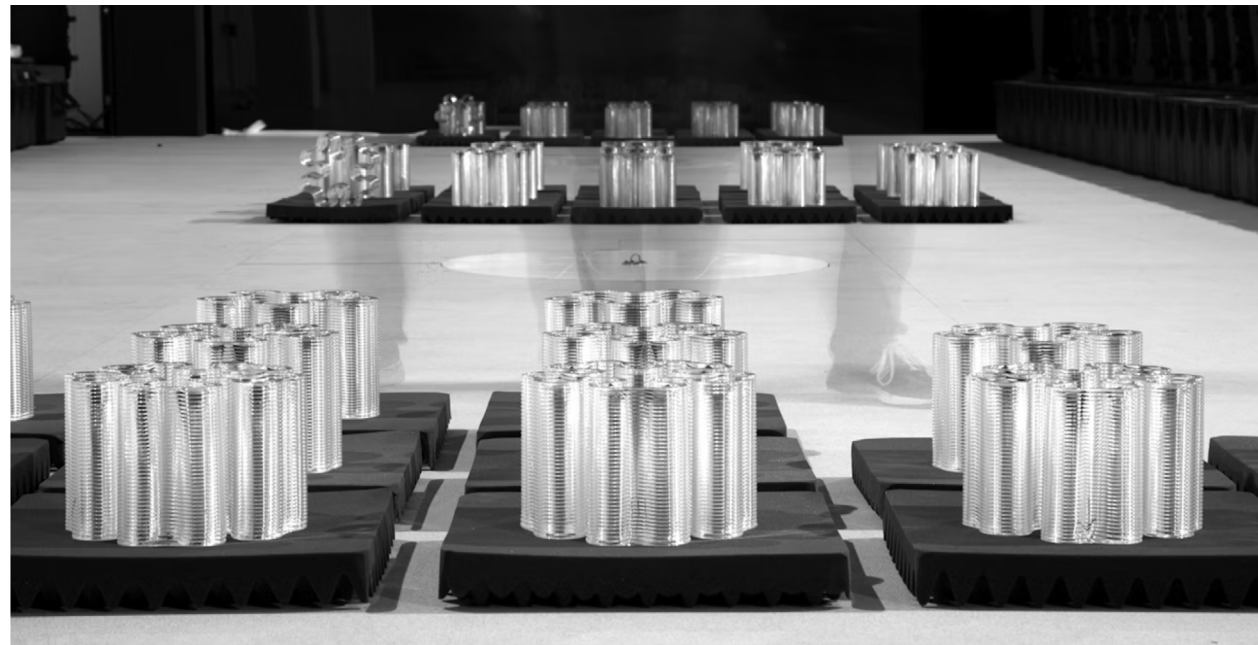


Figure 65 : Disassembled column, <https://oxman.com/projects/glass-ii>

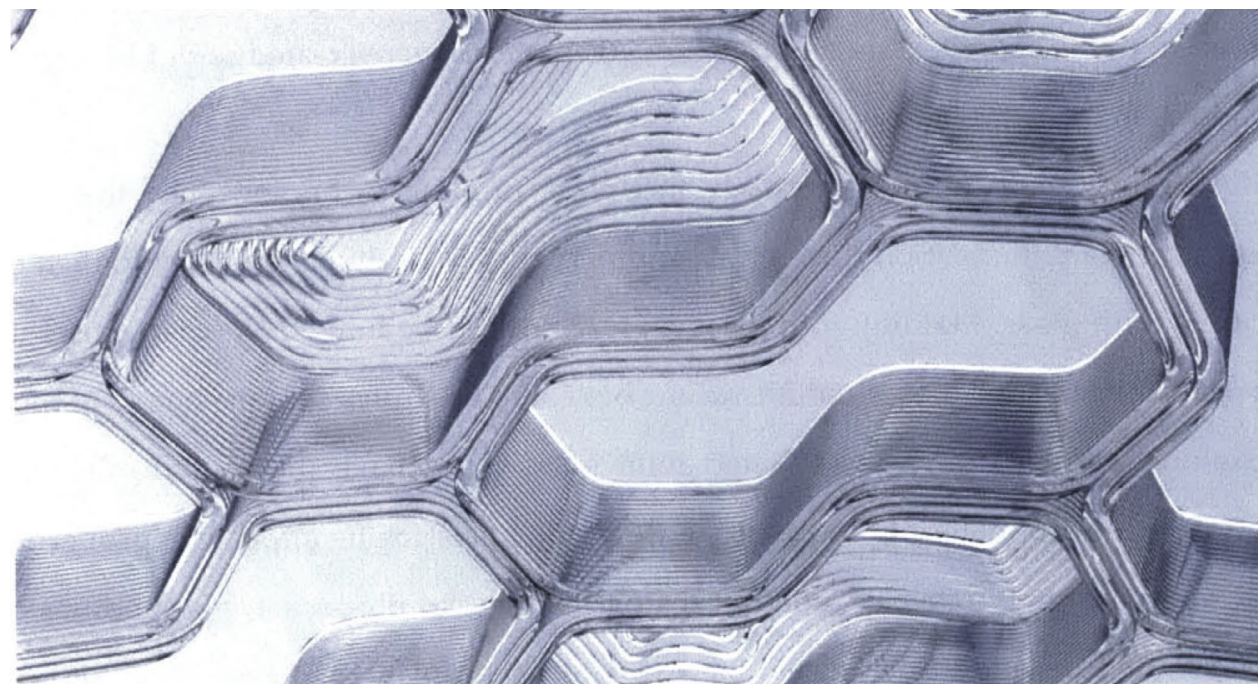


Figure 66 : Conceptual design of compressive shell structure comprised of 500 3D printed glass components (Klein, 2015)

4.3.2. Stereolithography (SLA) and digital light processing (DLP)

SLA and DPL are similar techniques that are both based on the selective curing under UV light of photosensitive resins layer by layer arriving at the final 3D shape. They differ in the way the light is directed; DPL uses a projector applying the light at each layer in a single pass, while SLA uses a laser that polymerize monomers into polymers. The glass parts manufactured with these techniques are of small size, high accuracy, are permeable and with excellent mechanical properties (Zhang et al., 2021). DLP is faster than the SLA method¹⁷. SLA using particle-laden resins is a more affordable alternative to FDM for high complexity and accuracy parts (Moore et al., 2020). On the downside it requires support structure that increases production time, the need for post processing and the risk of breaking the samples in the process (Zhang et al., 2021).

However, the transparent glass examples printed using SLA display limitations in the chemical composition, based on SiO₂ nano-particles. Compositions containing more than one oxides show greater potential for applications in medical, tech and telecommunication industry (Moore et al., 2020).

Recent research using the DLP technology and phase changing resins is promising paving the way for 3d printing of glass components with multi-oxide compositions. In order for them to become transparent they have to pass through pyrolysis

and sintering that dramatically reduce the volume of the object by 60% (Moore et al., 2020) (Figure 67).

4.3.3. Computed axial lithography (CAL)

Recently developed by the collaboration of University of California, Berkeley and Albert Ludwig University of Freiburg in Germany (Figure 68). This technique can print extremely high-definition microstructures with higher optical quality, design flexibility and strength. The size of the realised examples is still limited (The Engineer, n.d.).

4.3.4. Selective laser sintering (SLS) and Selective laser Melting (SLM)

In SLM method a high-power laser beam is directed towards a powdered material selectively consolidated by melting it. Glass powder is applied on the substrate that is then selectively melted. The process is repeated for each layer of the model. In SLS the material is not melted but sintered leading to different molecular structure, porosity etc. After printing objects are heat treated leading to noticeable shrinkage. The realized samples with SLM and SLS, as presented in the review paper of (Zhang et al., 2021) and through personal communication with TU Darmstadt are of small scale and further development is needed for larger scale prints.

Early attempts at 3D printing with sintered glass powder show potential towards industrializing

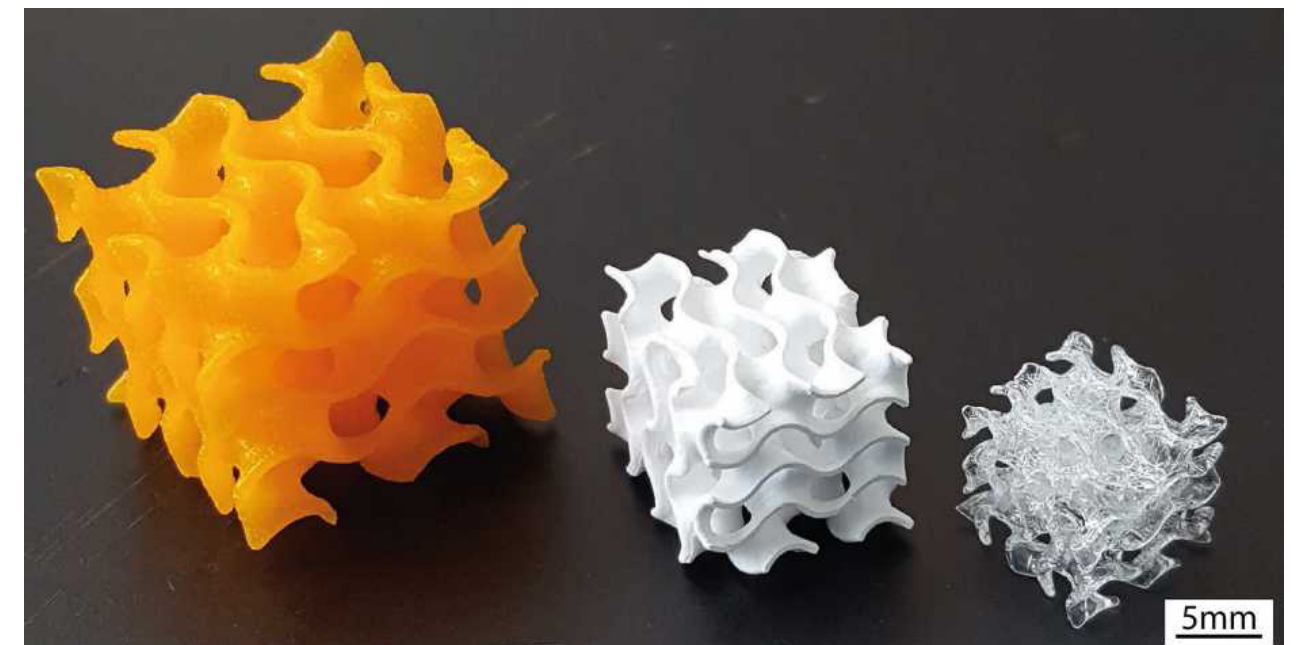


Figure 67 : Shrinkage of component printed with DLP technology, (Moore et al., 2020)

17. Personal communication with TU Darmstadt (prof. Seel, Matthias Martin and Chhadeh, Philipp Amir)

glass manufacturing process. Through vat photopolymerization and direct ink writing advancements have been made in high-resolution sintered glass printing. The lack of transparency, mechanical qualities, and slow rate of only 0.02 kg/h are some shortcomings that this method has. The significant shrinkage and distortion that take place when the binder is removed during the sintering process present another difficulty in scaling this indirect technology (Inamura et al., 2018).

4.3.5. Direct ink writing (DIW)

DIW shares similarities with FDM. In DIW a semi-solid ink is extruded through a nozzle as in FDM. The printed object is rapidly solidified then heat treated and sintered arriving at the desired glass object.

The ink involved in this technic must fulfill a set of requirements regarding its shaping and rheological properties and its pore formation during drying. On the contrary to FDM method, DIW does not require high temperature for glass printing. Elements produced via DIW show good transparency, are non-porous, have lower shrinkage and bigger sizes can be printed. On the downside, this method is subject to the limitations of extrusion-based technologies. The accuracy is confined by the nozzle size, the shape freedom is limited by the path of the nozzle and drying time is long (Moore et al., 2020; Zhang et al., 2021).

Comparison of 3D printing of glass

Commercially produced sintered glass objects are available, although they are very delicate and have an opaque appearance due to incomplete densification of the glass powders. Such problems have persisted despite the most recent trials with glass SLM; the resulting items are opaque and have inferior mechanical qualities. Furthermore, polishing requires a lot of work and the effort to access all parts of the geometry can lead to fracturing of the sample (Klein, 2015).

FDM requires melting the raw material beyond 1,000 °C. High temperature is not required in other methods of 3D printing of glass. The later methods of printing soda-lime glass circumvent the substantial shrinkage and post-processing of typical powder-based techniques. Up until now FDM methods seem the most promising for fabricating large scale structural components.

In the new process, the starting powder is fastened by an inorganic binder, whereas the mould in the conventional process takes its form by using an organic binder. The fixing of powders by the inorganic binder is caused by a sol-gel reaction of precursor materials. Therefore, the new mould process is more environmentally friendly and simpler than the conventional process. The inorganic binder system for the in situ process was prepared from a mixture of tetraethyl orthosilicate and poly(dimethyl siloxane) as SiO₂ precursor, and so-

dium methoxide as Na₂O precursor. The prepared samples show a fracture strength of about 5 MPa, indicating that the in situ process can be applied to the fabrication of moulds having high mechanical properties (Kim et al., 2011).

4.4. Fabrication methods comparison

Each fabrication method comes with its own set of advantages and disadvantages. When designing an all-glass structure is good to have an overview of the available methods and be aware of the effect those methods have on the aspects of the design. Table 4 gives an overview of the fabrication methods currently available for glass. Depending on the design requirements a different fabrication method might be ideal.

Summarizing the findings of Table 4 we see that laminated glass structures are good in terms of redundancy and structural behaviour due to the highly controlled float glass properties and the multilayer design. On the downside they are hard to recycle and result in high waste generation during their production phase. The lamination process results in slender elements (limited total thickness) with directional transparency and non-homogeneous structural behaviour.

Cast glass is recyclable and has full transparency potential. The main challenges of cast glass are the lack of redundancy due to a less controlled production method and, depending on the casting method, the need for post processing and mould waste. Size and shape limitations are mostly linked to the annealing time required.

3D printing of glass while it is still at an embryonic stage is the best method sustainability wise but has compromised optical quality, anisotropic structural behaviour and fabrication limitations in size and shape.

To understand in depth this preliminary and qualitative comparison between the most prominent fabrication methods for glass we need to dive into the different criteria that affect each aspect of the fabrication. The fabrication method that are chosen are:

- Lamination of AWJ cut glass parts
- Kiln casting with the aid of disposable 3D printed sand moulds
- 3D printing of glass

The next chapter introduces four main categories of criteria based on which the fabrication methods are accessed on.

Table 4: Comparative table between different binders for 3D printed sand moulds ((ExOne, 2023)

	+	-
Laminated	<p>Predictable structural performance</p> <p>Low safety factor</p> <p>Redundancy</p>	<p>Waste generation</p> <p>Difficult to recycle</p> <p>Directional transparency</p> <p>Structurally non-homogeneous</p>
Cast	<p>Recyclable</p> <p>Potential for full (non-directional) transparency</p> <p>Structurally homogeneous (isotropic)</p> <p>Shape and size freedom</p>	<p>Mould waste*</p> <p>Need for post processing (rough surface) *</p> <p>No redundancy</p> <p>Size and shape confined by annealing time</p>
3D printed**	<p>Zero waste</p> <p>No post processing</p> <p>Recyclable</p>	<p>Structurally non-homogeneous</p> <p>Directional transparency (visible layering)</p> <p>No redundancy</p> <p>Currently limited print volume</p>

* Depending on the mould type, applies mainly for disposable moulds (Oikonomopoulou, Bhatia, et al., 2020)

** For FDM method

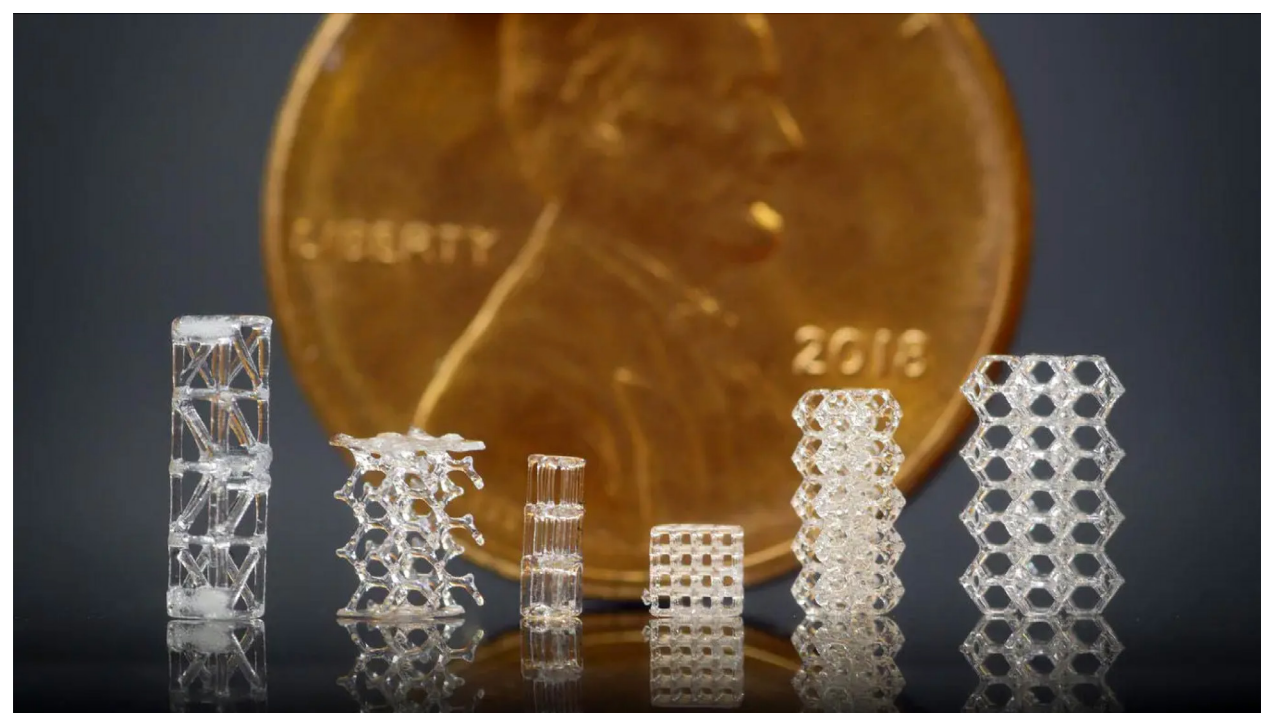


Figure 68 : Microstructures of glass made by CAL AM method, (The Engineer, n.d.)

5

ASSESSMENT CRITERIA

In this chapter, the three fabrication methods for glass within the scope of this thesis are assessed based on a set of criteria related to structural performance, visual quality, fabrication limitations, and sustainability. This comparative study acts as a guide, helping to select the preferred fabrication method based on the soft criteria set during the design phase.

Introduction

To access the three different fabrication methods (1. lamination of AWJ cut glass parts, 2. kiln casting with the aid of disposable 3D printed sand moulds and 3. 3D printing of glass), it is important to establish assessment criteria. Some criteria are measurable while others are abstract/observation based. This categorization has to do with feasibility, given the limited time of this thesis some assumptions and generalizations are made to arrive at a conclusion.

There are four main categories: Structural, optical, sustainability and fabrication limitations (Figure 69).

- Structural deals with redundancy and structural performance.
- Optical deals with transparency and finishing quality.
- Sustainability in terms of waste generation and recyclability.
- Fabrication limitations is the biggest group and is subdivided into fabrication cost, need for post process, size limitation, shape limitation, ease of connection and transportation.

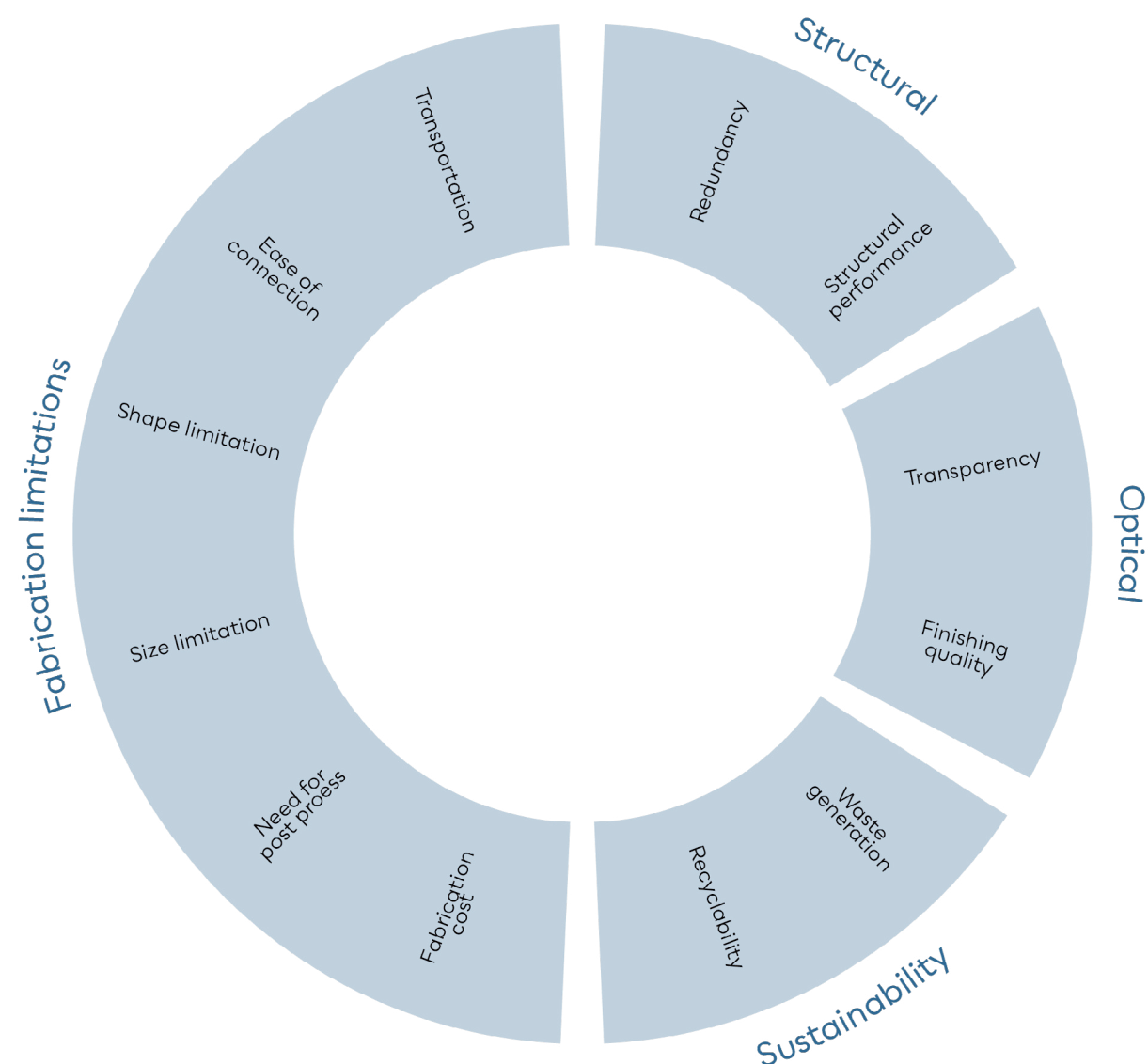


Figure 69 : Spider diagram of the four main categories and the assessment criteria that the comparative is based on for the different fabrication methods for glass

5.1. Structural

(Friedman, 1952) noted that the tensile strength of materials is different than the strength/ maximum resistance of a structural element. Three are the main factors that influence the values: technological, structural and operational (Rodichev et al., 2018). A material's structural behaviour is affected:

- by its mechanical properties,
- by its production method, functionality, overall dimensions, and volume distribution
- and by external factors such as heat, loads and time.

5.1.1. Redundancy (safety)

"To make glass safe, it must be redundant (capable of carrying after failure of a major part) and not ductile". (Nijse, 2003)

Redundancy in structural applications of glass is assessed based on the risk of failure, the predictability of the structural behaviour and the safety factor required.

Glass is a brittle material and displays significant difference between its tensile and compressive strength. Tensile strength is at least an order of magnitude lower than its compressive strength. The microscopic flaws in the material restrict the tensile strength of glass in the range of 40-80 MPa (Inamura et al., 2018). Thus, failure of glass is always caused by local tensile stresses. Even when a glass component is only loaded under compression due to buckling and the effect of Poisson's ratio, peak tensile stresses develop causing failure in lower compressive stress values than the theoretical ones (Oikonomopoulou, 2019). Due to the brittle nature of glass, the inability for plastic deformation and the low fracture toughness failure is sudden, impacting negatively the safety of a structure (Rodichev et al., 2018).

Failure of glass can be caused by external factors (impact, loading, thermal shock, etc.) or by residual stresses and/or by flaws inherent to the material (Bristogianni, 2022; Oikonomopoulou, 2019). While a risk analysis for external factors is almost always necessary in glass structures, the fabrication method is directly connected with residual stresses and flaws in the material.

AWJ cut laminated Float glass

Laminated glass structural components have been extensively analysed and realized in various built projects. The biggest advantage of AWJ cut laminated glass components is its great and calculable structural performance and post fracture load bearing capacity. Float glass panels (usually between 2-7 layers, in extreme cases up to 11 (Eckersley O'Callaghan, 2018; Li & Ren, 2011)) are glued together under heat and pressure. The interlayer is either PVB or similar soft adhesive material. The advantage of the laminated elements is that if one or more layers are damaged or fail loads transfer through the interlayer to the intact glass layers (Cruz, 2013). The properties of the interlayer are crucial in the post fracture behaviour of the components. Usually even after failure of all layers the laminated elements remain as one single object (Centre for the Protection of National Infrastructure, 2019). Such structure can warn the user before failure allowing for a safe evacuation in case of fatal failure. Overall, laminated structural glass elements tend to display lower risk of failure, a more predictable structural behaviour and lower safety factors than cast or 3D printed elements. Laminated glass structures are extensively more extensively studied and realised and have a more calculable structural behaviour.

Complex manufacturing technique can display higher chances for flaws or errors than can reduce the safety of the structure. The process starts with the float glass production, followed by the AWJ cutting in the desired shape and finally laminating of the pieces. While AWJ cutting can be performed in pre laminated glass it is not suggested (Shivaji Rao & Satyanarayana, 2020) as it can lead to rougher edges and longer cutting times. Float glass production process has been optimized and refined since its introduction by Pilkington (1959). Currently high-quality standards are implemented ensuring no flaws or residual stresses in the material. Meaning that redundancy is not hindered by the material. Abrasive waterjet cutting can lead to rough edges. Surface roughness can lead to local peak stresses and early failure of the component. In that case additional post processing by polishing, grinding or etching is needed. To avoid that a set of settings during the cutting must be adjusted to reduce the roughness of the edge. During lamination, several factors can affect the quality of the final product. Float glass production results in panels that are not perfectly flat due to the deformation caused by the rollers. This should be considered in the alignment of the panels. If the panels are laminated incorrectly stresses can develop. Cleanliness of the glass parts, pressure, temperature and correct cooling are also important. Improper set up

can lead to bubble formation or incorrect binding of the layers.

Redundancy of AWJ cut laminated float glass is linked with the structural performance, waste generation, recyclability, need for post process, size limitation and shape limitation criteria.

Redundancy comes with some trades of sustainability-wise. Due to the lamination process it is hard to separate and recycle the materials. Waste in form of cut out parts are generated during water-jet cutting. Nesting algorithms utilize glass panes more efficiently and cut-out parts can be recycled but require additional energy and has higher environmental impact. Redundancy also relates with shape and size limitations directly linked with the available size of autoclaves, size of glass panes and number of layers that can be laminated. Currently the standard size of glass panes is 6000 x 3210 mm (Saint-Gobain, n.d.) but can reach up to 20000 x 3210 mm (Sedak, n.d.). (Sedak, n.d.) can laminate parts up to 20000 x 3210 mm.

Kiln cast glass

Cast glass components lack the established properties of laminated glass. For that reason, the rating of the criteria derives from experimental data and bibliographical research.

Flaws in glass can be distinguished in three main categories: surface flaws, edge flaws and inclusions (Figure 70)(Molnar et al., 2012). Surface flaws can be any kind of scratch, dent or discontinuity of the surface caused during the production of the glass but also during its service life by impact, debris, thermal shock, chemical corrosion, contact with other materials or glass pieces etc. (Oikonomopoulou, 2019). Edge flaws are like surface flaws. Inclusions (Figure 71) are categorized by (Bartuška, 2008) into stones, seeds and cords. All the flaws can cause peak stresses that lead to early failure of the glass component.

Spontaneous failure of cast glass introduces a level of unpredictability in its structural behaviour. To tackle this issue several measures can be considered. Higher safety factor can be introduced to ensure that after loading the local tensile stresses are not exceeded. Post processing of the surface by means of grinding and polishing can significantly reduce the surface flaws in size ensuring an overall better structural performance.

Design can solve this issue. By laminating a sacrificial layer of float glass, the structural members are protected from impact, vandalism, etc. Some manufactures (Haverkamp, n.d.; tgc, n.d.) have developed liquid safety coating that can be applied in any glass surface. The coating holds the structure

together preventing shards or splinter of glass from detaching.

For customized and complex glass structures, extensive experimental validation under mechanical testing is necessary, when accessing the compressive and tensile strength and subsequently to avoid over dimensioning and/or high values of safety factor (Oikonomopoulou, 2019; Rodichev et al., 2018). (Koniari, 2022) used a safety factor for kiln glass structures of 4.5 (refer to next sub-chapter).

As a result, redundancy of cast glass relates to structural performance and can be linked to recyclability criteria in case safety coatings are used.

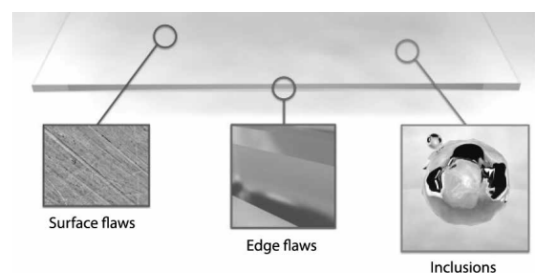


Figure 70 : Three categories of glass flaws according to (Molnar et al., 2012)

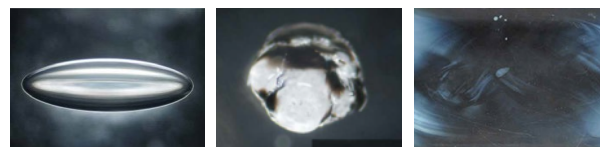


Figure 71 : Inclusion flaws in glass, from left to right: Bubbles, stones and cord. Image source (left and middle) (Molnar et al., 2012), (right): (Oikonomopoulou, 2019).

3D printed glass (FDM)

3D printing of glass is still in embryonic experimental state. Limited data can be found in bibliography. Like structural cast glass components, 3D printed components display no redundancy. After printing a lengthy annealing process ensures that no residual stresses are present.

The lack of standards and established properties requires extensive experimental validation to arrive at a value for the tensile strength of 3D printed components. In the work of (Inamura et al., 2018) a safety factor of 10 is used resulting in tensile strength 10 times lower than the tested one and over dimensioning of the structural elements. The high safety factor is associated with the small size of the tested samples and the high divergence in resulting values.

Redundancy is linked with structural performance. In this case due to limited data available no correlation can be observed between other criteria.

5.1.2. Structural performance

“A good structure must warn by deformation, i.e., cracking noises or whatever signals that an overload and fatal loss of integrity is imminent”. (Nijse, 2003)

Structural performance is access based on isotropic/anisotropic behaviour, the effect of size to the formation of internal flaws, residual stresses and strength. Glass as a material displays an almost perfectly linear elastic structural performance and has high degree of sensitivity to technological defects and damage during its service time (Rodichev et al., 2018). Furthermore, the load bearing capacity of glass is proportional to the time interval of the applied load and the surface area (Weller et al., 2008).

AWJ cut laminated float glass

Laminated glass structural components have anisotropic structural behaviour. This relates to the design and is dictated by the limited number of layers that can be bonded together. Structural members are usually slender with high ratio of width to depth ratio. Buckling can be an issue in such components loaded under compression. Between the different types of flaws discussed in chapter 5.1.1, edge flaws have a major effect on the strength of glass (Molnar et al., 2012). This means that tensile strength of glass is lower at the edge than further away from the edge (Louter, 2011).

Normally when the glass is waterjet cut then the cut edge is not very smooth, but it can be post-processed, e.g., by fire polishing or mechanical polishing. As stated by (Sanders et al., 2021) the accuracy of the AWJ cutting affects the strength of the glass. Samples of AWJ cut and core drilled annealed and toughened glass were drilled. The authors of the paper note that with the former method the holes were not perfectly round. The somewhat elliptical holes resulted in lower tensile strength compared to the core drilled samples. Under bending annealed glass samples displayed even higher difference, with the AWJ cut part performing worse. While circular holes are not necessary in all design can be a strong indication of the accuracy and the surface quality that waterjet cut edges do have.

As described above the inherited redundancy mechanism of such elements results in higher design values. In this regard the ability to use annealed, heat strengthened and toughened glass in lamination further improves the design tensile strength values. Also, the behaviour of laminated float glass has been extensively studied and evalu-

ated and we can have more precise strength values and use lower safety factors, thus resulting in more lightweight structures. Thus, structural performance of laminated glass is related to redundancy and finishing quality.

Kiln cast glass

Cast glass components display structural homogeneity and isotropic material behaviour as glass has a non-crystalline amorphous molecular structure.

Size of the cast glass components affects the structural performance. (Louter, 2011) states that the larger the size of the specimen the higher the chances for a large critical flaw within the volume. This means that size and structural performance are inversely proportionate, also referred as the inverse scale factor (Bristogianni, 2022; Louter, 2011; Oikonomopoulou, 2019)

Residual stresses relate to the annealing of the glass components and the difference between the minimum and maximum cross section of the voluminous components. Annealing time is important to allow for homogeneous cooling throughout the volume of the glass object. Uneven cooling of the volume leads to faster cooling and shrinkage of the outer surface and slower cooling of the centre volume. The outer surface is in compression and the centre volume in tension, any flaw or disruption in the surface can release the stresses difference between the inside and the outside areas leading to unpredictable failure. Residual stresses can be accessed in a qualitative manner using a cross polarization filter and a light source (Figure 72) (Oikonomopoulou, 2019).

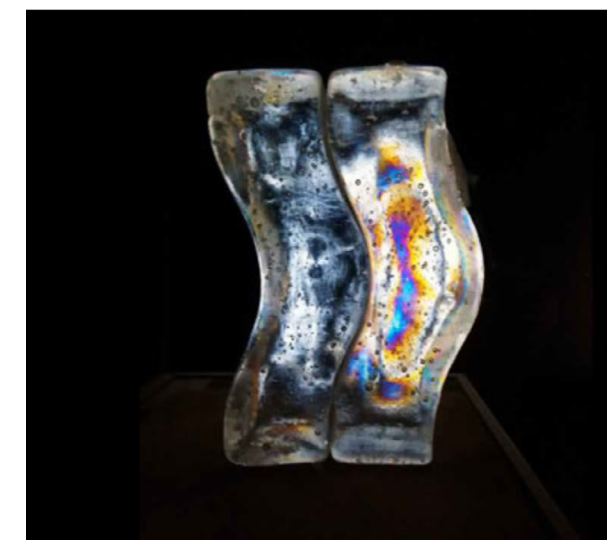


Figure 72 : Stress concentration as seen through a polarised filter. A qualitative way to check residual stress on glass components (Oikonomopoulou, 2019)

Strength of cast glass is restricted by flaws. Flaws in glass casting appear at a higher rate than that observed in the float glass industry. The main reason for that is the lack of automation and inspection in the fabrication method. The ones greatly affecting the risk of failure are the surface flaws (Bristogianni, 2022). When components are loaded surface cracks exposed to positive crack opening forces propagate and create peak tensile stress (Figure 73). When the peak stress value exceeds the maximum tensile stress of glass, the component fails. Since glass is brittle the failure is sudden, and the system is unable to carry any load post fracture.

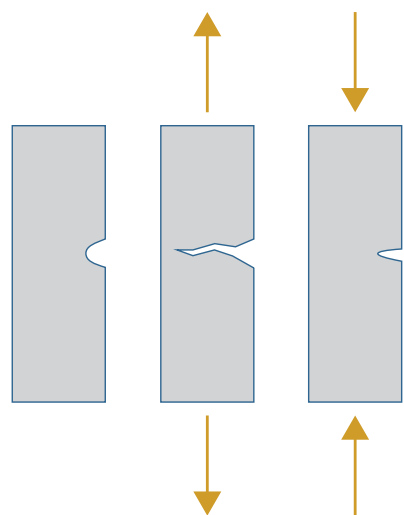


Figure 73 : Crack propagation positivity due to tensile stress, edited from (Damen, 2019)

Cast glass is also subject to the inverse scale effect which implies that the larger the component, the higher the probability of critical flaws within it (Bristogianni, 2022; Oikonomopoulou, 2019). This translates in a decrease in the probabilistic strength with massive cast glass piece expected to have a reduced strength compared to an equivalent sized structure fabricated via laminated float glass¹⁸.

To arrive at a specific value for the tensile strength of borosilicate cast glass we can assume that the ratio of tensile strength over flexural strength of float glass is the same. Through the research of (Bristogianni et al., 2020) we can derive the flexural strength of borosilicate cast glass. In the work of (Koniari, 2022) tensile strength for borosilicate float glass is considered as 45 MPa arriving at a tensile strength of 29 MPa for borosilicate cast glass. Through extensive literature review the maximum value for tensile strength of borosilicate float glass is 32 MPa. This results in a tensile

strength for cast glass of 20.5 MPa.

Flexural strength for cast soda-lime glass as tested in 4 point bending tests displays a wide range of results from 35 to 170 MPa (Rodichev et al., 2018), 51–71.5 MPa (Veer, 2007), 53–129 MPa (Yankelevsky et al., 2017). The size and polishing of the samples affect the results. Higher flexural strength is expected with additional polishing.

Structural performance of cast glass elements correlate with redundancy, finishing quality, shape limitation and criteria.

3D printed glass (FDM)

The strength values of this paragraph refer to a modified soda lime glass used by (Inamura, 2017b; Klein, 2015) for its low working temperature and wide working range.

The interface between two consecutive layers can display poorer mechanical properties than the rest of the volume. Improper adhesion of the layers can lead to de-lamination and failure of the sample (Belter & Dollar, 2015; Bertoldi et al., 1998). Preliminary 3-point bending tests parallel to the layers conducted by (Klein et al., 2015) confirm the assumption.

3D printed glass components have anisotropic structural performance. (Klein et al., 2015) states 40% difference between the major and minor axis. Loading perpendicular to the plane of the layer (major axis) displays the best performance. More extensive testing has been performed by (Inamura et al., 2018) in annealed and chemically tempered samples under 3-point bending. The resulting tensile strength for annealed glass on the major axis was 51 MPa and in the minor axis 41 MPa. Chemical strengthened glass samples lead to inconclusive results in strength value with high deviation. Result from the data above can only be used as a general approximation since the sample size is small and the testing is not performed under 4 point bending.

Structural performance connects with redundancy, finishing quality and shape limitation criteria.

Comparison

In literature a plethora of values is mentioned regarding the structural values of glass. In Table 5 a summary of the key finding can be found. Values should be used with caution as most of the values are indicative and are used as a base for this thesis. Experimental validation for cast and 3D printed glass is still limited.

Table 5: **Disclaimer: use values with caution.** Indicative values of the structural strength of glass. Data for cast and 3d printed glass are limited. Fields with ukn. are unknown

Soda lime	S.	Flexural strength	S.	Tensile strength	S.	Compressive strength	Units
Float	ff,fl,s	69	ft,fl,s	30-35 or 45 ¹⁹	fc,fl,s	300-420 up to 1000 ²⁰	
Cast	ff,c,s	44	ft,c,s	29 ²¹		Ukn.	
3D printed		Ukn.	ft,3,s	51 or 41 ²²		Ukn.	
Borosilicate							MPa
Float	ff,fl,b	69 ²³	ft,fl,b	22-32 ²⁴	fc,fl,b	260-350 up to 500 ²⁵	
Cast	ff,c,b	44 ²⁶	ft,c,b	20.5 ²⁷	fc,c,b	500 ²⁸	
3D printed		Ukn.		Ukn.		Ukn.	

The German standard DIN 18008 provided the following equation for the design strength of glass structures:

$$R_d = \frac{k_{mod} * k_c * f_k}{\gamma_M} = 0.22 * f_k$$

which is equivalent to a safety factor of 4.5 for cast glass.

k_{mod} = Modification factor for calculating the effect of load durations (0.4 for medium duration of loads)

k_c = Design coefficient normal (1.8)

f_k = Normal limit stress

γ_M = Material factor (1.8)

R_d = Rated value of the resistance to stress failure

19. In Granta EduPack 2021 R2 a tensile strength for soda-lime glass is stated in a range of 30-35 MPa. (O'Regan, 2015) reports that the tensile strength of soda-lime glass is 45 MPa.

20. Different values are stated in the bibliography. For float soda-lime glass compressive strength as high as 1000 MPa is reported (Ashby & Jones, 2006; Weller et al., 2008). In Granta EduPack 2021 R2 a compressive strength for soda-lime glass is stated in a range of 300-420 MPa.

21. As used in the thesis of (Koniari, 2022). Calculated using "rule of 3" since ff,fl,s, ff,c,s and ft,fl,s are known

22. (Inamura et al., 2018) for major and minor axis. Results from 3-point bending test. Actual values are expected to be lower under 4-point bending testing. Limited number of samples

23. As reported in (Oikonomopoulou, 2019) for borosilicate glass in form of float glass panels.

24. In Granta EduPack 2021 R2 a tensile strength for borosilicate glass in the range of 22-32 MPa

25. In Granta EduPack 2021 R2 a compressive strength for borosilicate glass in the range of 260-350 MPa. Mechanical testing in the work of (Oikonomopoulou et al., 2017) shows higher values.

26. MSc thesis of (Koniari, 2022) uses 44 MPa as the flexural strength of borosilicate glass. This value is close to the mean value mentioned in the work of (Bristogianni et al., 2020).

27. Calculated by the author using "rule of 3" method with known ff,fl,b, ff,c,b and ft,c,b. resulting in $ft,c,b = 32/69 * 44 = 20.5$ MPa

28. Based on tests conducted on borosilicate glass bundled columns by (Oikonomopoulou et al., 2017)

18. On laminated float glass elements, the failure of one ply is not that critical, also the automated, highly controlled production process ensures little presence of flaws and thus better structural performance.

Table 6: Design values for soda lime and borosilicate glass, as calculated by the author.

Soda lime	S.	Design tensile strength	Borosilicate	S.	Design tensile strength	Units
Float	fd,t,fl.s	10 ²⁹	Float	fd,t,fl.b	7.1	MPa
Cast	fd,t,c,s	6.4	Cast	fd,t,c,b	4.5	
3D printing	fd,t,3,s	4.1	3D printing	fd,t,3,b	Ukn.	

5.2. Optical

Glass is often correlated with the notion of transparency and spotless quality. This criterion is based on qualitative and quantitative assessment. Major flaws and the level of finish accuracy can be detected by optical inspection or other electronic means (e.g., microscope, etc.).

5.2.1. Transparency

Transparency is access qualitative in terms of colour change, opacity and roughness of the final product.

AWJ cut laminated float glass

AWJ results in a Laminated glass has directional opacity. As seen in the (Figure 74) the structure is transparent in the vertical direction (perpendicular to the laminae) while is completely opaque when seen parallel to the layers (Koopman, 2021). Careful lamination is imperative for the final optical quality. During the process bubbles can form affecting the optical homogeneity. The directionality of the transparency can be undesirable for certain applications (e.g., archaeological sites). Float glass used in the lamination process is of high optical quality and surface roughness is minimal compared to other fabrication methods for glass.

Redundancy and shape limitation criteria relate to transparency. Multiple layers of glass result in higher opacity and better structural performance.



Figure 74 : Directional transparency of laminated glass as displayed in the project Glass wipe by (Eckersley O'Callaghan, 2018)



Figure 75 : Directional transparency of laminated glass as displayed in the project Glass wipe by (Eckersley O'Callaghan, 2018)

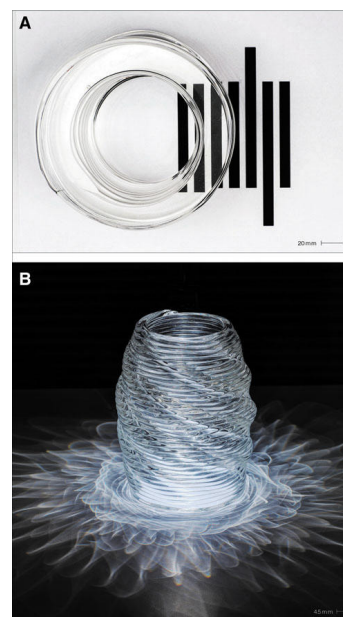


Figure 76 : Directional transparency of 70-mm-tall cylinder printed with the FDM method using G3DP. Polishing of the top and bottom edge resulted in high transparency(Klein et al., 2015).

Kiln cast glass

The transparency of kiln cast glass elements is affected by several factors. Type of glass, firing temperature, type of mould, coatings applied in the moulds and post processing being the main factors seen in bibliography (Bhatia, 2019; Giesecke & Dillenburger, 2022; Oikonomopoulou et al., 2020). Cast glass on steel or graphite mould can have full non directional transparency as seen on Figure 75. When cast on 3DPSM then main factor that hinders transparency is that grains of sand consolidate with the glass object resulting in an opaque and rough object. In cast glass transparency is interlinked with finishing quality, fabrication cost and need for post processing.

3D printed glass (FDM)

Glass printed with FDM method displays directional transparency like the laminated components. The components are printed layer by layer resulting in a transparent but optically distorted projection of the background when seen from the side. This is evident in the work of (Inamura, 2017b; Klein, 2015). The intricate caustic patterns caused by the refraction of light is considered as a design asset by the architects (Figure 76A). While it gives a unique property in the 3D printed glass it is a subjective design choice that cannot be avoided with the current means available. In the (Figure 76B) it is clearly depicted that perpendicular to the layers of printing the glass component is fully transparent. According to (Klein et al., 2015) top and bottom sides were polished using cerium oxide.

Other methods for additive manufacturing of glass present varying levels of transparency but they do not display significant potential for applications on bigger scale thus they are not accessed further.

Finishing quality, need for post processing, fabrication cost and shape limitations inherit to the

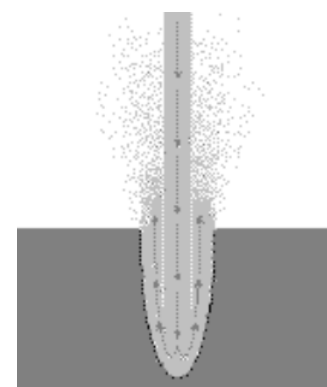


Figure 77 : Flow of water while cutting (Ramulu et al., 2005)

fabrication method are interrelated with transparency.

5.2.2. Finishing quality/ accuracy

Finishing quality can be optically inspected to determine the level of precision or in other words the deviation from the desired shape and the surface quality. Depending on the case it can be defined quantitative and qualitative. Finishing quality is strongly related with the need for post processing and the structural performance, especially of the cast glass component.

AWJ cut laminated Float glass

According to (Ramulu et al., 2005) the hole cut using this method is substantially wider than the jet stream, which is primarily connected to the additional wall erosion caused by the forceful upward ejection of the jet out of the blind cavity (Figure 77).

Float glass industry has an allowable deviation of 0.3 mm for float glass of 12 mm and 0.5 mm for 15 mm thick glass according to (EN 572-2:2012, 2012; Sanders et al., 2021). Several factors affect the accuracy and finishing quality of AWJ cut parts. Water pressure, size and flow of the abrasive material, nozzle cross section and length, cutting distance, angle of impact.

In single sheet float glass elements, the outer edge of an AWJ cut piece displays some surface roughness (Dudutis et al., 2020). Float glass edges are slightly inclined in some cases a value as high as 4-5 degrees from perpendicular angle is mentioned (Dudutis et al., 2020), other research shows a significantly lower divergence between 1/10th to 1/100 (ShivajiRao & Satyanarayana, 2020). The later results are more reliable as calibration of waterjet cutter has been performed and experimentation with abrasive size, abrasive flow rate, water pressure and stand-off distance were performed. Internal cuts with small size must be avoided, in the

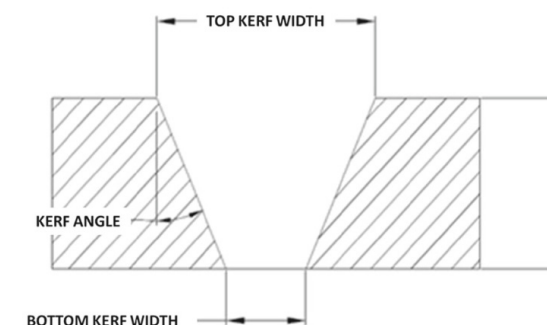


Figure 78 : Kerf angle, (ShivajiRao & Satyanarayana, 2020)

29. This value is indicative and is related to the type of glass and load case combination. For heat strengthened glass the design value is 45 MPa and for fully tempered glass is 80 MPa (Feldmann et al., 2014).

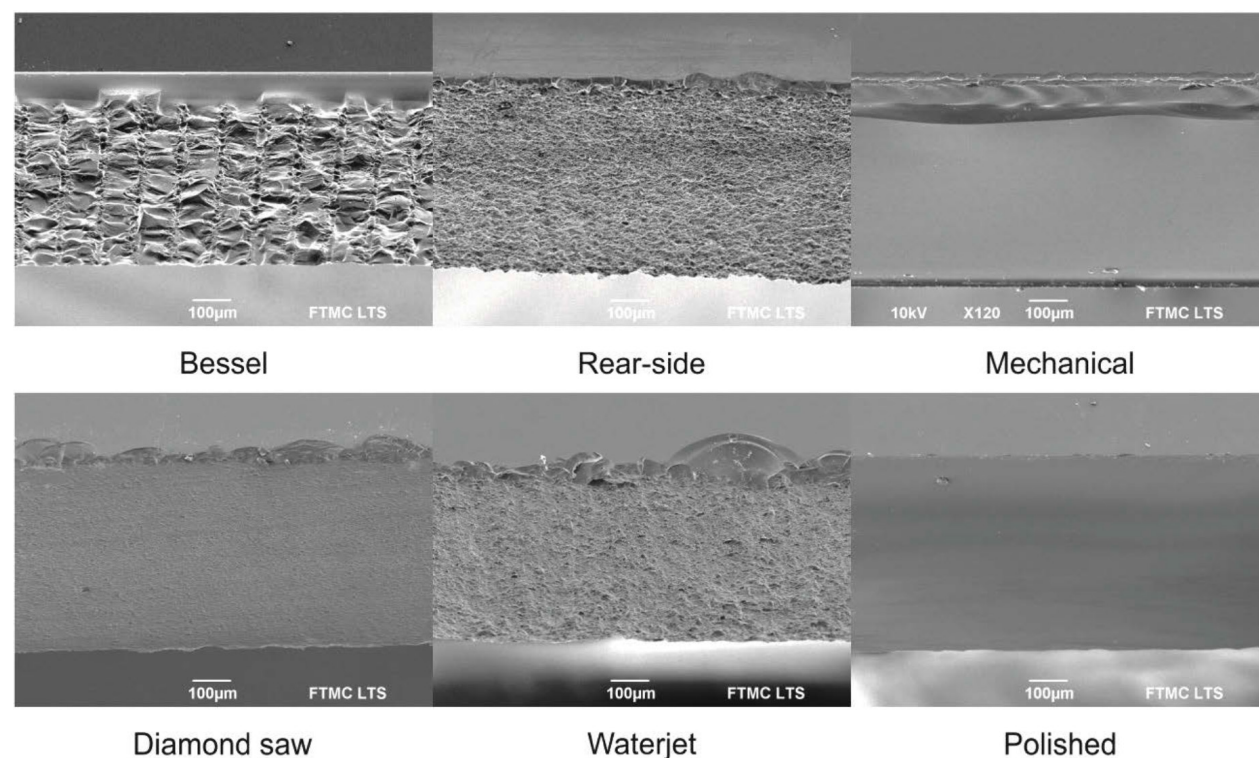


Figure 79 : Side walls of glass cut using different cutting methods, scanning electron microscope (Dudutis et al., 2020)

example of (ShivajiRao & Satyanarayana, 2020) circular holes with diameter of 5 mm where drilled with a centre to centre distance of 40mm. In some of the experimentation abrasive clogging of the hole has been noticed so small diameter holes are not suggested. Drilling close to another hole can result in increased stresses due to inherited flaws and consequently to failure of the material.

AWJ of laminated glass displays rougher surface than the single sheet. Chipping de-lamination or entrapment of abrasive in between glass layers appears, since the kinetic energy of the waterjet is reduced as the thickness of the material increases (ShivajiRao & Satyanarayana, 2020).

In principle, AWJ cutting on laminated pieces had higher diameter deviation at the exit hole at the bottom of the element and most of the times a negative kerf angle (Figure 78) was noticed. In the single float glass sheet kerf angle appears to be positive (ShivajiRao & Satyanarayana, 2020).

Finishing quality connects with structural performance and need for post processing criteria.

Kiln cast glass

The resolution of the 3DPSM affects the accuracy of the cast object. The resolution is linked to the size of the sand grain used. The stated accuracy is 0.1– 0.38 mm³⁰. Residual parts of the 3DPSM tend to stick on the cast glass components leaving them with rough surface. Application of coatings can improve the optical quality and reduce the need for post processing, reducing the overall cost and feasibility of production. Real life application³¹ of cast glass display ~1.5 mm standard size deviations (Oikonomopoulou et al., 2022). This deviation is a function of the size of the elements. For bigger cast elements higher deviation in size is expected and relates to the shrinkage.

Finishing quality connects with structural performance, transparency, fabrication cost and need

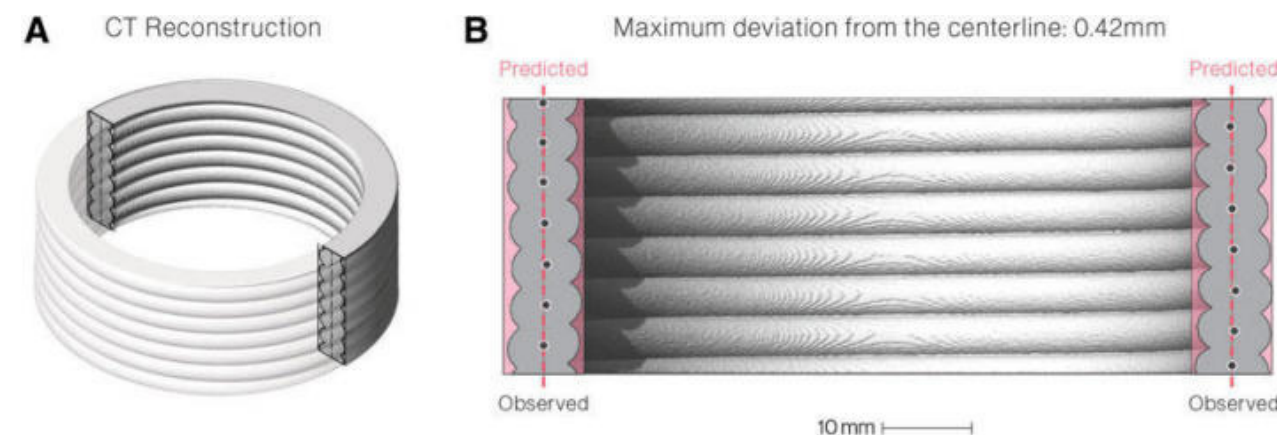


Figure 80 : Deviation from the desired geometry. CT reconstruction of the printed geometry using the G3DP (Klein et al., 2015)

for post processing criteria.

3D printed glass (FDM) *values for G3DP

3d printed glass components display visible layering because of the way it is fabricated. This unique optical finish affects the structural behaviour of glass as discussed in chapter 4. In the work of (Klein et al., 2015) a deviation of layer width was 0.19 mm and of the centre of the layer 0.13 mm. A maximum of 0.42 mm in deviation was (Figure 80) observed that led to a tolerance value of 0.5 mm. The accuracy is affected by the pressure and nozzle orifice manufacturing.

Finishing quality in this fabrication method correlates with transparency, fabrication cost and need for post process. Due to the absence of contact surface when produced (mould) surface roughness has not been evaluated, this means that on the contrary to kiln casting surface quality and structural performance do not relate.

Overview

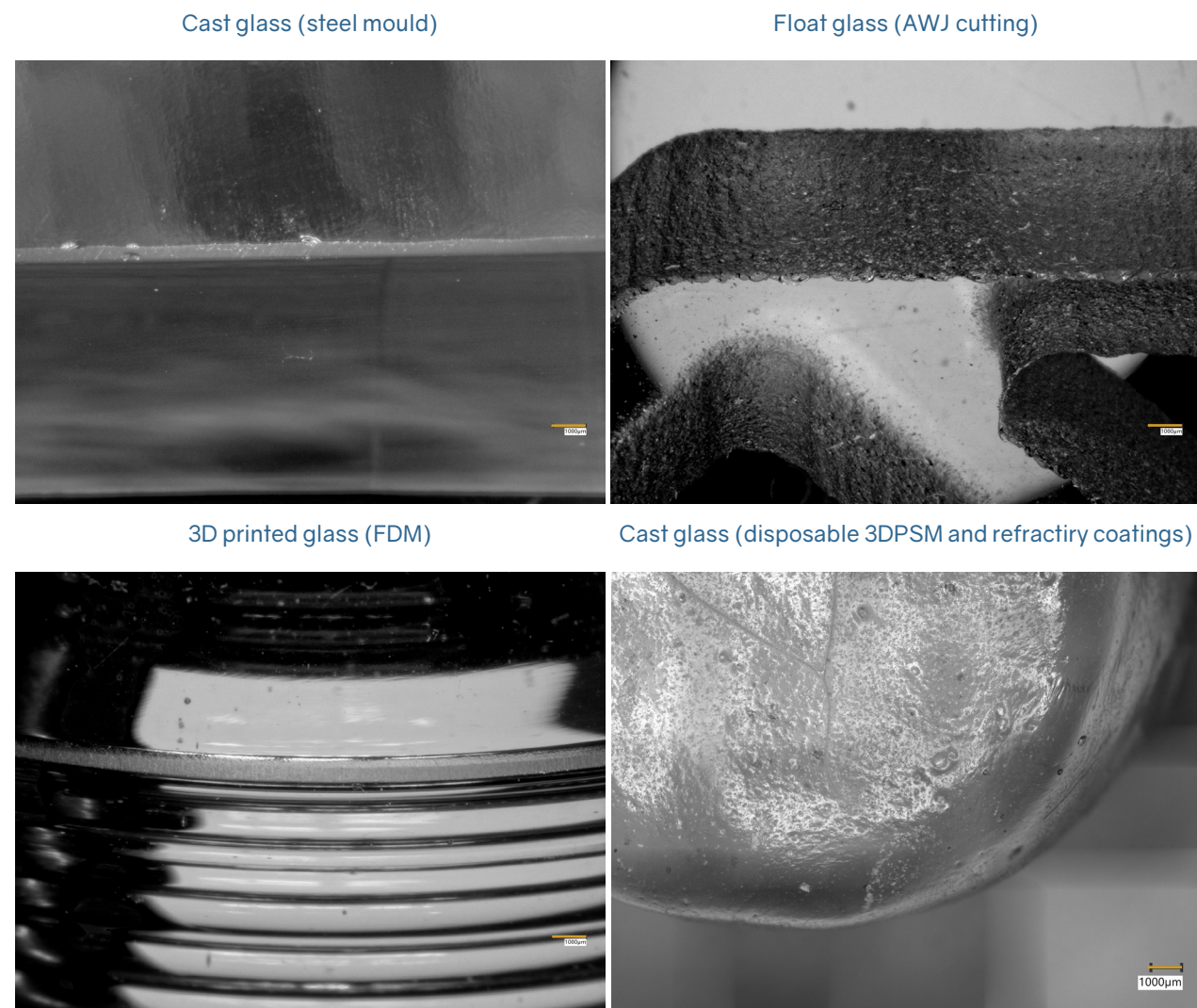
An overview of the surface quality of glass fabricated through different methods can be seen on Table 7. The images were captured using the VHX-7000 Digital microscope. All specimens except for the last one is placed on an inclination of approx. 45° so both side and top parts are visible.

Cast glass on steel moulds has great finishing quality both at top and side faces. Abrasive water jet float glass has a rough surface especially at the side edge where the jet stream cuts the material. Surprisingly also the top side displays some spots which are most likely abrasive material particle that bond with the glass during the cutting process. 3D printed glass using the FDM method displays great top and side surface quality. The top and bottom sides are polished as mentioned earlier. Finally kiln cast glass experiments using disposable moulds (3DPSM) and combination of coatings yielded some satisfactory results regarding the surface quality, results discussed in detail on the following chapter.

30. (ExOne, 2023) mentions layer height between 0.26 – 0.38 mm

31. Soda-lime cast glass solid bricks produced with steel moulds and foundry casting used in Crystal house, brick size 240 × 110 × 53 mm and weight 3.5 kg display a deviation of 1.5 mm according to (Oikonomopoulou et al., 2022). Resolution of ExOne S-Print 3D printer according to (Szymański & Borowiak, 2019) is 100 µm and layer thickness between 240 µm to 380 µm.

Table 7: Surface quality of glass fabricated with different fabrication method.



5.3. Sustainability

Sustainability is a current topic that affects all aspects of life. The building industry is one of the biggest emitters of greenhouse gases and end of life waste generated (25–30% of all waste generated in the EU according to (Surgenor et al., 2018)). Sustainability implemented during the design and production of a building component can reduce material use. Imperative for sustainability is also circularity which aims at closing the material loops in the building sector. Specifically for glass manufacturing, the main sub criteria that are accessed: waste generation and recyclability. Waste generation considers primary and secondary production methods. Recyclability takes into consideration feasibility and efficiency in the recycling process.

5.3.1. Waste generation *during production

Waste generation during: a. Primary processing and b. Secondary processing

AWJ cut laminated Float glass

In this fabrication method waste are generated during AWJ cutting and lamination. Depending on the desired shape and how it fits in the standard float glass sheets the amount of glass cut off can vary. These cuts can be remelted and turn back to float, however, they do require additional energy. During cutting big amounts of water is used and abrasive material. During lamination interlayer film is also cut to shape leaving unused pieces.

Kiln cast glass

Casting of glass with 3DPSM produces some was. Mould material is disposable and is thrown away after casting is complete. The mould leftovers are contaminated with binders and coatings which makes it difficult to recycle. In the thesis of

(Bhatia, 2019) it is briefly mentioned that the sand of 3DPSM is reusable. Theoretically sand can be cleaned and reused for printing new moulds, especially when inorganic binder is used which is water soluble and non-toxic.

If vents and pouring basin are needed during casting, there are chances that some minor glass wastes are generated. During polishing and grinding minimal amounts of glass is ground from the surface (lab experience).

3D printed glass

This method has virtual zero waste during production. The production of each piece happens in one continuous tread but due to limitations of the current technology the first 2-3 layers of the print are rough and are usually cut off. Like float or cast glass and depending on the recipe used for printing these parts can be recycled or cut into pieces and placed on the kiln cartridge.

Correlations

Waste generation has negative impact on the fabrication cost in AWJ cut laminated float glass and kiln casting method. In kiln casting waste generation also relates with the need for post process and shape limitation criterion. In 3D printing waste is generated due to technical and material limitation that result into inconsistencies of the first layers can be linked to shape limitation criterion. In AWJ laminated float glass waste generation is also directly connected with the redundancy of the structure.

5.3.2. Recyclability

On the one hand, glass is an unsustainable material due to the high working temperatures and lengthy cooling process. On the other hand glass is 100% recyclable and can be recycled perpetually (Musgraves et al., 2019). Despite that currently recycling is only limited in soda-lime food containers (reaches up to 79% for EU + UK, (FEVE, 2021)). In the building sector there is huge potential in glass recycling as it can be seen in the work of (Bristogianni, 2022).

AWJ cut laminated Float glass

Float glass industry has high standard of quality meaning that they only recycle glass of the purest quality. Glass cut offs created during AWJ cutting of glass can be recycled and used back in float glass line. In fact, glass cullets reduce the energy consumption and prolong the life span of the furnace (Nilsson & Persson, 2007; Worrell et al., 2008). Recycling of the interlayer of glass is pos-

sible but so far effort focus on PVB (Martín et al., 2020). Laminated glass elements pose difficulties in recycling. With the technologies at hand, only 50–60% of clear glass fragments and interlayer are recoverable. The leftovers end up in landfills or downcycled into bottles, aggregated or insulating materials (glass wool). The main reason has to do with the high degree of contamination and different chemical composition (Bristogianni & Oikonomopoulou, 2022b). Efficiency and purity of the individual components will undoubtedly rise as technologies in the field progress. The cost of this technology will also rise, making it economically unviable for low-volume processing (Šooš et al., 2021).

Kiln cast glass and 3D printed glass

Depending on the material used for the disposable moulds the material can be reusable. In case of silica plaster moulds the material end up in the landfill but with 3DPSM sand can theoretically be cleaned and reused. The avoidance of adhesives or foils in these production methods also yields contaminant-free glass which is 100% recyclable. In case safety coatings are used to ensure a more redundant structure glass can be contaminated making recycling more challenging.

Sustainability wise glass casting is more flexible. Different types of glass and recipes can be mixed when casting and different glass recipes can be cast in the same furnace and without incurring production loss. Waste glass streams that are not recycled (e.g., art glass, laboratory glass, etc) can be used. Hence cast glass has the potential of reducing the accumulation of glass waste, use less energy and reduce CO₂ emissions. Specifically, literature indicates that for each tonne of recycled cullet 1.2 tones (850kg been sand) of raw materials are saved (Hestin et al., 2016; Surgenor et al., 2018). For every 10% of recycled cullet added to the melting batch energy consumption is reduced by 2.5–3% (Nilsson & Persson, 2007) which translates in a reduction of 300 kg of CO₂ emissions per tonne of cullet used (Hestin et al., 2016). Another advantage of the use of recycled cullet is that the service life of the oven can be extend by up to 30%, due to the lower temperatures required for melting and batches that are less corrosive (Worrell et al., 2008). From an aesthetic point of view recycled glass has a unique appearance and can result in original and unprecedented patterns such the ones seen on Figure 81. The playful look and blend of transparency/ opacity and colours can be considered as a characteristic of added value, especially for highly customized cast glass shapes this

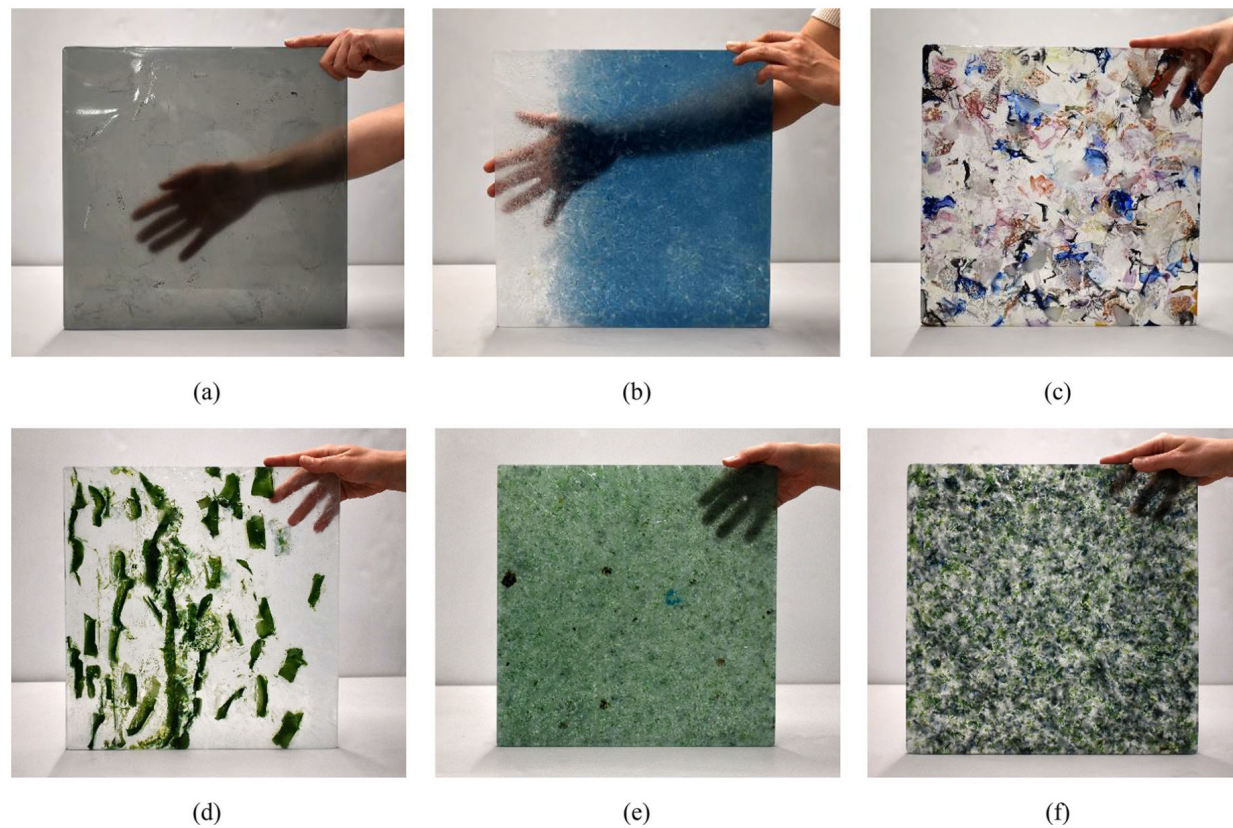


Figure 81 : Kiln-cast glass panels (350*350*10 mm) made at TU Delft from glass waste cullet. Namely Cathode-Ray Tube (CRT) front screen (a), transition float glass from clear to blue (b), CRT back screen and crystal coloured glass (c), enamel float glass (d), automotive glass (e) and oven doors (f). (Bristogianni & Oikonomopoulou, 2022a)

Correlations

In AWJ laminated float glass method recyclability and waste generation is interlinked with redundancy since the more redundant, more plies, the more difficult it is to recycle. On kiln casting recyclability criterion is linked to redundancy in case a safety coating is used. If recycled or waste glass is used for casting transparency can be compromised in favour of lower environmental footprint. The same can be true for 3D printed glass.

5.4. Fabrication limitations

Fabrication limitation criterion is trying to assess the different limitations that are posed by the three fabrication methods for glass. This criterion is broken down in six sub criteria that are the most important when designing a glass structure of complex and customized form.

5.4.1. Fabrication cost

This sub criterion considers the cost involved in primary production, secondary production, raw materials and annealing time (annealing time is standardized for float glass but plays a great role in the cost and feasibility of cast and 3D printed glass). While primary, secondary production and raw material cost can be compared on a qualitative way, annealing time can be compared in a quantitative manner. Annealing time can increase the cost of production since it requires higher amounts of energy to maintain the annealing chamber in the appropriate cooling cycle but also due to the prolonged occupancy of the chamber.

AWJ cut laminated Float glass

AWJ laminated float glass has a complex production method, float glass, AWJ cutting and lamination. A variety of machinery and materials are used resulting in complex and costly process. Regarding annealing time, the float glass manufacturing companies have optimized their processes and offer annealing time for different thicknesses of glass. For example, a 200 mm thick glass slab cooled from both sides takes approx. 27 days of annealing time (Bulls-eye Glass, n.d.).

Kiln cast glass

Kiln casting on disposable 3DPSM involves the binder process, coatings, and casting. This process used simpler materials and processes but requires more manual labour during coating and casting. Secondary processing, like grinding and polishing, can increase the cost. 3DPSM can be printed in a relative fast pace of up to 125l/h of volume build up (ExOne, 2023). Due to the custom and complex geometry secondary processes must be performed manually, while reaching all the points in the surface might prove challenging. In that sense cost is also affected by the need for post processing, finishing quality and transparency criteria.

As discussed in chapter 4.2 annealing time in cast glass is affected by many factors. The material properties and mass distribution/geometry play a crucial role as indicated in Equation 2. The maximum radius of the material is the factor that can exponentially increase the annealing time. A common example that proves the above mentioned is that of cast glass mirror blanks. The largest solid blank made from cast glass was 2.5 m in diameter and required 12 months of annealing for a maximum thickness of 325mm. In comparison the Giant Magellan blank has a diameter of 8.4 m and requires only one quarter of the annealing time, 3 months, for maximum thickness of 894mm. The huge difference in the annealing time is attributed to the material and mass distribution (Zirker, 2005). This example pinpoints the relation between cost and shape limitations criteria.

3D printed glass

The first experimentation of MIT with 3D printing of glass using FDM methods used a separate oven that followed the annealing cycle as displayed in the (Table 9). After printing the object is moved in the oven where the temperature is set at 480oC. For an element of 10kg in weight 1 hour is needed for the printing and 8 hours for annealing (Inamura, 2020). The object usually requires extra fine polishing to achieve a shiny finish. Cost is interlinked with the need for post processing criterion.

Table 8: Comparison between mass and annealing time

Soda-lime	Mass (kg)	Annealing time (hr.)
Cast glass	3.6 ³⁴	8
3D printed	10	8

Table 9: Annealing schedules use don 3D printed objects with G3DP (Klein, 2015)

Cooling rate (°C/h)	T (°C)	Dwell time (h)
-	480	1
25	400	-
50	150	-
50	80	-
120	20	-

32. Glass with 1/3 of thermal expansion coefficient is used in the later

33. Hollow honeycomb pattern is applied

34. For 210 x 105 x 65 mm bricks used in Crystal house (Oikonomopoulou, 2019; Oikonomopoulou, Bristogianni, Veer, & Nijse, 2018)

5.4.2. Need for post processing

Finishing quality, surface roughness and transparency are the key factors affecting this criterion.

AWJ cut laminated Float glass

Due to the nature of the material and even when proper settings are used (pressure, speed and distance from surface) chipping and sometimes failure of the specimen cannot be avoided (ShivajiRao & Satyanarayana, 2020). The microscope pictures of AWJ cut glass at Table 7 clearly indicated that the side surface requires post processing. Post processing of the edges of float glass is done through grinding and polishing using a diamond disk (Bukieda et al., 2020) or through chemical etching by immersion on solution of hydrofluoric (HF) and sulphuric (H₂SO₄) acid (Ward et al., 2011). Both methods help achieve better surface quality and can decrease the risk of failure due to the activation of surface flaws. In case post processing fabrication cost is expected to be higher and final strength higher (better structural performance).

Kiln cast glass

The use of the same principle can be applied on cast glass. Manual polishing using diamond disks of different grits: starting with 60 and going all the way up to 600 is currently used on kiln cast glass elements. The final polishing step that gives the shiny look is done using cerium oxide. The process is extremely time-consuming, significantly increasing the cost and the risk of inducing damage to the part.

Manual polishing using a polishing table or a hand-held rotary tool (e.g., bremel) has its limitations as it can be hard for the tools to reach at some point on an intricate geometry. Chemical etching might be a good alternative, but it is uncertain if it can be applied to voluminous objects or if it works better on edges. Where transparency is not important and for hard-to-reach surfaces sandblasting can be a good alternative. From the above surface we can conclude that the need for post process is linked to cost.

3D printed

As stated in the chapter 5.2 polishing is required for 3D printed glass objects at top and bottom side to achieve a transparent surface. Chemical etching and sand blasting should be applicable as well but no mention was found.

5.4.3. Size limitation

Size limitation in terms of min and max size as well as other limitations related to accuracy of each fabrication method. Size limitation is also linked with the nature of the material. It is considered that the likelihood of a significant defect, which would result in a weaker strength, increases as the size of the glass sample increases, assuming that the defects are distributed randomly across the surface. This phenomenon is known as the inverse scale effect (Louter, 2011).

AWJ cut laminated Float glass

The float glass industry has standardized production dimensions for glass panes. Standard size panels are called jumbo panes and are 6 x 3.21 m in size. Manufacturers can produce panels up to 20 m in length, but the max. width is either 3.21 m or 4.5 m. For those panels, the standard thickness of 2, 3, 4, 5, 6, 8, 10, 12, 15, 19 and 25 mm (Lyons 2010; Schittich et al. 2007; Patterson 2011). In building applications thickness used are between 4-19 mm with 25 mm been rarely produced (Oikonomopoulou, 2019). (Sedak, n.d.) can laminate parts up to 20000 x 3210 mm. Typically in structural applications no more than 7 plies of glass are laminated together, although a few examples with more plies can be found in literature. Lamination of more layers is usually performed with in situ use of adhesive as seen in House Laminata project. This increases the manual labour, hence affecting the cost and the ease of connection between glass interlayer. Transportation becomes more challenging the bigger the laminated elements.

Kiln cast glass

Size of cast elements are constricted primarily by the mould and secondarily by the annealing chamber size. When casting using disposable 3DPSM the maximum printing dimension differs according to the manufacturer and the type of binders used but is usually limited by the size of the printer bed. As reported by (Voxeljet, 2022) the maximum size of the printable volume is 4 X 2 X 1 m. (ExOne, 2023) states max dimensions for printing with the inorganic binder as 1,800 x 1,000 x 700 mm (1260 l in volume). The work of (Koniari, 2022) shows that with appropriate planning it is possible to overcome the size limitation of the moulds by segmenting the geometry in smaller interlocking pieces that can be produced with current means of technology. Regarding the minimum dimension of the wall thickness no prior research has been done specifically for glass, but values can be calculated empirically.

Research at ETH while casting concrete on

3DPSM indicated that thinner than 6-10 mm walls were unstable and could be easily damaged during the preparation of the mould for casting. When calculating the wall thickness the build of hydrostatic pressure at the deepest parts must be considered. Another size limiting factor is the overall size of the mould with 1.8 m² approaching the limit in terms of manipulation and stability of the piece. The use of a greater number of smaller mould parts can increase challenges while assembling and casting. A compromise between size, number of pieces, weight and logistical factors should be taken into account (Menges et al., 2017). On figure 82 segmentation of the mould geometry is done, based on maximum printable size and ability to manipulate. Interlocking positive-negative dents are used primarily for alignment during assembly.

Annealing chamber size is not necessarily a limiting factor as it can be easily custom-made but will increase the cost. See Giant Magellan Telescope blank 8,4 by 0.894 m. For this kind of customized piece, a custom annealing Lehr had to be manufactured.

Size limitation can relate to the fabrication cost. The minimum dimension of the thickest part of the geometry defines the total annealing time required, which consecutively affects the former. The bigger the size the more challenging the development of connections and transportation. Finally, shape and size limitations are interconnected as some limitations unique to glass, (e.g., min. size, max. size, undercuts, voids etc.) affect both criteria.

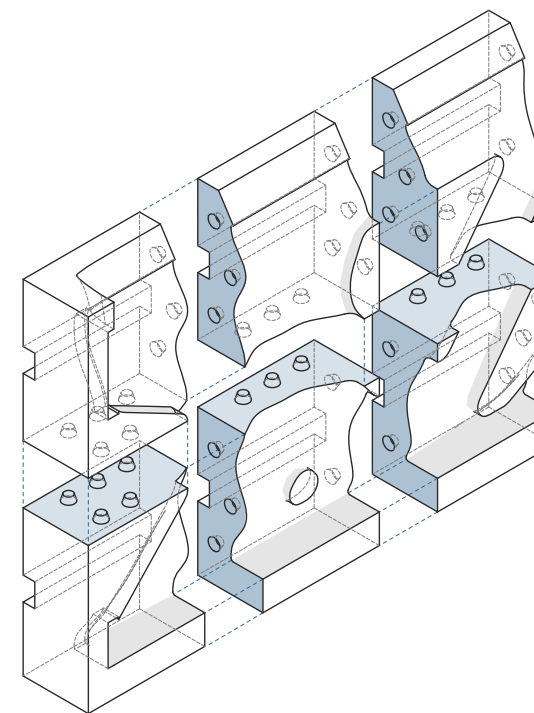


Figure 82 : Interlocking 3DPSM. Moulds can be split according to the maximum printable and manipulation size.

3D printed

Using FDM method for 3d printing of glass MIT managed in 2015 to produce components of complex form up to 250 mm by 250 mm by 300 mm at a flow rate of 2.2 kg/h (Inamura et al., 2018; Klein, 2015). This is 42 times faster than Micron3DP (first FDM printer developed for glass) and 118 times faster than a typical high-resolution vat photopolymerization printer (Inamura et al., 2018). In the year 2018, the second generation of this FDM 3d printer for glass was developed with improved speed, accuracy and size. The maximum printable area is up to 320 mm by 320 mm by 350 mm with a flow rate of 5.2 kg/h (Inamura et al., 2018). Other methods for AM glass vary in the amount of the detail and size but in principal are for printing smaller elements (Sivarupan et al., 2021). (MIT media lab 2018) states that using this technology they can print up to 30 kg of glass (Table 10).

This method is governed by the same principles in annealing as kiln casting, thus the size is linked to the fabrication cost.

Table 10: Comparative table of the 2 version of FDM printers developed by MIT, edited from (Inamura et al., 2018)

	Unit	G3DP	G3DP2
Platform			
X-axis	mm	250	320
Y-axis	mm	250	320
Z-axis	mm	250	320
Print volume	cm ³	18.75	35.84
Reservoir size	kg	2.1	25.5
Material ratio	%	4.6	29
Process			
Nozzle size	mm	10	11.5
Print rate	mm ³ /s	240	570
Flow rate	kg/h	2.2	5.2

5.4.4. Shape limitations

Shape limitations are defined as the level of geometrical freedom affected by the material and the fabrication method. Undercuts, edge trim, voids are among the geometrical constrictions observed in glass fabrication methods.

AWJ cut laminated Float glass

This method displays low shape freedom. As it has been seen in realized projects in chapter 3. Undercut and voids are hard to create for the following reasons: avoiding foil leaking into the voids while melting, geometrically overlapping of the plies is needed to allow for adequate contact surface, limitation in the number of laminated elements. Lamination of multiple layers is challenging, requires additional labour and can increase the overall fabrication cost. For above mentioned reasons, the realization of such structures is time and cost inefficient.

Shape and size limitations are closely related as the max. number of layers that can be laminated affects in a sense the size of the structure.

Kiln cast glass

Kiln casting has high shape freedom. A complex geometry with undercuts is possible. In the fabrication of Giant Magellan Telescope pressured water has been used to clean the remaining mould material from undercuts. However, fully encapsulated voids are not possible. The complexity of the shape does not increase the price or the production time. Sharp edge and 90° corners should be avoided as they can create stress concentration (Figure 83). When designing the mould a pouring basin and exhaust vents are needed to allow for flow of glass and to ensure that glass fills 100% of the mould. Due to hydrostatic pressure build up and depending on the size of the required geometry the walls of the mould must have adequate thickness to avoid collapse during casting. (ExOne, 2023) suggest using wall thickness of at least 20-25 mm for small scale sample with a max. dimension of 300 mm. Casting larger objects will require much higher values of minimum wall thickness. Manufacturers provide some information regarding the strength of the binder and in the work of (Stefana-

ki, 2020) and according to Voxeljet company the bending strength range of 3DPSM is between 220-300 N/cm².

Regarding glass the cross-sections do not have to fall in a specific range but rather abrupt changes in cross-section should be avoided. This is because a significant difference in mass distribution can lead to uneven cooling times, resulting in localized stress concentrations that can lead to fractures. Additionally, care should be taken to avoid sharp and thin edges, as these will cool more quickly than the rest of the component and increase the risk of cracking. To mitigate these risks, thin elements and sharp edges should be avoided and replaced with elements of a minimum dimension and round edges, respectively (Koniari, 2022).

In kiln cast glass shape limitation criterion affects the structural performance and is linked to

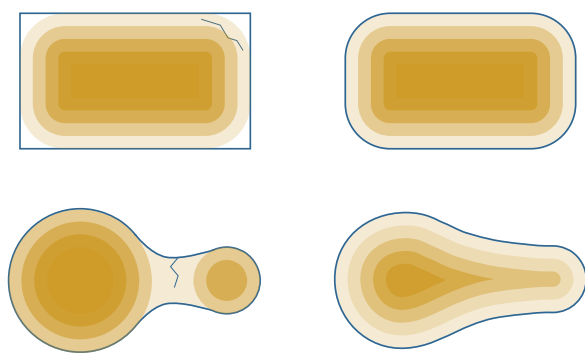


Figure 83 : Shape limitations in glass casting. Edited from (Damen, 2019). Top: avoid sharp corners as they cool down much faster than the rest of the mass leading to possible cracking. Bottom: Avoid abrupt cross-section change.

size limitation criterion.

3D printed

This fabrication method has some limitation regarding its shape expression. Objects should be produced on a continuous interrupted thread. Extreme over hangs are not possible without the introduction of a supporting structure while the first layers need to be cut after printing. Another shape limiting factor is the visible layering inherent to the manufacturing process. In that sense structural performance (anisotropic), transparency and waste generation are interconnected with the shape limitation criterion

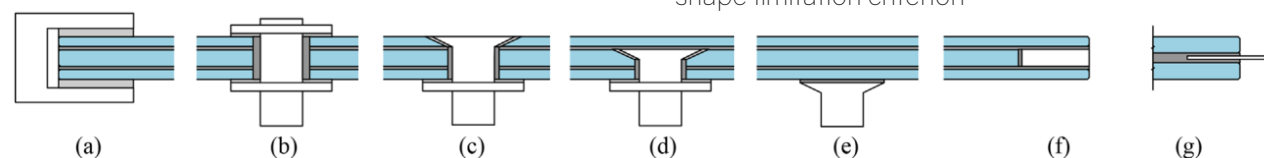


Figure 84 : Connection typologies used in structural glass applications. a) Clamped; b) bolted; c) bolted with countersunk bolt; d) hybrid with countersunk bolt; e) adhesive; f) embedded with thick insert; g) embedded with thin insert (Bedon & Santarsiero, 2018)

5.4.5. Ease of connection

Ease of connection in terms of glass-to-glass connection and glass to other materials (e.g., steel, etc.)

AWJ cut laminated Float glass

Lamination of float glass as expected and been the most documented and widely use in structural glass applications has a variety of connections and has the higher ease of connection. The work of (Bedon & Santarsiero, 2018) summarises the most common typologies of connections (Figure 84). The material used is stainless steel and in some cases titanium as it has the same expansion coefficient with soda lime glass. The metal piece can then be connected to foundations or other materials. Adhesives and/ or structural silicone is also used.

Kiln cast glass

Connections for kiln cast glass applications are the same as on hot poured glass. Adhesives, UV cured epoxies, neoprene, TPU, PU and other soft interlayer are most commonly used (Oikonomopoulou, 2019; Oikonomopoulou, Bristogianni, Veer, & Nijse, 2018; Oikonomopoulou et al., 2022). Also in the work of (Oikonomopoulou, Bristogianni, Barou, Jacobs, et al., 2018) interlocking connection for kiln cast glass is explored. Reinforcement of kiln cast glass with steel or titanium displays potential (Bristogianni & Oikonomopoulou, 2022a) and while at experimental stage can create more connections freedom in the future for such parts.

3D printed

Lastly the least documented fabrication method is that of 3D printing of glass. The only know structural application is that of Glass II were silicon film interlayer between the pieces and a post tensioned steel system is used to hold the structure together.

This criterion might be unrelated to any other. Only size can somewhat affect the easy of connection, bigger piece is harder to connect or requires the development of a custom-made connection. In any case since this thesis address highly customized glass shapes a customized connection system is expected.

5.4.6. Transportation

Transportation considers all the logistical difficulties regarding moving the glass piece on site and the construction and installation sequence at the location. The maximum allowed for a size of truck allowed within European union and specifi-

cally in Greece is 12 m X 2.55m X 4m (Figure 85). The case study location is not directly accessible via road, which mandates the arrival of the glass piece will arrive until the car parking via truck and the use of a helicopter for the final assembly of the structure. The size restriction of the truck applies to all the methods to allow for easier and more economic transportation of the structure.

AWJ cut laminated Float glass

In the example project of the glass cantilever at the Bründl Kaprun flagship store, installation and transportation proved challenging due to its location above the river. The cantilever, which is made of glass, weighed approximately 9 tons, and had to be lifted with the use of a crane from the street side and placed on the fourth floor of the existing building. Additionally, the glass walkway had to be able to withstand significant forces such as its own weight, payload, wind and snow. To ensure its durability, the laminated safety glass was put through a tensile test before installation. This involved applying calculated forces to the glass multiple times and gradually increasing the load until the glass broke under the pressure (seele, 2021).

Kiln cast glass

Apart from the limitation of the size of trucks, specifically for cast glass elements produced using 3DPSM transportation of the moulds is also crucial. This type of mould is friable and custom solutions should be found, such as the integration of a protective bed of unbounded sand contained within a closed 3D printed box. This way the piece is supported until it is ready to be used for casting. (Menges et al., 2017). Transportation is linked to size limitation criterion.

3D printed

Due to its small size elements fabricated with this technique don't present any difficulty different that the transportation of a fragile object.

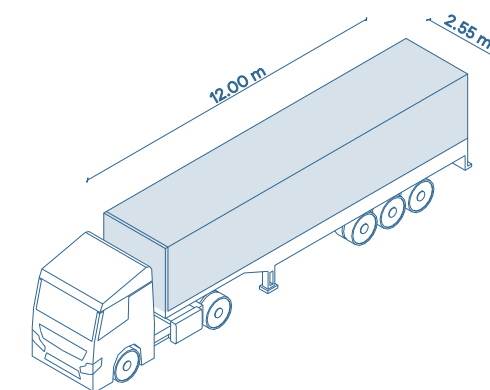


Figure 85 : European box truck max. dimensions that primarily limit the transportation of glass components.

5.5. Conclusions

The table below displays a qualitative overview of the assessment (performance) per fabrication method for glass (Table 11).

From the above it can be derived that according to the prioritized performance criteria, the most suitable fabrication method can already be pre-selected (Figure 86).

Among the three fabrication methods discussed, water-jet cutting and bonding of float glass is the best choice in terms of structural performance due to the well-documented and controlled properties of float glass and the redundancy of a multi-layered solution. On top of those factors the possibility for further improving the tensile strength of the component by tempering and the use of the lowest safety factor between the fabrication methods, can result in the most lightweight solution. On the downside, optical performance is hindered by the directionality of the layers, while there are considerable size limitations (especially thickness) and shape restrictions (connected to the planarity of the panes). This method is the least sustainable with high waste generation and hard to recycle final components.

Casting glass is the optimal choice for achieving transparency and size and shape freedom. The main limitation in terms of size is the annealing time, which can be minimized by optimizing the geometry and by using glass with low thermal expansion coefficient. The main disadvantage of this fabrication method is the need for post-processing to arrive at a smooth surface, linked to the use of disposable moulds for creating customized components. Another drawback of cast glass components is the lower strength values compared to float glass due to the less controlled casting process, lack of quality standards, and the inverse scale effect (for larger glass components). This necessitates the use of increased safety factors, resulting in a heavier structure compared to float glass, thus a monolithic glass structure lacks redundancy. Sustainability wise cast glass is a good option and displays potential in terms of recoverability and recyclability of the material.

Finally, additive manufacturing (AM) of glass, while still in the experimental phase, could potentially be the most environmentally friendly option, with almost no waste and minimal need for post-processing. However, this technique faces challenges like those of laminated glass regarding optical performance (directional), as the deposited glass layers are visible. Additionally, AM glass has the lowest overall structural performance and is limited by various fabrication constraints, although some limitations such as size and shape

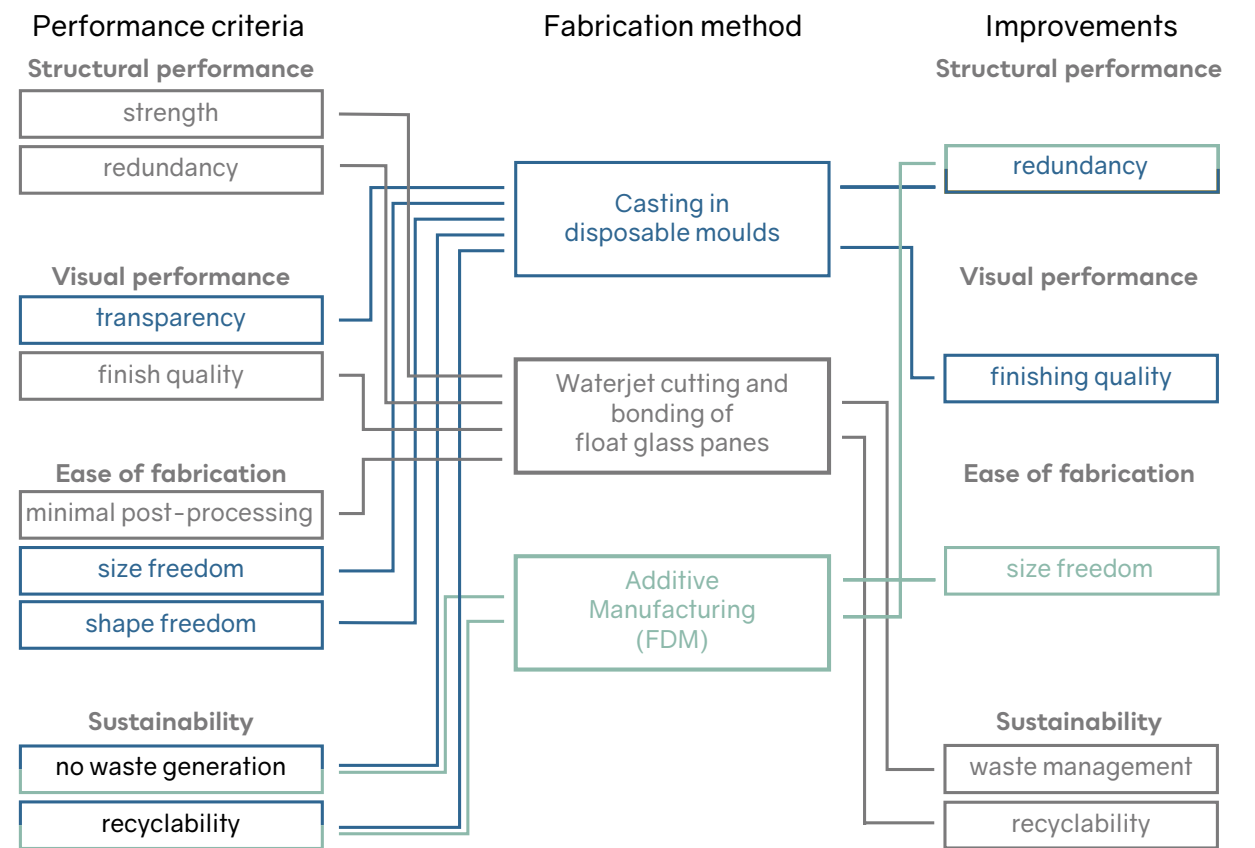


Figure 86 : Performance criteria linked to each fabrication method and suggested improvements per fabrication method.

Table 11: Qualitative comparison of different fabrication methods for glass based on a custom set of criteria.

Criteria	Structural		Optical		Sustainability		Fabrication limitations					
	Redundancy	Structural performance	Transparency	Finishing quality	Waste generation	Recyclability	Fabrication cost	Need for post process	Size limitation	Shape limitation	Ease of connection	Transportation
Laminated	High	High	Medium	High	High	Low	High	Low	Medium	High	High	Medium/High
Cast	No	Medium	High	Low	Low	High	Medium	High	Low	Low	Medium	Medium/High
3D printed	No	Low	Low	Medium	No	High	High	Medium	High	Medium	Low	Easy

*Colors indicate if something is considered an advantage or disadvantage, blue for exceptional, green for advantage, orange for neutral and red for disadvantage.

constraints can be attributed to its embryonic state of development.

To realise the complex correlations between the different domains and criteria some spider diagrams were developed. The main purpose of those diagrams is to visualize the interlinking criteria via lines. On the AWJ cut one a lot of lines meet at the redundancy criterion. This is logical considering that redundancy of this structure is its biggest advantage structurally and its biggest disadvantage sustainability wise. On the kiln cast one we can clearly see the relation between surface quality, transparency, structural performance as well as the secondary connection to redundancy and cost. On the AM manufacturing one a lot of lines connect to the optical category highlighting the direction transparency and the anisotropic structural behaviour. Those diagrams can be seen at the appendix.

Having said that and based on the set of soft criteria set on chapter 2.2; minimal optical footprint, optical transparency, sustainable fabrication and shape-size freedom; the preferred fabrication method for the realization of the observatory in Vikos Gorge is **casting on disposable moulds**. Surface quality can be improved through lab experimentation with the aim of obtaining a good surface quality directly after de-moulding. Redundancy which is not one of the main soft criteria but imperative for all built structures will be explored through research by design (chapter 7) (e.g., by segmentation or lamination of a sacrificial layer) (Figure 85).

6

FABRICATION EXPERIMENTATION

The chapter documents the lab experiments done in the glass lab as part of this thesis. The research sub questions that aims to answer are:

Focusing on kiln-casting using disposable 3D printed sand moulds (3DPSM):

- a. How to improve the surface quality and optical quality of structural glass elements?
- ii. Which is the preferred firing schedule and maximum temperature that glass can be cast on the provided 3DPSM?
- iii. Which is the potential of applying different coatings on 3D printed sand moulds in improving the surface quality and finishing texture of complex-shaped cast glass components?

Introduction

Based on the optical transparency, sustainability and shape-size freedom criteria, as defined at the case study chapter and the available means within TU Delft, casting in 3D printed sand moulds (3DPSM) is selected over the other fabrication methods. Kiln-cast components display structural homogeneity, are 100% recyclable, produced with zero glass waste, have high shape and size freedom, and can reach full non-directional transparency. Typically 3DPSM are used for hot pouring of metal with significant shorter contact time at high temperature. Kiln casting requires a prolonged exposure to high temperatures, hence the behaviour of these moulds is unknown.

Currently kiln casting of glass in disposable 3DPSM results in a translucent and rough surface that requires post processing. The need for post processing increases the cost and affects the feasibility of such complex shaped glass components. The use of refractory coatings is common in metal casting and initial testing for glass show promising results by ETH.

6.1. Overview

As discussed in previous chapters, while casting using steel moulds can lead to full and non-direction transparent glass elements; casting glass in disposable 3DPSM results in a rough and opaque surface. This is evident in previous experimental

work within the Glass group of TU Delft and previous thesis (Bhatia, 2019) (Figure 87).

Sand grains of the disposable moulds tend to adhere to the glass, mandating post-processing. Post processing with means of polishing leads to higher manufacturing costs while it can compromise the structural integrity and dimensional accuracy of the component.

The spider diagram (Figure 88) highlights the focus of this chapter which is to explore ways to improve the surface quality and transparency of kiln cast glass, thus reducing the need for post processing and cost. The issue of structural performance and redundancy is explored through research by design.

Previous research at ETH focusing on foundry casting in 3D-printed sand moulds fabricated with Inorganic binders and coated with a combination of Zirkofluid and graphite-water dispersion yielded promising results in terms of optical and surface quality.

Current experimental work focuses on the further investigation of coatings that can yield a completely smooth and transparent surface quality in kiln-casting of glass. Two sets of experiments are conducted. The first one explores the **maximum firing temperature** that the provided 3DPSM can be used at. The second one evaluates **different coatings**, coatings combinations and application methods on different temperatures to arrive at the optimal kiln casting set up.



Figure 87 : Left kiln cast glass using disposable 3DPSM (Bhatia, 2019). Right foundry cast glass using steel moulds. Difference in the surface quality is evident (Oikonomopoulou, Bristogianni, Veer, et al., 2018)

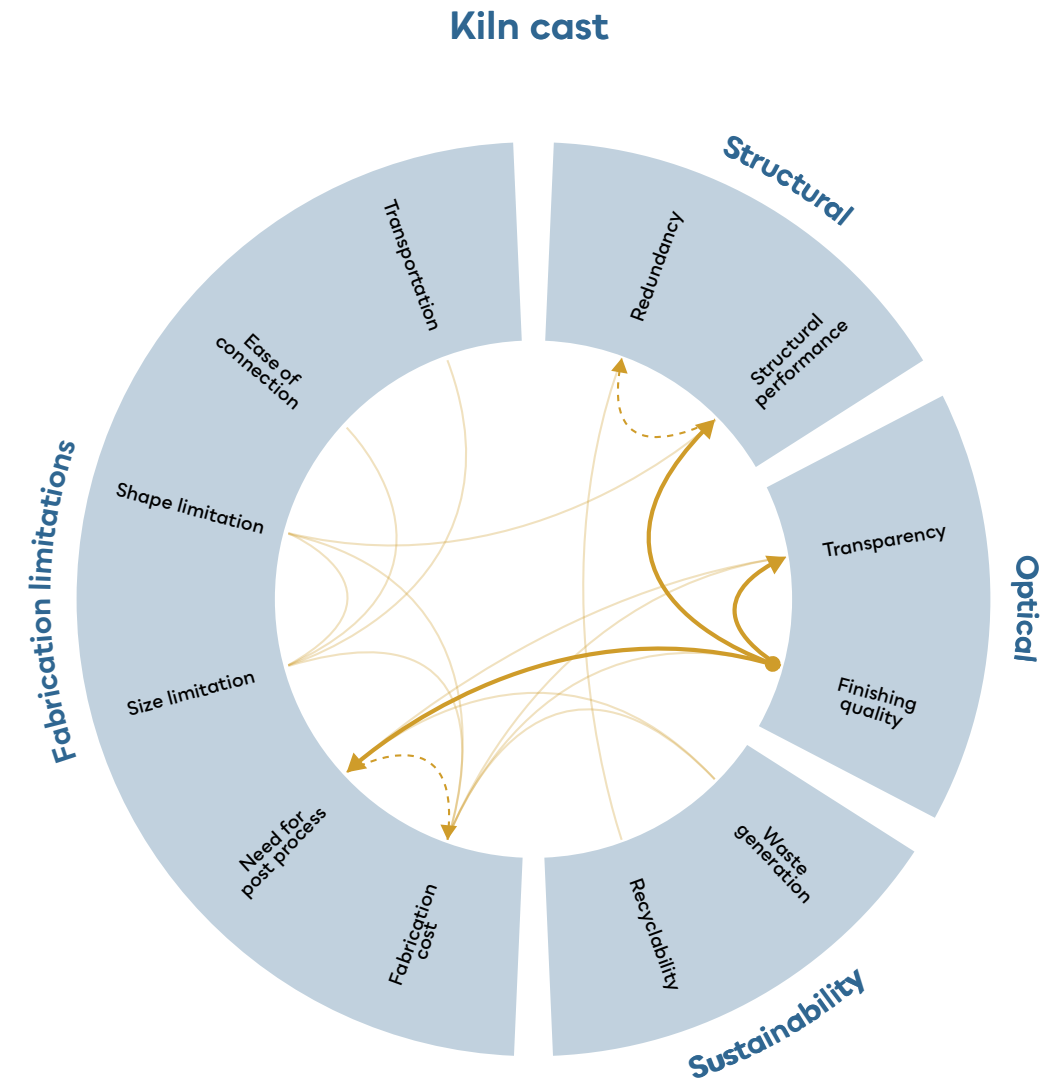


Figure 88 : Finishing quality effect on different domains of kiln cast glass, focus on transparency and need for post processing.

6.2. Experiments set up

The lab experiments would not have been possible without the contribution of ExOne which provided the 3DPSM and Hüttenes Albertus that offered the coatings.

6.2.1. Moulds

The moulds used in those experiments are produced through binder jetting additive manufacturing method using Inorganic binder. Two types of sands were tested (Figure 89): quartz (white colour) and ceramic/ synthetic (terracotta colour). The moulds were printed into two geometries (Figure 89): a bar and a cube geometry with a cylindrical hole. The former is used for the annealing schedules experiment (first set) and the latter for the

coating experiments (second set).

Binder

Inorganic binder used on the provided moulds is preferred over other binders for its relative low cost and its non-toxic nature (Szymański & Borowiak, 2019). Inorganic binder is based on a sodium silicate chemistry (water glass). This means that the cured moulds are hygroscopic and should be used in the shortest time possible or stored on a low humidity environment (ExOne, 2023). The use of water based coatings can be detrimental for the binder capacity and spirit based coatings are usually preferred ('Coatings for Moulds and Cores', 2000). If an aqueous coating is used, it should be dried as soon as possible either by use of hot air blower or by placing the mould into an oven at 180-250°C for 10-60 minutes (Roller et al., 2016).

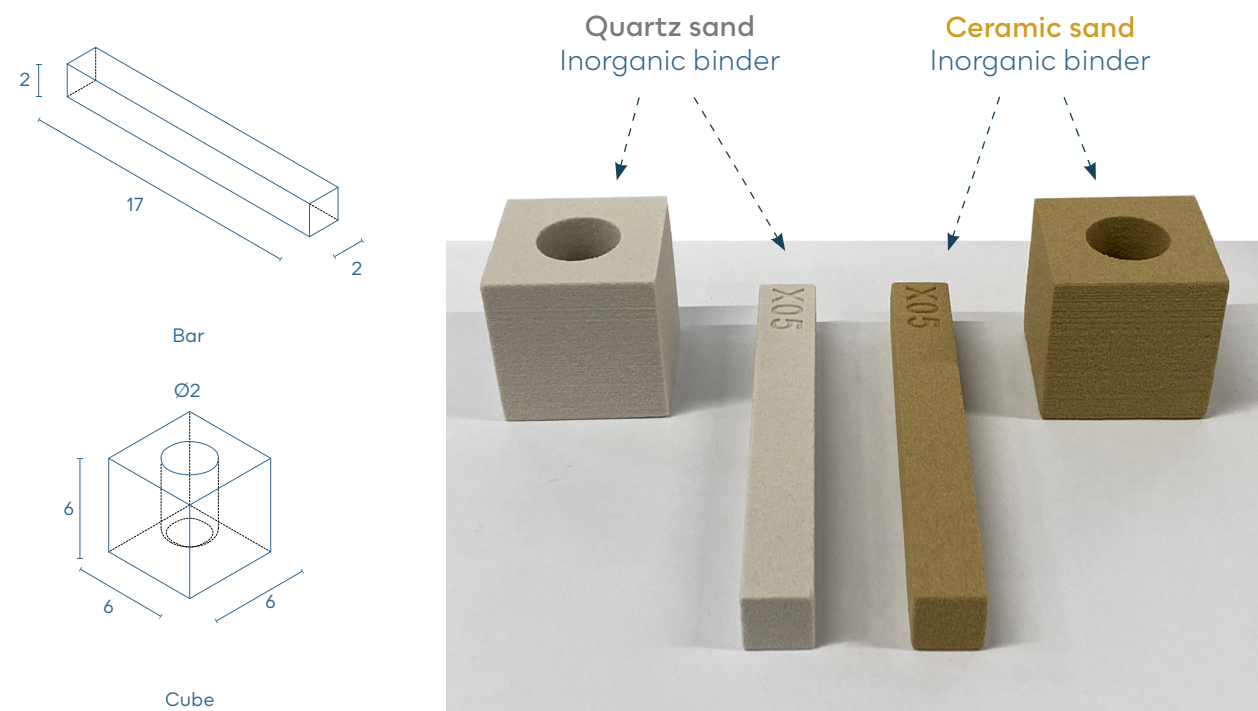


Figure 89 : Mould geometries and types of sands used for the experiments (dimensions in cm).

Cast properties can be adjusted by dosing various additive quantities and the strength of the printed cores is regulated by the amount of binder (ExOne, 2023). The amount of binder is somewhat determined by the thermal expansion coefficient of the sand. In the case of quartz sand moulds, the expansion coefficient of the sand is greater than that of the ceramic sand, thus requiring higher amount of binder to maintain its form during casting³⁵.

6.2.2. Coatings and protective layer

Coating materials are usually comprised of one or more base materials, binders, and pH regulators. These materials are suspended in a liquid carrier (Roller et al., 2016) which for Zirkofluid is isopropanol and for Arkopal B 5 is water. Zirkofluid is based on zircon silicate. The different numbers symbolize different grain size, fine grain for the 6672 and coarser for the 1219³⁶. Arkopal B 5 is based on graphite.

The coatings and protective layers used during those experiments, their solvent as well as the dilution ratio per application method are summarized in Table 12 and Table 13.

Table 12: Comparative table of the 2 version of FDM printers developed by MIT, edited from (Inamura et al., 2018)

Name	Solvent	Dilution (Flow/ Immersion application) ³⁷	Provider
Zirkofluid 1219	Isopropanol	~ 40% wt.	Hüttenes Albertus
Zirkofluid 6672	Isopropanol	~ 10% wt.	Hüttenes Albertus
Arkopal B 5	Water	~ 30% wt.	Hüttenes Albertus

35. Personal communication with ExOne (Andreas Müller and Leonhard Stöckle)

36. Personal communication with Hüttenes Albertus (David Hein)

37. Personal communication with Hüttenes Albertus (David Hein)

Table 13: Protective layers used during the experiments.

Name	Solvent	Dilution (Brush application)	Provider
Shelf-primer	Water	N/A	Bullseye glass Co.
Crystalcast	Water	~ 33% wt. (2/1 ratio) ³⁸	Provetro gruppo

6.3. Annealing schedules

The offered 3DPS moulds are typically used for foundry casting (hot pouring) of aluminium or iron which takes place at lower temperatures and considerably lower contact time and considerably less exposed time to high temperatures when compared to glass. Indicative in the work of (Anna Gowsalya & E. Afshan, 2021) temperature of molten aluminium don't exceed ~850°C and max temperature for the mould is not above 200°C. The behaviour of such moulds for kiln casting has not been tested above 900°C (Bhatia, 2019; Giesecke & Dillenburger, 2022) and for prolonged exposure to high temperatures necessary for the proper annealing of glass components.

This series of experiments explores the following for kiln casting of glass on disposable 3DPS moulds:

- the maximum service temperature
- the effect of prolonged exposure to heat
- the effect of coatings and maximum temperature on the ability to cast glass
- compatibility of coatings and sand

The moulds described at 6.2, are placed in the oven following different annealing cycles. Results are evaluated qualitative: 1) through visual inspection and 2) by scratching the surface.

Different annealing schedules (Figure 89) with different max. temperature and heating up rate are tested. In total 4 annealing schedules with 3 distinct maximum temperatures: 1120°C, 970°C and 870°C. For the schedule of 1120°C two heating up rates are tested: 50°C/h and 30°C/h. Depending on the maximum firing temperature a different composition of soda-lime glass is used: float glass for 1120°C and Bullseye (Tekta AK90) for 970°C and 870°C schedules. All tests are performed inside a Rohde ELS 1000 S.

While this series of experiments focuses on the behaviour of the mould on different annealing schedules and max. temperatures, coatings are introduced to have an overview of the final set up and get insight for the next series of experiments. To do so small dents are scraped off the surface of the bar shaped moulds using a small spoon (Figure 91). Different coatings are applied on the small cavities, left to dry and then glass shards are placed in them. The set up is then placed in the oven. The coatings used on those experiments can be seen at Table 12. The coatings are applied undiluted for brush application and diluted for flow or immersion application.

38. Diluted based on ease of application decided by author.

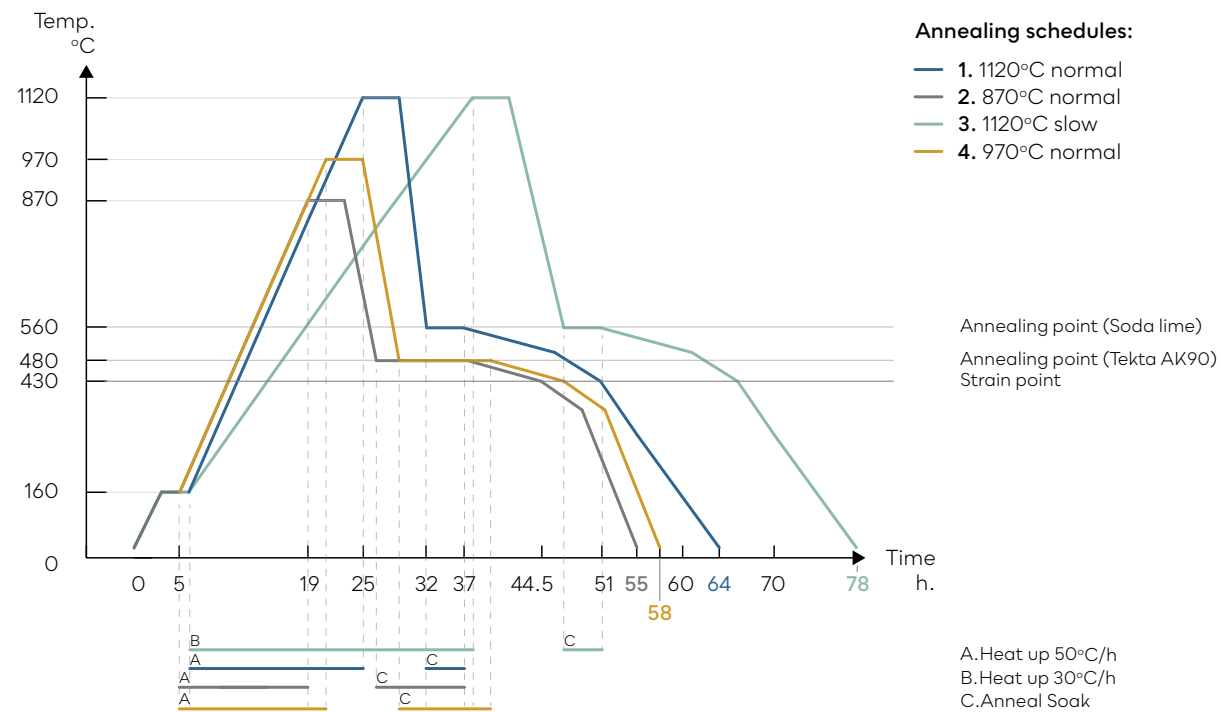


Figure 90 : Annealing schedules used for the experiments of this chapter. Temperature - time graph.

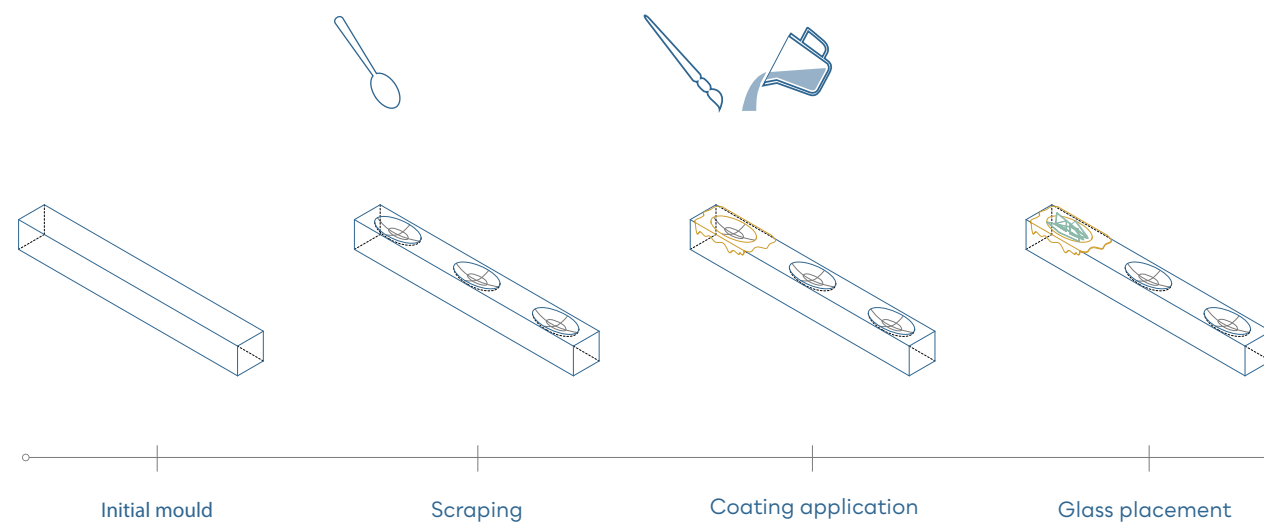


Figure 91 : Preparation of bar shaped moulds for annealing schedule and coatings tests.

6.3.1. Quartz sand moulds

The annealing schedule 1120°C normal (Figure 90) was tested first. For quartz sand moulds (white colour) this temperature proved to be unsuitable for glass casting. Tests at this schedule result in mould cracking at multiple points and glass adhesion to the sand and coating. Mould has no bearing capacity after firing and collapses at touch. After adjusting the firing schedule by reducing the heating up slope from 50°C/h to 30°C/h (1120°C slow)

and embedding the bars in sand the results were less intense in terms of cracking, but glass still penetrates the mould and adheres to it.

Tests at 970°C yielded interesting results. An untreated bar was placed on top of the sand and two that went through the process described at (Figure 92) were embedded in sand. The untreated one showed no cracks after firing. The mould material scrapes easily after firing but displays better carrying capacity. The coated bar shaped samples

6.3.2. Ceramic (synthetic) sand mould

had cracks only were the Zirkofluid 1219 and 6672 was applied regardless of the application method. This is the first indication of some kind of coating incompatibility in terms of thermal expansion coefficient between the sand of the mould, the coating and glass. This result is also contradictory to the finding on literature which suggest spirit-based coatings (e.g., Zirkofluid) over water based (e.g., Arkopal B 5 (graphite water)).

Finally tests at the lowest temperature (870°C) displayed the expected results in terms of mould integrity and casting quality for glass. Glass doesn't penetrate the mould at this temperature but adheres to the coating and sand making it hard to remove. Arkopal B 5 applied via brushing (undiluted) resulted in a somewhat transparent surface with minor sand adhesion.

Ceramic sand moulds (terracotta colour) performed differently than the quartz sand moulds. This type of mould maintained its integrity even at 1120°C. While the integrity of the mould is not an issue glass adheres to the sand making it impossible to have a clear and transparent surface. General observation at all temperatures is that this mould became harder after firing. De-moulding is hard and requires immersion of the mould in water and the use of hammer to free the glass piece. This observation is in line with the work of (Szymański & Borowiak, 2019) that mentions that inorganic binder gains higher final strength making release more difficult. According to (ExOne, 2023) the strength of the cores is determined by the amount of binder used. In fact on ceramic sand moulds lesser amount of binder is used compared to quartz sand³⁹. Ceramic sand manufactured using a full synthetic sand that has spherical shape and displays low expansion (Figure 94), allowing for the use of lower amount of binder to obtain the same adhesion between sand grains.



Figure 92 : Results for quartz sand moulds and different annealing schedules, 3DPS mould specimens after the firing schedule.

39. Personal communication with ExOne

6.4.2. 1120°C normal

As seen in the table above three types of moulds were used, Quartz sand, ceramic sand and Crystal-cast moulds (based on silica plaster, produced by investment casting on a reusable mould positive).

Quartz sand moulds were coated with:

- single layer of the three coatings (brush and flow application),
- triple layer of crystal cast (brush) and two times immersion of a) Zirkofluid 1219 plus Arkopal B 5 and b) Zirkofluid 6672 plus Arkopal B 5

- two times immersion Arkopal B 5

Ceramic sand moulds were coated with:

- a triple layer of crystal cast (brush) and two times immersion of a) Zirkofluid 1219 plus Arkopal B 5 and b) Zirkofluid 6672 plus Arkopal B 5

- a triple layer of Crystalcast (brush) and two times immersion of Zirkofluid 6672

- two times immersion Arkopal B 5

The Crystalcast moulds have been coated with:

- two times immersion of a) Zirkofluid 1219 plus Arkopal B 5 and b) Zirkofluid 6672 plus Arkopal B 5

Overall results of those application are that sand, coating, and protective layers attach to the glass. This depends on the combination of protective layer and coating but the results regarding the sand cores are consistent. Glass cast on Crystalcast showed less consistent results. During de-moulding specimens coated with Zirkofluid (1219 and 6672) displayed surface chipping and breaking. The ones coated with Arkopal B 5 maintained the shape and integrity but have a rough and opaque finishing quality.

6.4.3. 970°C normal

Initial tests at 970°C and application of the three main coatings via brush and flow (single and double) at both sands (quartz and ceramic) displayed similar results with the ones at 1120°C. Sand adheres to the glass specimens. While results are not promising in terms of finishing quality, they indicate that some coatings are more compatible with a specific type of sand.

Quartz sand

The combination of quartz sand mould and zirkofluid coatings led to cracking of the coating layer. The cracking of the coatings allows glass to penetrate the mould and attach to the sand. Samples examined from the contact side have intricate veining patterns matching the shape of the cracks on the coating. From top glass shows cracking. Graphite based coating (Arkopal B 5) does not display any cracking of the glass or of the coating (Table 16).

Ceramic sand

For ceramic sand moulds the results are similar but with the exact opposite compatibility. In this case veining is not noticed but cracking of the glass is present on specimens treated with Arkopal B 5. Noteworthy is the fact that samples coated with Zirkofluid 6672 (both flow and brush application) failed spontaneously long after the release from the mould. As discussed in the annealing schedule experiments chapter cores fabricated with this kind of sand were difficult to separate from the cast element. The sample that was not coated cracked in half when trying de-moulding. The use of a hammer for de-moulding might be one of the reasons leading to the spontaneous failure of the above-mentioned samples. Another possible explanation is that the combination of coating, sand type and glass have different expansion ratios that lead to stress concentration which is released after de-moulding (Table 16).

Coatings compatibility

The possible incompatibility of the sand can be caused partly by the difference in the expansion coefficient of the materials. (Roller et al., 2016) suggests that ceramic sand has similar expansion coefficient/temperature curve with zircon sand. While the expansion coefficient of the zircon-based coatings might be different this can be a good approximation. Data for graphite⁴⁰ are not consistent. Expansion coefficient values for graphite were retrieved from Granta EduPack 2022 R1 (Table 15) and were converted to expansion percentage using the following formula:

$$\Delta L = \frac{\alpha \times \Delta T}{L_0} \times 100, (\%)$$

ΔT = temperature difference (°C),

α = Linear thermal expansion coefficient (°C⁻¹)

L_0 = initial length (m), 1 m

There is no correlation between the expansion coefficient of graphite-based coatings and quartz sand. The expansion of soda lime glass is higher than that of ceramic sand and lower than that of quartz sand. This graph suggests that quartz sand might be preferred over ceramic sand mould for casting of glass when thermal expansion coefficient is taken into consideration. For proper casting of glass integrity of the mould need to be taken into consideration. As mentioned before ceramic sand mould maintain its bearing capacity after firing making it ideal for larger scale prototypes.

Table 15: Expansion coefficient of graphite and soda lime glass as percentage of the initial length.

	Linear thermal expansion coefficient $\alpha(10^{-6}/^{\circ}\text{C})$	Temperature (°C)	Expansion %
Graphite	2.09	20	0
	2.9	409	0.113
	3.56	798	0.138
	4.08	1190	0.159
	4.5	1580	0.175
Soda lime	9	0	0
	9	300	0.27

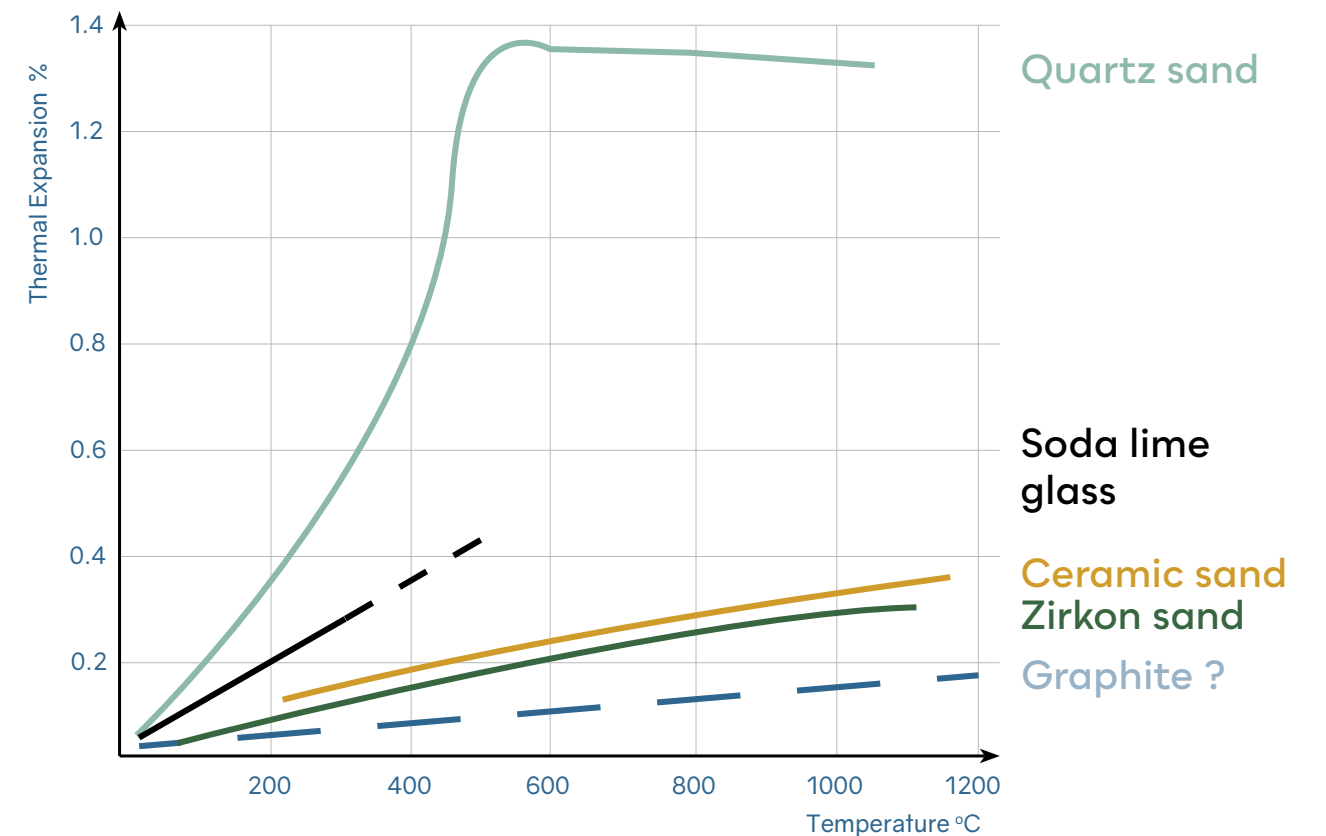
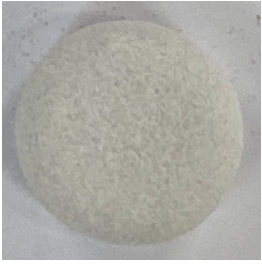
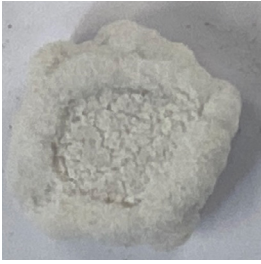
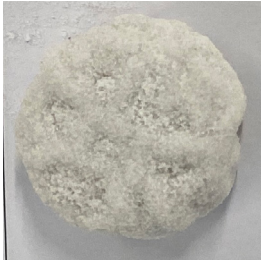
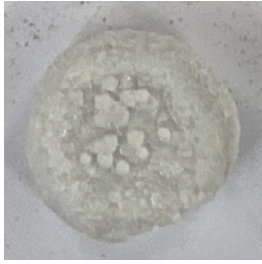
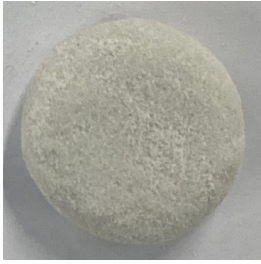


Figure 94 : Thermal expansion (%), temperature (°C) graph, edited form (Roller et al., 2016)

40. Data are retrieved for pure graphite to get a measurable approximation of the expansion coefficient of graphite-based coatings.

Table 16: Results at 970°C for quartz sand and ceramic sand moulds. Veining pattern is visible on the contact surface when isopropanol-based coatings are applied on quartz sand moulds. Application of the water-based coatings on ceramic sand mould results in cracking of the glass.

Annealing schedule	Protective layer	Sand type	Side	Coatings						Coating	
				No	Zirkofluid 1219		Zirkofluid 6672		Arkopal B 5		
					Flow	Brush	Flow	Brush	Flow		Brush
970°C normal	No	Quartz sand	Contact								2X
			Top								
		Ceramic sand	Contact								
			Top								

Protective layer (Table 17)

Thus far the experiments have resulted in an opaque and rough surface. A protective layer between the mould and the coating was introduced. Two materials were used: Crystalcast and Shelf-primer (kiln wash). The protective layer was applied with the use of soft natural brush (brush application) on three layers with a minimum drying time at room temperature of 1.5 hrs. between each layer. The former one is used in the glass lab of TU Delft for investment casting, through lost wax technique and it is based on silica plaster and has been tested successfully on temperatures of up to 1000°C (Oikonomopoulou, Singh Bhatia, et al., 2020). The latter is used as a separator for glass with unknown maximum service temperature.

Shelf-primer

Results from the shelf-primer on quartz sand moulds and single flow application of the three coatings are not promising. Glass adheres to the sand making the separation impossible. Further testing is advised using ceramic sand moulds.

Crystalcast

This protective layer displayed the first relatively good results at this temperature in terms of transparency and surface quality of the contact side. For the initial testing, a single layer of Zirkofluid 1219 and of Akropal B 5 was tested yielding the first satisfactory result. Samples were cleaned using water, isopropanol and a sponge. Surface is not perfect but sand is not attached to the contact side. The next batch of specimens were coated with two layers of coating via brush and flow application (Table 18). In the latter set of specimens the higher thickness of the coatings did not deliver better surface quality results. Coatings attached to glass making it impossible to separate. The next logical step is to reduce the temperature to 870°C and evaluate the best combinations of sand, coating, protective layer and application method.

Table 17: Overview of the protective layers used at 970°C with quartz sand moulds and ceramic sand moulds.

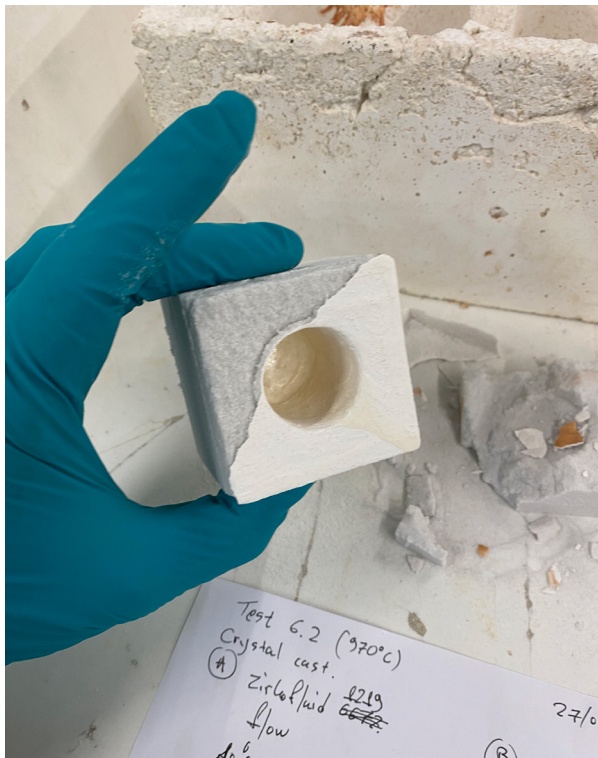
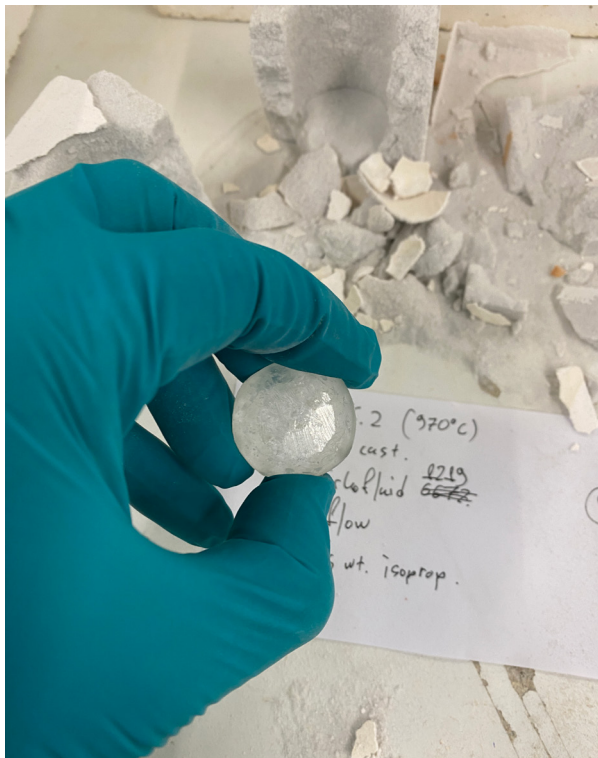
Annealing schedule	Sand type	Protective layer	Overview	Top	Contact
			970°C normal	Quartz sand	Crystalcast
	Ceramic sand	Shelf-primer			

Table 18: Surface quality of the contact side, first row for single layer of coating and bottom row for dual coating application. Images in orange frame ceramic sand moulds, rest quartz sand moulds. Justification of the reason some of the experiments were not conducted can be found at the bottom left.

Annealing schedule	Protective layer	Sand type	Side	Coatings						Coating	
				No	Zirkofluid 1219		Zirkofluid 6672		Arkopal B 5		
					Flow	Brush	Flow* (2X)	Brush	Flow		Brush
970°C normal	Crystalcast 3X Brush	Quartz sand	Top	1.		2.		2.		2.	1X
			Contact								
		Ceramic sand	Top	1.		2.		2.		2.	
			Contact								

Reasons why experiments were not conducted:

1. Similar to casting on Crystalcast mould
2. Protective layer is used so coatings behaviour is expected to be similar regardless of the mould sand

6.4.4. 870°C

From the annealing schedule experiments, we have some preliminary indication that this is the ideal temperature for kiln casting of glass using 3DPSM. More extensive experimentation at this temperature shows promising results. Considering the results from the previous tests at higher temperatures only Crystalcast has used as protective layer and applied Arkopal B 5 on quartz sand moulds and Zirkofluid 1219 and 6672 on ceramic sand moulds. The best results are summarized in Table 20.

Quartz sand

The best results in terms of transparency and optical quality are observed when a dual layer of Arkopal B 5 via brushing is applied directly on the coating. Each layer has been dried using a hot air blower immediately after application to minimize the detrimental effect of the water-based coating on the binder. The use of crystal cast does not further improve the surface quality.

Ceramic sand

Application of Zirkofluid 1219, 6672 by either brush or flow application direction on the mould yielded opaque contact surface. The use of Crystalcast as a protective layer showed really promising results, especially 6672 (flow). The latter offered the best surface quality and transparency.

Coatings on Crystalcast moulds

The idea of applying the coatings directly on crystalcast moulds emerged while de-moulding some of the moulds that had protective layer. Crystalcast even after firing maintained its integrity forming a thin wall casting vessel/mould as it can be seen in Figure 95.

The three coatings were applied on two layers via brush method. The results are especially promising for Zirkofluid 1219 and 6672. Noteworthy is the fact that while glass surface is transparent is not totally smooth. The brush strokes from coating application are visible which suggests that flow or immersion application method might be more suitable to achieve the best surface quality (Table 19).



Figure 95 : Crystalcast protective layer after de-moulding from quartz sand mould.

Table 19: Surface quality of glass cast on crystal cast moulds and the use of the 3 coatings, application of the coating two times using a brush. Brush strokes are visible.

Annealing schedule	Mould type	Side	Coatings			Coating
			Zirkofluid 1219	Zirkofluid 6672	Arkopal B 5	
			Brush	Brush	Brush	
870°C normal	Crystalcast mould	Top				2X
		Contact				

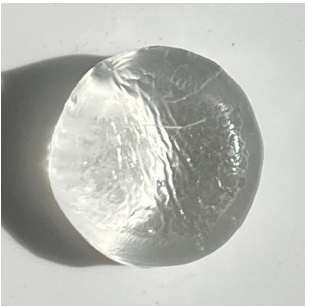
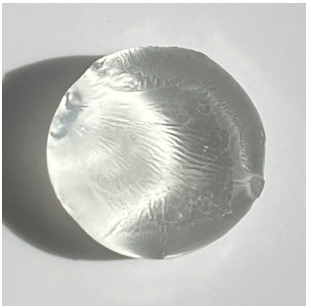
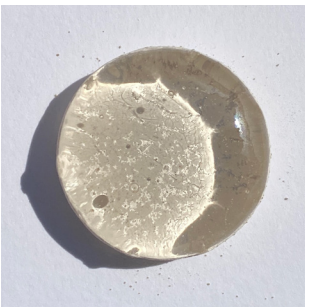
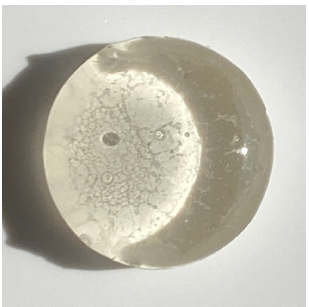
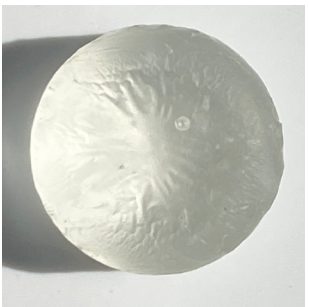
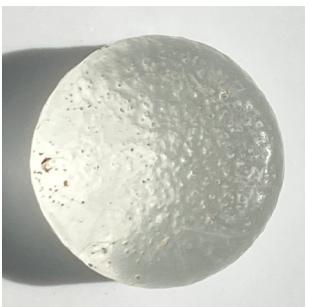
Table 20: Surface quality of contact side at 870°C normal with (top part) and without (lower part) the use of a protective layer. Justification of the reason some of the experiments were not conducted can be found at the bottom left. Continues at the next spread.

Annealing schedule	Protective layer	Sand type	Side	Coatings						Coating	
				No	Zirkofluid 1219		Zirkofluid 6672		Arkopal B 5		
					Flow	Brush	Flow	Brush	Flow		Brush
870°C normal	Crystacast 3X Brush	Quartz sand	Top	1.	2.	2.	2.		4.	2X	
			Contact								
	No	Quartz sand	Top	2. & 3.	2. & 3.	2. & 3.					
			Contact								

Reasons why experiments were not conducted:

- 1. Similar to casting on Crystacast mould
- 2. Possible coating and mould sand incompatibility
- 3. Coatings applied on a single layer on initial tests. Results were not promising
- 4. Not tested since results for brush application without the use of coating were good

Table 20: continue

Annealing schedule	Protective layer	Sand type	Side	Coatings						Coating	
				No	Zirkofluid 1219		Zirkofluid 6672		Arkopal B 5		
					Flow	Brush	Flow	Brush	Flow		Brush
870°C normal	Crystacast 3X Brush	Ceramic sand	Top	1.		2.		2.		2.	
			Contact								
	No	Ceramic sand	Top						2.		
			Contact								

2X

Reasons why experiments were not conducted:

1. Similar to casting on Crystalcast mould
2. Brush application is less preferred as it leaves visible brush marks on the surface of the mould and glass (after casting).

6.5. Hot pouring

Additional testing at 1380°C has been performed using the hot pouring method. Even though the focus of the thesis is kiln casting, this test was conducted as it can provide good insight on the factors that affect the surface quality, such as 1. heat, 2. total exposure time on high temperature and 3. the combination of the two. After hot pouring the specimens were placed directly in the annealing oven at 480°C following the part of the schedule of 870°C normal after the 26 hrs. mark (approximate total dwell time 28 hrs.).

For this experiment two types of glass were used: a. Bullseye (3 crucibles) and b. John Lewis recipe (1 crucible). The glass was heated up at 1380°C (dwell for approx. 1 hr.) and then poured into the 3DPSM. The protective layer and coating combinations used are:

- 1) Quartz sand + Arkopal B 5 application 2x Flow (6 s.) + Bullseye glass
- 2) Quartz sand + Arkopal B 5 application 2x Flow (6 s.) + John Lewis glass
- 3) Quartz sand + Zirkofluid 6672 2x Flow (6 s.) + Arkopal B 5 application 2x Flow (6 s.) + Bullseye glass
- 4) Ceramic sand + Zirkofluid 6672 2x Flow (6 s.) + Bullseye glass

After de-moulding all specimens presented a contact surface with no sand or coating adhesion. The last two specimens (3, 4) displayed uneven surface quality which was considerably better at top and bottom of the glass piece. During the hot pouring flames and smoke were present on samples 3 and 4. Smoke entrapment is visible inside the glass (black spots, Table 21) and crystallization zones in the middle of those specimens. Overall, in all samples and regardless of the coating used the bottom contact surface has inclusions in high density when observed under the microscope. The side contact surface presents less inclusions. This test, while successful in terms of sand adhesion, indicates that hot pouring at lower temperature might display better surface quality with less inclusions and inhomogeneity. This test confirms that there is a correlation between, temperature and exposure time, in the effectiveness of the coating. It seems that the maximum temperature has less influence on the effectiveness of the coating with time been the key factor.

Table 21: Hot pouring results, contact and side surface

Annealing schedule	Protective layer	Sand type	Side	Coatings				Coating
				Arkopal B 5	Arkopal B 5 (John Lewis)	Zirkofluid 6672	Zirkofluid 6672 + Arkopal B 5	
				Flow	Flow	Flow	Flow	
870°C normal	No	Quartz sand	Contact					2X
			Side					
	Crystacast 3X Brush	Ceramic sand	Contact					
			Side					



Figure 96 : Hot pouring of glass on 3DPSM, left: Telesilla Bristogianni, right: author, image credits: Marcel Billow



Figure 97 : Hot pouring of glass on 3DPSM, cutting of glass string, behind: Telesilla Bristogianni, front: author. Image credits: Marcel Billow

6.6. Conclusions

The experimental work conducted thus far indicates, that at 870°C annealing schedule, the combinations with the best finishing quality are (i) moulds printed with quartz sand coated with Arkopal B5® or Crystalcast and Arkopal B5 and (ii) moulds printed with synthetic (ceramic) sand coated with Crystal Cast and Zirkofluid® (6672, 1219) implying that 3D-printed moulds from Crystalcast could be a promising solution. Especially, the combination of Crystalcast and Zirkofluid 6672 applied on ceramic sand moulds gave very promising results in terms of surface quality. Nevertheless, the application process is complex. Crystalcast is diluted on water and Zirkofluid is based on isopropanol which means that the protective layer needs to be completely dry before the coating is applied. Zirkofluid 6672 requires special respiratory protection. Those peculiarities result in a thick coating layer which can compromise the dimensional accuracy⁴¹ and increase the cost. Even though the application of a water-based coating (Arkopal B5) on a water glass binder is detrimental to its structural integrity, application of Arkopal B5 directly on quartz sand mould offers the second-best surface quality and has a simpler application method with the only drawback being the need for quick drying after application. The latter is only true when the coating is applied via brush. When the same coating is applied via flow directly on quartz sand mould the results are not good (Table 20). Flow application most likely results in a thinner layer due to the dilution ratio and has higher water content that reacts with the binder.

Another downside of brush method is that in larger and more complex shaped moulds all point cannot be reached efficiently, and brush strokes will be visible on the glass surface. For this reason, flow application of the coating is preferable and easier to automate on larger scale production. This can be an issue for the protective layer as well. Currently the protective layer is applied using a brush.

Personal communication with ExOne indicated that higher amount of binder is used on quartz sand mould compared to ceramic sand ones to account for the higher rate of expansion of the sand. This can possibly explain why ceramic sand mould displayed poor surface quality and penetration of glass when combined with a water-based coating at 970°C. In this case the lesser amount of binder is more severely affected, leading to inferior surface quality and compromised integrity of the mould. Or

41. The difference in diameter of the cylindrical samples with and without the use of Crystalcast as measured on one sample at the lab is 5mm. This translates to an approx. 2.5 mm difference in radius of offset when designing an object. This accuracy is proportional to the size of the object but can be crucial for smaller components or details.

in other words, one can conclude that the higher amount of binder on quartz sand mould and quick dried had a less severe effect on the carrying capacity resulting in good surface quality. The tests at 970°C were conducted without quick drying of the Arkopal B5 coating which could have affected the results. The application method as well as the dilution of the coatings also affects the effectiveness of the coating as observed on the application of Arkopal B5 directly on quartz sand mould.

Overall, regarding the annealing cycle, there seems to be a correlation between time and maximum temperature, affecting the effectiveness of the coatings. This assumption is verified by the hot pouring experiments. During the hot pouring experiment coatings and moulds were exposed to maximum temperature of approx. 1380°C for a short period of time (minutes) and annealed for 28 hrs. at temperatures lower than 480°C. The kiln cast samples at 970°C were exposed to temperatures higher than 480°C for 30 hrs. and annealed following the same schedule as the hot poured samples. The fact that the results of kiln casting at 970°C were poor (sand and coating adhesion to glass) while the hot pouring samples had a transparent surface indicates that the prolonged exposure to high heat greatly affects the performance of the coatings. Up to today the optimum annealing schedule for kiln casting of glass on such moulds is the 870°C normal (55 hrs. total dwell time). Even at this temperature the discolouration of the coatings is visible and can be observed in the Figure 99 where Arkopal B5 coating applied on same type of mould and with same application method.

Finally the roadmap of the experiments arriving at the optimum set up can be seen on Figure 101.

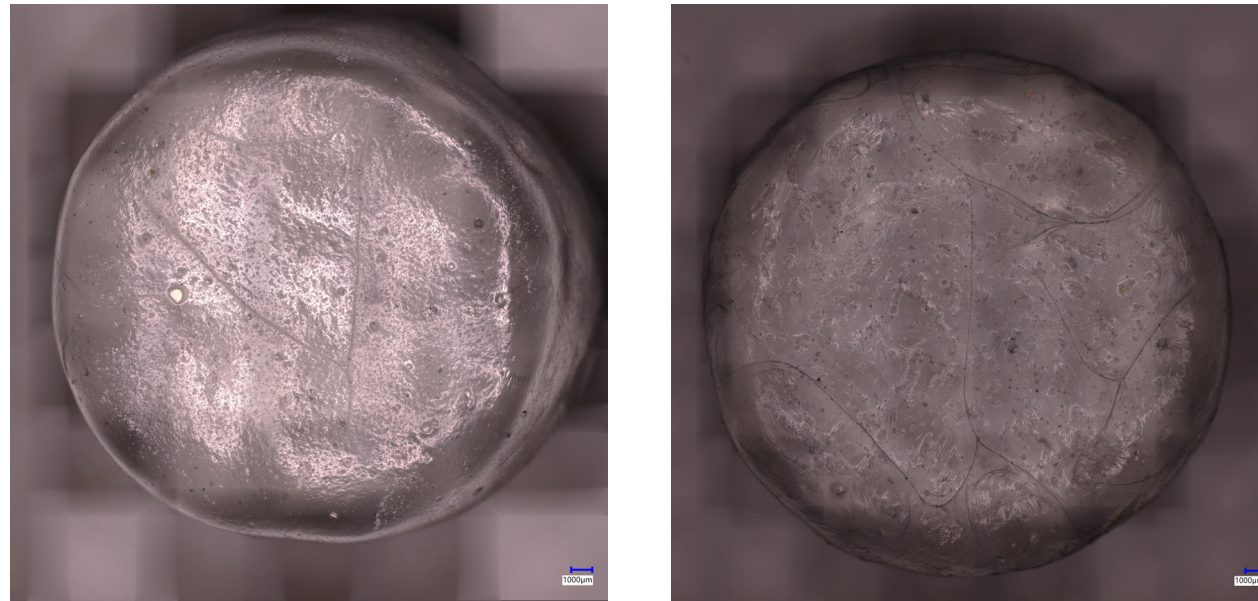


Figure 98 : Microscope images of the surface quality of the most promising moulds, coatings, and annealing schedule (870°C) combination.



Figure 99 : Left Arkopal B 5 applied on quartz sand mould two times via flow application after the annealing schedule at 870°C.. Right same set up after hot pouring and annealing of glass. Colour difference is a clear indication of some kind of deterioration of the coating due to the prolonged exposure to high temperature.

6.7. Discussion – Next steps

The two set of experiments gave a good understanding of the challenges involved on kiln casting of glass using disposable 3DPSM. As seen on the experiments above, the optimal set up is defined by a plethora of factors (Figure 100):

- the annealing schedule,
- the difference in thermal expansion coefficient between glass, sand and coating,
- the binder (amount),
- the type of sand,
- the application method and
- the coatings used.

To achieve the best optical and surface quality all the above-mentioned factors should be taken into consideration. The maximum firing temperature and the total dwell time are detrimental for the mould integrity but can also reduce the effectiveness of the coatings used. Thermal expansion coefficient of the moulding material, glass and coating are important on the final surface and optical quality. The amount of binder (also defined by the sand type) can result in different coatings compat-

ibility. Different application methods also affects the surface roughness with flow or immersion been the most prominent ones. Finally, the coating in combination with the application method and the thickness of its layer have the greater impact on the surface quality of kiln cast glass.

The quest to arrive at a smooth and transparent surface quality is not complete and still requires further experimentation at 870°C with the most prominent combinations of coatings by scaling up and increasing the complexity of the geometry. Scaling up the geometry will require longer dwell time at higher temperatures to allow for proper melting and complete casting. The extra time as seen on the experiments can have detrimental effect, but the magnitude of its affects is still unknown.

Apart from that more extensive testing with thicker layer, e.g., 2x Immersion, and quick drying of the water-based coatings after application at 970°C schedule is advised to arrive at more complete conclusions for this temperature.

Finally, tests using Crystalcast moulds and flow application of the coatings is also advised to confirm that the surface quality and transparency is better than that of brush application.

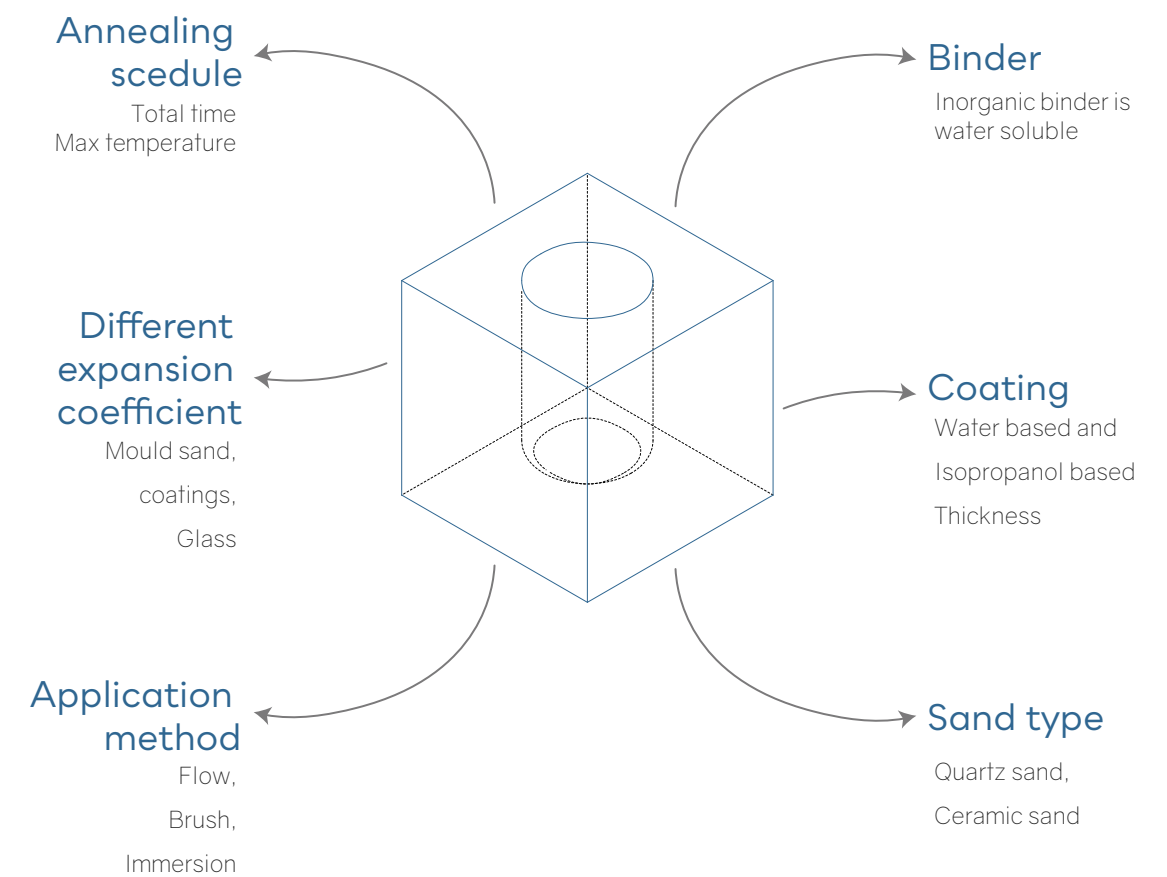
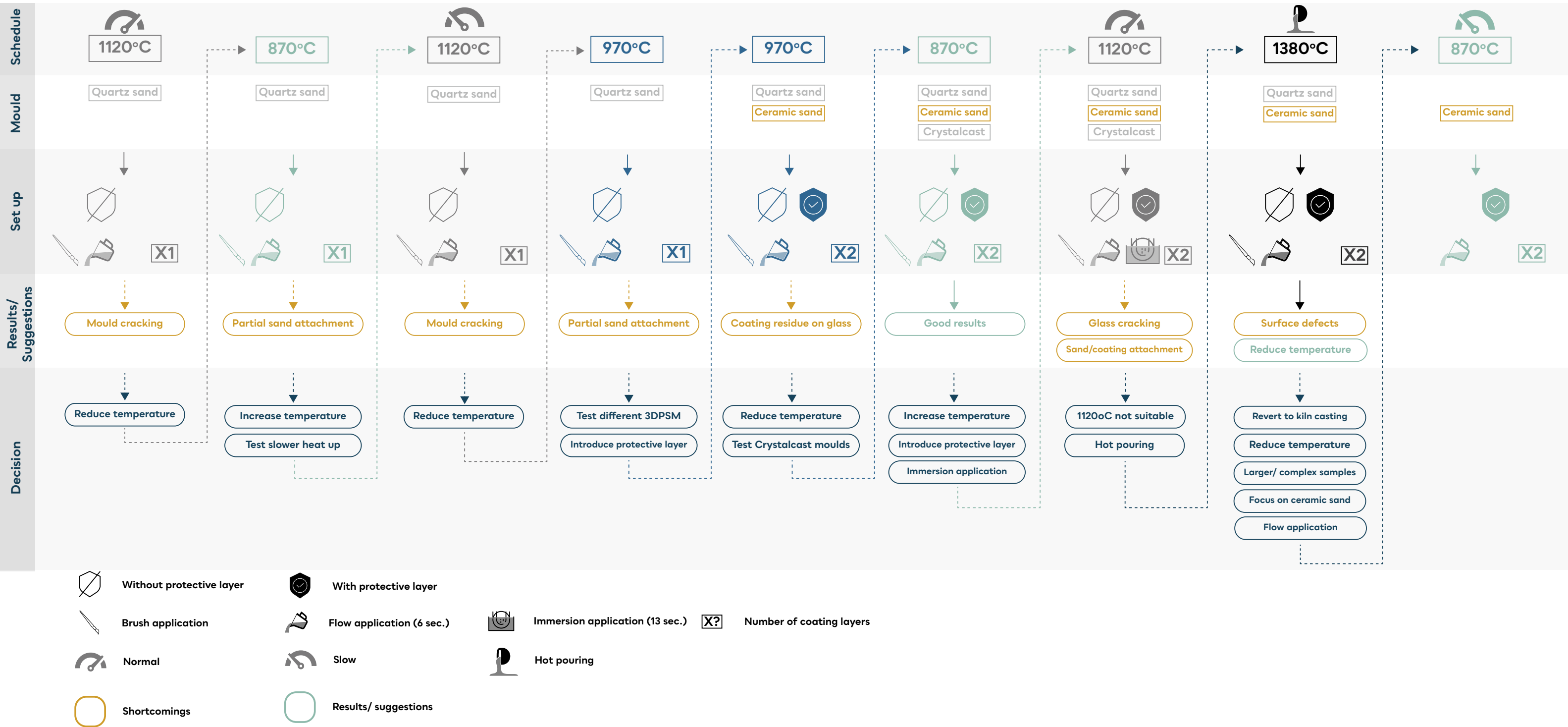


Figure 100 : factors that affect the surface quality of kiln cast glass using 3DPSM.

Figure 101 : Decision roadmap of the experiments conducted arriving at the optimal set up. The optimal set up concluded is: ceramic sand moulds coated with Crystalcast protective layer and flow (x2) application of Zirkofluid 6672. This set up is going to be further tested on larger scale geometry with a more complex form.



7

FINAL DESIGN & REDUNDANCY

This chapter described the process of design of the case study and aims at answering the second research sub question:

Focusing on kiln-casting using disposable 3D printed sand moulds (3DPSM):

- b. How to improve redundancy and safety of structural glass elements?
 - i. In which ways can design help improve safety of cast glass structures?

Ir. Anna Maria Koniari kindly offered her expertise and her custom developed Matlab TO code for glass making the optimization of the design possible. Due to limitation on the RAM (random access memory) required for the calculations the optimization simulations were held using a desktop computer with 2 Intel(R) Xeon(R) CPU E5-2640 v4 @ 2.40GHz processors and 64 GB installed RAM which has kindly offered by Ir. Hans Hoogenboom from VR-lab. Even with this amount of RAM the number of finite elements that could be used where limited to approx. 2100. Post processing of the output values using McNeal's Rhinoceros 7 and grasshopper plug was necessary to arrive at the final pseudo-3D geometry. The process is presented in the following chapter starting by introducing the limitations of current software and going through the custom algorithm developed by A. M. Koniari.

7.1. Software limitations

“TOPOLOGY OPTIMIZATION OF SOLID STRUCTURES INVOLVES THE DETERMINATION OF FEATURES SUCH AS THE NUMBER AND LOCATION AND SHAPE OF HOLES AND THE CONNECTIVITY OF THE DOMAIN.” (Bendsøe & Sigmund, 2004)

Topology optimization in structures is a mathematical way to define the optimal material (isotropic) distribution within a defined domain, under a given set of objectives and constraints. Loads, support conditions, volume of the structure and optionally additional design limitations like location and size of predetermined voids or solid areas are the inputs. The size and the shape and connectivity of the structure are unknown. (Bendsøe & Sigmund, 2004).

The most common topology optimization formulations are:

- Minimization of compliance (maximization of stiffness objective) subject to a volume constraint
- Minimization of stress objective subject to a volume constraint
- Minimization of volume subject to a compliance constraint

A variety of topology optimization software is available nowadays as stated in the work of (Damen, 2019; Koniari, 2022; Koopman, 2021). Different algorithmic methodologies are used with the most prominent been that of SIMP. SIMP is preferred over other methods for its robustness of solution and mathematical validity of the calculations. SIMP briefly returns a black and white (grayscale) raster image of the discretized domain⁴². Each element of the domain gets one value between 0-1. This value defines the pseudo density function $\rho(x)$, where $\rho(x)=0$ stands for void and $\rho(x)=1$ stands for full material (Nathan et al., 2020). This method is sensitive to the number of finite elements. More finite elements results in higher generation of void since more efficient distribution of the mass is possible.

A full categorization of the software can be seen in (Figure 102).

In short, Millipede, Topos, Ameba and Karamba 3D are McNeal Rhinoceros plug-ins. Other commercial software is available such as Ansys Workbench, Autodesk Fusion 360, Simulia ABAQUS, etc. All software has an integrated FEM (finite element method) solver that allows for the verification of the structure produced via topology optimization.

Regardless of the algorithmic methodology that the software uses, the stress constrained topology optimization is usually performed based on von Mises failure criterion. This criterion is effective when used for ductile materials that have similar values of tensile and compressive strength. Glass as stated in chapter 3.6 is a brittle material with a significantly different values for tensile and compressive strength. The use of Drucker-Prager failure criterion is considered more suitable for brittle materials⁴³.

Other limitations are software specific such as the limited number of nodes that can be used in the educational license of ANSYS workbench which leads to time consuming optimization in iteration or the need to use of paid cloud computing time when it comes to Fusion 360.

	Homogenization	SIMP	Level Set	ESO / BESO
		✓	✓	
		✓	✓	
		✓	✓	
 Millipede	✓			
 TOPOS		✓		
		✓		
 Ameba				✓
 Karamba 3D parametric engineering				✓
3D TopOpt App		✓		
	✓	✓	✓	

Figure 102 : Topology optimization software per algorithmic method (Koopman, 2021)

42. Finite elements analysis is based on the discretization of a structural elements to a known number of elements, in a 2D case the domain can be imagined as a grid.

43. This criterion can, according to (Bruggi & Duysinx, 2012), extend the applications of TO application to pressure-dependent materials, such as concrete, polymers and composite structures.

7.2. Custom algorithm for TO of glass (Koniari, 2022)

As part of the MSc thesis of (Koniari, 2022) a custom 2D TO algorithm for cast glass was developed on the commercial coding software MathWorks MATLAB and was based on SIMP algorithm. The introduction of some unique features is necessary to address the peculiarities of glass as a material. These features are divided into two categories: 1. objectives and 2. constrains.

Objectives

Depending on the main objective of the optimization the algorithm can account for either **volume** or **compliance**. The second objective which is always used regardless of the first objective is the **filtering**. Filtering ensures for each iteration that the **minimum dimension** of cross section is respected. The minimum dimension is crucial to avoid fragile parts and small cross sections that can cool down quicker than the rest of the structure leading to stress concentration during annealing. Filtering is also important to avoid some algorithmic limitations, such as the checker board patterns, where structure appear to be stiffer on calculations but impossible to manufacture in real life.

Constrains

When volume is used as the main objective compliance fracture is used as constraint and vice versa. Maximum vertical deflection is used as a constraint based on the allowable deflection (formula $d < 500/L$). The **Drucker-Prager** failure criterion implemented through the introduction of an **asymmetry** ratio - s - defined as the compressive to tensile allowable strength limits such as that $s = \sigma_{comp} / \sigma_{ten}$. Principal stresses are checked with the allowable tension and compression values during the optimization ensuring a structurally feasible result. Finally, combined **annealing and manufacturing** criterion as part of the algorithm, checks the cross-section dimension with the maximum annealing time is within the limit set by the user. All parts of the structure should fall within a range to allow for homogeneous shrinkage and stress-free annealing of the glass component. Calculation of the maximum annealing time needed is done using Equation 2.

Table 22: Objectives and constrains as presented in the work of (Koniari, 2022).

	Main objective	Filtering	Volume	Compliance	Deflection	Principal stresses	Annealing & Manufacturing criteria	Drucker-Prager failure criterion
Volume	x	x		x	x	x	x	x
Compliance	x	x	x		x	x	x	x

7.3. Load cases

The proposed cantilevering structure is a bridge when it comes to structural calculations. The loading conditions are defined according to Eurocode 1 (EN 1991-1-1, 2002), chapter 6. The structure falls under the category of C5 (area susceptible to large crowds) and the suggested values for the imposed loads and the safety factors for this category of structures are presented in the Table 23.

The most commonly used load cases according to Eurocode 2 (EN 1992-1-1, 2004) for vertical loading, ULS (ultimate limit state) are the following:

- LC1: $s_p \cdot (\text{permanent}) + s_l \cdot (\text{live} + \text{snow})$
- LC2: $s_p \cdot (\text{permanent}) + s_l \cdot (\text{live} + \text{wind})$
- **LC3:** $s_p \cdot (\text{permanent}) + s_l \cdot (\text{live} + \text{snow} + \text{wind}/2)$ (downward facing wind)

LC3 is selected as it is the least favourable resulting in a higher distributed load. The total imposed load according to LC3 is **6.5 KN/m²** (5 KN/m² live + 1.2 KN/m² snow + 0.25 KN/m² downward facing wind) which is multiplied by 1.5 (safety factor) (Figure 103).

For horizontal structures (e.g., balustrades, fall protection e.t.c.) Eurocode 2 according to ULS suggests the following load case:

- LC4 = $s_p \cdot (\text{permanent}) + s_p \cdot (\text{wind}) + s_l \cdot (\text{live}) = 1.35 \cdot (\text{permanent}) + 1.35 \cdot (\text{wind}) + 1.35 \cdot (\text{live})$

Since the algorithm used for the optimization of the structure is developed for 2D, LC3 (ULS) is going to be used for the optimization of the bearing structure. LC4 will be used for the verification of vertical elements in the final design by for hand calculations and using ANSYS workbench.

Another important value to account for before the optimization of the geometry is the allowable deflection of the structure. According to Eurocode (EN 1990, 2002) the maximum vertical total deflection calculated for dead and imposed loads for rigid roofing of flooring elements is set as $L/500$ according to ULS and to $L/250$ for SLS (serviceability limit state). ULS load cases are going to be used for pre failure calculations and for post failure cases SLS will be used instead (ULS without the safety factors).

Table 23: Objectives and constrains as presented in the work of (Koniari, 2022).

	Type	Symbol	Value	Units
Imposed (short-term)	Live load	q_k	5.0-7.5	KN/m ²
	Snow	q_s	1.2 ⁴⁴	
	Wind	q_{lw}	0.5 ⁴⁴	
	Live load (fall protection) (LC4)	$q_{k,p}$	1	
Permanent	Self-weight (cantilever)	q_{sw}	9.8	KN/m ²
	Self-weight (float glass sacrificial)	q_{sws}	1.2	KN/m
	Self-weight (float glass fall protection)	q_{swp}	1.2	
	Live load (point)	q_k	3.5-4.5	KN
	Safety factor imposed	s_l	1.5	
	Safety factor permanent	s_p	1.35	

7.4. Design domain and input data

The design domain is set as a rectangle of 10 m in length and 2 m in height inspired by the realised case study Bruendl skywalk. The depth of the structure is not important for the optimization as the algorithm is limited in 2D. The total design domain of the structure can be seen on (Figure 103, 104) The domain is then discretised into quadrilateral (square) elements based on the maximum number of elements allowed by the RAM memory limitation (2100). In this case the size of the finite elements is 0.1 m and the number of elements at

x axis is 100 and at z axis 20 (Table 26). Common soda lime glass is used for this case study due to its lower cost as described at Table 2.

The input for the algorithm is summarised on the Tables 24-26. The main objective of the optimization the minimization of the mass/volume with the set of constraints as shown on Table 22 (first row).

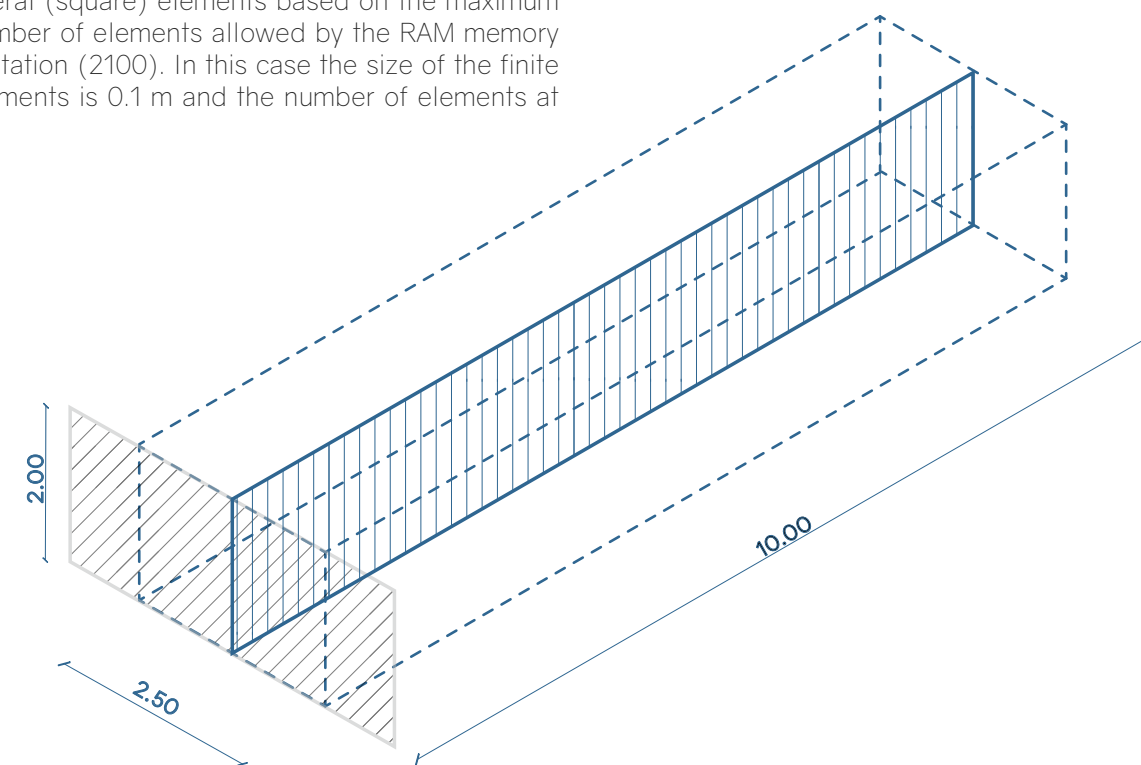


Figure 103 : Design domain dimensions and cross section used for the two dimensional optimization. Left is the fixed support and right the free end.

44. (Dlubal, n.d.)

Table 24: Input values for the algorithm, properties of soda lime glass

	Symbol	Units	Input values (Soda lime glass)
Young's modulus	E	GPa	70
Poisson's ratio	ν	-	0.22
Density	ρ	Kg/m ³	2500
Initial cooling range (annealing process)	ΔT	oC	553-485
Thermal expansion coefficient	αT	1/K	8.5×10^{-6}
Thermal conductivity	k	W/(m*K)	1.06
Specific heat capacity	cp	J/(kg*K)	870

Table 25: Constrain values

	Symbol	Units	Input values (Soda lime glass)
Design tensile strength	ft,des	MPa	6,4
Design compressive strength	fc	MPa	500
Deflection	d	m	L/500
Maximum annealing time	tann,max	s	432000 (5 days)
Minimum element dimension	dmin	m	0.3
Ratio of maximum to minimum element dimension	rann	-	2
Maximum permanent residual stress (after annealing)	$\sigma_{res,max}$	MPa	1

Table 26: Case study specific input data

	Symbol	Units	Input values (Soda lime glass)
Element size	d_FE	m	0.1
Number of elements x	nelx		100
Number of elements z	nelz		20
Length	d_ln	m	10
Width	d_wd	m	1
Height	d_ht	m	2
Initial density	xi		0.6
Compliance of virgin material	cmpl_init		0.7206

7.5. Geometry optimization

The optimization output is a table of values between 0-1 that represents the density for each of the finite elements within the design domain. This table, when translated into a grey-scale raster image gives an idea about the shape of the optimized geometry (Figure 106, top). The resolution of the picture is affected by the available RAM memory and is currently constricted to approximately two thousand pixels. Even at this resolution the algorithm required 2 days to converge (arrive at a feasible result satisfying the objective and constraints).

To arrive at a sensible design the results need to be post-processed. At this point a design decision must be taken informed by safety and redundancy of the structure.

7.6. Research through design/ redundancy of bearing structure

Two design variations have been explored as part of this thesis: a) a monolithic cast glass structure and b) a sliced design composed of multiple elements (Figure 105).

The first concept is a monolithic piece of cast glass. To be able to manipulate the geometry the data generated from the optimization are imported to grasshopper. By filtering the densities below a certain point, tracing and smoothing the outlines and extruding the 2D profile, arriving at the main bearing element. This idea has been previously implemented in the work of (Koniari, 2022) and results in a structure that can be structurally verified for the imposed load, but lacks redundancy in case of an accident or vandalism. A possible collapse of the main bearing structure at the edge of a cliff will have severe consequences with many predicted human casualties. To make a better-informed decision regarding the redundancy we use the risk analysis table that ABT uses to assess glass structures (Table 27). By constructing different scenarios, we can see if any of them require special action. A special action needs to be taken when the result of the equation: $RD = WS \times BS \times ES$ is higher than 70.

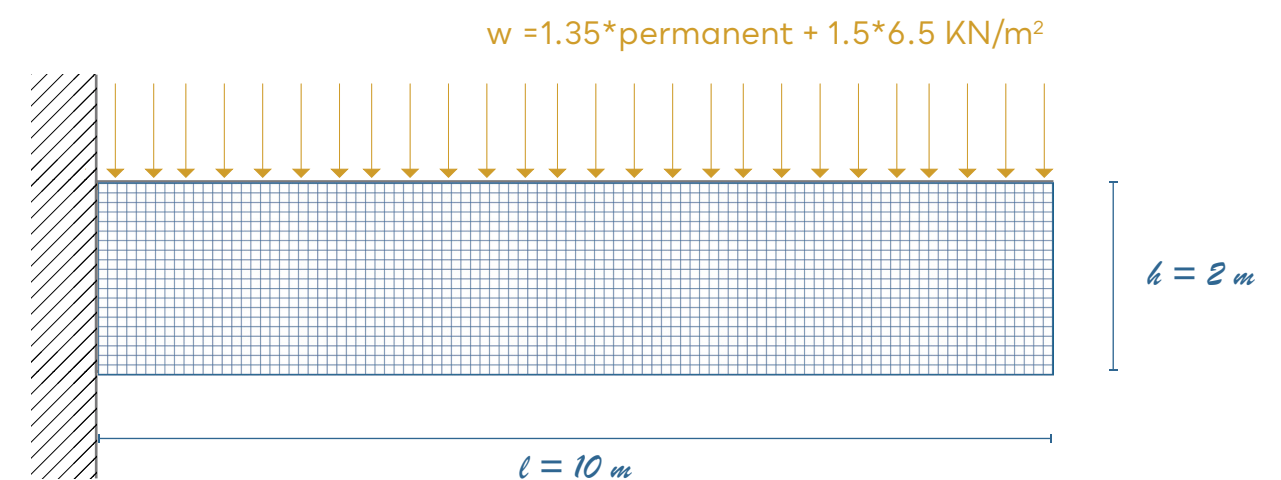


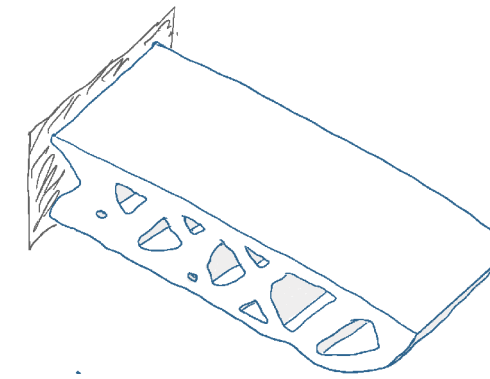
Figure 104 : Top: Free body diagram of the discretized domain used for topology optimization. Additional to the self weight (permanent) of the structure, a provisional 4cm float glass floor is accounted during the optimization.

Table 27: Risk analysis table, ABT.

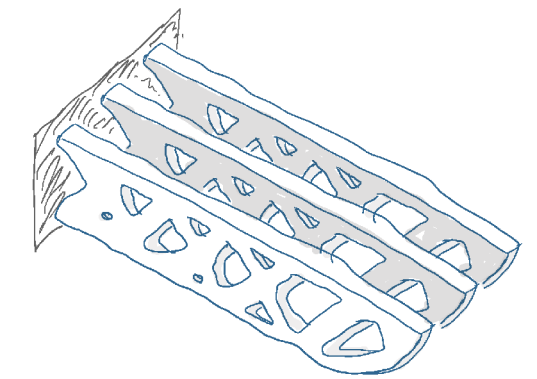
Probability intentional or unintentional	WS	Exposure of structural element	BS	Consequence at complete failure	ES
Virtual impossible	0.1	Very rarely	0.5	First aid	1
Practically impossible	0.2	Several times a year	1	Minor injury	3
Possible, but very unlikely	0.5	Monthly	2	Serious injury	7
Only possible in the longer term	1	Weekly	3	One dead	15
Uncommon, but possible	3	Daily	6	More than one dead	40
The best possible	6	Constantly	10	Catastrophe, many deaths	100
Can be expected	10				

Table 28: Risk analysis table for bearing structure zone.

Risk scenario	Description	Type of damage	WS	BS	ES	RD= (WS*BS*ES)	Action needed	
Bearing structure (cast glass)	Vandalism/accident	Internal or External/ rock or other sharp object drop	3	2	100	600	Imperative to introduce redundancy through slicing of the structure	
	Accident	Internal or External/ cleaning-maintenance tools collision	1	1	100	100		
	Accident	Car, truck, helicopter or other heavy vehicle crush	Complete breakage	0.5	0.5	100	25	no
	Terrorism	Explosion from bomb or gunfire	Complete breakage	0.5	0.5	100	25	no
	Accident	Landslide	Possible failure of bearing structure	1	0.5	100	50	no



Monolithic design



Sliced design

Figure 105 : Monolithic vs. sliced cast glass bearing structure design concepts

Based on the findings on (Table 28) the monolithic concept is considered as unsafe, and an alternative is explored that of a sliced structure. On a sliced structure if one of the fins breaks down spontaneously, the rest of the fins can redirect the load of the structure until safe evacuation. Having said that the output of TO is post processed based on the sliced design concept consisting of 3 fins (Figure 105, right).

Other redundancy strategies were considered but as mentioned in (Bristogianni & Oikonomopoulou, 2022a) there are hard to apply in cast glass. Specifically, tempering of cast glass is challenging due to the volume of the component. Chemical strengthening targets only the surface which is a fraction of the overall volume of the piece. Finally, lamination is hindered by the shrinkage of cast glass components as for the method to work it requires a virtually flat surface.

The output of the algorithm is imported in Grasshopper with the help of excel read component (Figure 107). A planar surface with the same dimension as the design domain is created and two thousand control points (same number as the values of densities) are introduced at the centre of each quadrilateral finite element. The density values are then remapped into the desired domain and converted into vectors that move the control points of the surface. The value of the vector is from 0 to 0.2 m reflecting in practice the maximum and minimum thickness of the structural elements. The result is an inherently smooth surface⁴⁵. A plane parallel to the initial one is used to filter out densities below one threshold that are considered as

non-contributing to the structure (in this case densities below 0.1). This step creates the unique pattern and defines the areas where holes are formed. The outline of the volume is extruded by a minimum amount to avoid elements that are too thin, hard to fabricate or prone to breaking. The thickness of the middle part is 0.075 m. The result is mirrored resulting in a symmetrical 3D shape with maximum thickness of 0.55 m and minimum thickness of 0.15 m. (Figure 106, bottom). Further refining the design, the geometry is edited manually filleting the edges of the holes and ensuring consistent thickness of the thinner element. The shape of the holes is better defined following the axis defined by the thicker parts of the geometry as can be seen on (Figure 106, middle) highlighted in orange.

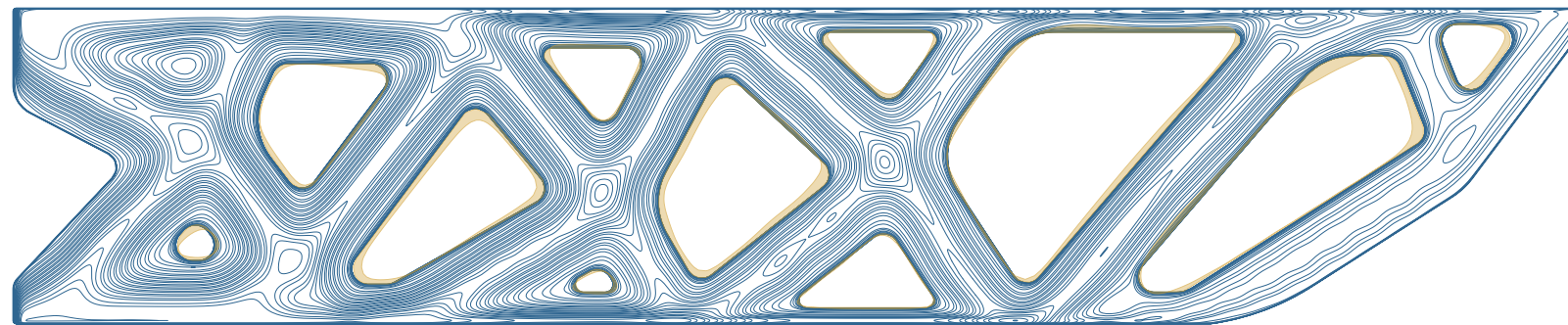
The post processed geometry is not the same as the output of the algorithm, but an interpretation based on a set of rules that arrives at a good approximation on how the structure would look like if a 3D TO algorithm was available for glass. Another advantage of this form is that it has a smooth shape with no abrupt changes on its cross section and can be easily manipulated for manufacturability.

On the downside the generated form uses slightly more material due to the smoothing process, hence slightly longer annealing time. The smoothing process would have been necessary for the monolithic design since the output resolution is rough. Given a computer with more RAM, the optimization output resolution would have been higher; with less post processing been necessary but greatly increased optimization time with the current software.

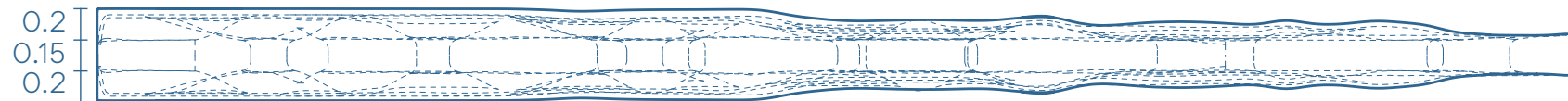
45. Arriving at a smooth geometry was particularly challenging by any other means. According to (Tedeschi & Wirz, 2014) geometries define by nurb curves are mathematically defined and hence smooth.



Algorithm output (side view)



Side view
Manual editing



Top view

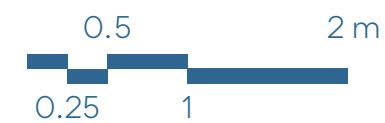


Figure 106 : Top: Output raster image from the TO algorithm of (Koniari, 2022). Middle: geometry after post processing, side and top view. Highlighted with orange the manual editing of the geometry removing inconsistencies in cross-section. Bottom: top view of the voluminous fin component.

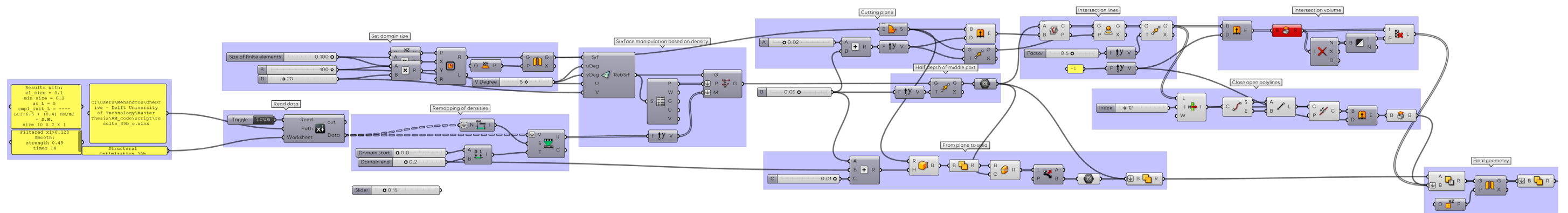


Figure 107 : Grasshopper script. From 2D table of numbers to 3D structural elements. The result of the script are then manually post processed to arrive at the final shape.

7.7. Research through design/ redundancy of side rails and floor

The final design of the case study can be seen in (Figure 108). The cast glass bearing structure is the base where a floor and protective rails are placed completing the observatory design and making the structure safe to use. As depicted in (Figure 108) there are 3 distinct zones in the structure, a) the side rails, b) the floor and c) the bearing structure. Each of the zones has a different exposure to risk and have different intervals of maintenance. In terms of exposure, the side rails and the floor are the most

exposed to vandalism, accidents and everyday wear. The main bearing structure is manufactured out of cast glass and redundancy is solved through slicing, while exposure is limited due to its position.

Floor zone

Starting with the floor zone, which should be first and foremost a flat surface accessible to people. Producing this element by casting would not make any sense cost and manufacturing wise, lamination of float glass is chosen as the preferred fabrication method, leading to a more lightweight and redundant structure that it is easy to replace

in case of an accident. The introduction of an extra sacrificial layer is advised based on the finding of risk analysis for this component (Table 29).

Side rail zone

Moving to the side rails here the choice of manufacturing method needs to weigh in factor such as redundancy, safety and total weight of the structure. A TO cast glass side rail is possible but according to the risk analysis will require a sacrificial layer to account for accidents and possible vandalism. Given the fact that vandalism is possible and in case of total failure multiple people can be exposed

to extreme height without any protection; hence lamination of float glass is preferred (see Table 30 for risk analysis). In fact, to arrive at a more intricate pattern and a design that matches the bearing elements lamination of AWJ cut plies can be implemented for this part. Contrary to the argument of sustainability and minimal visual impact set for the design of this case study these zones safety cannot be delt in a better way and a compromise must be made to design a feasible structure.

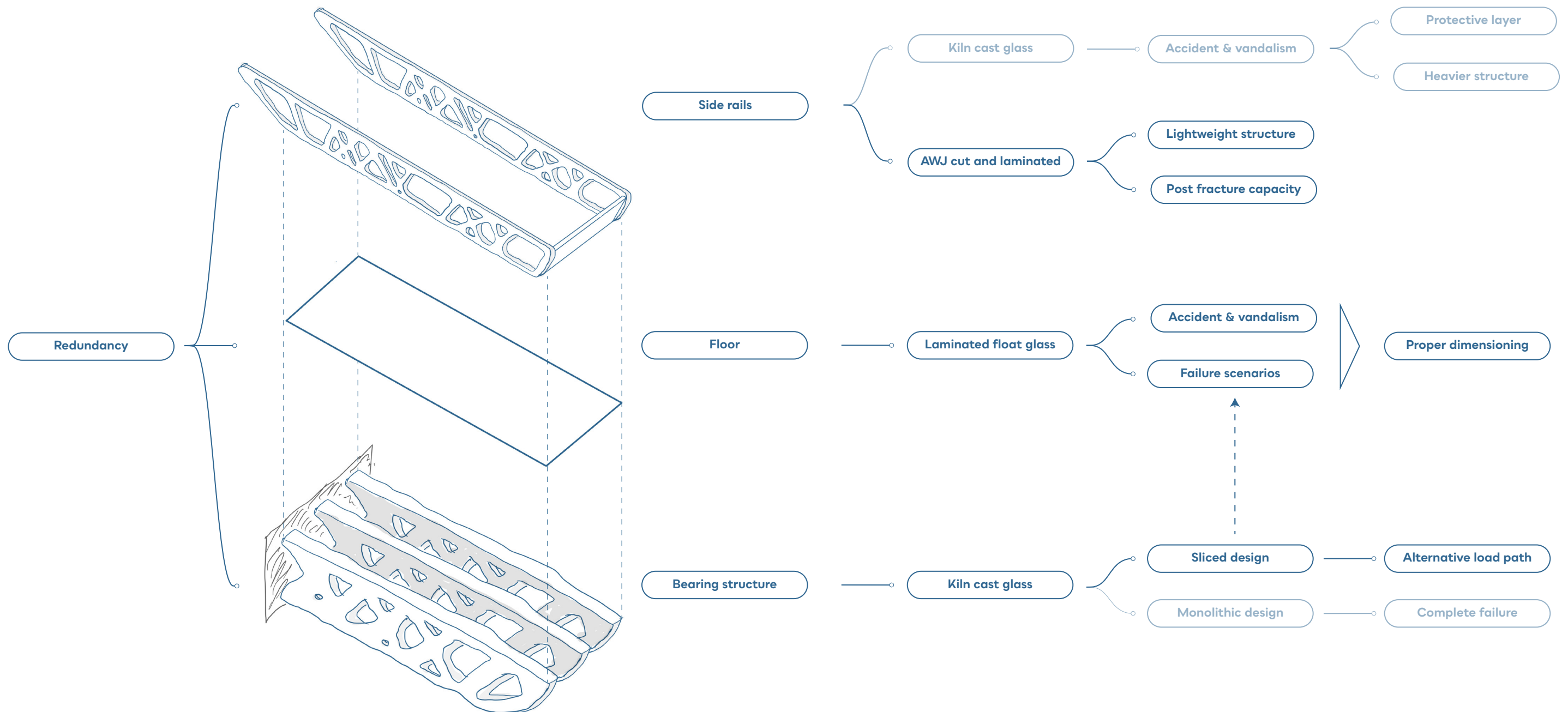


Figure 108 : Schematic division of the structure in 3 zones based on exposure to risk and decision tree diagram.

7.7.1. Dimensioning (floor)

Taking safety, a step further, the floor elements are calculated under two failure scenarios. The aim is for the floor elements to be able to carry the imposed load even after the failure of one of the cast glass fins. The calculations are done according to SLS to determine the number and thickness of layers needed for this element.

After some quick first calculations, the top scenario (that of side fin failing) (Figure 109) is considered the worst in terms of deflection and stresses (see appendix for hand calculations). The side rails are anchored on the concrete and in case of a fin failure they can act as an alternative path beneficial to the floor element until safe evacuation. For

that reason their self weight is not taken into account in the calculations. The worst-case scenario can be seen on Figure 109 and the calculations are results are summarised at Table 31.

For the floor structure according to SLS calculations and the risk analysis it is suggested to use one extra sacrificial layer of heat strengthened glass of 12 mm laminated using a PVB interlayer. Calculations according to ULS also confirm the calculations of SLS and display that even **3 layers of 15 mm** display tensile strength well below the design strength. To maintain a lightweight structure, I choose a total of **4 layers of 15 mm laminated heat strengthened glass**.

Table 29: Risk analysis table for the floor zone.

	Risk scenario	Description	Type of damage	WS	BS	ES	RD=(WS*BS*ES)	Action needed
Floor (laminated float glass)	Vandalism	Hammer, rock or other sharp object drop	Damage on top side or more layers	3	6	40	720	Lamination of sacrificial layer
	Accident	Car, truck, helicopter or other heavy vehicle crush	Complete breakage	0.2	1	100	20	no
	Accident	Landslide	Damage on more than one layers	1	0.5	15	7.5	no
	Terrorism	Explosion from bomb or gunfire	Complete breakage	0.5	0.5	100	25	no

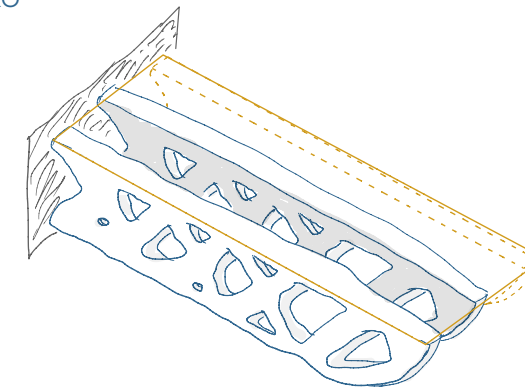
Table 30: Risk analysis table for the side rail zone.

	Risk scenario	Description	Type of damage	WS	BS	ES	RD=(WS*BS*ES)	Action needed
Side rails (if cast)	Vandalism	Internal or External/ hammer, rock or other sharp object drop	Complete breakage	3	6	40	720	Switch to different fabrication method, lamination of float glass
	Accident	Car, truck, helicopter or other heavy vehicle crush	Complete breakage	0.2	1	100	20	no
	Accident	Drone, bike crush	Possible damage	3	2	7	42	no
	Accident	Internal or External cleaning-maintenance tools collision, rock or other sharp object drop	Complete breakage	1	2	40	80	Introduce protective-sacrificial layer
	Terrorism	Internal/ external explosion from bomb or gunfire	Complete breakage	0.5	0.5	100	25	no
	Natural cause	Wildlife/ Birds, running through.	Possible damage	3	2	7	42	no

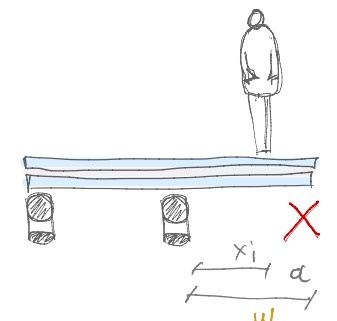
SLS calculations

Side fin failure scenario

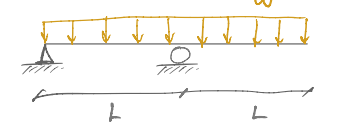
Axo



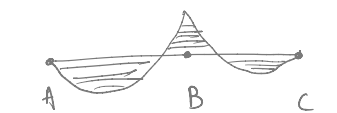
Section



FBD



BMD

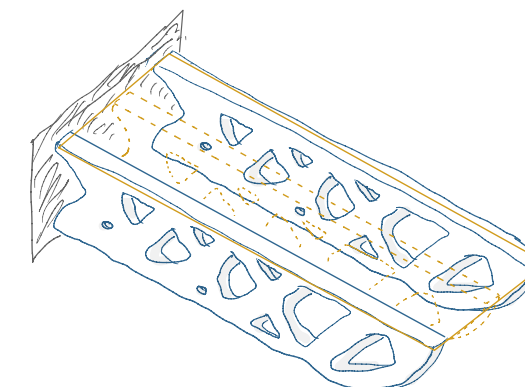


$$M(B) = \frac{w a^2}{2}$$

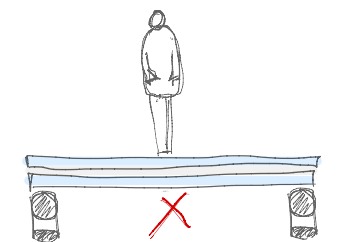
$$\Delta x(\max) = \frac{L}{4} \frac{w x_1^4}{EI}$$

Middle fin failure scenario

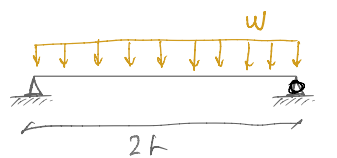
Axo



Section



FBD



BMD



$$M(x) = \frac{w(2L)^2}{8}$$

$$\Delta x(\max) = \frac{5w \cdot (2L)^4}{384EI}$$

Figure 109: SLS calculation scenarios according to different failure scenario. Top, fin failure scenario. Bottom, middle fin failure scenario. For each scenario: axonometric, section, free body diagram (FBD), bending moment diagram (BMD) and formulas used for the hand calculations (formulas retrieved from structx.com).

Table 31: Risk analysis table for bearing structure zone.

	Layers * thickness	Allowable deflection	Deflection (max)	Bending moment (max)	Design shear stress	Shear stress (max)
SLS	3 * 15 mm		8.8 mm	5.93 KNm		21.5 MPa
	4 * 12 mm	5 mm	7.4 mm	6.01 KNm	45 ⁴⁶	15.7 MPa
	4 * 15 mm		3.8 mm	6.25 KNm		10.4 MPa
ULS	4 * 15 mm	2.5 mm	0.12 mm	2.25 KNm	45	3.8 MPa

ULS calculations

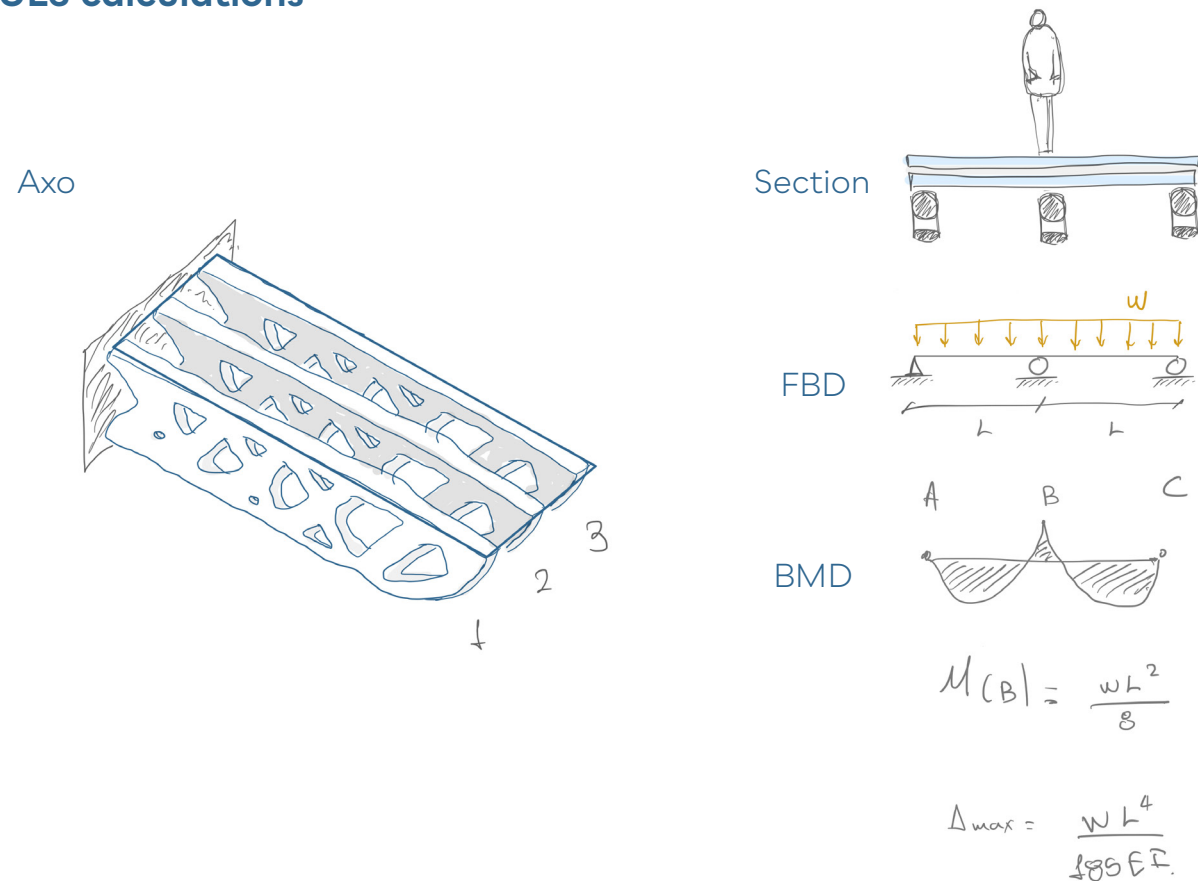


Figure 110 : ULS calculations according to formulas from structx.com.

7.7.2. Dimensioning (side rail)

To define the number of plies for the side rail some basic hand calculations were made that are summarized on Table 32. Calculations according to ULS scenario checks height wise for simplified model with full cross section. Lengthwise the results indicate that more than 5 layers of 15 mm heat strengthened glass are needed to fall within the allowable deflection which will lead into a thick elements and approximation of the actual geometry. Ansys is used to further validate the results and define the exact thickness needed for this element.

After some experimentation with different thicknesses, it seems that a more appropriate combination of layers is: **3 times 15 mm AWJ cut**, and heat strengthened glass pieces according to the design that can be seen on Figure 108 and **2 full layer of AWJ cut** and heat strengthened glass as fall protection. So, in total the laminated elements of the side rail are comprised of **5 layers of 15 mm heat strengthened glass**. The load applied in this case is LC4 (Table 23) without the safety factor for self-weight (as gravity has a fixed value on ANSYS workbench software). The model is set up with fixed supports at 3 ends and bonded connection between the plies of glass. Automatic meshing of 25 mm in size is used. This set up resulted in maximum deformation of 5.7 mm and maximum tensile strength of 38.22 MPa which is within the allowable limits (Figure 111).

Table 32: Hand calculations for side rail

	Layers * thickness	Allowable deflection	Deflection (max)	Bending moment (max)	Design shear stress	Shear stress (max)
ULS height	3 * 15 mm	2.4 mm	1.8 mm	2.12 KNm	45	7.7 MPa
	3 * 15 mm	22.4 mm	130 mm	-	-	-
ULS length	4 * 15 mm	22.4 mm	54 mm	-	-	-
	5 * 15 mm	22.4 mm	28 mm	-	-	-
ANSYS	5 * 15 mm		5.7 mm		45	38.22 MPa

46. According to DIN 18008-1:2020 the design strength for prestressed glass is $R_d = k_c \cdot f_k / \gamma_m$. For values for heat strengthened glass: $k_c = 1$, $f_k = 80$ MPa and $\gamma_m = 1.5$, $R_d = 45$ MPa.

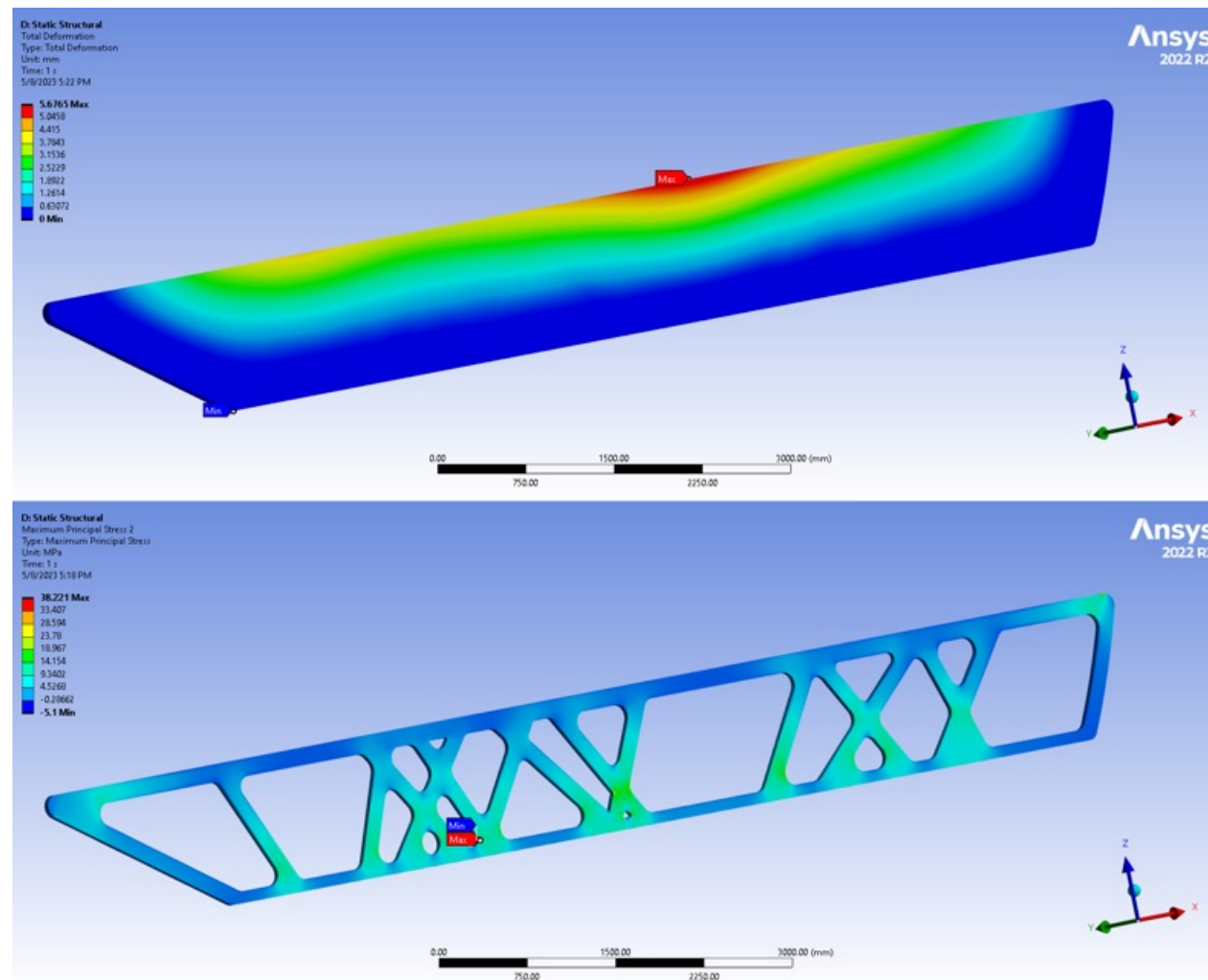


Figure 111 : Top: maximum deformation of side rail under LC4. Bottom: Maximum principal stresses of the infill part. Verification has been done using ANSYS workbench commercial software using a student license. Calculations were made for the 5 layer structure which are then hidden to reveal the pick stresses on the patterned glass elements.

7.8. Detailing

In the work of (Bristogianni & Oikonomopoulou, 2022a) titanium Grade 2 (99.3% Ti) bars are used to reinforce a soda lime silica glass (Float: 75% SiO₂, 12% Na₂O, 8% CaO). The combination yielded successful results under kiln casting at 1120°C. Expansion coefficient of the two materials is similar allowing for a stress-free annealing. When it comes to the connection of the glass cantilever to its concrete foundation at the fixed end, a ductile material is necessary to pick up the bending moment and tensile stresses. The design of the mould in pieces can allow for a custom titanium connection to be pre-installed during assembly of the mould and then kiln casting of glass can happen around it. The open mould design based on the findings regarding coatings allow for easier application and placement of the titanium reinforcement. The glass/titanium components can be transferred at location and fixed using a simple plate and bolt anchor fixed in the reinforced concrete foundation as

can be seen on Figure 113.

For the connection of the side rail to floor part embedded steel sockets can be used at both elements allowing for easy fixing on site (Figure 112). The side rail is also attached to the concrete wall at the beginning of the observatory.

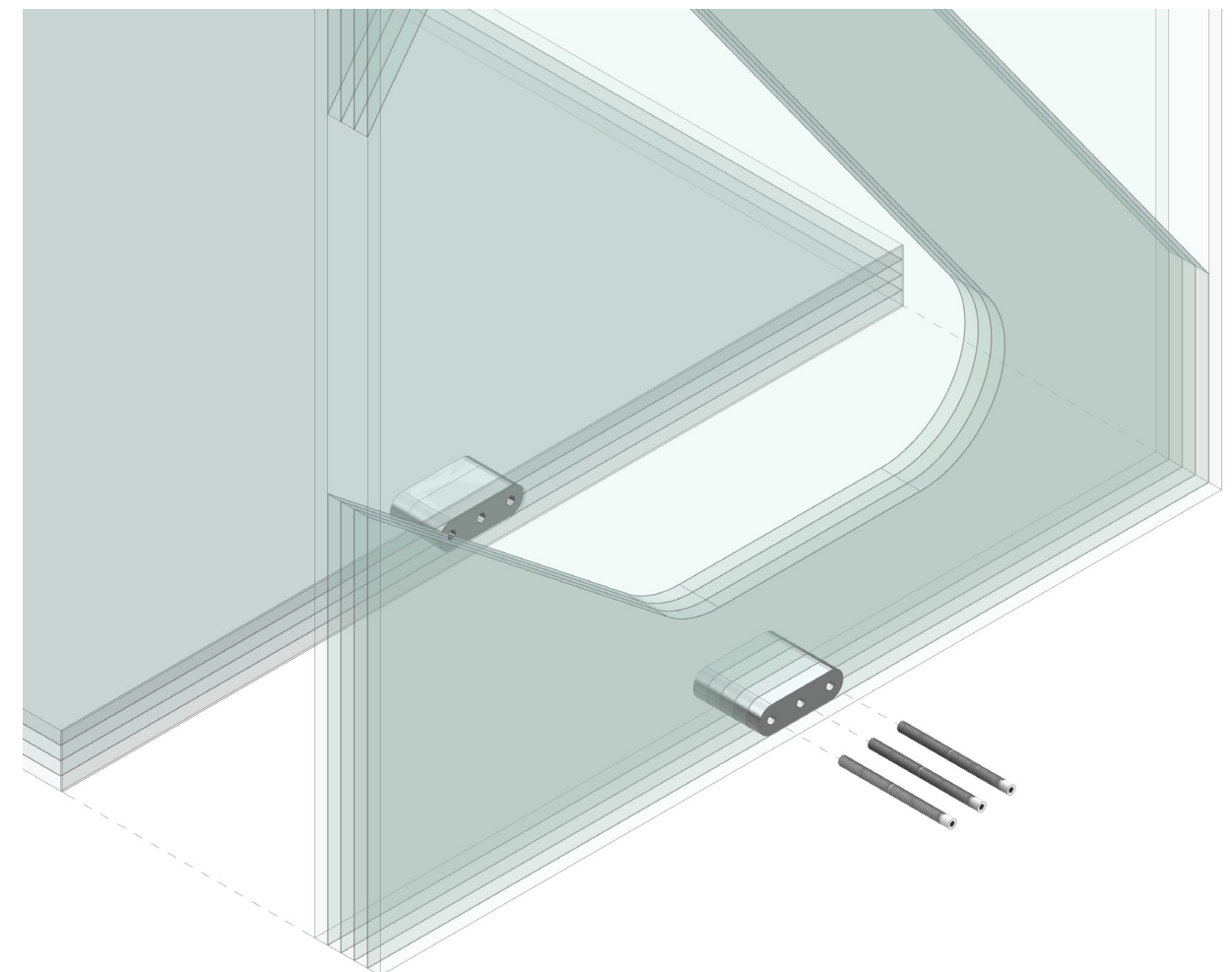


Figure 112 : Floor to side rail embedded connection.

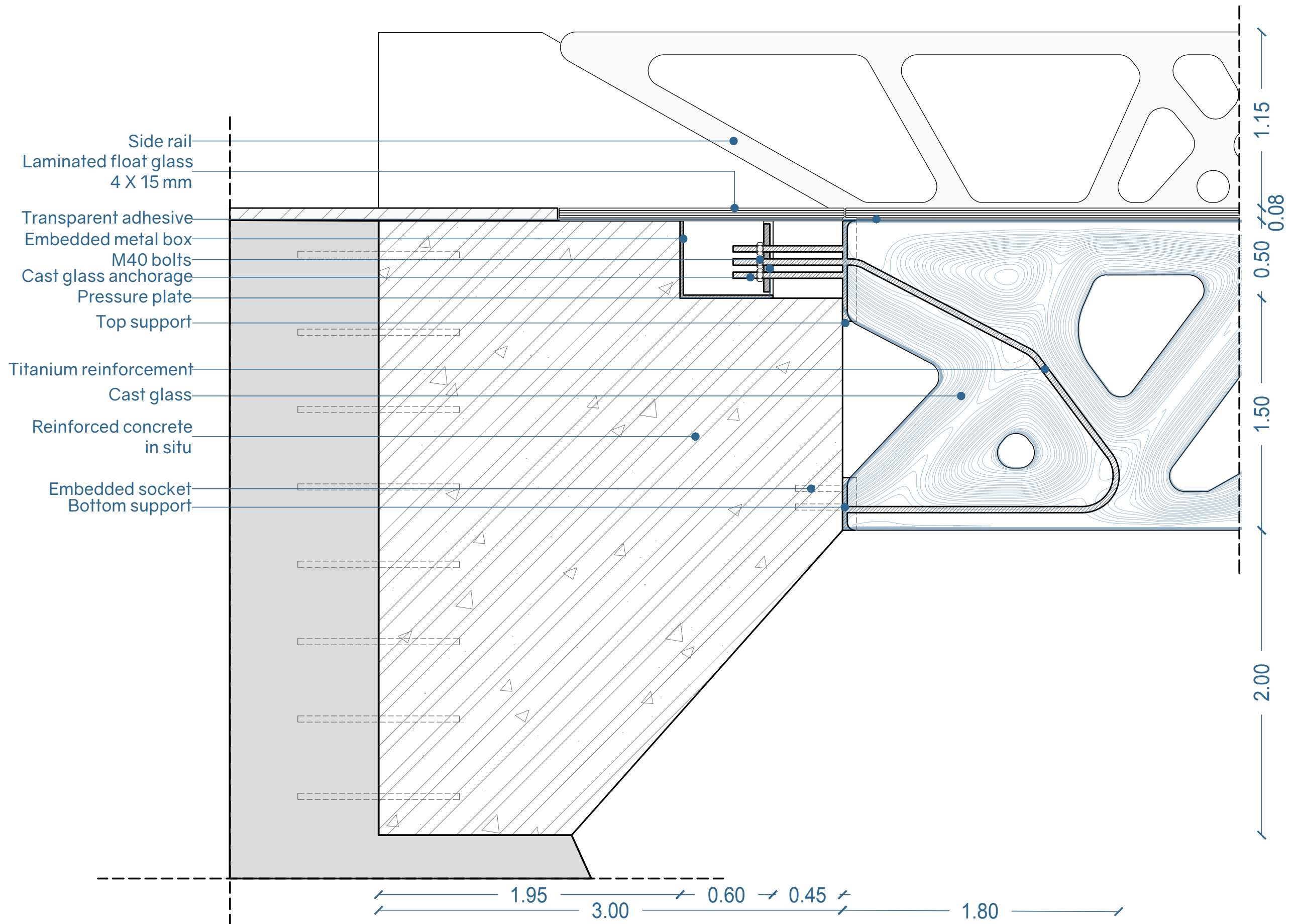
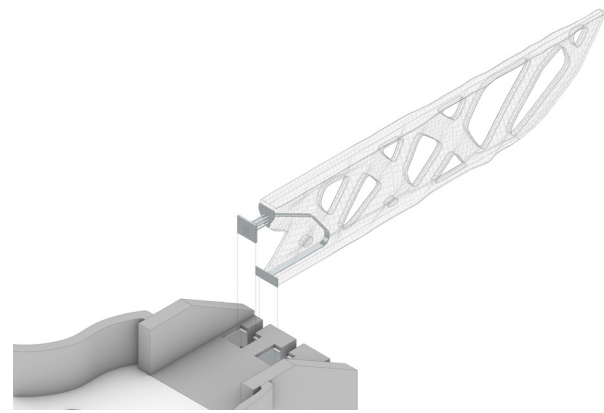
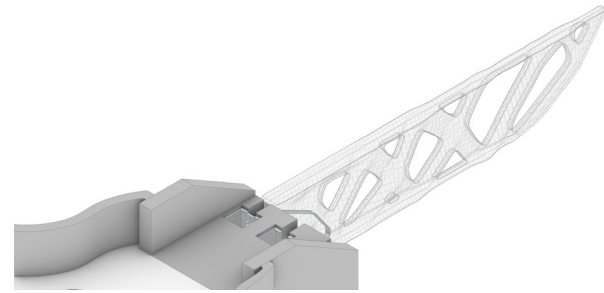


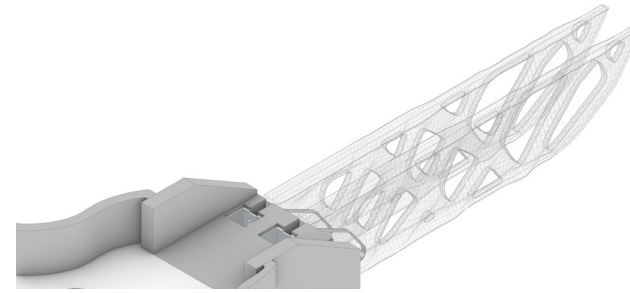
Figure 113: Titanium reinforcement and connection of fin with concrete foundation, section



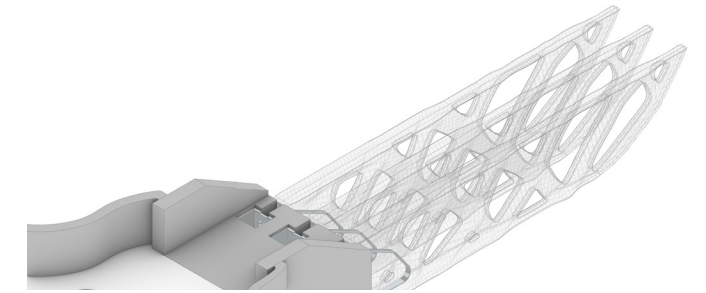
1 Placement of the fin from top with the help of a helicopter.



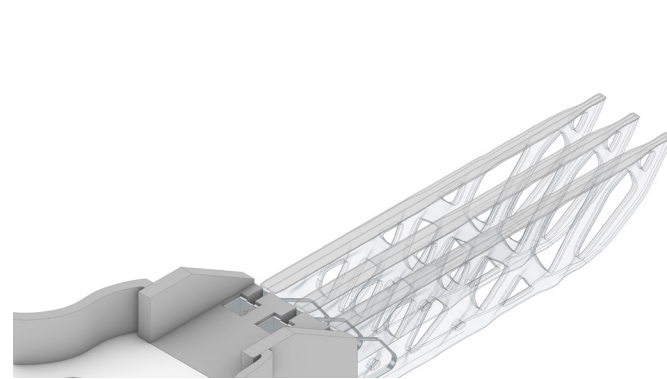
2 Alignment and tightening of the pressure plate with the embedded steel box of the concrete foundation. Fixing of the bottom support using bolts.



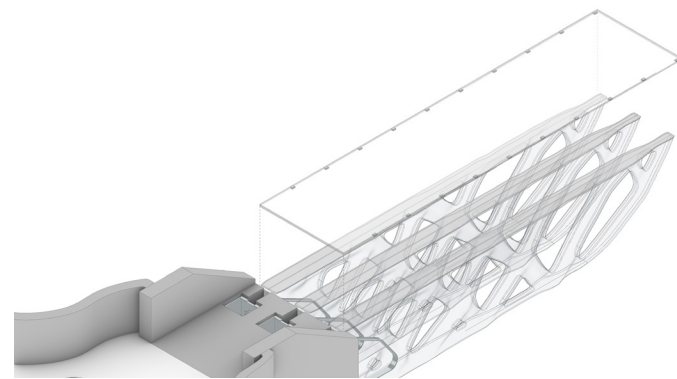
3 Repeat process for second fin.



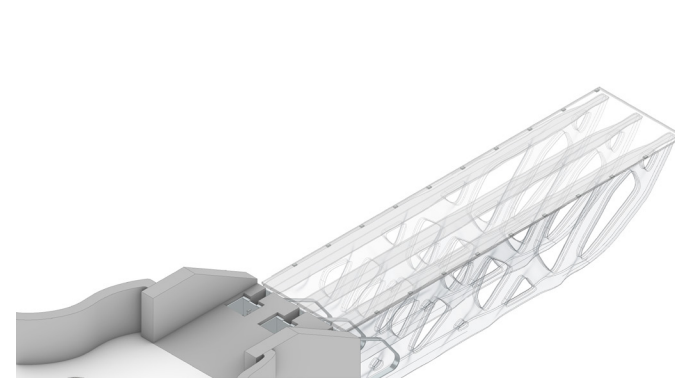
4 Repeat process for third fin.



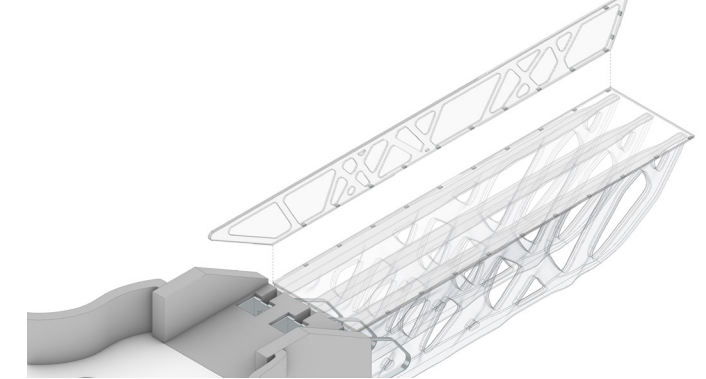
5 Application of transparent adhesive on the top side of fins.



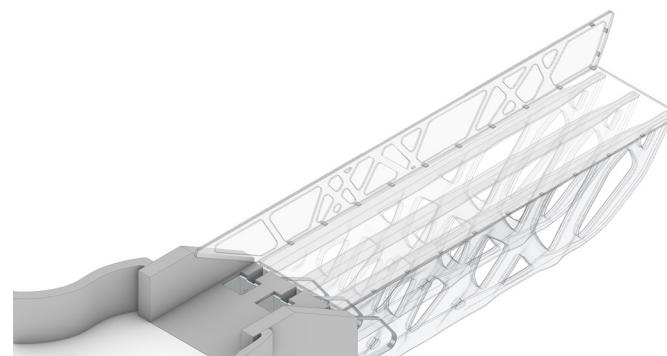
6 Alignment of the laminated float glass floor element.



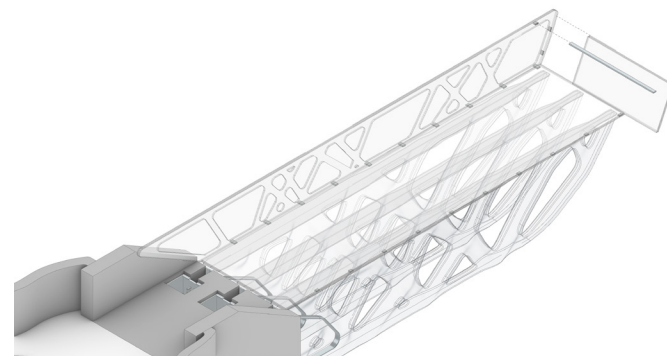
7 Fixing of the laminated float glass floor element.



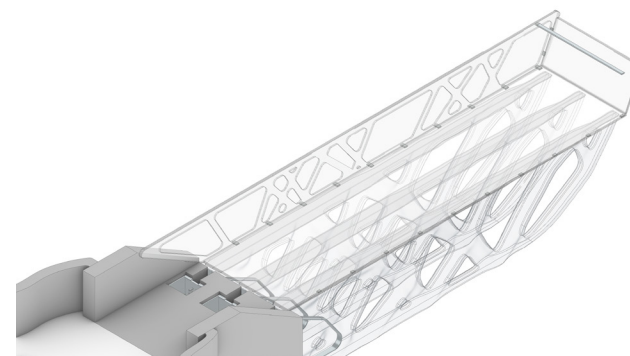
8 Placement of the first side rail.



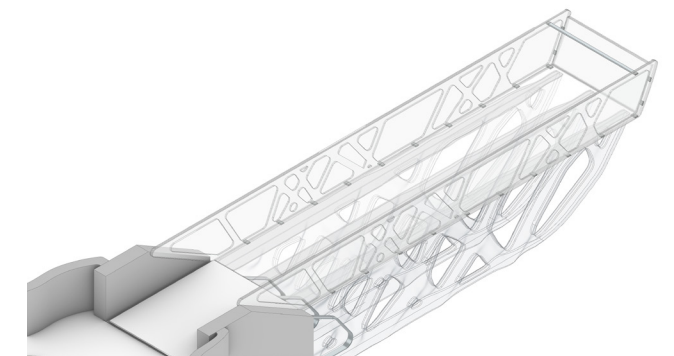
9 Bolting of the first side rail element.



10 Placement of the end panel and the hand rail.



11 Bolting of the end panel and the hand rail.



12 Placement and fixing of the second side rail.

Figure 114 : Assembly sequence of the glass observatory

7.9. Assembly sequence

The glass fins elements including the reinforcement, connection and pressure plate can fit on a single truck with maximum dimensions of 12 x 2.55 x 2.5 m. (Figure 118). The floor and end panel also fit within the standard dimensions of a box truck (Figure 85). Side rail components length is slightly longer than 12 m. and a longer truck with a semi-trailer that can reach up to 16 m. is needed. Transported from the manufacturing facility to the parking lot next to the site is done via trucks but placement on site requires a helicopter.

Before the placement of the glass structure an insitu reinforced concrete structure is constructed. The structure is anchored to the rock and has embedded metal box that acts as the connection interface. Glass fins are transported with the help of a helicopter from the parking lot nearby. The elements are slide from top and are aligned with the connection interface (1-2). The tightening plate on top is tightened and the bottom support is fixed using bolts(3). The process is repeated for the other 2 fins (4). Transparent adhesive is added at the top side of the fins. The floor unit is transported again with the help of a helicopter, aligned and glued (5-7). Side rail is inserted vertically, aligned with the embedded connection of the floor unit and is bolted (8-9). The end panel and the hand rail is placed from the side and fixed in a similar manner. The process is repeated for the second side rail (10-12). The structure is ready for use. The complete assembly sequence is explained at Figure 114.

7.10. Verification of bearing structure

Verification of the structural elements proved to be harder than expected. To accurately calculate the stresses using ANSYS workbench, proper conversion of the geometry was needed. Some assumptions and simplification were necessary given the limited knowledge on non-linear analysis and of how to model reinforcement inside glass. Initial simulations showed good results with the default coarse meshing (automatically assigned by ANSYS workbench) and fixed support at the flat side edges of the model. To make sure that the results were correct a more refined mesh was used, resulting in tensile stresses above the design limit for cast glass. To figure out whether this is an issue of the geometry or the way the model was set up the geometry was smoothened out at the pick stress point. Again, the results were above the design limit. This indicated that something was wrong with the meshing and modelling on ANSYS. Singularity issues are sometimes present on finite elements verification softwares. At this point a different approach for the placement of the fixed.

The titanium reinforcement volume is subtracted from the glass volume. Fixed support is assigned on all surfaces created from the geometrical subtraction (boolean difference). This change yielded good results with the default mesh. After mesh refinement I ended up with a simulation with good results well within the design limits. The set up and result of this simulation can be seen on Figure 115-117 on the right. For the verification of the structure LC3 was used adding 3 KN/m for the self-weight of the side panels and floor.

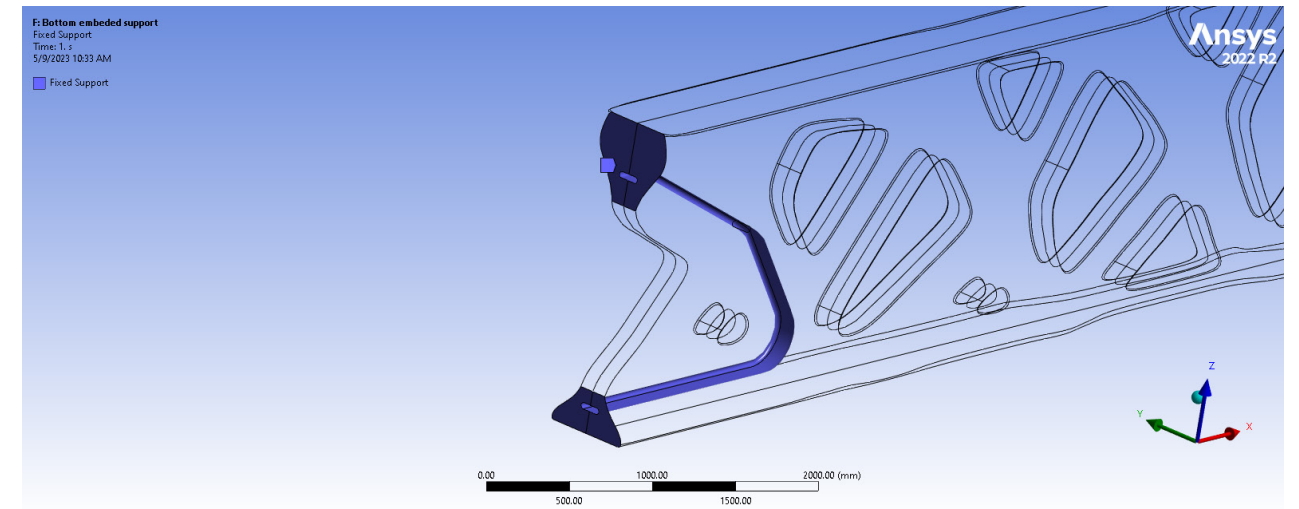


Figure 115 : Fixed supports as assigned for the FEA simulation on ANSYS workbench software.

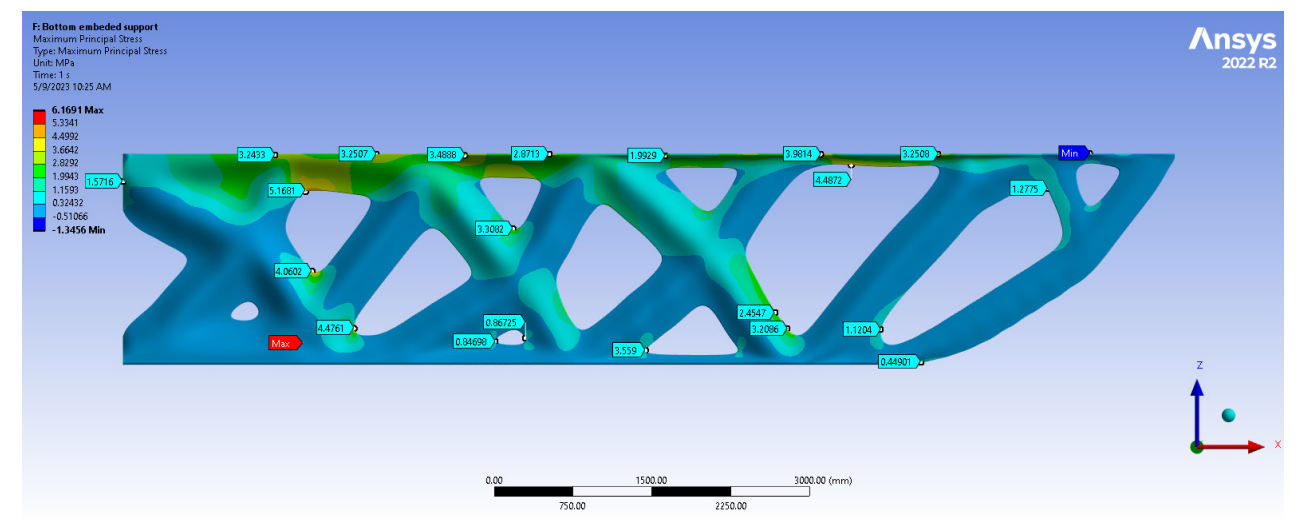


Figure 116 : Maximum stress at the structure as verified on ANSYS workbench. Maximum tensile value is present internal cavity where the titanium reinforcement will be placed. 10 mm mesh size.

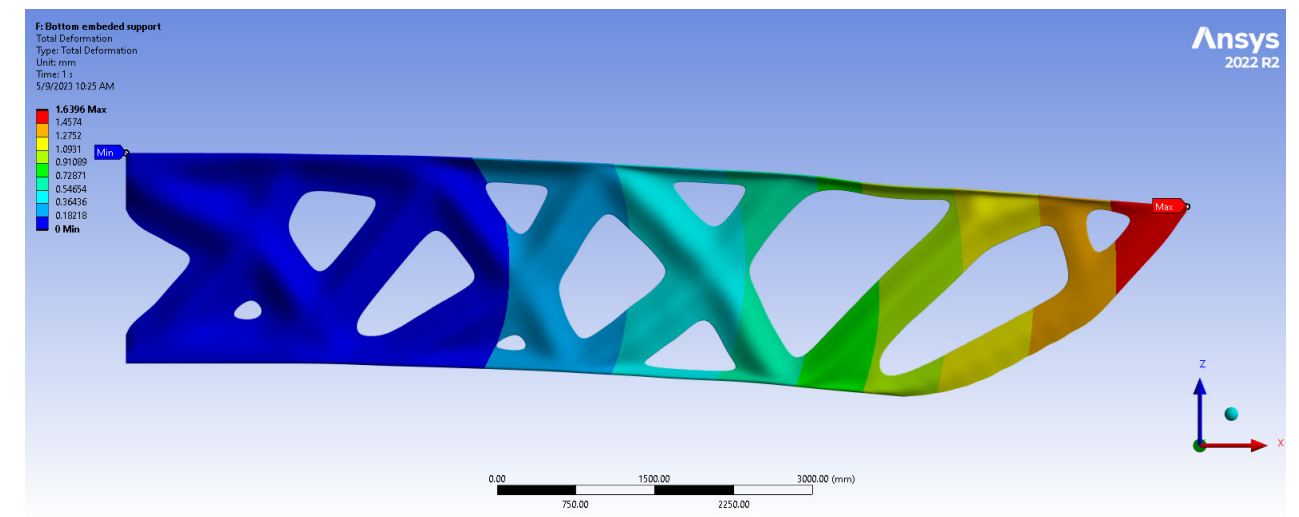


Figure 117 : Maximum deflection at the structure as verified on ANSYS workbench. 10 mm mesh size.

7.11. Final geometry

The structural validation of the bearing elements of the structure was crucial on the consolidation of the design. The final design of the all glass bridge-observatory on Vikos gorge can be seen on the following Figures 119-123. The overall size of the walking platform is 2.5 m. wide and 10 m. long.

Revising the soft criteria set in chapter 2, the vision of the final design as presented in the render (Figure 122) has a minimal optical footprint, offers great view of the gorge by extending 10 m. over the cliff, is definitely a unique structure and the fabrication method can use the cut off of the waterjet cut side rails and other recycled material for the casting of the fins. The production of the fins can become even more sustainable if glass waste streams are used such as oven doors, enamel, bottles, windscreens etc. In this case the transparency of the structure is compromised (see Figure 152 for an impression)

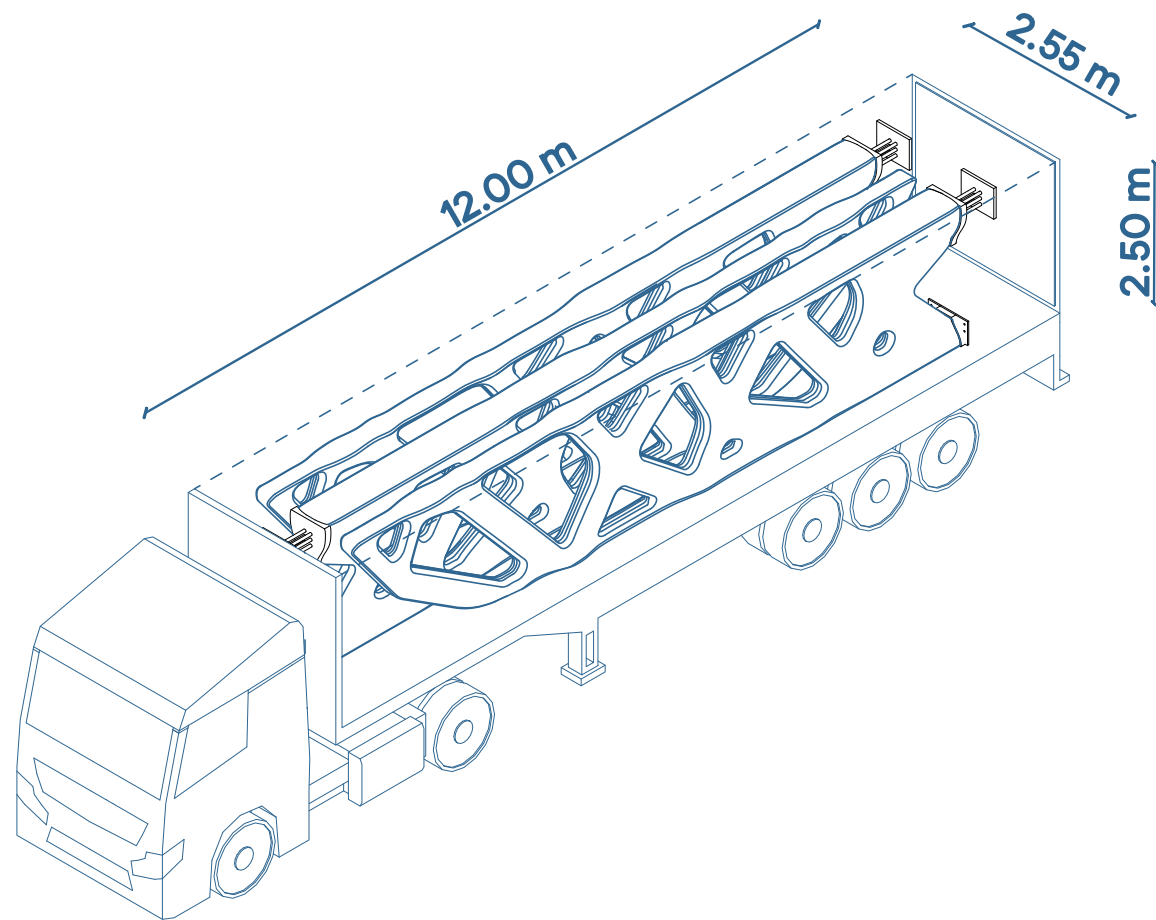


Figure 118 : Fin components transportation. Height smaller than the standard size. Each fin weights approx. 12 tons. All three can be carried in a single shipment. The weight limit for EU truck with ordinary trailer , such the one in the figure above, is 40 tones.

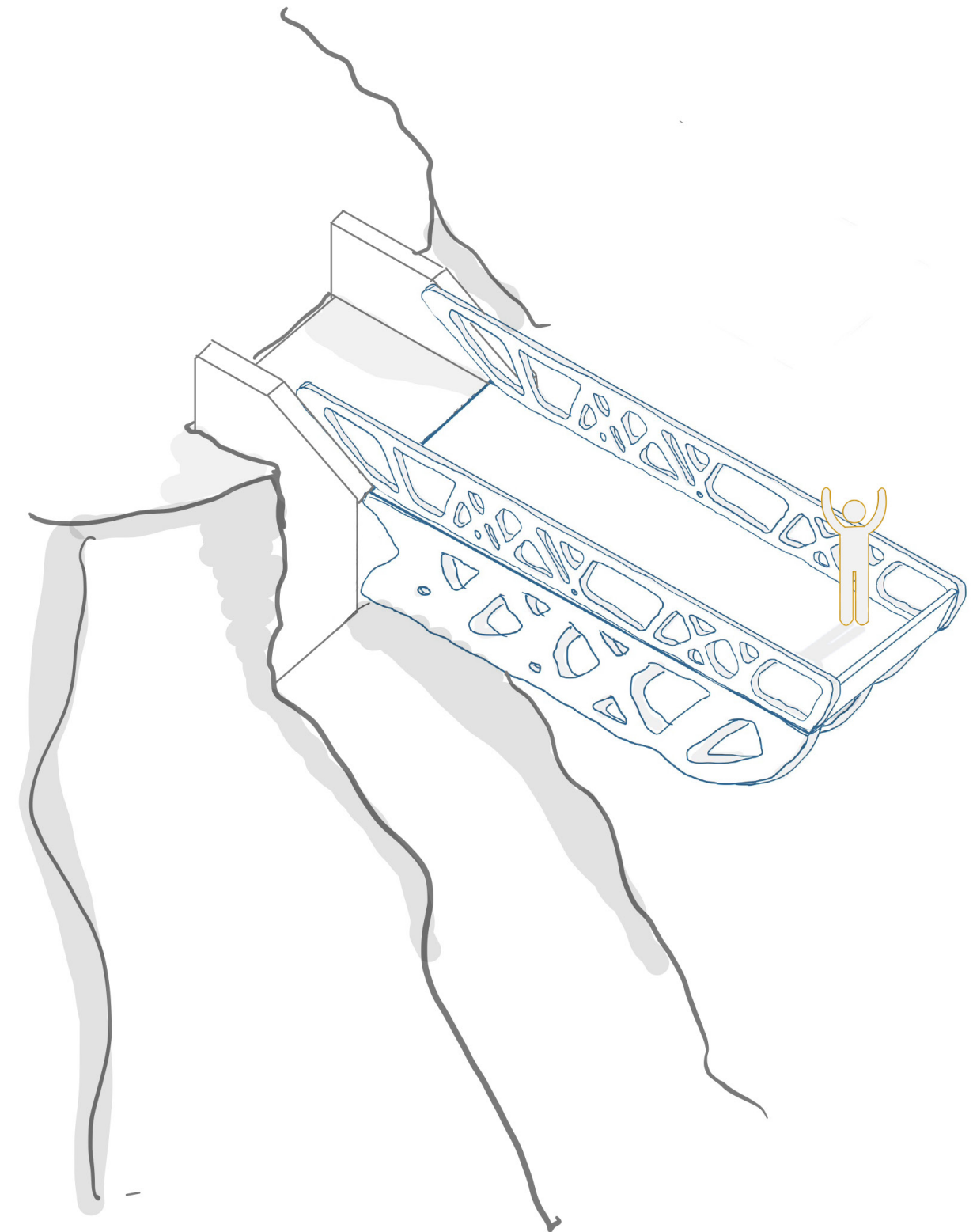


Figure 119 : Axonometric view (sketch) of the final design of the all glass observatory in Vikos gorge.

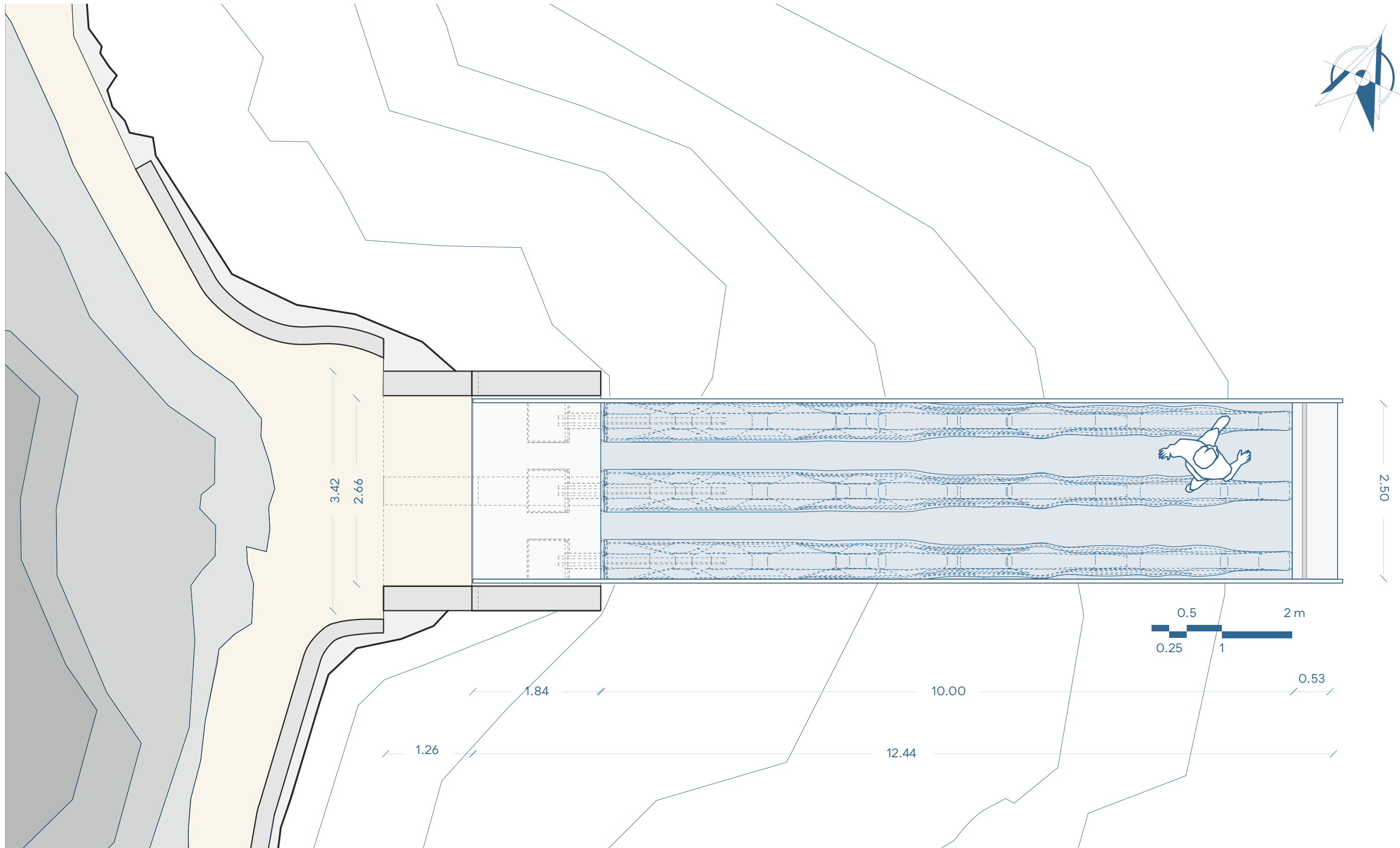


Figure 120 : Plan view of the final design at the edge of the cliff.

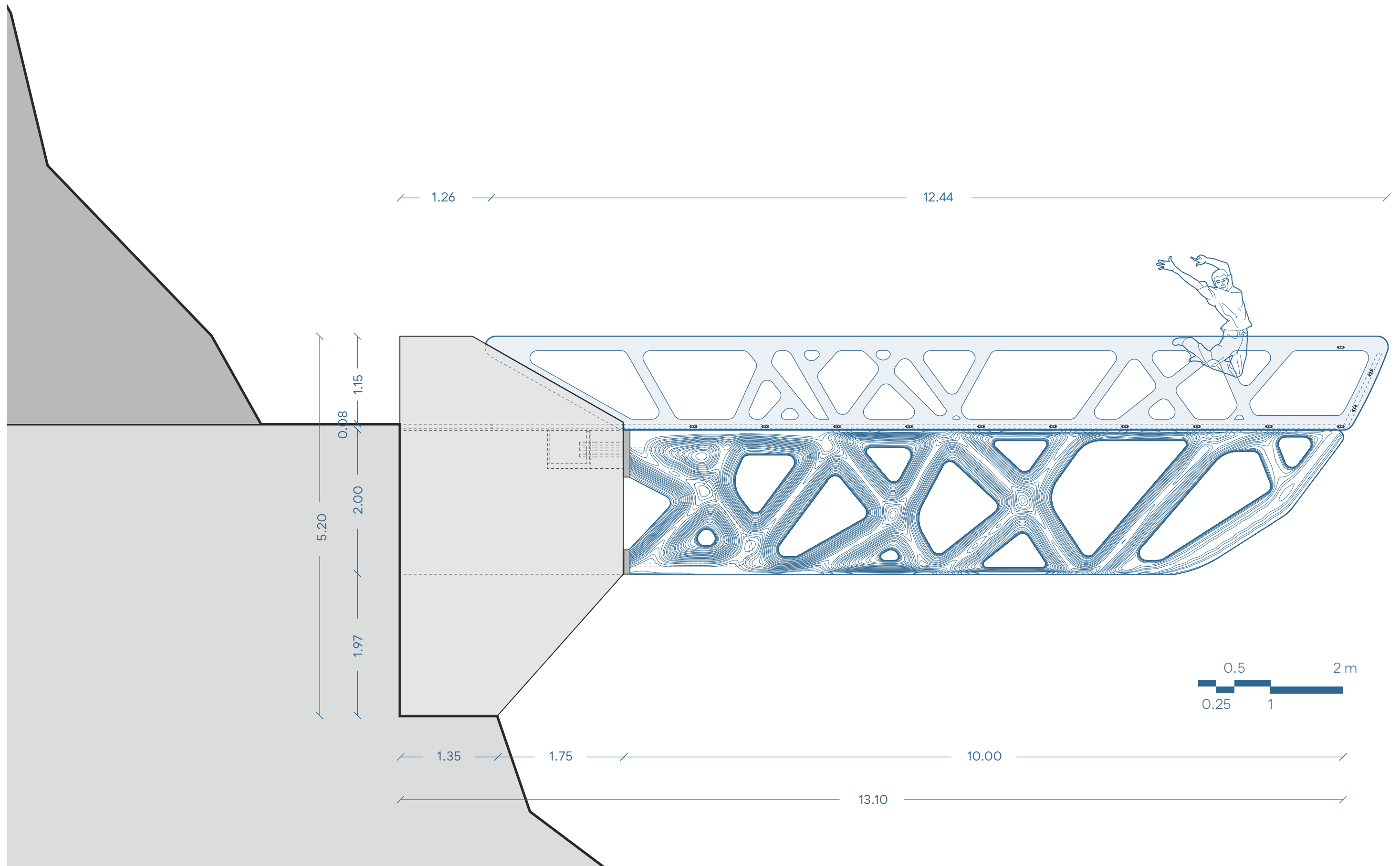


Figure 121: Elevation view of the final design.



Figure 122 : Rendered view of the all glass bridge observatory. The two different fabrication methods are visible. Cast glass at the bottom and lamination of AWJ cut glass at the top.



Figure 123 : Rendered view of the final design as envisioned during the night. Minimal light or biofluorescent tapes can be used to highlight the walkable path.

8

PROTOTYPING

The results from previous lab experiments are scaled up to further validate the results and understand factor that can be at play on larger scale samples. Additionally the fabrication process of a scaled glass prototype of one of the fins is documented.

8.1. Scaling up the coatings results

As concluded at chapter 6.6 scaling up of the moulds is crucial to further validate the results of the coatings and protective layer. Larger size samples of topologically optimized beams for 4 point bending test, as part of another research project currently running at Glass lab of TU Delft, are used to apply the findings from the coatings experiments (Figure 125).

The geometry has a minimum glass dimension of 8 mm. Small pieces of the geometry can break while in the oven resulting in contamination of the glass and failure of the mould leading to leakage of the glass. This is something that should be avoided. After extensive discussion ceramic sand was preferred for the larger geometries as it is considered to have better chances of success for larger geometries as from previous tests proved to be more robust after firing. The samples are fired on a slightly modified 870°C normal annealing schedule to allow for proper melting of the increased amount of glass. The mould was coated with Crystalcast and Zirkofluid 6672 (2X flow) following the suggestions of the coatings experiments. The dimensional discrepancy of Crystalcast (approx. 2.5 mm offset outwards) is taken into account during the preparation of the geometry for printing.

The application of the Crystalcast via brushing was somewhat challenging. Some spots of the mould are hard to reach which makes the process time consuming. Spraying of the Crystalcast mixture using a typical spray bottle was not successful ending up at clogging the outlet of the spray immediately. Flow application of the mixture leaves a lot of clogs at the surface leading into an uneven surface something that is not desired.

After firing (at 870°C normal +2 hrs., Figure 124) the mould maintained its integrity and casting is considered successful verifying the finding regarding the annealing cycles for ceramic sand mould (Figure 126).

The resulting surface quality of the cast glass elements is not the same as the one received from testing on smaller samples. Compared to prior experiments conducted on complex shaped geometry using 3DPM made of silica sand and CHP binder the results are improved. Sand adhesion is prevented, but results are far from the benchmark optical quality and transparency of the glass cast on steel or graphite moulds.

On possible reason why the surface of the glass is not as transparent as on the previous experiments can be the extended exposure of the coating to the maximum temperature. Those extra couple of hours can rendering the coating ineffective making it adhere to the glass. Other possible reason behind it can be the thickness of the coating as in some parts the quality is better than other. This can also be linked to the application of the protective layer (Crystalcast). For longer exposure at high heat an even thicker coating layer might be necessary. Finally, another explanation can be that some chemical reaction induce crystallization of the glass surface making it opaque.

Examination under the microscope shows coating adhesion to glass and rough surface, pointing towards the temperature and coating assumptions (Figure 127). Further testing is needed using thicker coating layer or a shorter annealing schedule such the one used for the first experiments. Hot pouring can also be a good alternative option.

The complete preparation of the mould to arrive at the cast glass object can be seen on Figure 128.

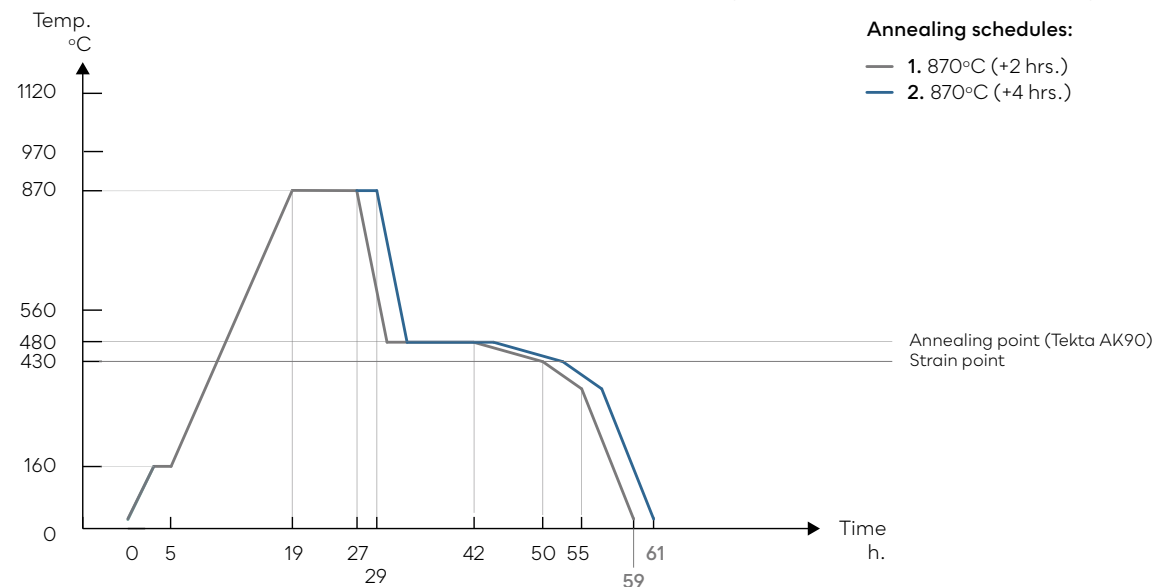


Figure 124 : Modified 870°C normal firing schedule for scaled-up experiments and prototype.



Figure 125 : Larger size moulds of TO beam geometries printed on ceramic sand with Inorganic binder, ExOne. Large dimension approx. 35 cm in length.



Figure 126 : Mould after firing. Some chipping of the crystalcast protective layer with a part of the sand mould.



Figure 127 : Microscope image of the cast surface on the larger sized sample (contact). Ceramic sand mould coated with Crystalcast and Zirkofluid 6672. Part of the surface is transparent and part of it is more translucent.

1 Crystalcast protective layer. Dried for 3 days at ambient temperature



2 Coating application (Zirkofluid 6672, 2X flow). Drying of 1,5 hrs between each layer



3 Glass (Bullseye) placement



4 Mould after firing at 870°C



5 Demoulding and cleaning using a sponge and water



6 Final glass element



Figure 128 : From 3DPSM to cast glass component.

8.2. Prototyping

One of the fins is chosen as the geometry for prototyping. The model is scaled down (1:25) and adjusted to fit the minimal dimension of wall thickness at all points defined by the shape and size fabrication limitations of 3DPSM as seen on chapter 5.4.3 and 5.4.4.

8.2.1. 3DPSM idea

As seen at Figure 129 two different ideas were explored.

The first one is an interlocking system made from multiple 3DPSM parts that when combined result into the casting geometry. This idea is uncertain if it will work effectively against the hydrostatic pressure build up that the glass will induce during kiln casting and whether the sand pieces will maintain their integrity holding the mould together.

The second idea is based on previous research at TU Delft and follows the same concepts of (Bhatia, 2019) where steel bolts are used to hold the pieces together.

In both cases, the set up is going to be placed inside a heat resistant concrete container and compacted with sand. This set up can help counteract the capillary effect on the moulds. The design opts for a two parts mould than allows for easy applica-

tion of the protective layer and the coating. Ideas regarding a fully closed mould were quickly ruled out for this type of mould.

To ensure that glass can reach all points some additions were made. A venting pipe was added to prevent air entrapment on closed cavities. A glass tank was added at the top acting as a buffer zone between the flower pot and the desired geometry, allowing homogeneous distribution of the melted glass and adequate time for it to flow inside the complex shape.

Unfortunately the prototype could not be realised within the time frame of the thesis.

8.2.2. Lost wax technique/ Crystalcast mould

Since the previous method was not feasible within the time frame of this thesis as an alternative the lost wax technique was used.

To begin with, a wax positive model is needed. This step proved to be more challenging than expected. Two different possibilities were explored. First 3D printing using a wax based filament was tested. This proved to be challenging for the size and the shape of this case study. Issues like wax warping and/or deforming were present hindering the process (Figure 130).

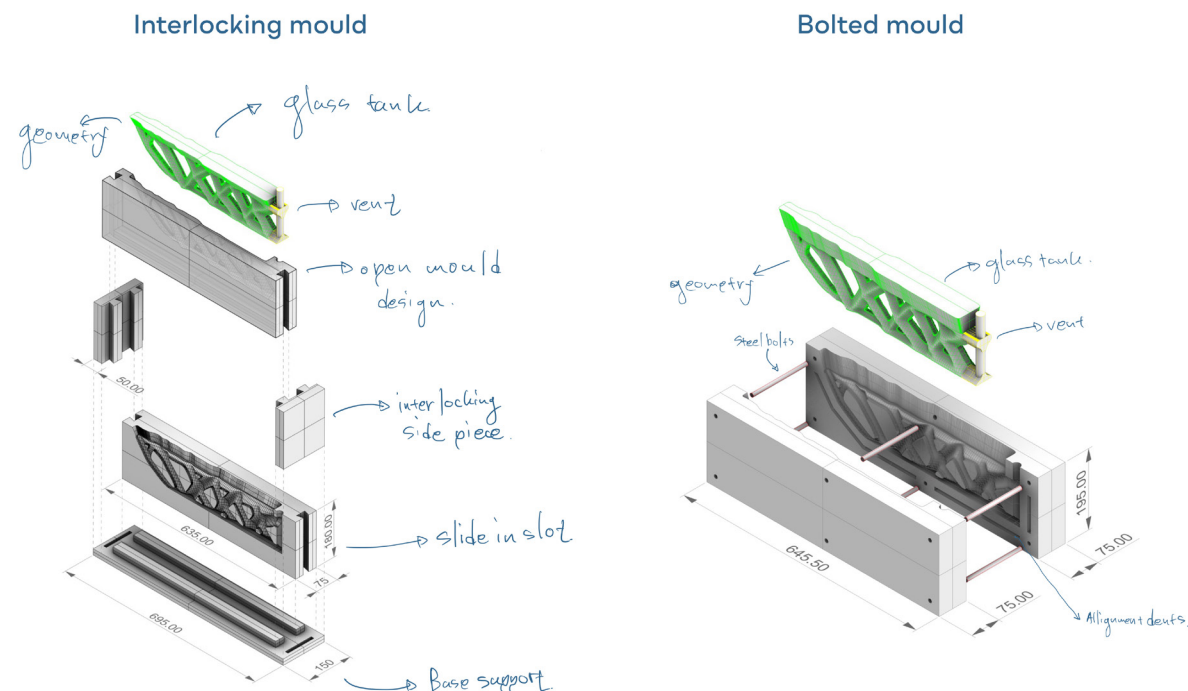


Figure 129 : Different ideas discussed with ExOne for the prototyping geometry. Left: interlocking 3DPSM moulds. Right: bolted mould based on the principle used for previous experiments as part of the work of (Bhatia, 2019).

The second idea that was explored was to 3D print the negative of the wax prototype using PETG and then cast the wax positive in it. PETG was chosen as a material for its high melting temperature (around 260°C) much higher than the melting temperature of wax (approx. 65°C). After some initial failed attempts the method worked. The most challenging part was to define the minimum dimension that could be released without any damage to the wax model. Some initial attempts can be seen on Figure 131.

After fine tuning the geometry, the two 3D printed negatives were coated with a good amount of Vaseline, aligned and clamped together. The edges were shield with clay to avoid any wax leakage (Figure 132). Melted wax was poured in the closed cavity. After cooling down the wax prototype was released with the help of pressurised air to avoid any damage to the wax (Figure 134). The wax was polished with acetone, arriving at a smooth surface. The next step is to investment cast the wax positive in Crystalcast. When the mould has dried adequately it was placed upside down and with the help of a steam generating device the wax melted, leaving the negative mould for glass casting.

At this point mould integrity issues arose. After de-waxing the mould displayed a lot of cracks at its thinnest elements. This is most probably caused by the way the geometry was designed and its minimum dimension (8 mm). This value is probably too low for this type of material causing local strain on the Crystalcast during setting.

The process was repeated and this time the steaming process was monitored more closely. Even with reduced de-waxing time the result was the same. Cracking was present at the thinnest elements of the mould. Regardless the strongest mould was locally repaired with some Crystalcast mixture (typical mixing ratio 1 part water and 2.8 parts Crystalcast). After drying the mould was coated with Zirkofluid 6672 (X2 flow). Finally, the set up was placed in the oven and two terracotta flower pots were placed on top containing the required amount of glass (Bullseye). The set up was fired following the 870°C normal +4 hrs (Figure 124).

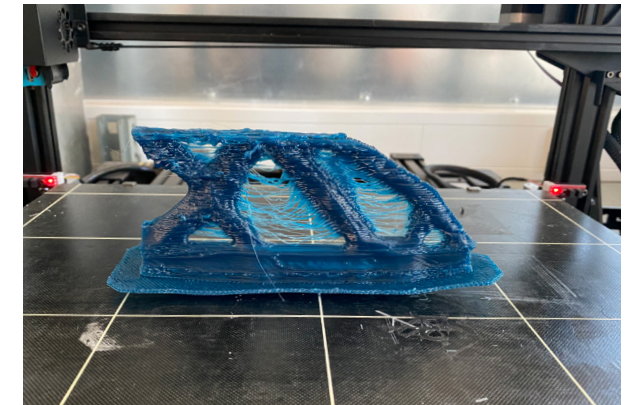


Figure 130 : 3D printing using a wax based filament. Warping and deformation of the geometry are visible. Different settings were tested but none was successful.



Figure 131 : Wax prototype after release from the PETG negative moulds. Geometry was scaled down 1:2 for this test to allow for quicker printing and to get some first impression of what needs to be improved. In this case the cross-sections are too small, thus the wax becomes fragile during separation.

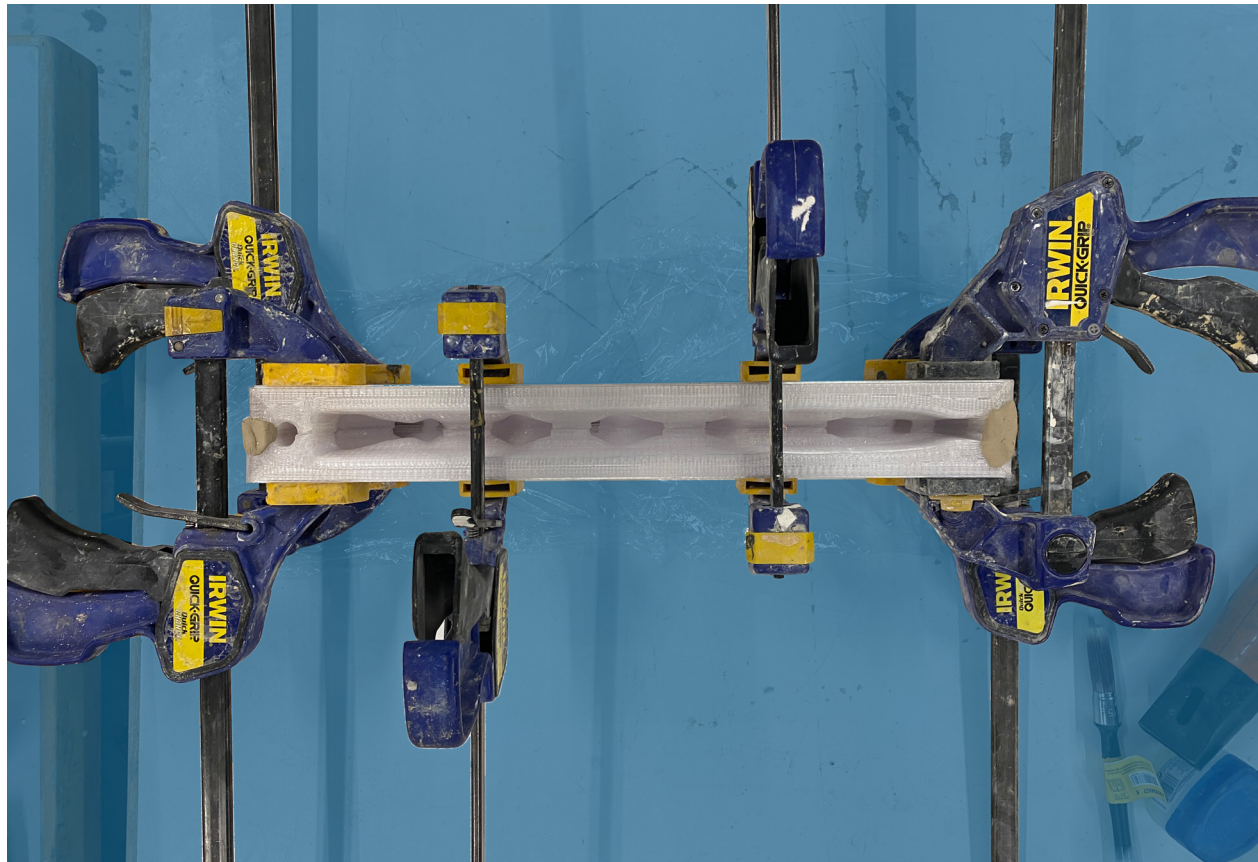


Figure 132 : Clamping and sealing of the two PETG negatives.

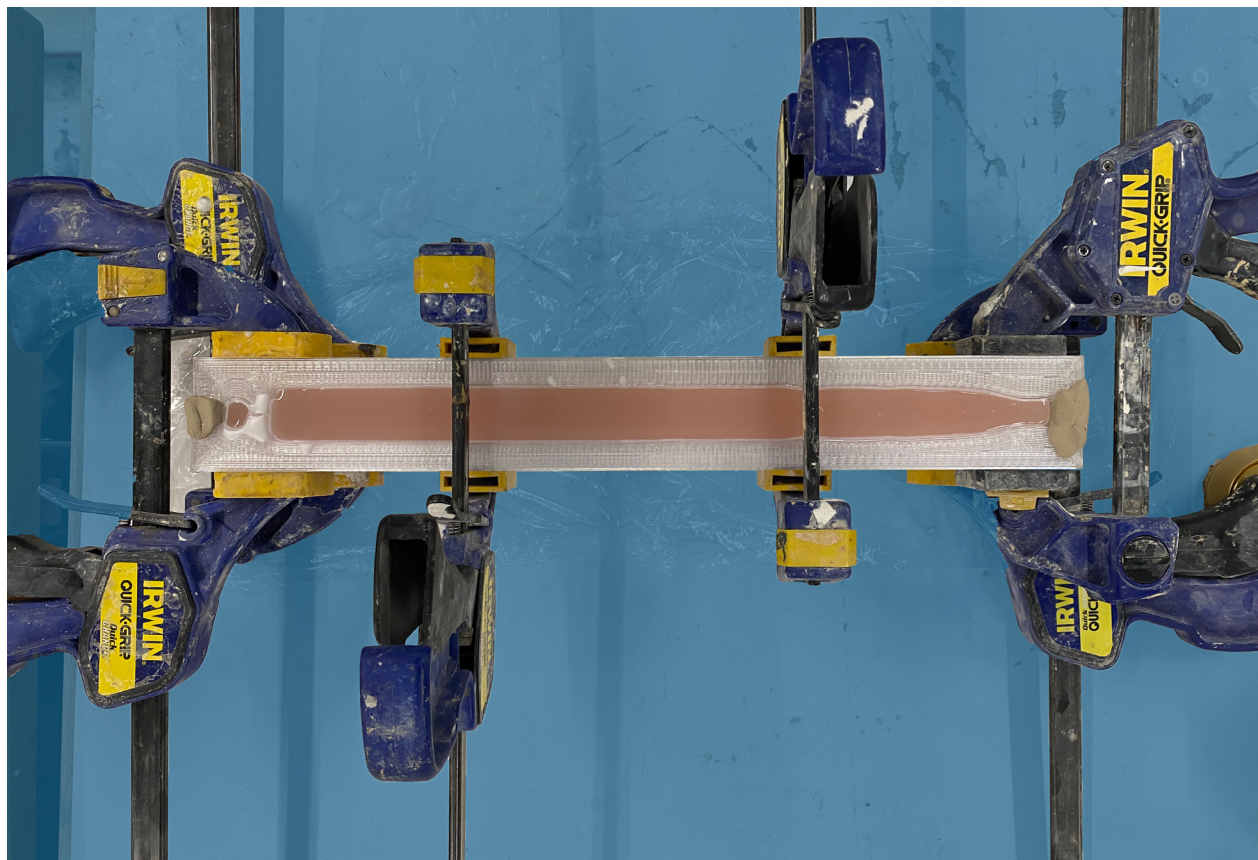


Figure 133 : Wax pouring inside the cavity. Picture taken during the cooling down.

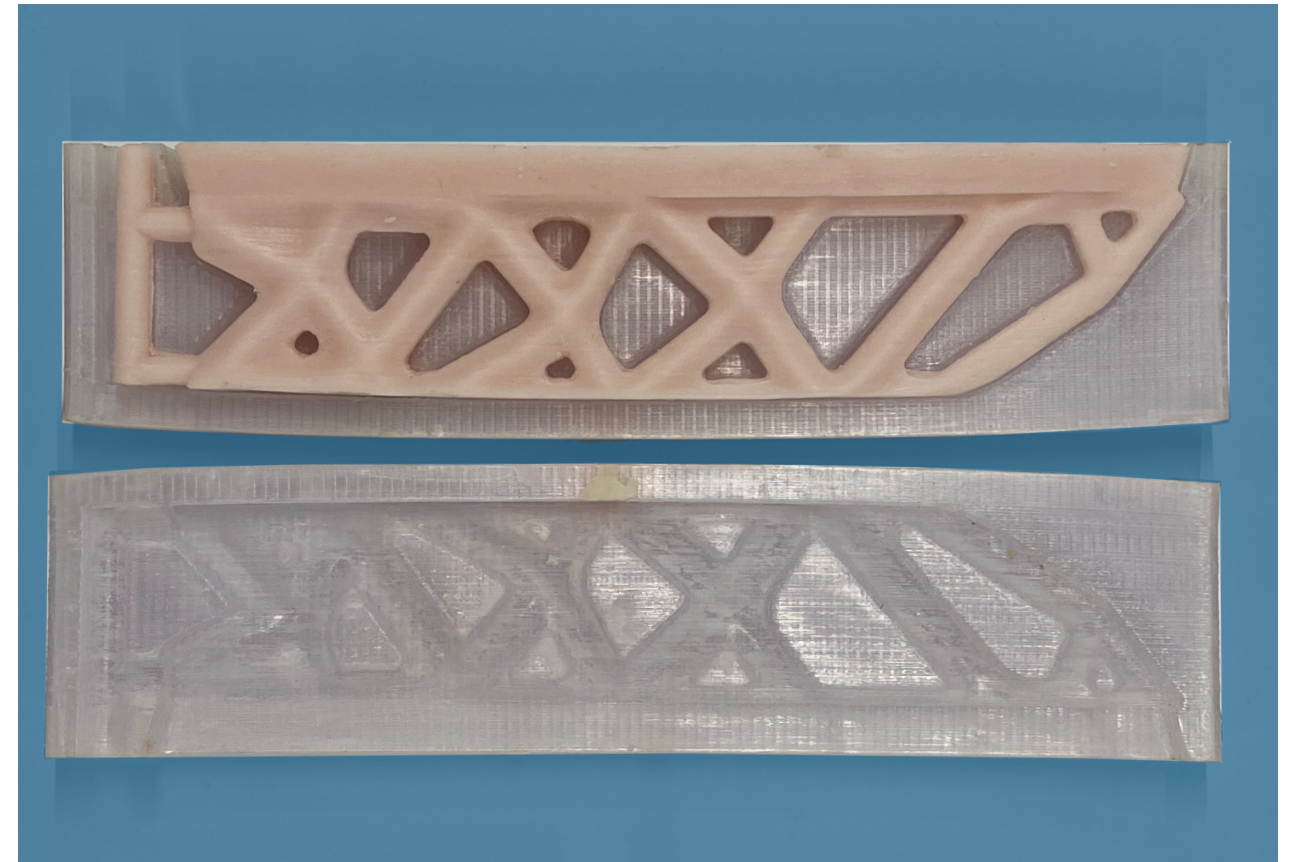


Figure 134 : Demoulding of the wax prototype using pressurised air at the edges. The skew of the mould is evident.

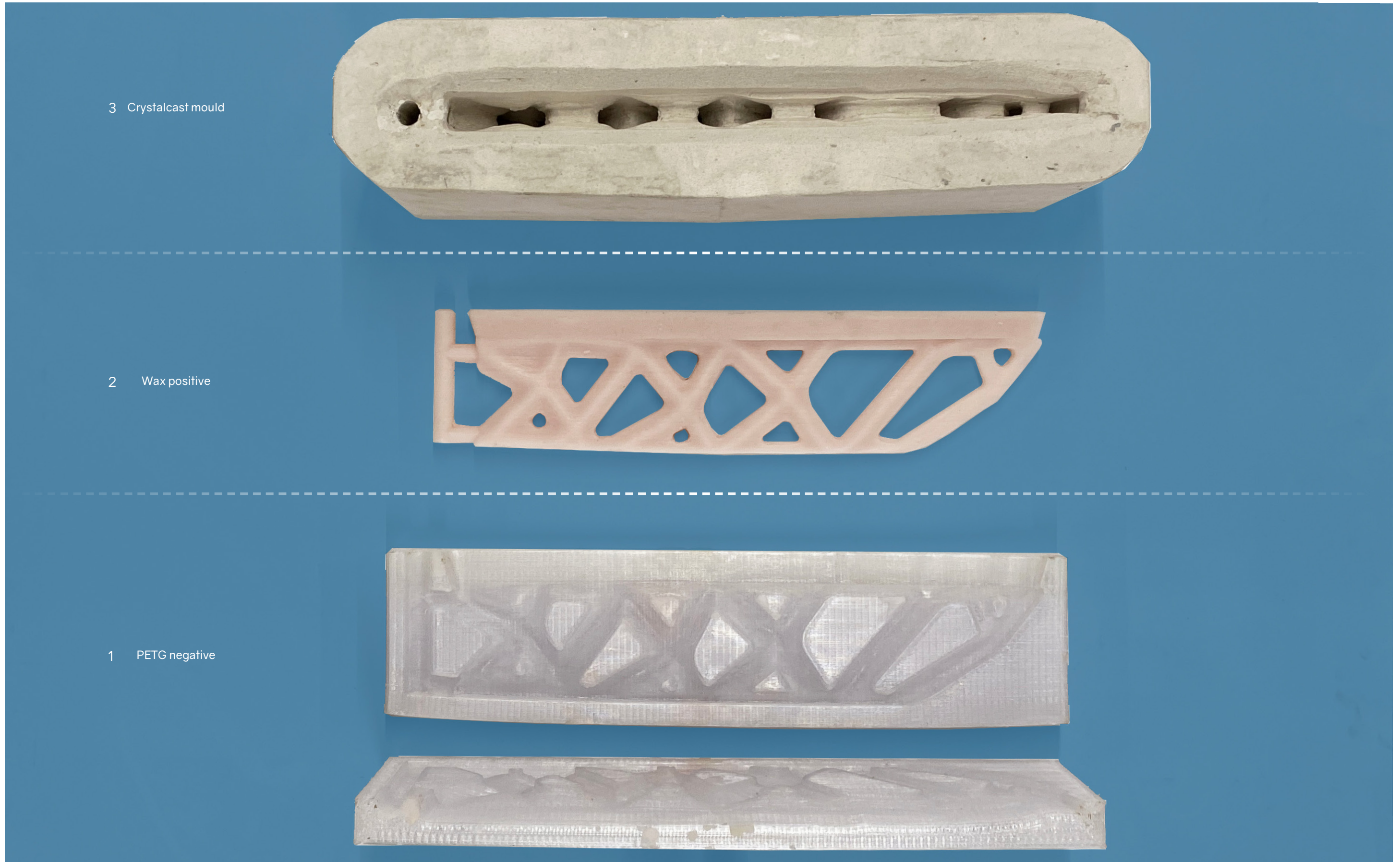
Comparison

The two different processes, that of 3DPSM and that of lost wax technique are compared at Figure 136. It is clear that the lost wax technique includes more steps making it more time consuming and laborious. Such process is unfavourable for such customized and complex geometries as it increases the cost, time and difficulty in fabrication. Another drawback of this method is that the number of steps hinders its dimensional accuracy. Inaccuracies can be caused either due to the misalignment of the two negatives or the printing accuracy. The accuracy of the printing is something that can be tackled using a higher quality printer with smaller nozzle. The misalignment can be prevented by designing a male-female connection interface. On the positive side coating application on Crystalcast moulds is considerably easier as the coatings is poured in the closed cavity and then poured out. When 3DPSM are used an extra layer of Crystalcast via brush application is required that is connected with difficulties in the application and reaching 100% of the surface. Finally, the alternative of directly 3D printing (FDM) on a wax based filament should be further explored. Tweaking and altering of the settings can lead to better print quality and reduced fabrication steps. Alternatively SLA printing on a wax based resin is worth exploring.

8.3. Fabrication

In the following images the lost wax process as realised for the production of the scaled glass prototype is displayed Figures 135-146.

After firing (870°C normal +4 hrs) the mould was left overnight to cool down properly. The next day was submerged in water to allow for easier release. The Crystalcast part was then removed with ease but the coating was still attached to the mould. A wire sponge and bremel using the brush head, were used to remove the residues leaving the surface smooth and transparent. The coating layer worked with this set up and could withstand the prolonged exposure to heat but whether the resulting surface quality is better than that of if Crystalcast requires further testing and inspection under the microscope.



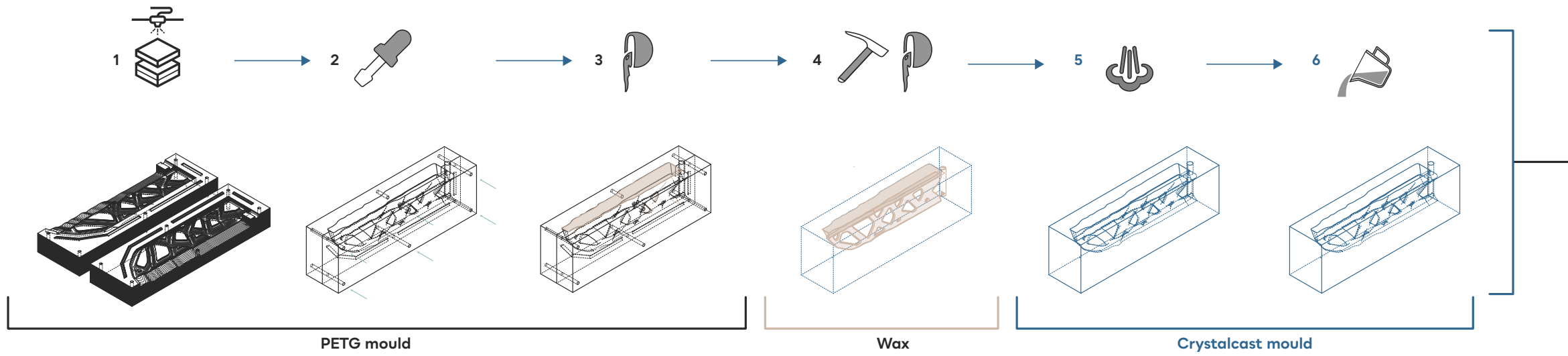
3 Crystalcast mould

2 Wax positive

1 PETG negative

Figure 135 : Lost wax technique. From PETG negative to Crystalcast mould.

LOST WAX TECHNIQUE



3DPSM

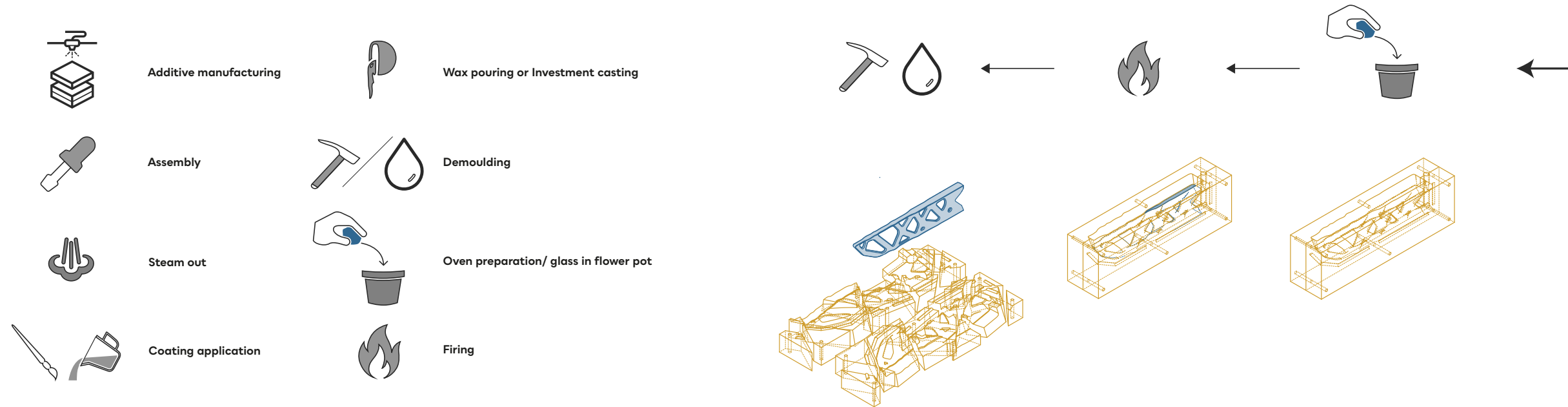
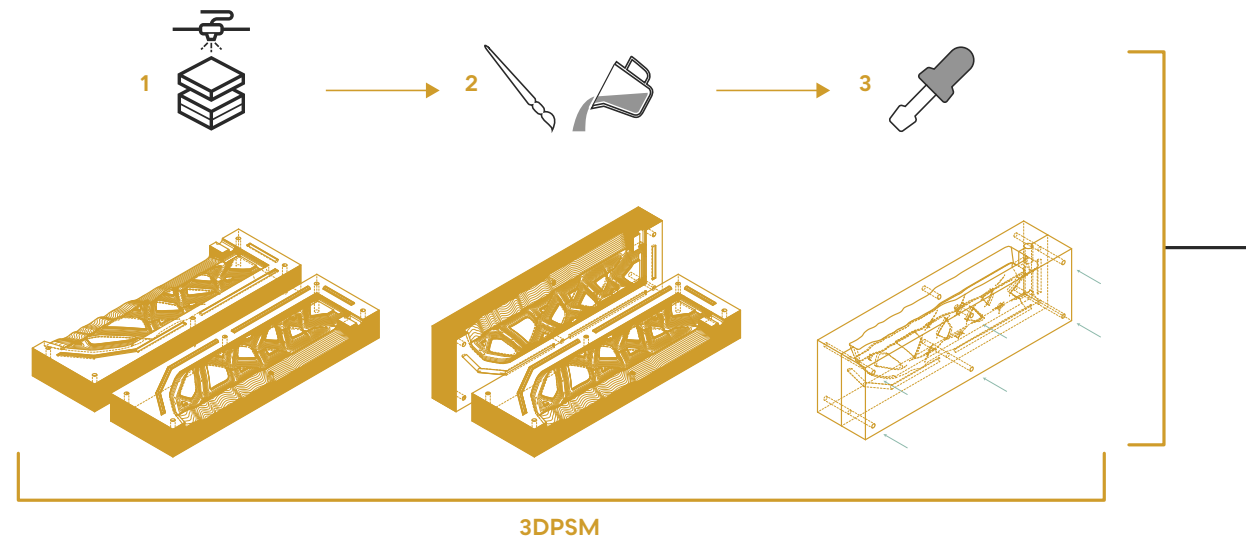


Figure 136 : 3DPSM vs. Lost wax technique process for glass. Considerably less steps and materials are involved for the kiln casting of glass when 3DPSM are used.



Figure 137 : Investment casting of the wax positive. Mould set up.

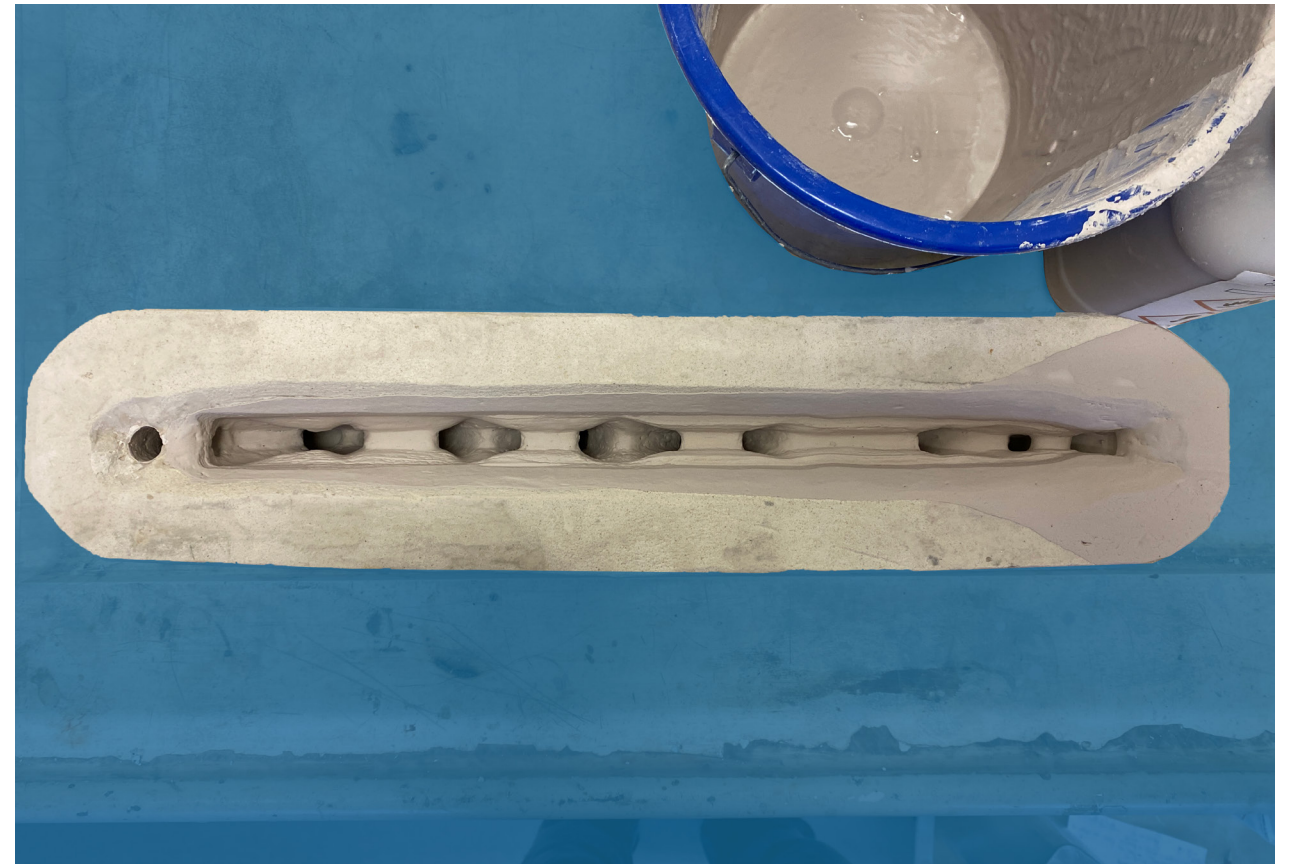


Figure 139 : Flow application of the coating.

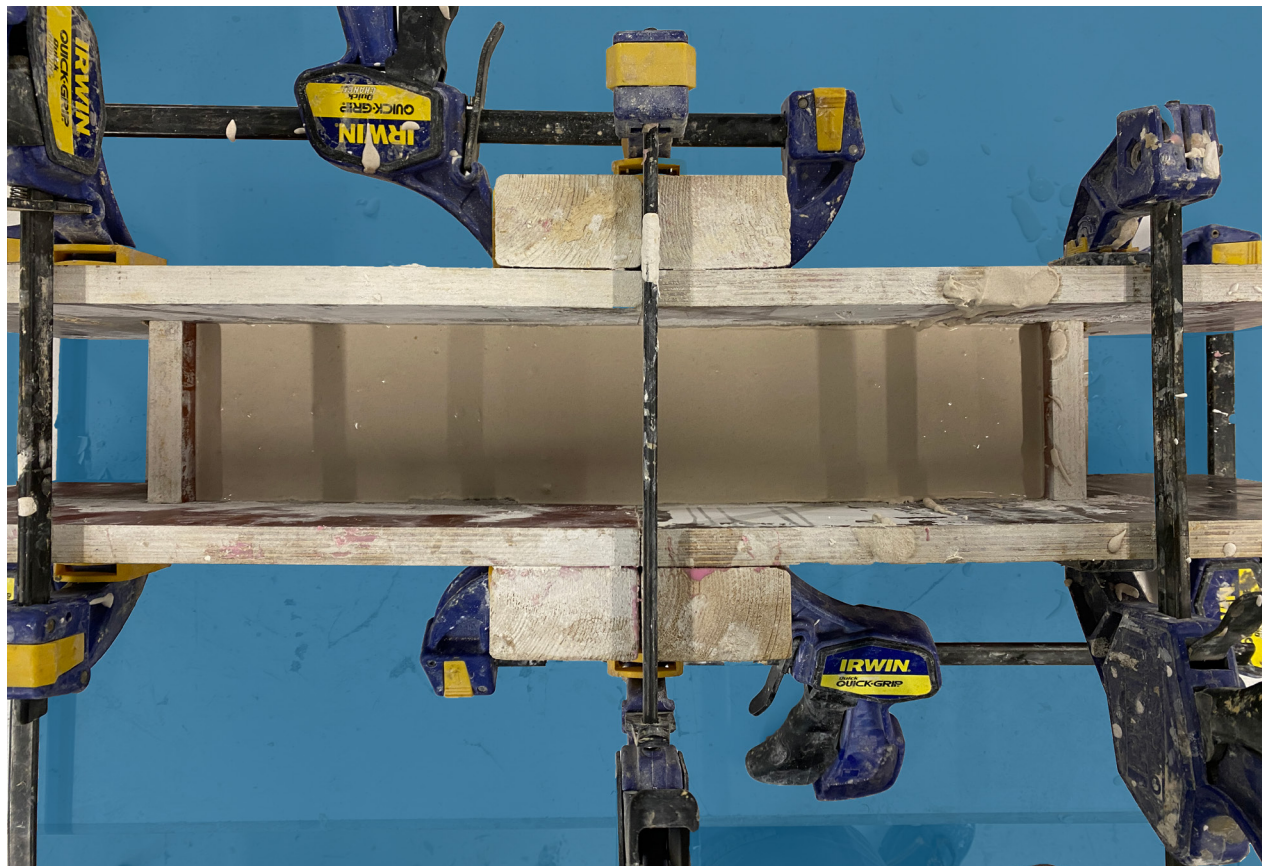


Figure 138 : Investment casting of the wax positive. Crystalcast pouring and setting.



Figure 140 : Flowerpot set up inside the oven. Before firing.

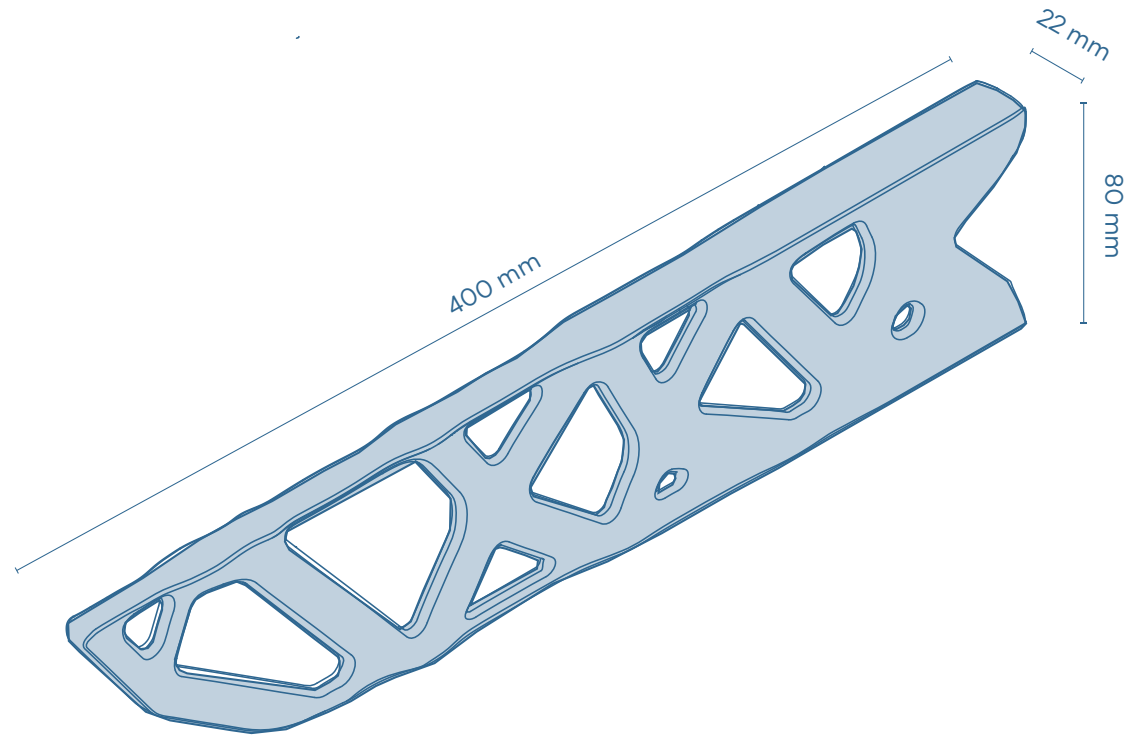


Figure 141 : Dimensions of the prototype. The minimum element dimension used is 8mm.

Table 33: Volume and weight of glass used for the prototype.

	Volume (m3)	Density Bullseye (kg/m3)	Bullseye weight (kg)	Weight + 10% (kg)
Shape	0.000272	2480	0.674	0.742
Shape + vent + tank	0.000427	2480	1.058	1.164



Figure 142 : Glass prototype after demoulding. Coating is attached to glass but can be cleaned relatively easy with the use of a sponge and bremel.

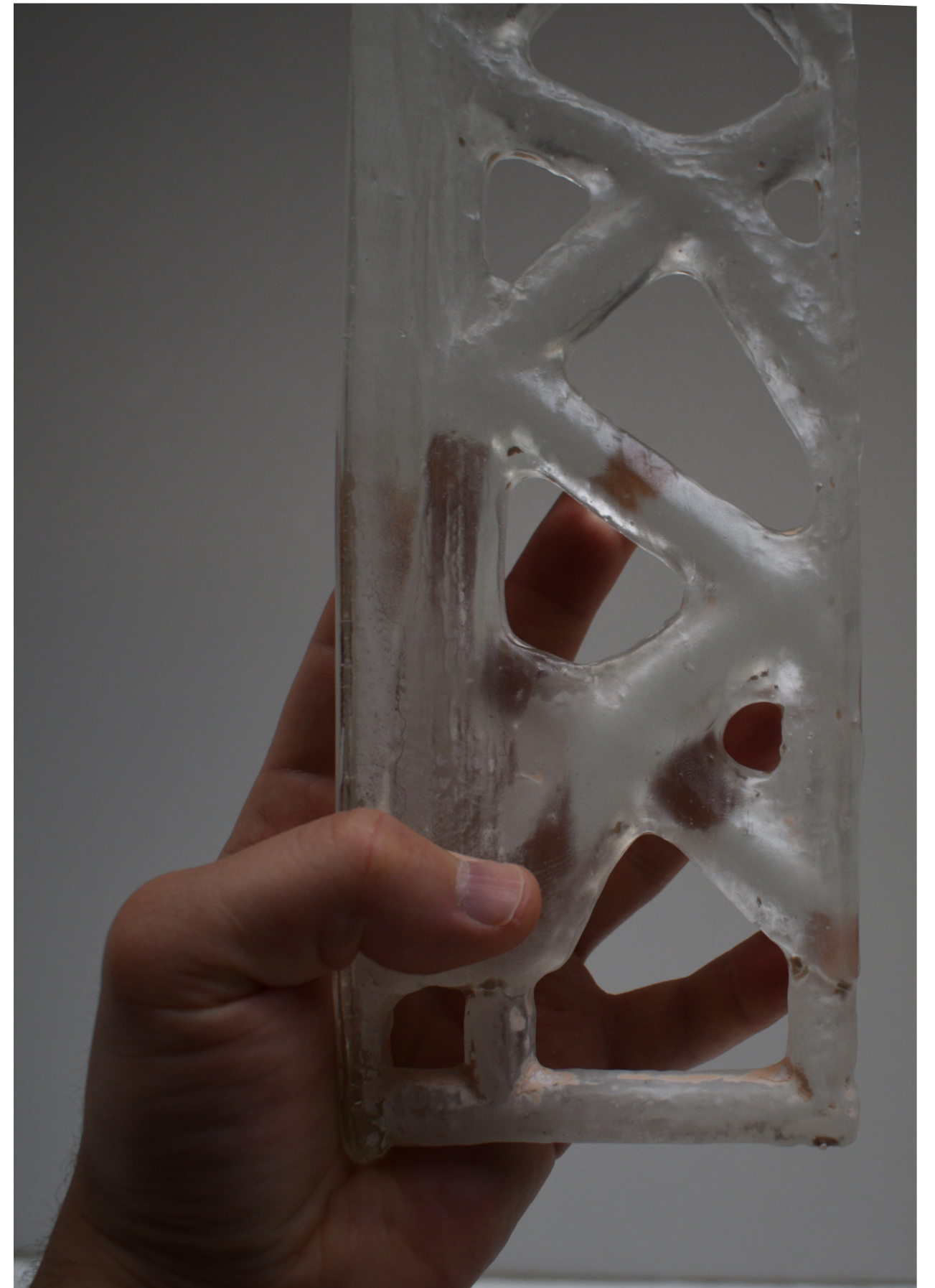


Figure 143 : Glass prototype after cleaning with the help of a sponge. Bremel was also used with a rotating soft brush removing most of the coating residue.



Figure 144 : Prototype after cutting the vent and glass tank using a diamond blade saw.



Figure 145 : Finally after all this hard work I get to play with the prototype and the wax model. Image credits: Marialena Toliopoulou

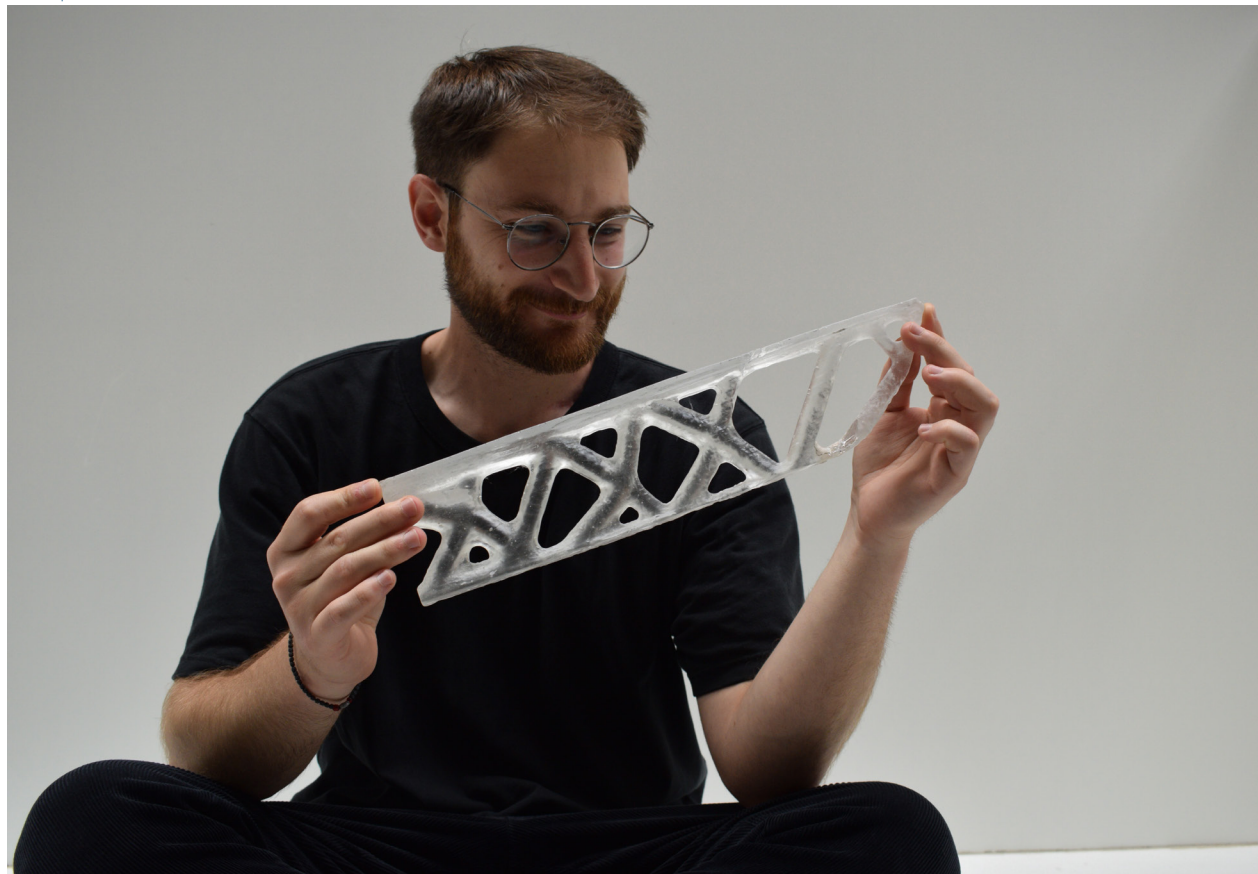


Figure 146 : Admiring the glass prototype. Image credits: Marialena Toliopoulou

8.4. Full size fabrication

The largest disposable mould made for glass casting is that of the great Magellan telescope bank. The diameter of the cast glass piece is 8.4 m. (Figure 147).

For the case of this thesis a slightly longer mould is needed. The total dimension of the mould are 10.55 m x 1.12 m X 2.55 m. Fabrication is not possible in a single piece; limited by the technology and practical aspects, such as handling and application of the coatings. The mould can be segmented based on the maximum size that can be handled with relative ease as indicated in the work of (Menges et al., 2017). On Figure 148 the segmentation on 48 pieces is visible. The individual pieces of the mould have interlocking interface that allows for easy alignment. Additional supports are needed to keep the mould together during casting comprised of the side planes (box) and the bottom support (Figure 148). The minimum wall thickness is defined by the hydrostatic pressure build up. In this case the minimum wall thickness is 26 cm (detailed calculations can be found in appendix).

The glass tank and the vent are also necessary for this mould to allow for glass to reach 100% of the geometry. The titanium connection is placed before closing the mould inside a pre-designed slot.

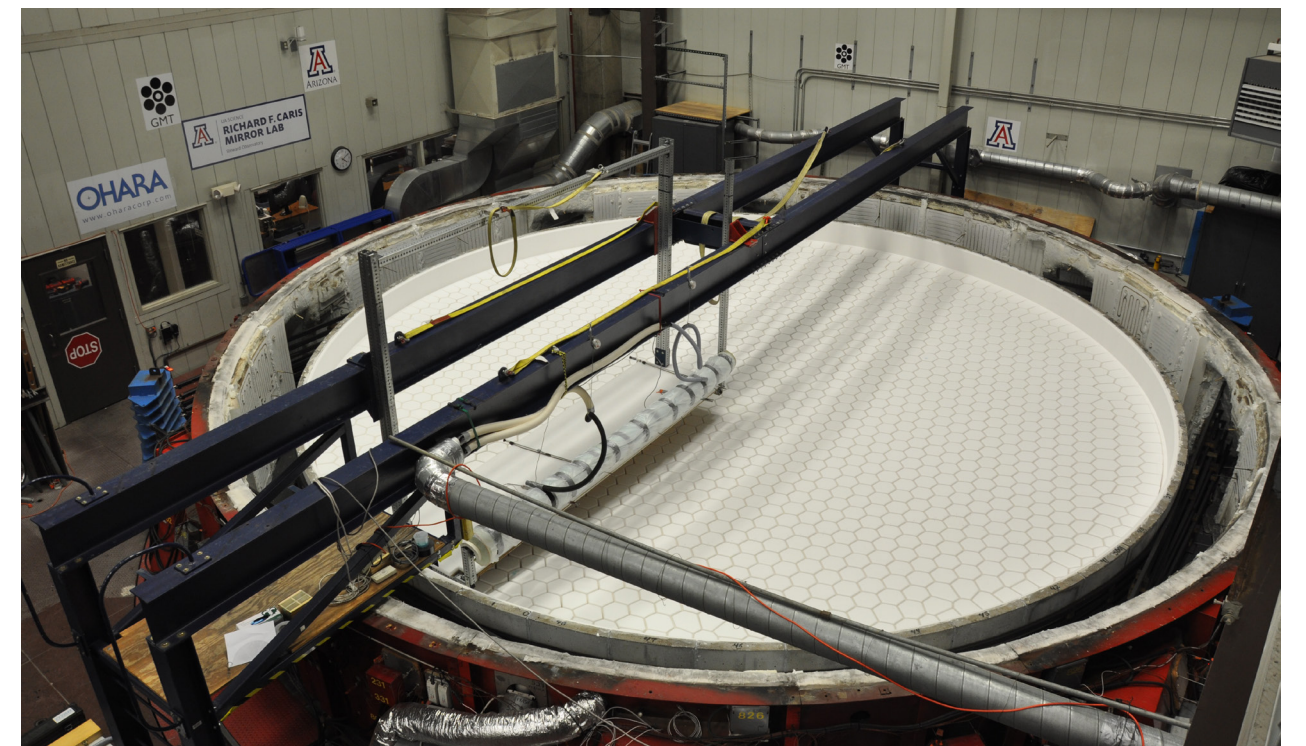


Figure 147 : Magellan telescope mirror blank. Image credits: Faidra Oikonomopoulou.

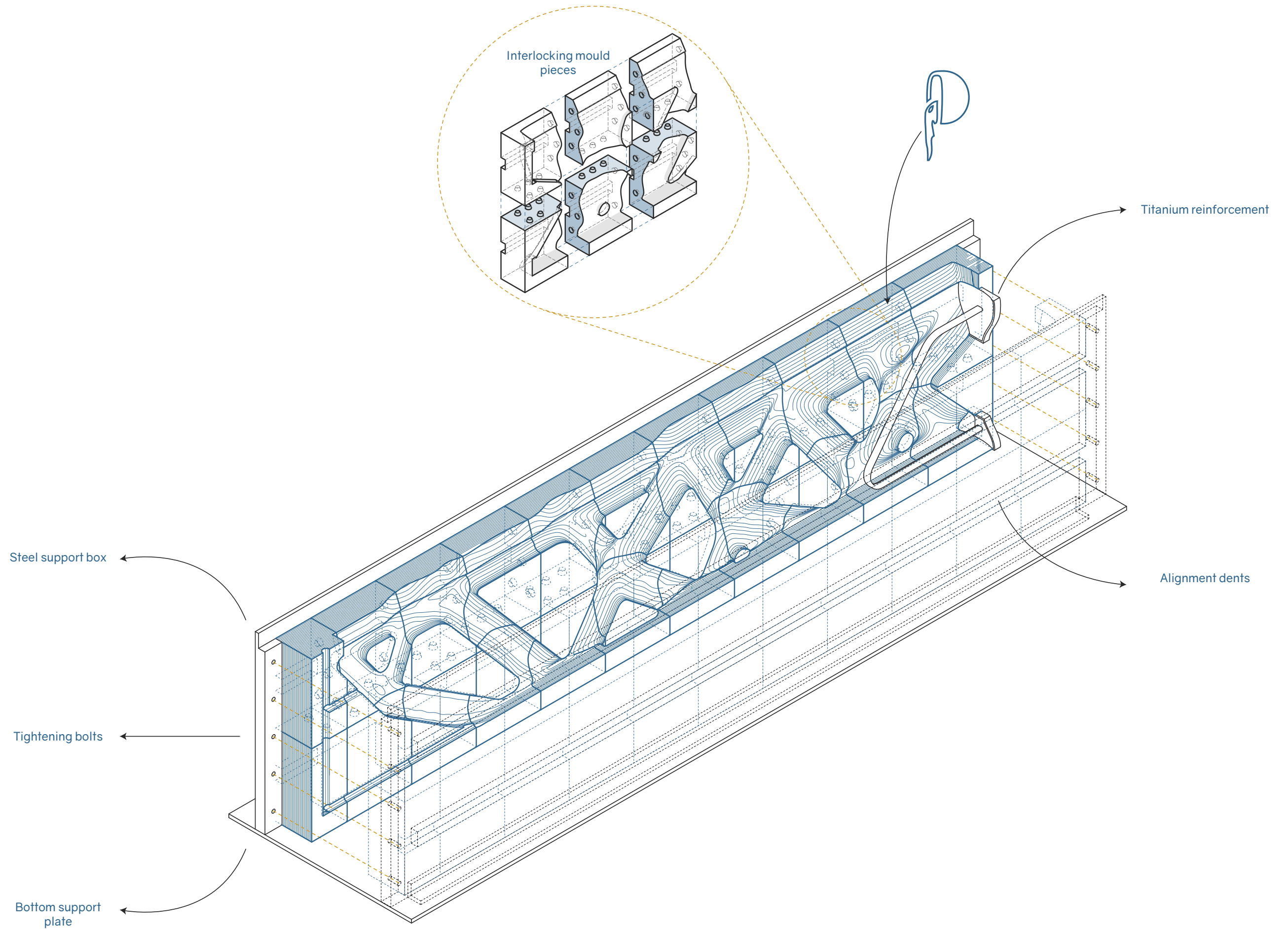


Figure 148 : Mould is comprised of 48 parts (24 on each side). Total mould size 10.55 m x 1.12 m X 2.55 m. Max segment size of 1 m X 1.2 m X 0.56 m.

9

CONCLUSIONS & REFLECTION

9.1. Conclusions

Thinking of glass, the first thing that comes to mind is its transparency or perhaps its brittleness that makes it fragile. Not a lot of people think of glass as a structural material with unique architectural and aesthetical expressions. Fascinated by the possibility, I embarked on the quest to bring glass giants to life or in other words mass optimized glass structures of substantial size. To do so I had to dive into different and niche fields of knowledge, to name a few: glass, glass fabrication methods, refractory coatings, TO and mould fabrication. The knowledge obtained by those fields helped me scratch the surface of the complex interplay of kiln cast glass using 3DPSM. Sharing the vision of previous MSc thesis; that complex and customized glass structures can become a reality in the not-so-distant future, this thesis adds to the existing knowledge and introduces an all-glass observatory deck as a case study.

The introduction of the case study serves as a means to an end; with the main focus of this thesis been the exploration of the fabrication possibilities of kiln cast glass on disposable 3DPSM. The biggest shortcoming of this fabrication method for glass is the resulting rough and opaque surface quality. To tackle this issue refractory coatings and protective layers were used. While the idea of using coatings for improving surface quality on casting is not new, the specific set up and material application hasn't been tested in depth. Further research is needed to arrive at more concrete conclusions, but this thesis arrived as some first promising results, pointing out the next steps and underlining the possibilities that lie within this fabrication method for glass; bringing the realization of glass structures one small step closer.

When searching for the best fabrication method for complex and customized glass forms, no method can tick all the boxes in terms of structural and optical performance, sustainability and fabrication freedom/ feasibility. The decision highly depends on the soft criteria set during the design phase. Specifically cast glass on disposable moulds seem to have the highest shape and size freedom, making it ideal for voluminous glass applications but is highly constricted by its lack of redundancy and the rough surface, making its production, cost and time inefficient. Those setbacks become the starting point for parallel research: one experimental and one through research by design.

Experimental research

The experimental research focuses on improving the surface quality aiming to arrive at an optically transparent and smooth surface directly after demoulding. This can reduce the need for post processing and thus cost and time. Research on the effect of the maximum firing temperature, annealing schedule (total dwell time) and coatings combinations yielded promising results. The best results were received for kiln cast samples tested at 870°C degrees and up to 55 hrs. with the best (optically) being the combination of ceramic sand moulds with Crystalcast and Zirkofluid 6672. Especially the use of Crystalcast (which is the standard material used for everyday casting of glass in the lab) performed well when used as a protective layer, maintained its integrity and forming a thin wall casting vessel/mould. If this material could be used for 3D printing of moulds, the laborious lost wax technique currently implemented for complex shapes could be avoided.

Overall, all the experiments conducted using 3DPSM indicated that there is a relation between time and temperature and the longer the exposure to high heat the worse the performance of the coatings. Hence the poorer the surface quality. The exact relation is not known, and further experimentation is needed to determine that.

Experimentation on more complex and larger geometry confirms the assumption of heat-time relation to the effectiveness of the coating. Larger samples require longer exposure at the maximum temperature to allow for proper melting of the glass. Those extra couple of hours affected the optical quality greatly resulting in adhesion of the coating to the glass. The results are improved when compared to previous kiln cast glass experiments (Figure 149, left) and no sand adhesion is present but the optical quality is far from the benchmark quality of glass cast on steel moulds (Figure 149, right). The improved surface quality translates into reduced post processing, thus time and cost for the production. In that sense the series of experiments are somewhat successful and hopefully further testing can fine tune the set up. However elimination of the post processing on larger elements cast on 3DPSM seems difficult.

Apart from temperature factor, for a smooth and transparent cast glass surface, a smooth mould surface is imperative. Application of the protective layer and coatings greatly affects the final finishing quality of the mould surface. Flow application is preferred as it results in a smooth finish quality and can cover even the most complex shaped moulds. Closing with the experimental part, on the small samples the application was straight forward and all points could be reached. When the

geometry was scaled up the application of Crystalcast proved more challenging especially reaching narrow parts of the geometry. This suggest that a different application method than brushing should be explored for the protective layer of Crystalcast. Since Crystalcast dries quickly after mixed with water the best guess can be a spraying system that mixes the two components at the outlet might be the most effective.

Finally, the time-heat affect on coating effectiveness is expected to be even more severe for larger glass objects. This means that the findings of those experiments is unclear if they are applicable to larger scale glass casting.



Figure 149 : Left kiln cast glass using disposable 3DPSM (Bhatia, 2019). Middle: current experiments as continuation of (Koniari, 2022) work and through application of the findings during this thesis. Right foundry cast glass using steel moulds. Difference in the surface quality is evident (Oikonomopoulou, Bristogianni, Veer, et al., 2018). Results are somewhat successful resulting in less sand adhesion and more transparent surface but further research is necessary to arrive at a result closer to that on the right.

Research by design

The research by design part focuses on safety and redundancy of the case study. While the initial aim was to create a full cast glass structure, safety wise this would not have been feasible. Certain design techniques were implemented, supported by an extensive risk analysis. The bearing structure started as a monolithic cast glass piece and ended up spliced in three. In doing so, complete failure of the bearing structure is less probable. The second strategy that was implemented is the division into three zones based on risk. The final design is a combination of two manufacturing methods, casting for the bearing structure and AWJ cutting and lamination, for the floor and side rails structures. The latter are prone to ware and accidents, vandalism or other causes. Redundancy of the structure is certainly improved, but the final structure deviated from the initial soft criteria of sustainably, since lamination of AWJ cut parts has high waste generation and results in components that are hard to recycle. Nevertheless, as discussed above there is no such thing as the most suitable fabrication method for all the soft criteria and depending on what is prioritized (in this case safety) some compromises must be made.

Geometry optimization

To close off with, while it is not the focus of this thesis, geometry optimization still displays a lot of difficulties. Apart from the limitation related to the current algorithm (2D), the translation of the results into geometry is not streamlined and manual editing and verification is still needed. The process is crucial to ensure that the final post processed geometry is structurally sound. At the same time automation requires advanced computational skills and understanding of the optimization process. These factors can become a knowledge barrier for the common user. For prototyping additional manual editing of the geometry is necessary to incorporate the limitations of each fabrication method and account for the scaling of the geometry. Fabrication limitation criteria can be incorporated on the optimization algorithms in the future. Finally, while the geometry generated is optimized the final post processed shape is somewhat altered resulting in an approximation of the optimal design.

9.2. Limitations

The main limitation on the experimental part has to do with time and materials. Within the time-line of an MSc thesis many tasks need to be complete leaving limited time for conducting the experiments. Within the available time the maximum number of experiments were conducted. At the end the issue was the number of available moulds which define the number of experiments.

Case study wise the biggest limitation faced was the optimization process which in essence requires a separate study of its own. Optimization algorithm requires advance understanding of the finite element's theory. The output requires a method for post processing to arrive at the final design. This part is still underdeveloped while as part of this thesis some steps were taken towards automating, the process still requires manual tweaking and some subjective interpretations when filtering the results. The overall design and validation process is thus mostly manual which is attributed to the specificity of application and the early stages of development.

9.3. Discussion

Depending on the intended application of the structure and the decisions and priorities set during the design phase the preferred fabrication methods for an all-glass structure can be preselected. As presented in this thesis, shape and size freedom, full and non-directional transparency and manufacturing with a method that can ensure recyclability and recoverability of the material are the top priorities. Based on the roadmap (Figure150) casting was chosen for the realization of the case study of all glass bridge observatory.

If the design prioritized a lightweight, thin and redundant structure, then based on the roadmap the preferred fabrication method would be lamination of AWJ cut parts. In the latter case the design is expected to look like the depiction on Figure 151.

Lamination of float glass has an extensively studied structural behaviour resulting in a higher design strength and a lower safety factor compared to cast glass, especially when heat strengthened glass is used.

Transparency-wise lamination of float glass has directional transparency while cast glass can achieve full transparency.

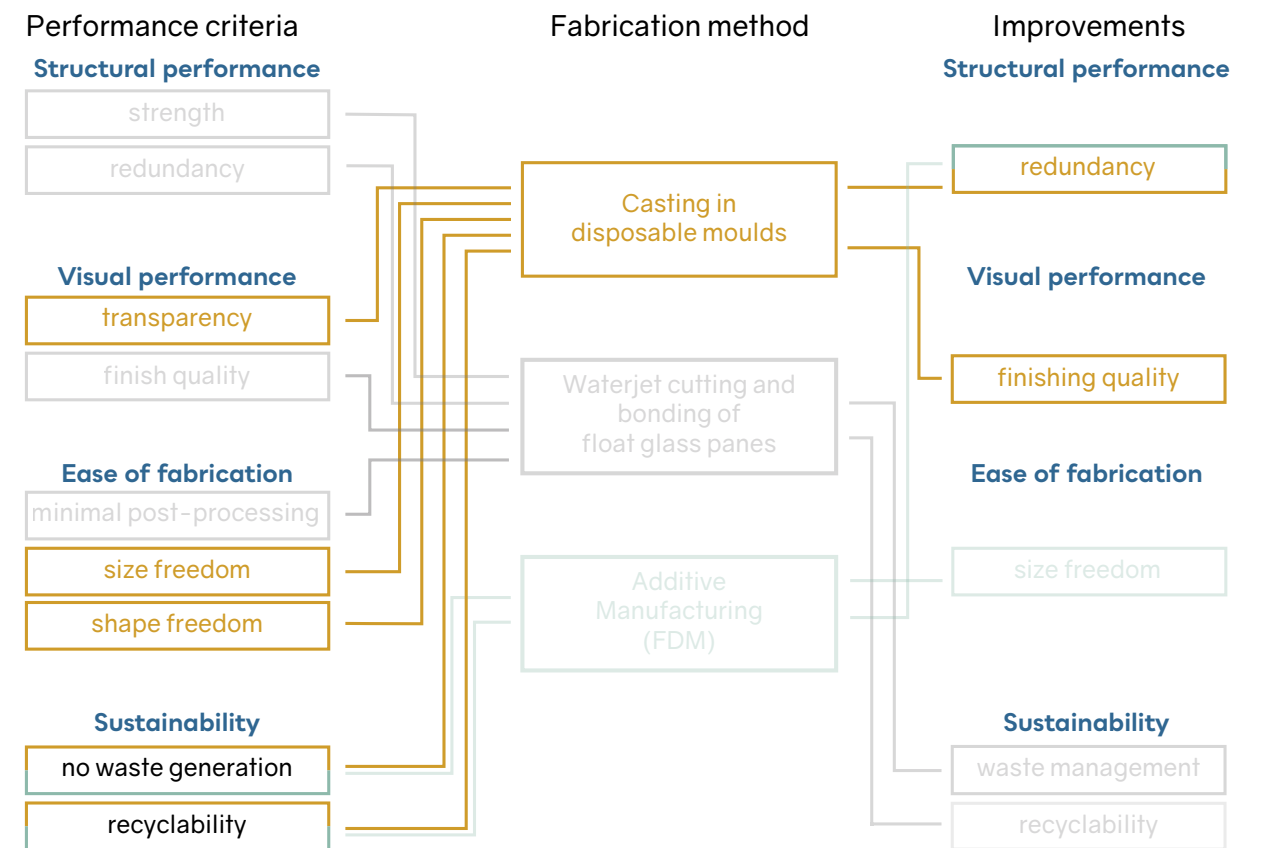


Figure 150 : Road map were the reason behind the selection glass casting for the realization of the case study are visible and the potential improvements that led to the experimental part and research through design.

Table 34: Comparison of AWJ cut and laminated vs. kiln cast glass on 3DPSM structure, based on structural, optical, sustainability and fabrication criteria.

		AWJ cut and laminated	Kiln cast glass on 3DPSM
Structural	Design strength	Up to 45 MPa	6.4 MPa
	Redundancy	Yes	No
Optical	Transparency	Directional transparency	Full transparency or semi opaque*
	Finishing quality	Good	Medium
Sustainability	Waste generation (glass)	High	Low
	Recyclability	Partial	Full
	Material	Raw (primary resources)	Raw or recovered/ recycled
Fabrication limitations	Recommended shape	Planar, can have sharp edges	3D, smooth edges

* If waste streams are used then transparency can be compromised in favour of sustainability. Unique patterns and colours can be used as an aspect of the design.

Sustainability-wise, cast glass components can be made from recovered or recycled glass reducing energy and raw material consumption. Cast glass components are 100%recyclable since no adhesives or lamination material is used. Lamination of float glass structures is not easily recyclable and due to the high standards of the float glass industry, raw material is usually preferred in the production.

Finally shape and size freedom is different for each fabrication method. AWJ and laminated float glass structures can have sharp edges and are limited: 1) thickness-wise (max. number of plies that can be laminated), 2) by the size of the panes and 3) by the minimum member size (to avoid breakage during the cutting process). Cast glass produced on 3DPSM components should ideally have 1) a homogeneous mass distribution, 2) smooth edges and 3) the min and max size of the members to allow for a sufficient mould thickness (Table 34).

To sum up, on one hand, casting seems to be an overall more flexible fabrication method for glass. As can be seen in the figures 152, different types of finishes can be achieved and different recipes of glass can be used. The surface roughness observed on cast glass on disposable moulds can be used as a design aspect that is unique to cast glass.

The roughness can be post processed using sand-blasting resulting in a uniform frosted look that is translucent. We can imagine a cast glass structure out of a recycled glass. Or even glass that looks like marble. Such structure will have a unique, almost artistic, appearance, offering new possibilities and in terms of architectural expression, while at the same time reducing the waste, promoting a more circular built environment and redefining the standards of beauty and quality within the glass industry.

On the other hand, casting of glass is as much a form of art as much as it is science. Extended validation, testing and experimentation is involved in the development of cast glass building products in real life. This translates into high cost, hindering the feasibility of such structures. However, through the years cast glass structures have captivated the imagination of architects and engineers and I personally feel that the exploration of the limitation and possibilities is the essence of the building technology studies. I am glad that I had the opportunity to study this fascinating topic as an architect and soon to be engineer.

9.4. Next steps

Important next step for this research is to further scale up the results. Scaling up the results will give important insight on the effectiveness of the coating and the overall set up.

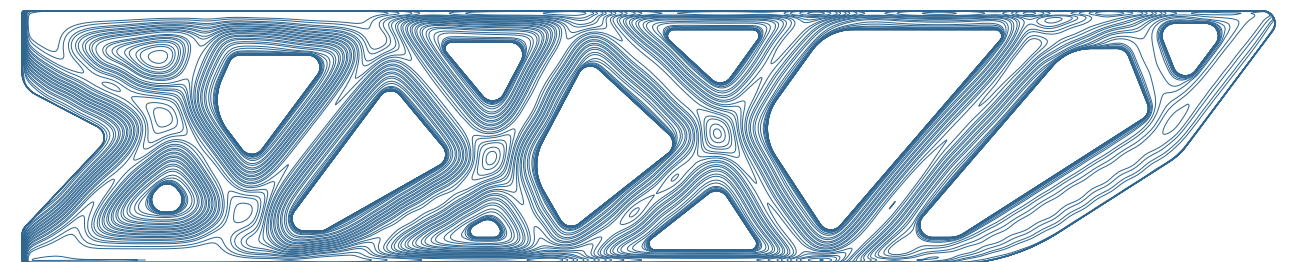
Structural testing of scaled up results can help define to what degree the roughness of the cast glass surface affects the structural performance of the components.

The Crystalcast mould used for prototyping yielded improved results than the equivalent 3DPSM with the use of the same coating. As discussed in the conclusions this highlights the potential that 3D printing of Crystalcast moulds can have both for architectural and art applications.

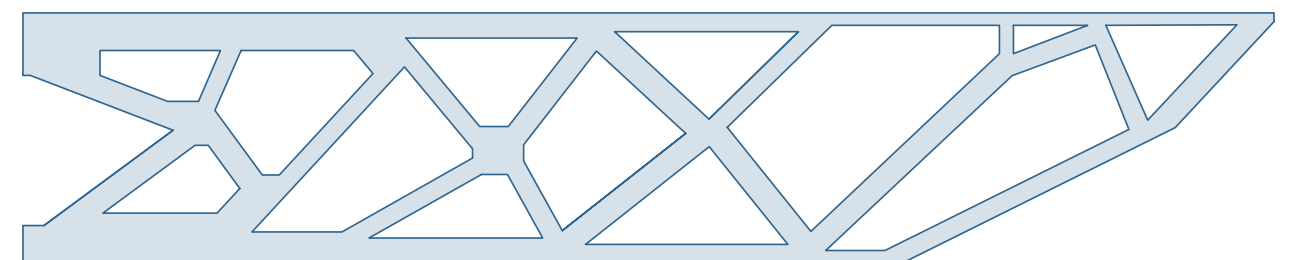
Further development of the optimization software for glass and implementation of automated post processing based on the limitations per fabrication method.



Algorithm output (side view)



Cast glass



AWJ and lamination of float glass

Figure 151 : From the output of the algorithm to the final geometry. Alternative designs outcome based on the selected fabrication method. The difference is clear. If the structure was made out of laminated float glass the architectural expression could have been totally different with sharp edges and a more lightweight structure.

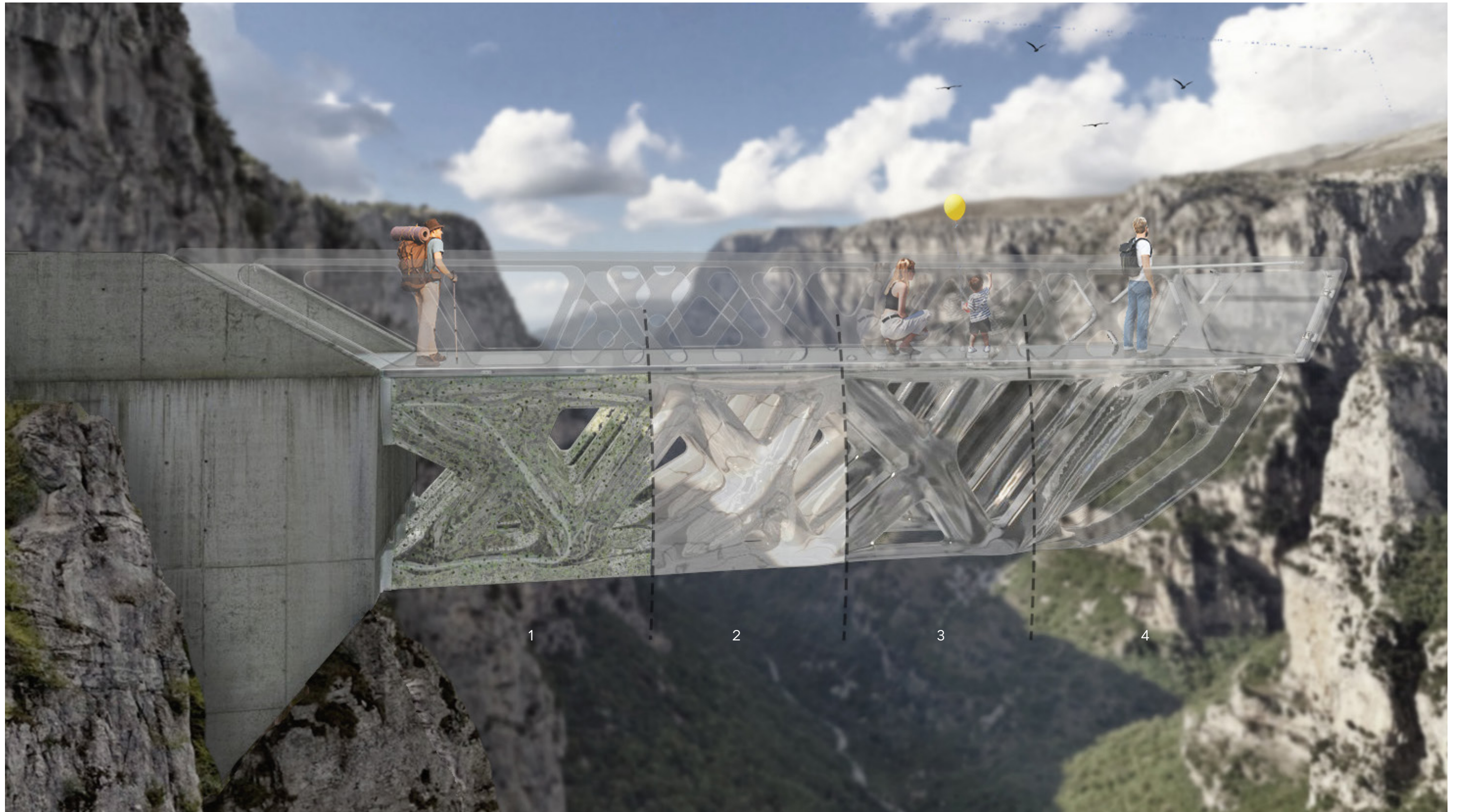


Figure 152 : Cast glass fin with different glass recipes and finishes. From left to right: 1. car glass or oven doors, 2. fully crystallized recycled glass (marble), 3.frosted finish (no post processing), 4. Polished finish (clear).

9.5. Reflection

Graduation process

How is your graduation studio topic positioned in the studio?

This thesis with title "Bringing Glass Giants to life, Fabrication of mass-optimized glass components of complex form" introduces a novel all-glass structure design and involves two chairs within the Building Technology master track: the Structural Design & Mechanics chair and the Building Product Innovation chair. The former provides the necessary knowledge regarding glass as material and glass casting, topology optimization, structural verification and input related to lab experimentation. The building product innovation chair provides insight on the current means of production, assessment criteria for each fabrication method, detailing of connections and overall feasibility of the design. The combined knowledge of both chairs helps push the boundaries of glass design and fabrication towards the creation of a material efficient, safe to use, sustainable, and feasible glass structures of complex and custom shape, providing a unique aesthetic. The interdisciplinary approach of this work reflects the essence of the building technology track and compliments the holistic and diverse take that the MSc AUBS has towards architecture.

How did the research approach work out (and why or why not)? And did it lead to the results you aimed for? (SWOT of the method)

The complexity of the topic dictated an approach of the topic using several methodologies. The thesis consists of four parts: literature review, comparative study, lab experimentation and research by design. The primary focus is the lab experimentation with the aim to enable better surface quality and transparency of kiln cast glass on disposable moulds (3DPSM). The research is supported by a state-of-the-art literature review on glass, topology optimization and glass fabrication methods. Additionally, the development of a case study linking the work with a real-life scenario and setting context, requirements and functionality. The approach worked as expected with all parts came together in the end. Research yielded promising results, the optimization of the geometry was performed and verified structurally.

How does the research lead to the design?

Novel glass structural applications display a unique set of material and fabrication peculiarities.

A complex research and design process was needed to understand the topics involved and arrive at a sensible research and design output. The research part was crucial in understanding the design limitations of glass, its material properties, the reason why TO is necessary and to familiarize oneself with the most promising glass fabrication methods currently available.

The introduction of a case study helped establish a set of soft criteria leading to the selection of the most appropriate fabrication method for glass. Research and design from this point on were intertwined leading to the next steps. This is especially evident in the lab experiments that were conducted with the aim of improving one of the main disadvantages of kiln-cast glass on disposable moulds (surface quality and transparency). Hence, connecting research, design and fabrication of complex and customized structural glass components. The final design serves as the means for further experimentation by prototyping.

Societal impact

To what extent are the results applicable in practice?

The research work of (Bristogianni, 2022; Oikonomopoulou, 2019) and the plethora of master theses from (Bhatia, 2019; Damen, 2019; Koninari, 2022; Koopman, 2021; Naous, 2020; Stefanaki, 2020) underlines the research potential on structural applications of cast glass within TU Delft. The importance of the research conducted in the glass lab is evident both in the academic and professional world with numerous publications and built examples (e.g., Crystal house, Qaammat Pavillion, Mirage). Apart from TU Delft other institutions (TU Darmstadt, MIT) display or have displayed in the past extensive research and interest towards the exploration of alternative fabrication methods of glass, highlighting the overall scientific relevance of the work. The experimental work as part of the thesis is going to be conducted in accordance with the ongoing research interest of the glass lab at TU Delft and involves companies (Ex One and HA) that sponsor materials for the research work, linking the topic of the thesis with the professional world.

While this thesis builds up and contributes to the above-mentioned knowledge, further investigation of the various factors that affect the surface quality and transparency of such components is needed. Further testing on larger scale and more complex geometry is needed.

Finally, this research is important for the work of artists and sculpturers were finishing quality and transparency on glass is important.

Does the project contribute to sustainable development? What is the impact of your project on sustainability (people, planet, profit/prosperity)?

Over the course of its history glass has transitioned from a fragile and opaque material to a durable, optically transparent, structural material that shows great potential in architectural and structural applications. Glass innovation is directly connected with advancements in many fields of science and society such as optical (lenses, mirrors and prisms), communications (glass fibers), automotive, renewable energy (solar panels), biology, medicine so on so forth. Glass is still relatively new in the structural world, compared to other materials, but displays great potential that can revolutionize the future application in the field of building industry, architectural engineering and structural engineering.

Having that said that this thesis dealt with the limitations of current means of fabrication and researched the possibilities towards the realization of transparent, structurally safe, sustainable and feasible cast glass structural applications contributing a small piece of knowledge.

Cast glass structures are more sustainable than laminated float glass structure. Recovered material that would have otherwise end up on the land field can be used reducing the raw material consumption and energy used. On top of that such structures are recyclable helping close the loop leading in a more circular built environment.

The use of recovered glass waste in casting leads in the creation of unique pieces with unique patterns and colour that have an almost artistic expression. The unique appearance apart from the fact that leads towards a more circular built environment, unlocks new ways of architectural expression with glass and helps redefine the beauty standards within the industry.

How does the project affect architecture / the built environment?

Cast glass structures is a niche research field, but the realised examples are indicative of a real-life demand. The output of the design part is a slightly utopic, size wise, but showcases a vision towards all glass structures. The outcome of the above-mentioned experiments will further verify the findings enabling applications of kiln cast glass on larger and more complex shapes and unique architectural and structural value. Thus, pushing the boundaries of what it is possible both design and manufacturing wise.

10 REFERENCES

- American society of testing and materials. (n.d.). ASTM F42.
- Anna Gowsalya, L., & E. Afshan, M. (2021). Heat Transfer Studies on Solidification of Casting Process. In Z. Abdallah & N. Aldoumani (Eds.), *Casting Processes and Modelling of Metallic Materials*. IntechOpen. <https://doi.org/10.5772/intechopen.95371>
- Ashby, M. F., & Jones, D. R. H. (2006). *Engineering materials* (3rd ed). Butterworth-Heinemann.
- Bartuška, M. (2008). *Glass defects* (T. Flynn, Ed.; First edition). Glass Service, Inc.; Práh.
- Bedon, C., & Santarsiero, M. (2018). Transparency in Structural Glass Systems Via Mechanical, Adhesive, and Laminated Connections—Existing Research and Developments. *Advanced Engineering Materials*, 20(5), 1700815. <https://doi.org/10.1002/adem.201700815>
- Belter, J. T., & Dollar, A. M. (2015). Strengthening of 3D Printed Fused Deposition Manufactured Parts Using the Fill Compositing Technique. *PLOS ONE*, 10(4), e0122915. <https://doi.org/10.1371/journal.pone.0122915>
- Bendsøe, M. P., & Sigmund, O. (2004). *Topology Optimization*. Springer Berlin Heidelberg. <https://doi.org/10.1007/978-3-662-05086-6>
- Bertoldi, M., Yardimci, M. A., Pistor, C. M., GUYeri, S. I., & Sala, G. (1998). Mechanical Characterization of Parts Processed via Fused Deposition. University of Illinois at Chicago.
- Bhatia, Jvneet. (2019). SHAPING TRANSPARENT SAND IN SAND Fabricating topologically optimized cast glass column using sand moulds. TU Delft.
- Blocher Partners. (n.d.). Bründl Kaprun flagship store. <https://blocherpartners.com/en/projects/trade-culture/brundl-kaprun-flagship-store>
- Bohlin Cywinski Jackson. (2006, 2011). Apple Store, Fifth Avenue. <https://www.bcj.com/projects/retail/apple-store-fifth-avenue-new-york/>
- Bontemps, G., & Cable, M. (2008). *Bontemps on glass making: The Guide du verrier of Georges Bontemps*. Society of Glass Technology.
- Bristogianni, T. (2022). Anatomy of cast glass: The effect of casting parameters on the meso-level structure and macro-level structural performance of cast glass components [Delft University of Technology]. <https://doi.org/10.4233/UUID:8A12D0B1-FEE2-47F1-9FA9-FF56AB2E84C1>
- Bristogianni, T., & Oikonomopoulou, F. (2022a). Glass up-casting: A review on the current challenges in glass recycling and a novel approach for recycling "as-is" glass waste into volumetric glass components. *Glass Structures & Engineering*. <https://doi.org/10.1007/s40940-022-00206-9>
- Bristogianni, T., & Oikonomopoulou, F. (2022b). Reinforced glass: Structural potential of cast glass beams with embedded metal reinforcement. In A. Zingoni, *Current Perspectives and New Directions in Mechanics, Modelling and Design of Structural Systems* (1st ed., pp. 807–812). CRC Press. <https://doi.org/10.1201/9781003348443-132>
- Bristogianni, T., Oikonomopoulou, F., Yu, R., Veer, F. A., & Nijse, R. (2020). Investigating the flexural strength of recycled cast glass. *Glass Structures & Engineering*, 5(3), 445–487. <https://doi.org/10.1007/s40940-020-00138-2>
- Bruggi, M., & Duysinx, P. (2012). Topology optimization for minimum weight with compliance and stress constraints. *Structural and Multidisciplinary Optimization*, 46(3), 369–384. <https://doi.org/10.1007/s00158-012-0759-7>
- Brunet Saunier Architecture. (1995). Centre Administratif. <https://brunet-saunier.com/projets/centre-administratif>
- Bukieda, P., Lohr, K., Meiberg, J., & Weller, B. (2020). Study on the optical quality and strength of glass edges after the grinding and polishing process. *Glass Structures & Engineering*, 5(3), 411–428. <https://doi.org/10.1007/s40940-020-00121-x>
- Bulls-eye Glass. (n.d.). Annealing thick slabs. Retrieved 15 January 2023, from <https://www.bullseyeglass.com/methods-ideas/annealing-thick-slabs.html>
- Centre for the Protection of National Infrastructure. (2019). Introduction to Laminated Glass Interlayers. Centre for the Protection of National Infrastructure.
- Choi, H.-H., Kim, E.-H., Park, H.-Y., Cho, G.-H., Jung, Y.-G., & Zhang, J. (2017). Application of dual coating process and 3D printing technology in sand mold fabrication. *Surface and Coatings Technology*, 332, 522–526. <https://doi.org/10.1016/j.surfcoat.2017.07.035>
- Coatings for moulds and cores. (2000). In *Foseco Ferrous Foundryman's Handbook* (pp. 226–244). Elsevier. <https://doi.org/10.1016/B978-075064284-2/50017-X>
- Corning museum of glass. (2011, October 24). On a Pool of Tin: Float Glass. <https://www.cmog.org/article/pool-tin-float-glass>
- Cruz, P. J. (Ed.). (2013). Boosting European education on structural glass: COST action TU0905 training school. In *Structures and Architecture* (0 ed., pp. 329–334). CRC Press. <https://doi.org/10.1201/b15267-41>
- Cummings, K. (2002). *A history of glassforming*. A. & C. Black.
- Damen, W. (2019). *Topologically Optimised Cast Glass Grid Shell Nodes*. TU Delft.
- dbt. (2017). 3D Printed Slab. <https://dbt.arch.ethz.ch/project/topology-optimisation-3d-printed-slabs/>
- Divisare. (n.d.). Kruunenberg Architecten Laminate, a House of Glass. Retrieved 10 January 2023, from <https://divisare.com/projects/387294-kruunenberg-architecten-luuk-kramer-lamina-ta-a-house-of-glass>
- Dlupal. (n.d.). Retrieved 12 February 2023, from <https://www.dlupal.com/en/load-zones-for-snow-wind-earthquake/>
- Dudutis, J., Pipiras, J., Stonys, R., Daknys, E., Kilikevičius, A., Kasparaitis, A., Račiukaitis, G., & Gečys, P. (2020). In-depth comparison of conventional glass cutting technologies with laser-based methods by volumetric scribing using Bessel beam and rear-side machining. *Optics Express*, 28(21), 32133. <https://doi.org/10.1364/OE.402567>
- Eckersley O'Callaghan. (2018). Glass Wippe. <https://www.eocengineers.com/projects/glass-wippe-385/>
- EN 572-2:2012: Glass in building—Basic soda lime silicate glass products—Part 2: Float glass. (2012). Comité Européen de Normalisation.
- EN 1990. (2002). CEN.
- EN 1991-1-1. (2002). CEN.
- EN 1992-1-1. (2004). CEN.
- ExOne. (2021). 3D Printing with Inorganic Binder. https://www.exone.com/Admin/ExOne/media/Sand-Binders/210310_X1_Handout_Inorganic_Binder_EN_2021-03_www.pdf
- ExOne. (2023). 3D Materials & Binders. <https://www.exone.com/en-US/3d-printing-materials-and-binders/sand>
- Feldmann, M., Kasper, R., Abeln, B., Cruz, P., Belis, J., Beyer, J., Colvin, J., Ensslen, F., Eliášová, M., & Galuppi, L. (2014). Guidance for European structural design of glass components: Support to the implementation, harmonization and further development of the Eurocodes. European Union.
- FEVE. (2021). Europe's glass value chain reaches a major milestone at 79% glass collection for recycling. <https://feve.org/glass-value-chain-hits-79-glass-collection/>
- Friedman, Y. B. (1952). *Mechanical properties of Metal*. Metallurgy.
- Galjaard, S., Hofman, S., Perry, N., & Ren, S. (2015). *Optimizing Structural Building Elements in Metal by using Additive Manufacturing*. 13.
- Giesecke, R., & Dillenburger, B. (2022). Three-dimensionally (3D) printed sand molds for custom glass parts. *Glass Structures & Engineering*, 7(2), 231–251. <https://doi.org/10.1007/s40940-022-00176-y>
- Giroux Glass. (n.d.). Grand Canyon Skywalk. Retrieved 14 January 2023, from <https://giroux-glass.com/project/grand-canyon-skywalk/>
- glaston. (n.d.). The future of flat lamination. Retrieved 21 January 2023, from <https://glaston.net/machine/prol/>
- Guinness world records 2005 (Special 50th anniversary ed). (2004). Guinness World Records.
- Hauser & Wirth. (n.d.). Roni Horn. Retrieved 29 April 2023, from <https://www.hauserwirth.com/hauser-wirth-exhibitions/5931-roni-horn-13/>
- Haverkamp. (n.d.). OPALFILM® Liquid Film. Retrieved 18 January 2023, from <https://www.haverkamp.de/en/sun-protection-film-technology/architecture/lacquer/product/opalfilm-liquid-film-special>
- Hestin, M., de Veron, S., & Burgos, S. (2016). Economic study on recycling of building glass in Europe. Deloitte Sustainability.
- Hubert, M. (2015). IMI-NFG Course on Processing in Glass Spring 2015.
- Inamura, C. (2017a). Towards a New Transparency: High Fidelity Additive Manufacturing of Transparent Glass Structures across Scales. MIT.
- Inamura, C. (2017b). GLASS II - APPLICATION. <https://www.chikara-inamura.com/GLASS/GLASS-II-APPLICATION>
- Inamura, C. (2020). Glass Additive Manufacturing. Paper presented at the Challenging Glass Ghent University.
- Inamura, C., Stern, M., Lizardo, D., Houk, P., & Oxman, N. (2018). Additive Manufacturing of Transparent Glass Structures. *3D Printing and Additive Manufacturing*, 5(4), 269–283. <https://doi.org/10.1089/3dp.2018.0157>
- Jet Edge. (n.d.). The Advantages of 5-Axis Waterjet Cutting Machines. Jet Edge Waterjets. Retrieved 13 January 2023, from <https://blog.jet-edgewaterjets.com/water-jet-machines/advantages-of-5-axis-waterjet-cutting-machines>
- Jipa, A., Bernhard, M., Meibodi, M., & Dillenburger, B. (2016). 3D-Printed Stay-in-Place Formwork for Topologically Optimized Concrete Slabs [Application/pdf]. 10 p. <https://doi.org/10.3929/>

ETHZ-B-000237082

Kim, E.-H., Lee, J.-H., Jung, Y.-G., Lee, C.-S., & Paik, U. (2011). A new in situ process in precision casting for mold fabrication. *Journal of the European Ceramic Society*, 31(9), 1581–1588. <https://doi.org/10.1016/j.jeurceramsoc.2011.03.013>

Klein, J. (2015). Additive Manufacturing of Optically Transparent Glass. <http://www.liebertpub.com/doi/10.1089/3dp.2015.0021>

Klein, J., Stern, M., Franchin, G., Kayser, M., Inamura, C., Dave, S., Weaver, J. C., Houk, P., Colombo, P., Yang, M., & Oxman, N. (2015). Additive Manufacturing of Optically Transparent Glass. *3D Printing and Additive Manufacturing*, 2(3), 92–105. <https://doi.org/10.1089/3dp.2015.0021>

Koniari, A. M. (2022). Development of a Topology Optimization Algorithm for a Mass-Optimized Cast Glass Component. TU Delft.

Koopman, D. (2021). The Topology Optimised Glass Bridge [TU Delft]. <http://repository.tudelft.nl/>

Le Bourhis, E. (2014). *Glass: Mechanics and technology* (2. ed). WILEY-VCH.

Li, Y., & Ren, S. (2011). *Building decorative materials*. Woodhead publ.

Louter, P. C. (2011). *Fragile yet Ductile: Structural aspects of reinforced glass beams*. s.n.

Lusas. (n.d.). Cantilevered glass canopy, Tokyo. Retrieved 26 December 2022, from <https://www.lusas.com/case/civil/cantilevered.html>

Martín, M., Centelles, X., Solé, A., Barreneche, C., Fernández, A. I., & Cabeza, L. F. (2020). Polymeric interlayer materials for laminated glass: A review. *Construction and Building Materials*, 230, 116897. <https://doi.org/10.1016/j.conbuildmat.2019.116897>

Menges, A., Sheil, B., Glynn, R., & Skavara, M. (2017). *Fabricate 2017*. UCL Press. <https://doi.org/10.2307/j.ctt1n7qkg7>

MIT News Office. (2015, September 14). Printing transparent glass in 3-D. <https://news.mit.edu/2015/3-d-printing-transparent-glass-0914>

Molnar, G., Molnár, L., & Bojtár, I. (2012). Preparing a comprehensive analysis of the mechanical classification of structural glass. *Materials Engineering*, 19.

Moore, D. G., Barbera, L., Masania, K., & Studart, A. R. (2020). Three-dimensional printing of multi-component glasses using phase-separating resins. *Nature Materials*, 19(2), 212–217. <https://doi.org/10.1038/s41563-019-0525-y>

Musgraves, J. D., Hu, J., & Calvez, L. (Eds.).

(2019). *Springer Handbook of Glass*. Springer International Publishing. <https://doi.org/10.1007/978-3-319-93728-1>

MVRDV. (2016). *Crystal Houses*. <https://www.mvrdiv.nl/projects/240/crystal-houses>

Naous, D. (2020). Topologically Optimised Cast Glass Shell Exhibition Booth. TU Delft.

Nathan, Palar, P. S., & Zuhail, L. R. (2020). SIMP versus level set function as an implicit representation model for structural topology optimization. 040003. <https://doi.org/10.1063/5.0005031>

Nijssse, R. (2003). *Glass in structures: Elements, concepts, designs*. Birkhauser-Publishers for Architecture.

Nilsson, L., & Persson, P.-O. (2007). *Cleaner production: Technologies and tools for resource efficient production*. Baltic University Press.

Nolan, B. (2001, November). Life Behind glass. *FRAME*, 23.

Oikonomopoulou, F. (2019). Unveiling the third dimension of glass Solid cast glass components and assemblies for structural applications. TU Delft.

Oikonomopoulou, F., Bhatia, I. S., van der Weijst, F., Damen, W., & Bristogianni, T. (2020). Rethinking the Cast Glass Mould. An Exploration on Novel Techniques for generating Complex and Customized Geometries. 16.

Oikonomopoulou, F., Bristogianni, T., Barou, L., Jacobs, E., Veer, F. A., & Nijssse, R. (2018). Interlocking cast glass components, Exploring a demountable dry-assembly structural glass system. *Heron*, 63.

Oikonomopoulou, F., Bristogianni, T., Barou, L., Veer, F. A., & Nijssse, R. (2018). The potential of cast glass in structural applications. Lessons learned from large-scale castings and state-of-the art load-bearing cast glass in architecture. *Journal of Building Engineering*, 20, 213–234. <https://doi.org/10.1016/j.jobe.2018.07.014>

Oikonomopoulou, F., Bristogianni, T., van der Velden, M., & Ikonmidis, K. (2022). The adhesively-bonded glass brick system of the Qaammat Pavilion in Greenland: From research to realization. *Architecture, Structures and Construction*, 2(1), 39–62. <https://doi.org/10.1007/s44150-022-00031-2>

Oikonomopoulou, F., Bristogianni, T., Veer, F. A., & Nijssse, R. (2018). The construction of the Crystal Houses façade: Challenges and innovations. *Glass Structures & Engineering*, 3(1), 87–108. <https://doi.org/10.1007/s40940-017-0039-4>

Oikonomopoulou, F., Singh Bhatia, I., Van Der

Weijst, F., Damen, W., & Bristogianni, T. (2020). Rethinking the Cast Glass Mould. An Exploration on Novel Techniques for generating Complex and Customized Geometries. <https://doi.org/10.7480/cgc.7.4662>

Oikonomopoulou, F., van den Broek, E. A. M., Bristogianni, T., Veer, F. A., & Nijssse, R. (2017). Design and experimental testing of the bundled glass column. *Glass Structures & Engineering*, 2(2), 183–200. <https://doi.org/10.1007/s40940-017-0041-x>

Olabisi, O., & Adewale, K. (Eds.). (2015). *Handbook of Thermoplastics, Second Edition*. CRC Press. <https://doi.org/10.1201/b19190>

O'Regan, C. (2015). *Structural use of glass in buildings* (Second edition). Institution of Structural Engineers.

Pilkington company. (n.d.). Invention of Float Glass. Retrieved 10 January 2023, from <https://www.pilkington.com/en-gb/uk/about/heritage/invention-of-float-glass>

Rafael Viñoly Architects. (1997). Tokyo International Forum. <https://vinoly.com/works/tokyo-international-forum/>

Ramulu, M., Posinasetti, P., & Hashish, M. (2005). ANALYSIS OF THE ABRASIVE WATERJET DRILLING PROCESS. 16.

Rasmussen, S. C. (2012). *How Glass Changed the World* (Vol. 3). Springer Berlin Heidelberg. <https://doi.org/10.1007/978-3-642-28183-9>

Rodichev, Y., Veer, F., Strizhalo, V., Soroka, E., & Shabetia, A. (2018). Structural Strength of Laminated Glass. *Challenging Glass Conference Proceedings*, 453–462 Pages. <https://doi.org/10.7480/CGC.6.2168>

Roller, R., Buck, V., Schlotterbeck, M., Trauzedel, D., & Wintgens, R. (2016). *Fachkunde Gießereitechnik: Technologie des Formens und Gießens* (8., überarbeitete und erweiterte Auflage). Verlag Europa - Lehrmittel Nourney, Vollmer GmbH & Co. KG.

Saint-Gobain. (n.d.). Glass manufacturing process. Retrieved 18 January 2023, from <https://in.saint-gobain-glass.com/glass-manufacturing-process>

Sanders, K., Bos, F., ten Brincke, E., & Belis, J. (2021). Edge strength of core drilled and waterjet cut holes in architectural glass. *Glass Structures & Engineering*, 6(2), 131–145. <https://doi.org/10.1007/s40940-021-00146-w>

Schittich, C., & Lenzen, S. (Eds.). (2007). *Glass construction manual* (2., rev.expanded ed).

Birkhäuser.

Sedak. (n.d.). Retrieved 18 January 2023, from <https://www.sedak.com/en/>

seele. (2021). Bründl Sports Flagship Store. <https://seele.com/references/bruendl-sports-flagship-store-austria>

Shelby, J. E. (2005). *Introduction to glass science and technology* (2nd ed). Royal Society of Chemistry.

ShivajiRao, M., & Satyanarayana, S. (2020). Abrasive water jet drilling of float glass and characterization of hole profile. *Glass Structures & Engineering*, 5(2), 155–169. <https://doi.org/10.1007/s40940-019-00112-7>

Sivarupan, T., Balasubramani, N., Saxena, P., Nagarajan, D., El Mansori, M., Salonitis, K., Jolly, M., & Dargusch, M. S. (2021). A review on the progress and challenges of binder jet 3D printing of sand moulds for advanced casting. *Additive Manufacturing*, 40. <https://doi.org/10.1016/j.addma.2021.101889>

Šooš, L., Matúš, M., Pokusová, M., Čačko, V., & Bábics, J. (2021). The Recycling of Waste Laminated Glass through Decomposition Technologies. *Recycling*, 6(2), 26. <https://doi.org/10.3390/recycling6020026>

Stefanaki, M. I. (2020). *Glass giants, Mass-optimized massive cast glass slab*. TU Delft.

Surgenor, A., Holcroft, C., Gill, P., & DeBrincat, G. (2018). *Building glass into the circular economy How to guide*. UKGBC, British Glass, Verdextra, ARUP.

Szymański, P., & Borowiak, M. (2019). Evaluation of Castings Surface Quality Made in 3D Printed Sand Moulds Using 3DP Technology. In B. Gapiński, M. Szostak, & V. Ivanov (Eds.), *Advances in Manufacturing II* (pp. 201–212). Springer International Publishing. https://doi.org/10.1007/978-3-030-16943-5_18

Tedeschi, A., & Wirz, F. (2014). *AAD - Algorithms-Aided Design: Parametric strategies using Grasshopper* (First edition). Le Penseur publisher.

Tensinet. (n.d.). 11 March Memorial Madrid. Retrieved 29 April 2023, from <https://www.tensinet.com/index.php/component/tensinet/?view=project&id=4680>

tgk. (n.d.). Splinter-shield Lacquer 750ml. Retrieved 18 January 2023, from <https://www.tgk.de/en/products-shop/glass-processing-techniques/safety-techniques/6876/splinter-shield-lacquer-750ml>

The Engineer. (n.d.). 3D-printed glass micro-

structures built with strength. Retrieved 29 April 2023, from <https://www.theengineer.co.uk/content/news/3d-printed-glass-microstructures-built-with-strength/>

Trentinella, R. (2003, October). Roman Glass. The Metropolitan Museum of Art. https://www.metmuseum.org/toah/hd/rxls/hd_rxls.htm

Veer, F. (2007). The strength of glass, a non-transparent value. *Heron*, 52.

Ward, J. A., Fowler, A. C., & O'Brien, S. B. (2011). Acid polishing of lead glass. *Journal of Mathematics in Industry*, 1(1), 1. <https://doi.org/10.1186/2190-5983-1-1>

Watson, D. M. (1999). Practical Annealing In: 11th Biennial Ausglass Conference.

Wax Filament. (n.d.). Machinablewax. Retrieved 21 January 2023, from <https://machinablewax.com/wax-filament/>

Weller, B., Reich, S., & Ebert, J. (2008). Principles and Geometry of Modular Steel-Glass Space Structures. *Challenging Glass 1*, Vol. 1, 145–155.

Wikipedia. (2022). Vikos Gorge. https://en.wikipedia.org/wiki/Vikos_Gorge

Worrell, E., Galitsky, C., Masanet, E., & Graus, W. (2008). Energy Efficiency Improvement and Cost Saving Opportunities for the Glass Industry. An ENERGY STAR Guide for Energy and Plant Managers (LBNL-57335-Revision, 927883; p. LBNL-57335-Revision, 927883). <https://doi.org/10.2172/927883>

Yang, D. (2021). The Interplay between the Structural and Sustainable Performance of Laminated Glass. TU Delft.

Yankelevsky, D. Z., Spiller, K., Packer, J. A., & Seica, M. V. (2017). Fracture characteristics of laboratory-tested soda lime glass specimens. *Canadian Journal of Civil Engineering*, 44(3), 151–160. <https://doi.org/10.1139/cjce-2016-0374>

Yellin, D. (n.d.). Retrieved 30 December 2022, from <https://www.dustinyellin.com/>

Zhang, D., Liu, X., & Qiu, J. (2021). 3D printing of glass by additive manufacturing techniques: A review. *Frontiers of Optoelectronics*, 14(3), 263–277. <https://doi.org/10.1007/s12200-020-1009-z>

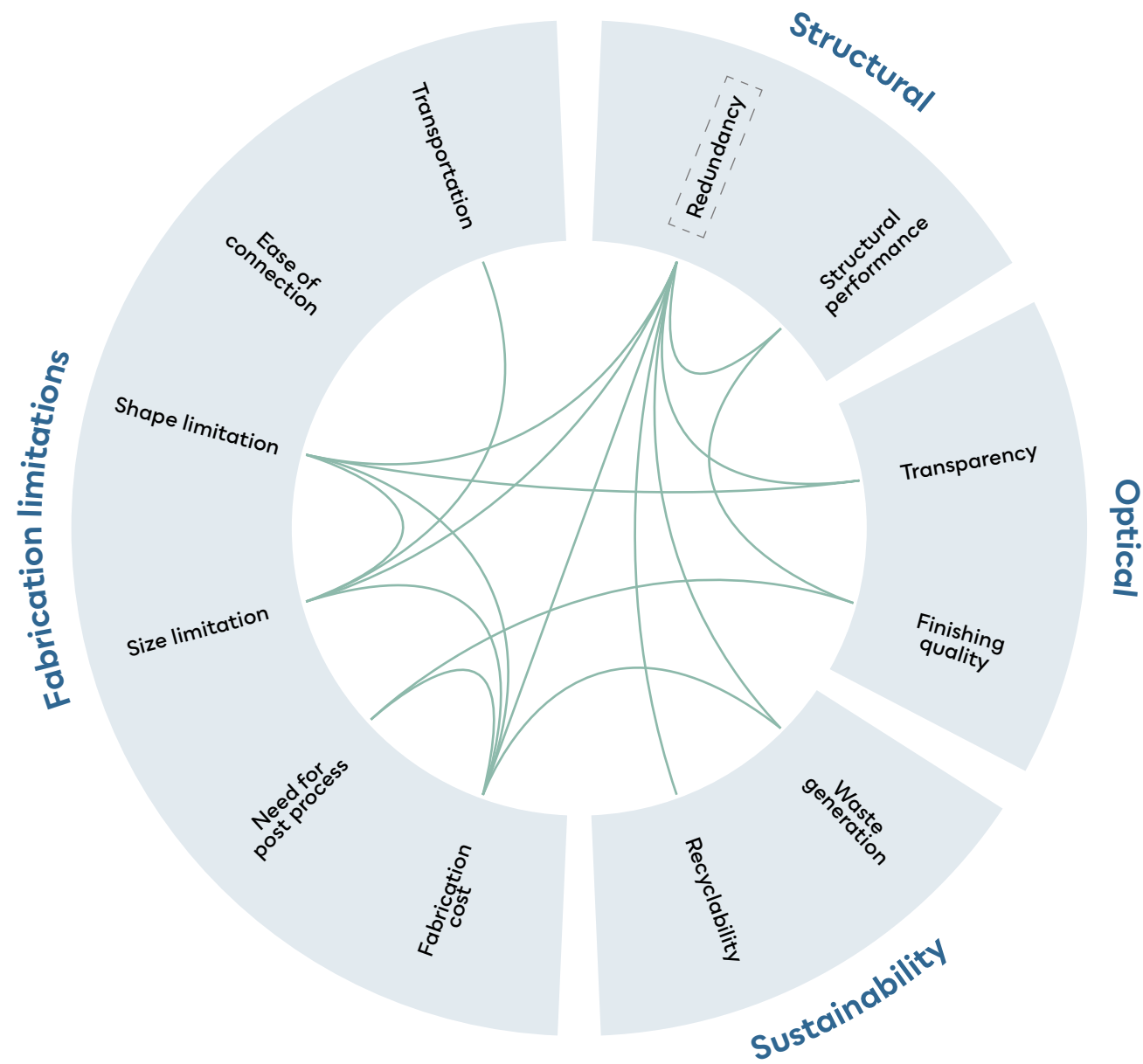
Zirker, J. B. (2005). *An Acre of Glass: A History and Forecast of the Telescope*. The Johns Hopkins University Press Baltimore.

Zoeller, D., & Muscato, C. (n.d.). The Crystal Palace in London: Building, Great Exhibition & History. Retrieved 12 January 2023, from <https://study.com/learn/lesson/crystal-palace-london-building-history.html>

11

APPENDIX

AWJ cut laminated float glass



Kiln cast

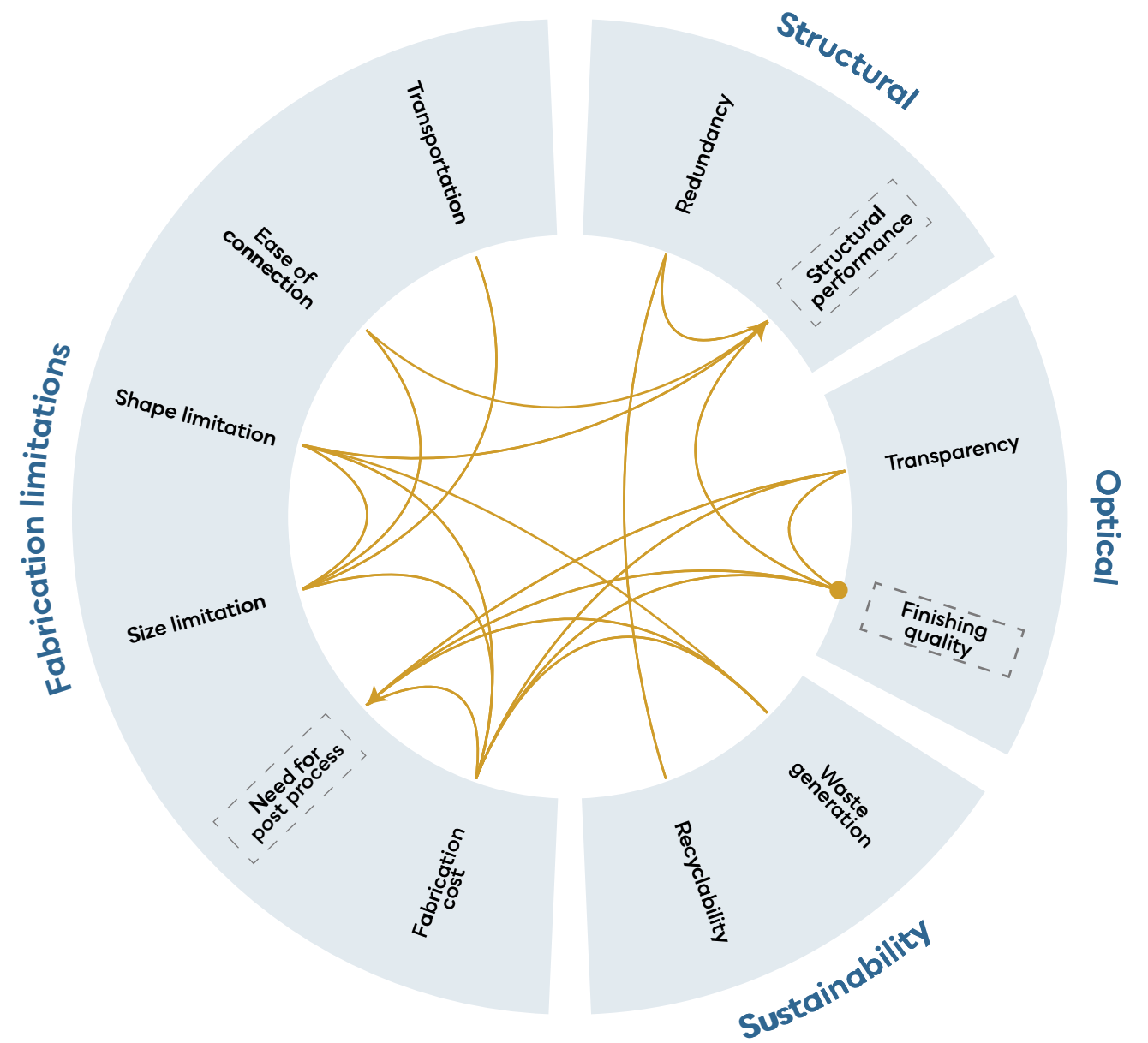


Figure 153 : Spider diagrams of interlinking assessment criteria for AWJ cut and lamination of float glass

Figure 154 : Spider diagrams of interlinking assessment criteria for kiln casting of glass.

3D printed glass

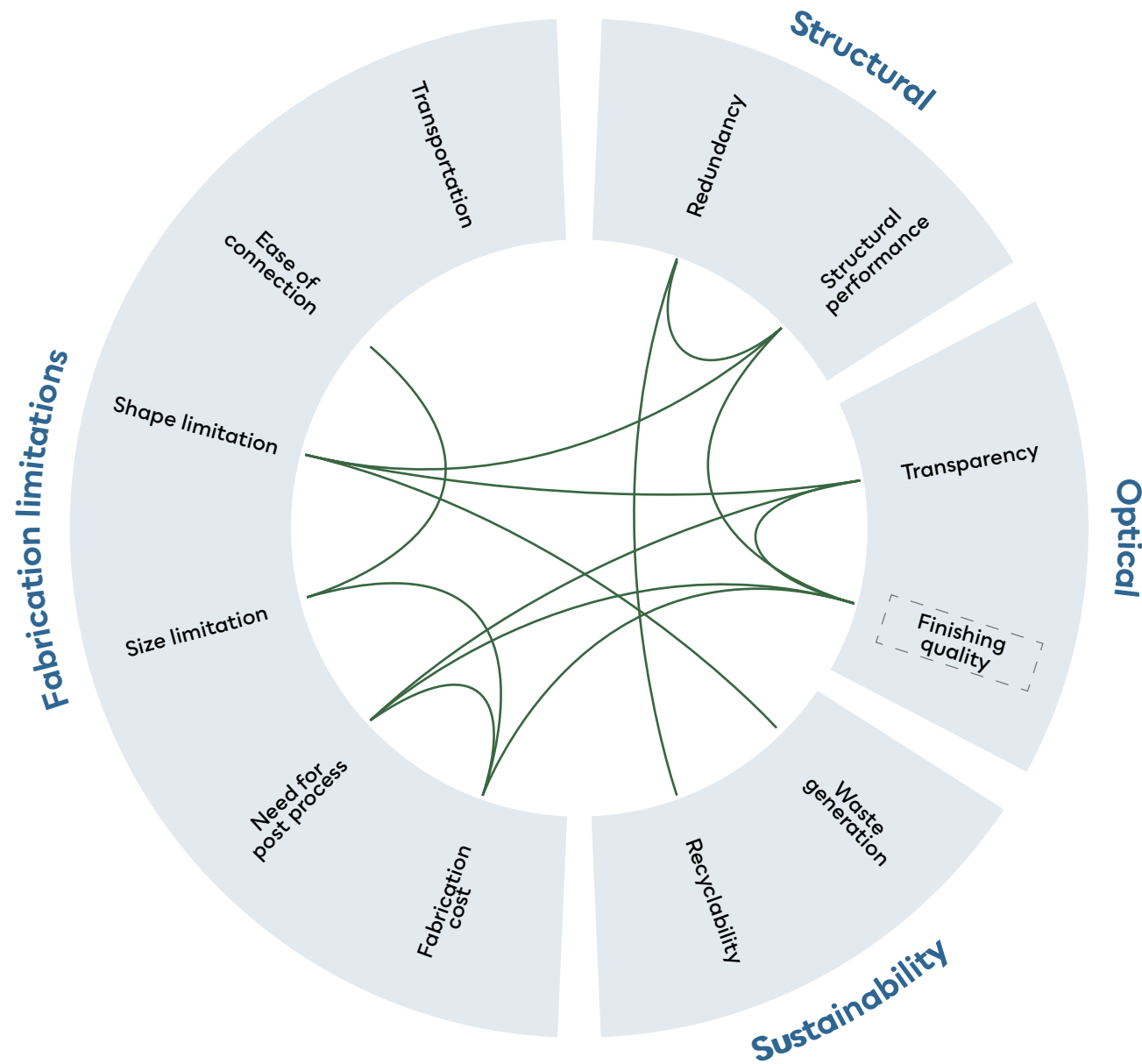


Figure 155 : Spider diagrams of interlinking assessment criteria for 3D printed glass.

Mould thickness calculation (Koninari, 2022; Stefanaki, 2020).

1) Thrust force calculation

$$F_A = p_A A = \left(\frac{p_t + p_b}{2} \right) \cdot A = \left(\rho g \cdot \frac{h_t + h_b}{2} \right) A$$

F_A = average thrust force

p_A = average pressure

A = area of the bottom surface = $0,4 \text{ m}^2$

p_t = pressure top

h_t = height top = 2 m

p_b = pressure bottom

h_b = height bottom = 0 m

$\rho = 2500 \text{ kg/m}^3$

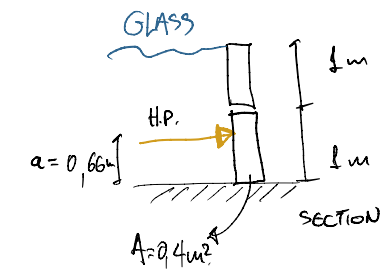
$g = 9,81 \frac{\text{m}}{\text{s}^2}$

$$F_A = 2500 \cdot 9,81 \cdot \frac{2}{2} \cdot 0,4 = 9,82 \text{ kN}$$

2) Bending moment

Hydrostatic pressure is applied on $1/3$ of the height.

$$M_{\text{max}} = F_A a = 9,82 \cdot \frac{2}{3} = 6,55 \text{ kNm}$$



3) Bending strength of 3DPSM (Voxeljet) $\sigma_{\text{bend}} = 220-300 \text{ N/cm}^2$

The min. value is used for the calculations:

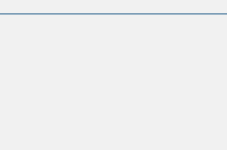
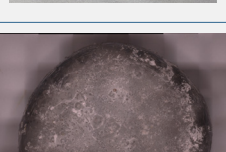
$$\sigma_{\text{bend}} = \frac{M_f}{I} = \frac{M_f}{\frac{1}{12} \cdot b \cdot d^3} \Rightarrow d = \sqrt[3]{\frac{6 \cdot M}{\sigma_{\text{bend}} \cdot b}}$$

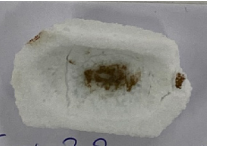
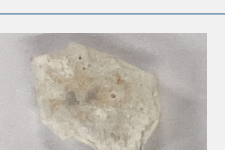
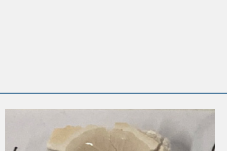
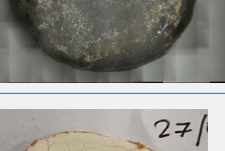
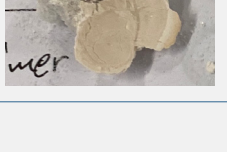
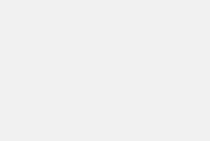
$$d = \sqrt[3]{\frac{6 \cdot 6,47 \cdot 10^3}{220 \cdot 10^4 \cdot 1}} \Rightarrow d = 0,26 \text{ m} \rightarrow 26 \text{ cm} \text{ minimum mould dimension.}$$

mould thickness for worstcase scenario piece.

Figure 156 : Hand calculations to define minimum mould thickness for the 1:1 fin element.

Figure 157 : Initial tests where consolidation of the sand is evident.

Annealing schedule	Nr.	Tested Geometry		Protective layer	Coatings		
		Cube	Bar		No	Zirkofluid 1219	
						Flow	Brush
1120°C normal	Test 1	1	2				
							
870°C normal	Test 2		2				
1120°C slow	Test 3		2				
970°C normal	Test 4		2				
							
	Test 5	1	Crystal cast	1			
				2			
				1			
	2	Shelf-Primer	1				

Coatings			
Zirkofluid 6672		Arkopal B 5	
Flow	Brush	Flow	Brush
			
			
			
			
			
			
			
			
			
			

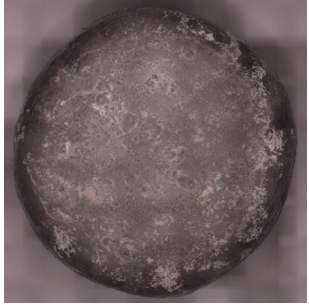
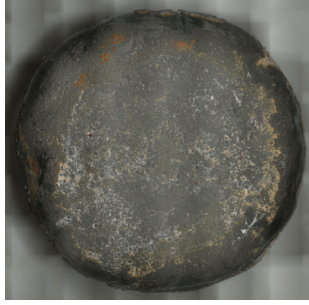
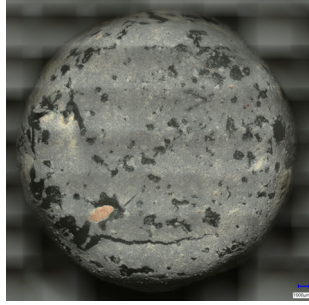
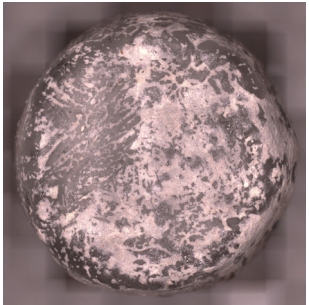
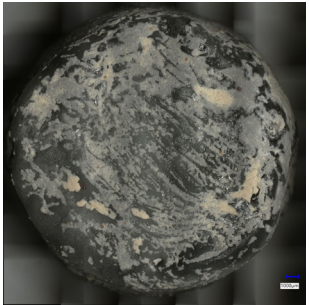
Annealing schedule	Protective layer	Sand type	Side	Coatings						Coating	
				No	Zirkofluid 1219		Zirkofluid 6672		Arkopal B 5		
					Flow	Brush	Flow	Brush	Flow		Brush
970°C normal	Crystalcast 3X Brush	Quartz sand	Contact								1X
											
		Ceramic sand	Contact								2X

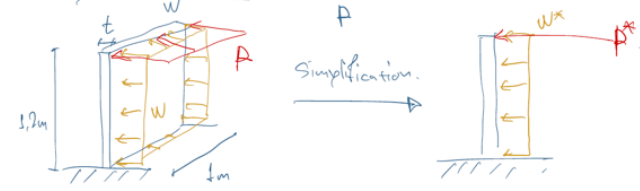
Figure 158 : Surface quality of the contact side. Captured using the microscope.

SIDE RAIL vertical (calculations for 1m long structure).

According to ULS the side rail must be able to withstand LC4:

no self weight in this direction

$$1,35 \cdot 24,7 \cdot t + 1,35 \cdot 0,9 \text{ (kN/m}^2) + 1,35 \cdot t \text{ (kN/m)} \Rightarrow 33,38t + 0,675 + 1,35 \text{ kN/m @ 1,2m}$$



Allowable deflection

$$L/500 = 1200/500 = 2,4 \text{ mm.}$$

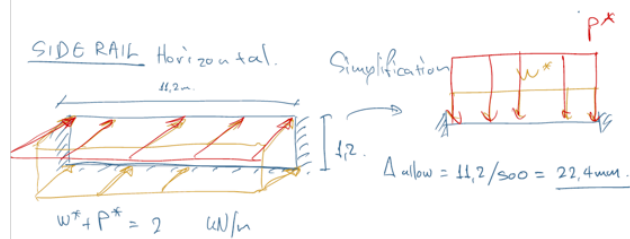
$$\Delta_{max}(w^*) = \frac{wL^4}{8EI}$$

$$\Delta_{max}(L^*) = \frac{PL^3}{3EI}$$

max deflection at the end.

for 3x15mm: $I = 7,6 \cdot 10^{-6} \text{ m}^4$, $t = 45 \text{ mm}$

$$\Delta_{max}(w^*) = \frac{0,68 \cdot 1,2^4}{8 \cdot 69 \cdot 10^6 \cdot 7,6 \cdot 10^{-6}} = 0,3 \text{ mm}$$



for 3x15mm $t = 0,045 \text{ m}$ $I = \frac{1}{12} \cdot 1,2 \cdot 0,045^3 = 9,1 \cdot 10^{-6} \text{ m}^4$ or $9,1 \cdot 10^{-6} \text{ m}^4$

$$\Delta_{max} = \frac{wL^4}{8EI} = \frac{2 \cdot 11,2^4}{8 \cdot 69 \cdot 10^6 \cdot 9,1 \cdot 10^{-6}} = 130 \text{ mm}$$

for 4x15mm $t = 0,06 \text{ m}$ $I = \frac{1}{12} \cdot 1,2 \cdot 0,06^3 = 21,6 \cdot 10^{-6} \text{ m}^4$ or $21,6 \cdot 10^{-6} \text{ m}^4$

$$\Delta_{max} = \frac{2 \cdot 11,2^4}{8 \cdot 69 \cdot 10^6 \cdot 21,6 \cdot 10^{-6}} = 94 \text{ mm}$$

for 5x15mm $t = 0,075 \text{ m}$ $I = \frac{1}{12} \cdot 1,2 \cdot 0,075^3 = 42 \cdot 10^{-6} \text{ m}^4$

$$\Delta_{max} = \frac{2 \cdot 11,2^4}{8 \cdot 69 \cdot 10^6 \cdot 42 \cdot 10^{-6}} = 28 \text{ mm}$$

See analysis.

$$\Delta_{max}(L^*) = \frac{1,35 \cdot 1,2^3}{3 \cdot 69 \cdot 10^6 \cdot 7,6 \cdot 10^{-6}} = 1,9 \text{ mm}$$

$$\Delta_{max}(tot) = 0,3 + 1,9 = 2,2 \text{ mm} < 2,4 \text{ mm}$$

$$M_{max1} = \frac{w \cdot L^2}{2} = \frac{0,68 \cdot 1,2^2}{2} = 0,49 \text{ kNm}$$

$$M_{max2} = PL = 1,62 \text{ kNm}$$

$M_{max}(tot) = 2,12$ or $2,12 \cdot 10^3 \text{ Nm}$

$$y_{max} = 45/2 = 22,5 \text{ mm}$$

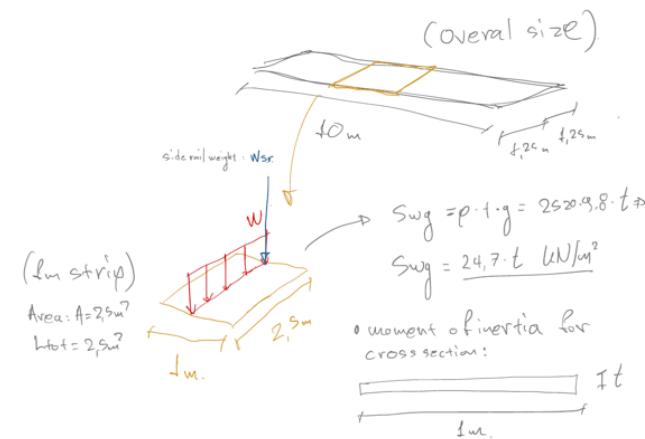
$$\sigma_{max} = \frac{M_{max} \cdot y_{max}}{I} = \frac{2,12 \cdot 10^3 \cdot 22,5}{7,6 \cdot 10^{-6}} = 7,7 \text{ MPa} < 25 \text{ MPa}$$

Side rails can be manufactured by laminating 3 layers of annealed glass and 1 layer of fully tempered float glass as sacrificial layer on the inner side.

SLS

Hand calculations worst case scenario (A)

Dimensioning of the sacrificial layer for the worst case scenario (A) when one of the side fins fails (break)



The load case and allowable deflection are defined according to SLS. In this case the allowable deflection is $L/250 \Rightarrow 1250/250 = 5 \text{ mm}$

L.C. = self weight + live = $24,7 \cdot t + 0,9 \text{ kN/m}^2$

for 3x15mm $t = 45 \text{ mm}$ $w = 7,6 \text{ kN/m}^2 \rightarrow w^* = 7,6 \text{ kN/m}$

$$I = \frac{1}{12} b h^3 = \frac{1}{12} \cdot 1000 \cdot 45^3 = 7,6 \cdot 10^{-6} \text{ m}^4$$

$$\Delta(x,c) = \frac{1}{4} \cdot \frac{7,6 \cdot 1,2^4}{69 \cdot 10^6 \cdot 7,6 \cdot 10^{-6}} = 8,8 \text{ mm}$$

$M_{max} = \frac{w \cdot a^2}{2} = \frac{7,6 \cdot 1,2^2}{2} = 5,53 \text{ kNm}$ $\sigma_{max} = \frac{5,53 \cdot 22,5}{7,6 \cdot 10^{-6}} = 16,5 \text{ MPa}$

for 4x15mm $t = 0,06 \text{ m}$ $w = 8 \text{ kN/m}^2 \rightarrow w^* = 8 \text{ kN/m}$

$$I = \frac{1}{12} b h^3 = \frac{1}{12} \cdot 1000 \cdot 60^3 = 18 \cdot 10^{-6} \text{ m}^4$$

$$\Delta(x,c) = \frac{1}{4} \cdot \frac{8 \cdot 1,2^4}{69 \cdot 10^6 \cdot 18 \cdot 10^{-6}} = 3,9 \text{ mm} < 5 \text{ mm}$$

$$M_{max} = \frac{w \cdot a^2}{2} = \frac{8 \cdot 1,2^2}{2} = 5,76 \text{ kNm or } 5,76 \cdot 10^3 \text{ Nm}$$

$$\sigma_{max} = \frac{M_{max} \cdot y_{max}}{I} \Rightarrow \sigma_{max} = \frac{5,76 \cdot 10^3 \cdot 30}{18 \cdot 10^{-6}} = 9,44 \text{ MPa}$$

$y_{max} = 60/2 = 30 \text{ mm}$

for 4x15mm $t = 0,06 \text{ m}$ $w = 7,7 \text{ kN/m}^2 \rightarrow w^* = 7,7 \text{ kN/m}$

$$I = \frac{1}{12} b h^3 = \frac{1}{12} \cdot 1000 \cdot 48^3 = 9,21 \cdot 10^{-6} \text{ m}^4$$

$$\Delta(x,c) = \frac{1}{4} \cdot \frac{7,7 \cdot 1,2^4}{69 \cdot 10^6 \cdot 9,21 \cdot 10^{-6}} = 7,4 \text{ mm}$$

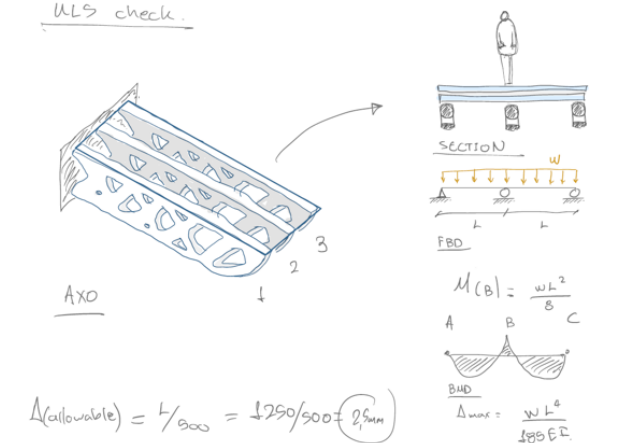
$$M_{max} = \frac{7,7 \cdot 1,2^2}{2} = 5,59 \text{ kNm}$$

$$\sigma_{max} = \frac{5,59 \cdot 30}{9,21 \cdot 10^{-6}} = 18,26 \text{ MPa}$$

$y_{max} = 48/2 = 24 \text{ mm}$

ULS check

for 4x15mm the deflection values are within the Eurocode requirement and design strength based on EN 1088. Since the stress is well below 45 MPa and even for 3 layers of 15mm HS glass stress doesn't go above 24,5 MPa no extra protective layer is going to be added to reduce weight and material use.



$$\Delta_{allowable} = L/500 = 1250/500 = 2,5 \text{ mm}$$

for 4x15mm for moment of inertia: $I = 18 \cdot 10^{-6} \text{ m}^4$

4x15mm for the load: $w = 9,75 + 7,35 \cdot t = 11,76 \text{ kN/m}^2$

$w^* = 11,76 \text{ kN/m}$

$$\Delta_{max} = \frac{11,76 \cdot 1,2^4}{185 \cdot 69 \cdot 10^6 \cdot 18 \cdot 10^{-6}} = 0,12 \text{ mm}$$

$$M_{max} = \frac{11,76 \cdot 1,2^2}{8} = 2,3 \text{ kNm or } 2,3 \cdot 10^3 \text{ Nm}$$

$$\sigma_{max} = \frac{M_{max} \cdot y_{max}}{I} = \frac{2,3 \cdot 10^3 \cdot 30}{18 \cdot 10^{-6}} = 3,8 \text{ MPa}$$

Scenario (B) (Middle fin failure)

$$2L/250 \Rightarrow 2500/250 = 10 \text{ mm allowable}$$

for 4x15mm $t = 60 \text{ mm}$ $w = 8 \text{ kN/m}^2 \rightarrow w^* = 8 \text{ kN/m}$

$$I = 18 \cdot 10^{-6} \text{ m}^4$$

$$\Delta_{max} = \frac{8 \cdot (2,5)^4}{384 \cdot 69 \cdot 10^6 \cdot 18 \cdot 10^{-6}} = 33 \text{ mm} < 40 \text{ mm}$$

$$M_{max} = \frac{8 \cdot 2,5^2}{8} = 6,25 \text{ kNm or } 6,25 \cdot 10^3 \text{ Nm}$$

$$\sigma_{max} = \frac{M_{max} \cdot y_{max}}{I} = \frac{6,25 \cdot 10^3 \cdot 30}{18 \cdot 10^{-6}} = 10,41 \text{ MPa}$$

Figure 159: Hand calculations for side rail.

Figure 160: ULS and SLS calculations for floor element.

